

METABOLOMICS OF UNHOPPED WORT AND BEER



Emilio Pliego Garcia

Supervised by: Dr Robert Falconer and Prof Duncan Cameron

A thesis submitted in fulfilment of the requirements for the degree of
Doctor of Philosophy (PhD)

The University of Sheffield
Faculty of Engineering
Department of Chemical and Biological Engineering

2020

Abstract

Beer is the second most consumed beverage in the world. The beer market has changed drastically in the last decades, especially with the rise of small-scale craft breweries, driven by the enthusiasm to experiment with unique and new recipes and cater to a market that appreciates artisanal products. Consumers' desire for more complex flavour profiles demands a better understanding of molecular explanations of how flavour arises in beer. The biochemical composition of beer is complex, comprising hundreds of compounds from different chemical classes arising by various mechanisms. There are a wide range of analytical approaches that can be implemented to study beer's composition and with the rise of highly sensitive extraction, separation, and detection methods, coupled to multivariate analysis models, emergent properties of beer can be revealed.

The aim of this PhD thesis is to design a brewing process based on modern brewing practices, take samples at various stages of the process, and then to analyse these samples using various mass spectrometry-based methods and a metabolomics workflow. Key compounds discriminant to each brewing stage were putatively identified, discussed, and compared between the methods; the methods themselves and the workflow implemented was critically assessed, along with their limitations and relative merits. The UPLC-MS approach results showed the most discriminatory power within sample classes, and a larger diversity of chemical classes was putatively identified from its results. A lack of food-related metabolomic platforms in the databases available makes the deeper analysis of these results still a challenge.

Compounds derived from phenolic amino acids (phenylalanine and tyrosine) show promise as precursors of flavour-active compounds. The phenylpropanoid pathway that is ubiquitous in plants and the phenyl-glycosides found attached to malt's husk could be sources of interesting flavour-active compounds that may be released and transformed during the brewing process.

Acknowledgements

I would like to express my acknowledgement to the people that supported me and offered guidance and advise along the course of this research:

All the staff and colleagues in the Chemical and Biological Engineering Department. To the staff of the Mass Spectrometry Centre at the Animal and Plants Science department, especially Dr Heather Walker, Prof Mike Burrell, and Mrs Gemma Newsome.

To my supervisors Dr Robert Falconer and Prof Duncan Cameron who helped the most in bringing this project to fruition.

And finally, to my family and friends who provided encouragement during my studies abroad.

Table of Contents

Abstract	i
Acknowledgements.....	ii
Table of Contents	iii
Table of Figures	vi
Table of Tables	xi
List of Abbreviations.....	xiii
1. Chapter 1: General Introduction.....	1
1.1 Brewing	1
1.1.1 Barley.....	2
1.1.2 Yeast	4
1.1.3 Water.....	4
1.1.4 Mashing.....	5
1.1.5 Boiling.....	7
1.1.6 Hops	7
1.1.7 Beer design considerations	8
1.3 The complex nature of beer chemistry	13
1.3.1 Vicinal diketones	14
1.3.2 Carbohydrates	14
1.3.3 Fusel alcohols	15
1.3.4 Esters.....	16
1.3.5 Aldehydes.....	17
1.3.6 Nitrogenous compounds.....	19
1.3.7 Sulphur compounds	20
1.3.8 Phenolic compounds.....	20
1.3.9 Compounds derived from the Maillard reaction	21
1.4 Mass Spectrometry for beer analysis.....	24
1.3.4 Principles of mass spectrometry.....	24

1.4.1 Extraction methods	26
1.4.2 Chromatographic methods	27
1.4.3 Metabolomics approach	27
1.4 Thesis aims	30
2. Chapter 2: Development of a brewing process and sampling method for metabolomics analysis	31
2.1 Introduction	31
2.2 Materials and methods	32
2.2.1 Brewing	32
2.4 Results and discussion.....	36
2.5 Conclusions	38
3. Chapter 3: Untargeted metabolomics analysis of brewing samples using matrix-assisted laser desorption/ionization – mass spectrometry and direct injection electron-ionisation – mass spectrometry.....	39
3.1 Introduction	39
3.2 Materials and methods	41
3.2.1 MALDI-MS	41
3.2.2 DI-MS.....	42
3.2.3 Data pre-processing and multivariate analysis	43
3.2.4 Development of a beer flavour compound database to use with MS data.....	44
3.3 Results	45
3.3.1 MALDI-MS	45
3.3.2 DI-MS.....	55
3.3.3 Statistical significance of the relative abundance between sample classes	58
3.3.4 Data processing and putative identification of discriminant compounds	64
3.4 Discussion.....	68
3.5 Conclusions	73
4. Chapter 4: Metabolomics of the liquid phase of brewing samples using ultra performance liquid chromatography – mass spectrometry.....	74

4.1 Introduction	74
4.2 Materials and methods	75
4.2.1 UPLC-MS.....	75
4.2.2 Data pre-processing and multivariate analysis	76
4.3 Results	76
4.3.1 Statistical significance of the relative abundance between sample classes	81
4.3.2 Data processing and putative identification of discriminant compounds	86
4.4 Discussion.....	88
4.5 Conclusions	91
5. Chapter 5: General Discussion	92
5.1 Comparison between MS techniques	92
5.1.1 Comparing the putative annotation results.....	92
5.1.2 Relative merits of the MS methods	94
5.2 Future recommendations	96
5.3 Conclusions	98
6. Bibliography	99
7. Appendix	109
A1 Method optimisation supplementary material	109
MALDI-MS method development	109
A2 Chapter 3 Supplementary material	126
MALDI-MS Supplementary Material	126
DI-MS Supplementary Material	140
A3 Chapter 4 UPLC-MS Supplementary Material	147

Table of Figures

Figure 1.1 Overview of brewing process (Adapted from Lewis and Young 1995).....	2
Figure 1.2 Longitudinal sectional view of a barley grain (left) and Scanning electron-microscopy (SEM) of starch granules (Sole and Griggs, 2005; Fuwa et al. 1979)	3
Figure 1.3 Typical pH and temperature enzyme ranges during mash (Adapted from (Palmer, 2006)).....	6
Figure 1.4 Beer's colour scale.....	9
Figure 1.5 Visual diagram of the composition of wort along the brewing process (Adapted from (Palmer, 2006))	12
Figure 1.6 Simplified diagram of the Ehrlich pathway (adapted from (Hazelwood <i>et al.</i> , 2008))	16
Figure 1.7 Simplified formation of aldehydes by lipid oxidation (Adapted from (Baert <i>et al.</i> , 2012))	18
Figure 1.8 Simplified diagram of the Strecker degradation	19
Figure 1.9 General structure of phenolic acids	21
Figure 1.10 Overview scheme of the Maillard reaction and its products, adapted from (van Boekel, 2006; Baert <i>et al.</i> , 2012)	23
Figure 11.11 Simplified diagram of the operating principles during ESI.....	25
Figure 12 The two main ionisation mechanisms during ESI: IEM model showing how analyte molecule is ripped from within the charged nanodroplet by the electrostatic forces (left); CRM model showing the nanodroplet's surface evaporates until only the charged analyte is left.	26
Figure 2.1 Picture of the distilling apparatus used for alcohol measurements	34
Figure 2.2 Mashing profile where the sampling points after each step are labelled.	36
Figure 2.3 Superimposed graph of Cell concentration, specific gravity, and ABV% (left). pH measurements (right).....	38
Figure 3.1 Simplified drawing of the operating principles during MALDI. The drawing shows the laser hitting the matrix:sample crystal lattice, the energy absorption, ionisation, and formation of molecular ions.....	39
Figure 3.2 QR code to access the beer flavour database (Permalink: https://drive.google.com/file/d/151leowuy3z3VYI5yvJTa2NvQ69-E7J_/view?usp=sharing).....	45
Figure 3.3 Sum total ion count (TIC) in positive (blue) and negative (orange) ionisation mode (MALDI-MS).....	46
Figure 3.4 Overall PCA score scatter plot (MALDI-MS positive mode). Labels on each point correspond to the time-point named in Chapter 2	47
Figure 3.5 PCA score scatter plot of the post-fermentation sample class (positive mode).....	47
Figure 3.6 PCA score scatter plot of the pre-fermentation sample class (positive mode)	48

Figure 3.7 OPLS-DA score scatter plot (positive mode)	49
Figure 3.8 Overall PCA score scatter plot (negative mode)	50
Figure 3.9 PCA score scatter plot of the post-fermentation sample class (negative mode)	50
Figure 3.10 PCA score scatter plot of the pre-fermentation sample class (negative mode)	51
Figure 3.11 OPLS-DA score scatter plot MALDI-MS (negative mode).....	51
Figure 3.12 Loadings column plot showing the most discriminant bins of the pre-fermentation sample class MALDI-MS (positive mode) normalised to unit length. Top discriminant bins are enclosed in black and were chosen for annotation.	52
Figure 3.13 Loadings column plot showing the most discriminant bins of the post-fermentation sample class MALDI-MS (positive mode) normalised to unit length. Top discriminant bins are enclosed in black and were chosen for annotation.	52
Figure 3.14 Loadings column plot showing the most discriminant bins of the post-fermentation sample class MALDI-MS (negative mode) normalised to unit length. Top discriminant bins are enclosed in black and were chosen for annotation.	53
Figure 3.15 Loadings column plot showing the most discriminant bins of the pre-fermentation sample class MALDI-MS (negative mode) normalised to unit length.....	53
Figure 3.16 Overall PCA score scatter plot in DI-ESI-MS.....	55
Figure 3.17 OPLS-DA score scatter plot in DI-ESI-MS.....	56
Figure 3.18 Loadings column plot showing the most discriminant bins of the pre-fermentation sample class (normalised to unit length). Top discriminant bins are enclosed in black and were chosen for annotation.....	56
Figure 3.19 Loadings column plot showing the most discriminant bins of the post-fermentation sample class (normalised to unit length). Top discriminant bins are enclosed in black and were chosen for annotation.....	57
Figure 3.20 Boxplots of the average %TIC detected at each discriminant bin of the pre-fermentation sample class (MALDI-MS positive mode). Upper and lower whiskers indicate upper and lower quartiles respectively; the rectangle represents the middle quartile range divided by the median value.....	60
Figure 3.21 Boxplots of the average %TIC detected at each discriminant bin of the post-fermentation sample class (MALDI-MS positive mode). Upper and lower whiskers indicate upper and lower quartiles respectively; the rectangle represents the middle quartile range divided by the median value.....	61
Figure 3.22 Boxplots of the average %TIC detected at each discriminant bin of the pre-fermentation sample class (DI-ESI-MS positive mode). Upper and lower whiskers indicate upper and	

lower quartiles respectively; the rectangle represents the middle quartile range divided by the median value.....	62
Figure 3.23 Boxplots of the average %TIC detected at each discriminant bin of the post-fermentation sample class (DI-ESI-MS positive mode). Upper and lower whiskers indicate upper and lower quartiles respectively; the rectangle represents the middle quartile range divided by the median value.....	63
Figure 3.24 MALDI-MS pre-fermentation chemical class proportional distribution of putatively identified compounds. Outer ring show the chemical class and inner ring shows the parent class....	65
Figure 3.25 MALDI-MS post-fermentation chemical class proportional distribution of putatively identified compounds. Outer ring show the chemical class and inner ring shows the parent class....	66
Figure 3.26 DI-ESI-MS pre-fermentation chemical class proportional distribution of putatively identified compounds. Outer ring show the chemical class and inner ring shows the parent class....	67
Figure 3.27 DI-ESI-MS post-fermentation chemical class proportional distribution of putatively identified compounds. Outer ring show the chemical class and inner ring shows the parent class....	68
Figure 4.1 Column plot of mean total ion counts in positive mode. Error bars indicate standard deviation.	77
Figure 4.2 PCA score scatter plot. The enclosed samples represent the sample classes identified	78
Figure 4.3 OPLS-DA Loadings column plot of the most discriminant features of the post-fermented sample class normalised to unit length (post-fermented-f1 pairwise comparison). Top discriminant bins are enclosed in black and were chosen for annotation.	78
Figure 4.4 OPLS-DA Loadings column plot of the most discriminant features of the post-fermented sample class normalised to unit length (post-fermented-pre-fermented pairwise comparison). Top discriminant bins are enclosed in black and were chosen for annotation.	79
Figure 4.5 OPLS-DA Loadings column plot of the most discriminant features of the F1 sample class normalised to unit length (post-fermented-f1 pairwise comparison). Top discriminant bins are enclosed in black and were chosen for annotation.....	79
Figure 4.6 Loadings column plot of the most discriminant features of the F1 sample class normalised to unit length (pre-fermented-f1 pairwise comparison). Top discriminant bins are enclosed in black and were chosen for annotation.	80
Figure 4.7 Loadings column plot of the most discriminant features of the pre-fermented sample class normalised to unit length (post-fermented-pre-fermented pairwise comparison). Top discriminant bins are enclosed in black and were chosen for annotation.	80

Figure 4.8 Loadings column plot of the most discriminant features of the pre-fermented sample class normalised to unit length (pre-fermented-f1 pairwise comparison). Top discriminant bins are enclosed in black and were chosen for annotation.....	81
Figure 4.9 Venn diagram of the most discriminant masses of the three sample classes identified	81
Figure 4.10 Boxplots of the TIC detected at each discriminant feature (mz/rt) of the pre-fermented sample class. Upper and lower whiskers indicate upper and lower quartiles respectively; the rectangle represents the middle quartile range divided by the median value.	83
Figure 4.11 Boxplots of the TIC detected at each discriminant feature (mz/rt) of the F1 sample class. Upper and lower whiskers indicate upper and lower quartiles respectively; the rectangle represents the middle quartile range divided by the median value.	84
Figure 4.12 Boxplots of the TIC detected at each discriminant feature (mz/rt) of the post-fermented sample class. Upper and lower whiskers indicate upper and lower quartiles respectively; the rectangle represents the middle quartile range divided by the median value.	85
Figure 4.13 Proportional distribution of putatively identified compounds in the pre-fermented samples. Outer ring show the chemical class and inner ring shows the parent class.....	86
Figure 4.14 Proportional distribution of putatively identified compounds in the F1 samples. Outer ring show the chemical class and inner ring shows the parent class.	87
Figure 4.15 Proportional distribution of putatively identified compounds in the post-fermented samples. Outer ring show the chemical class and inner ring shows the parent class.....	88
Figure 4.16 Proposed inter-relations of heterocyclic sulphur compounds.	91
Figure 5.5.1 Venn diagrams of shared discriminant bins and features between methods. Pre-fermentation sample classes (left) and post-fermentation sample classes (right). The F1 sample class was considered as part of the post-fermented in this comparison.....	93
Figure 5.5.2 From left to right: Avenanthramide 1s, Avenanthramide 2, Avenanthramide A, and Avenanthramide G	94
Figure 7.1 Mass spectra of three M64 replicates (MALDI-MS Positive mode Test 1)	111
Figure 7.2 Mass spectra of three MB replicates (MALDI-MS Positive mode Test 1)	112
Figure 7.3 Mass spectra of three F11 replicates (MALDI-MS positive mode Test 1)	113
Figure 7.4 Mass spectra of three F14 replicates (MALDI-MS positive mode Test 1)	114
Figure 7.5 Mean total ion counts for each sample in MALDI positive mode Test 1. Error bars show standard deviation.	115
Figure 7.6 PCA scatter plot of the fermentation samples (MALDI-MS positive mode Test 1)....	116
Figure 7.7 PCA scatter plot of the mash samples (MALDI-MS positive mode Test 1)	116

Figure 7.8 PCA scatter plot of all samples (MALDI-MS positive mode Test 1).....	117
Figure 7.9 Total ion counts of the diluted samples in positive and negative ionization modes (MALDI -MS test 2).....	118
Figure 7.10 Mass spectra of three replicates of the 100 fold diluted samples in positive ionization mode (MALDI-MS positive mode Test 2).....	120
Figure 7.11 Mass spectra of three replicates of the 1000 fold diluted samples in positive ionization mode (MALDI-MS test 2)	121
Figure 7.12 Mass spectra of three replicates of the 10000 fold diluted samples in positive ionization mode (MALDI-MS Test 2).....	122
Figure 7.13 Mass spectra of three replicates of the 100 fold diluted samples in negative ionization mode (MALDI-MS Test 2).....	123
Figure 7.14 Mass spectra of three replicates of the 100 fold diluted samples in negative ionization mode (MALDI-MS Test 2).....	124
Figure 7.15 Mass spectra of three replicates of the 10000 fold diluted samples in negative ionization mode (MALDI-MS Test 2).....	125
Figure 7.16 Mass spectra of three M64 replicates (MALDI-MS positive mode Chapter 3)	126
Figure 7.17 Mass spectra of three MB replicates (MALDI-MS positive mode Chapter 3)	127
Figure 7.18 Mass spectra of three F1 replicates (MALDI-MS positive mode Chapter 3).....	128
Figure 7.19 Mass spectra of three F14 replicates (MALDI-MS positive mode Chapter 3).....	129
Figure 7.20 Mass spectra of three M64 replicates (MALDI-MS negative mode Chapter 3)	130
Figure 7.21 Mass spectra of three MB replicates (MALDI -MS negative mode Chapter 3).....	131
Figure 7.22 Mass spectra of three F1 replicates (MALDI-MS negative mode Chapter 3).....	132
Figure 7.23 Mass spectra of three F14 replicates (MALDI-MS negative mode Chapter 3).....	133
Figure 7.24 Mass spectrum of a pre-fermentation sample (DI-MS positive mode Chapter 3) ..	140
Figure 7.25 Mass spectrum of a post-fermentation sample (DI-MS positive mode Chapter 3) .	141
Figure 7.26 Chromatogram of a pre-fermentation sample (UPLC-MS Chapter 4)	147
Figure 7.27 Chromatogram of a F1 sample (UPLC-MS Chapter 4).....	147
Figure 7.28 Chromatogram of a post-fermentation sample (UPLC-MS Chapter 4).....	148
Figure 7.29 Mass spectra of three replicates of the M64 sample (UPLC-MS Chapter 4)	149
Figure 7.30 Mass spectra of three replicates of the MB sample (UPLC-MS Chapter 4)	150
Figure 7.31 Mass spectra of three replicates of the F1 sample (UPLC-MS Chapter 4)	151
Figure 7.32 Mass spectra of three replicates of the F14 sample (UPLC-MS Chapter 4)	152

Table of Tables

Table 1.1 Enzymatic activity along mashing temperatures	6
Table 1.2 Gross chemical composition of whole hops (Lewis and Young, 1995)	8
Table 1.3 Hop Utilization percentage based on boiling time (Dornbusch, 2010)	13
Table 1.4 Amino acid classification according to their yeast uptake pattern in brewery conditions (Jones and Pierce, 1964)	20
Table 2.1 Results of the sieving. Results are reported as mean and standard deviation of three replicates.....	36
Table 2.2 Physical-chemical parameters of brew at different sample points. Results are reported as mean and standard deviation of three replicates.....	37
Table 2.3 Cell counting results.	37
Table 3.1 Synapt G2 specifications (Waters Corporation, UK).....	42
Table 3.2 DI-MS run parameters.....	43
Table 3 QStar Elite MS System technical specifications (Applied Biosystems)	43
Table 3.4 Top discriminant bins between sample classes. Putative identification of compounds for each sample class is referenced next to it by table number.....	54
Table 3.5 Results of <i>t</i> -test applied to discriminant pre-fermentation bins (left table) and post-fermentation bins (right table) of MALDI-MS positive mode. P value significant if $p < 0.05$; df = degrees of freedom; t = t value	58
Table 3.6 Results of <i>t</i> -test applied to discriminant pre-fermentation bins (left table) and post-fermentation bins (right table) of DI-ESI-MS positive mode. P value significant if $p < 0.05$; df = degrees of freedom; t = t value	59
Table 4.1 UPLC-MS tune settings	75
Table 2 Synapt G2-Si-Q-TOF technical specifications (Waters Corporation, UK).....	76
Table 4.3 Summary of one-way ANOVA applied to discriminant features of the pre-fermentation samples (left table), F1 samples (top-right table), and post-fermentation samples (bottom-right table). F = F value; P value significant if $p < 0.05$; df = degrees of freedom	82
Table 7.1 Putative identification of compounds discriminant to the pre-fermentation sample class (MALDI-MS positive mode).....	134
Table 7.2 Putative identification of compounds discriminant to the post-fermentation sample class (MALDI-MS positive mode)	137
Table 7.3 Putative identification of compounds discriminant to the pre-fermentation sample class (DI-MS positive mode).....	142

Table 7.4 Putative identification of compounds discriminant to the post-fermentation samples class (DI-MS positive mode).....	145
Table 7.5 Putative identification of features discriminant of the wort sample class (UPLC-MS)	153
Table 7.6 Putative identification of compounds of the discriminant features in the wort-f1 sample class (UPLC-MS).....	156
Table 7.7 Putative identification of compounds discriminant for the F1 sample class (UPLC-MS).....	161
Table 7.8 Putative identification of discriminant feature of the beer-f1 sample class (UPLC-MS).....	162
Table 7.9 Putative identities of features discriminant to the beer sample class (UPLC-MS).....	165

List of Abbreviations

- American Society of Brewing Chemists – ABC
- Analysis of variance – ANOVA
- Arabinoxylan – AX
- Cyano hydroxycinnamic acid – CHCA
- Dihydroxybenzoic acid – DHB
- Dimethyl sulfide – DMS
- Direct injection – DI
- Dry basis coarse grind – DBCG
- Dry basis fine grind -DBFG
- Electrospray ionisation – ESI
- European Brewery Convention – EBC
- Final gravity – FG
- Free amino nitrogen – FAN
- Full width half maximum – FWHF
- Gas chromatography – GC
- Headspace – HS
- International Bittering Units – IBU
- Liquid chromatography – LC
- Mass spectrometry – MS
- Matrix-assisted laser desorption ionisation – MALDI
- Moisture content – MC
- Molecular-input line-entry system – SMILES
- Multivariate analysis – MVA
- Original gravity – OG
- Orthogonal partial least squares discriminant analysis – OPLS-DA
- Principal component analysis- PCA
- Revolutions per minute – rpm
- Solid-phase extraction – SPE
- Solid-phase microextraction – SPME
- Specific gravity – SG
- Standard Reference Method – SRM
- Time of flight – TOF
- Total ion count – TIC
- Ultra-performance liquid chromatography – UPLC
- Vicinal diketones – VDK
- Windisch-Kolbach – WK

1. Chapter 1: General Introduction

1.1 Brewing

Beer is a fermented beverage with a very distinct flavour and mouthfeel, traditionally produced from the fermentation of malted barley, although other carbohydrate sources may be used, and flavoured with hops. The main ingredients to produce beer are water, malted barley, hops, and yeast; however, adjuncts in the form of grits, liquid extracts, or processed grains may be used to substitute certain ingredients, to supplement the process and/or reduce the processing time.

The process of brewing is really a discipline that combines biochemistry, botany, microbiology, and pure chemistry. Although brewing has been practiced since before 4000 BCE (Moll, 1994), the concepts from the applied sciences to optimise the process have only been gradually applied for the past 150 years. Aspects such as: adjusting pH and temperature during the mashing to achieve a more efficient extraction; controlling the environment during the fermentation to ensure the quality of the yeast culture; and controlling for undesirable bacterial and fungal contaminants, had previously only been overcome by the empirical and pragmatic efforts of brewers and the intrinsic properties of beer itself.

For example, brewing has several aspects that make infection difficult (but not impossible) under normal circumstances: hops have natural antimicrobial properties (De Keukeleire, 2000); the pH drops during fermentation from 5.0-5.2 to 3.8-4.0 (Priest and Campbell, 2003); the concentration of CO₂ rises and further develops the anaerobic conditions; and the concentration of ethanol increases as the waste product of the fermentation of yeast. Brewers unknowingly evolved the brewing process to overcome potential infections while their main concerns were others. The main drivers for changing brewing practices were the availability of the supplies, the desire for a better quality product, greater control and efficiency, economy, and decent profit. Additionally, these drivers were limited by external factors such as consumer preference and government policies about taxation related to alcohol consumption.

The overall process diagram of brewing is shown in Figure 1.1, from the handling and preparation of malt to beer dispense. In brief: malted barley milled to a certain size; then the fermentable sugars are extracted into the water through a process called mashing; the mash is then filtered into the sweet wort which is then boiled vigorously; then during the boiling the hops are added at a specific schedule to control for bitterness and aroma; the next step is to cool the hopped wort quickly while preventing infection; then the boiled wort is whirlpooled to remove suspended solids transferred into the fermentation vessel and pitched with the yeast, where it will continue fermentation for weeks; finally,

the green beer can be filtered or supplemented with agents that aid with clarification before the packaging and/or dispense method of choice.

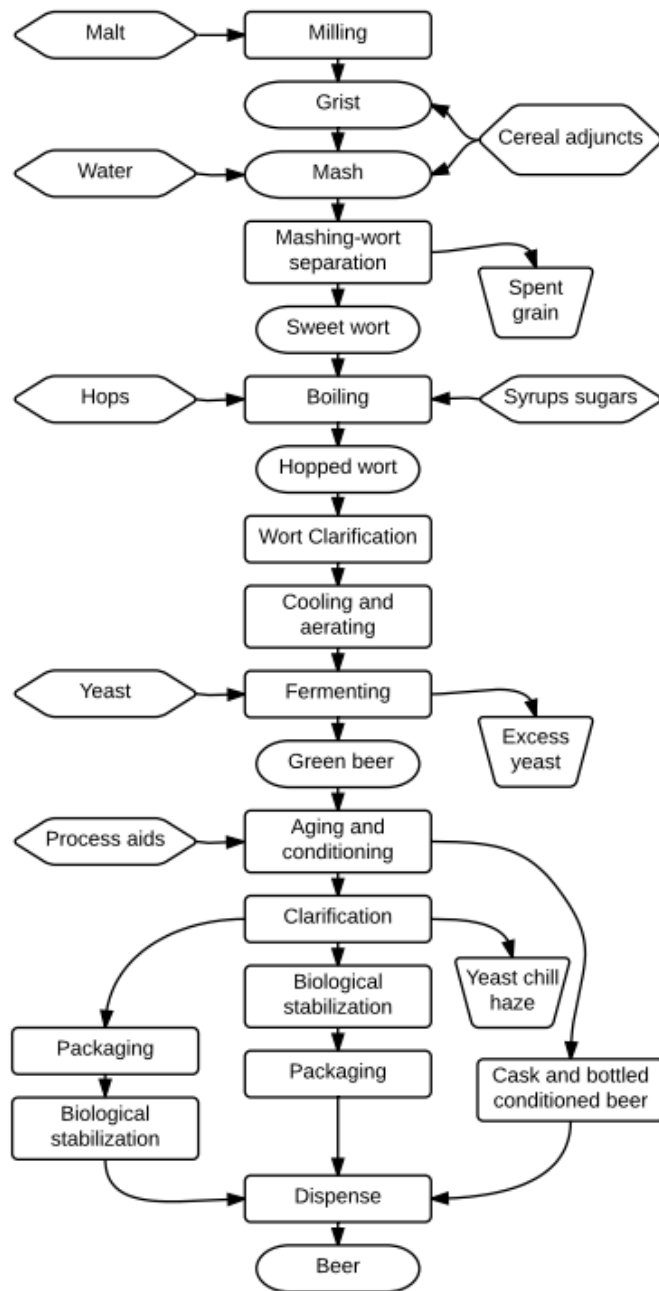


Figure 1.1 Overview of brewing process (Adapted from Lewis and Young 1995)

1.1.1 Barley

As it is barley (*Hordeum vulgare*) is unsuitable for mashing and has to undergo the process of malting in order to provide the wort with the necessary enzymes, carbohydrates, and nitrogenous compounds to ensure a successful fermentation. Malting consists in the controlled germination of the barley kernel up to a stage where the content of hydrolytic and proteolytic enzymes is stimulated into biosynthesis and diffuses from the embryo into the endosperm, which will make them able to infuse

into the water during mashing. The protein content in malting barley is of 10-12% (Baxter and Hughes 2001). By controlling the humidity and time of the germination, maltsters achieve a desirable degree of modification in accordance to the brewer's requirements, usually it is desirable for most of the starch to remain intact.

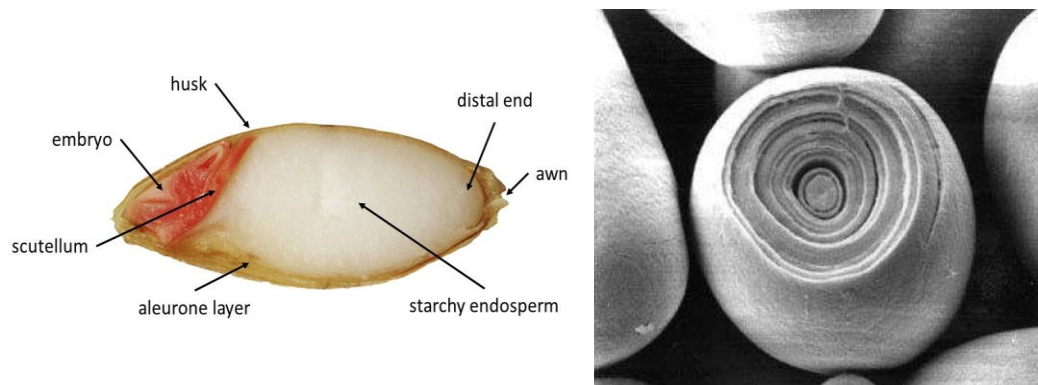


Figure 1.2 Longitudinal sectional view of a barley grain (left) and Scanning electron-microscopy (SEM) of starch granules (Sole and Griggs, 2005; Fuwa et al. 1979)

Afterwards, the kilning consists in drying the green malt from 45-50% to 3-5% moisture content with currents of heated air. The objective of kilning is to stop the germination process while conserving the integrity of the enzymes produced during the germination. The temperature of the air during the kilning is controlled in order to produce a wide variety of malts. Lighter kilned malts (up to 85 °C) produce lager beers; higher temperatures (90-100 °C) give lightly coloured and flavourful pale ale malts; specialty malts with flavours that range from toffee and caramel to sharp astringent roasted malts are roasted at much higher temperatures (200 °C). Kilning is unsurprisingly the most energy intensive stage of the malting process (Briggs, 1998).

1.1.1.1 Malt

Malting barley is classified as either six-row or two-row based on their grain symmetry and morphology (Briggs, 1998). Six-row malt tends to have a thicker husk and higher protein content and thus a higher starch conversion potential. Malt quality is determined by the choice of grain and the skill of the maltster. Brewers are concerned with several variables that are used to assess malt quality. A malt specification sheet will contain these variables in order for the brewer to adjust quantities and process parameters within their brewing system. These variables are determined by standard, laboratory-perfect mashes in where theoretical maximum values can give brewers an idea of the highest yields possible with that batch of malt and how to optimally use that particular malt in recipes. Depending on the organization responsible on obtaining these benchmark values (American Society of Brewing Chemists or the European Brewing Convention), the units of measurement employed may vary, but can be mathematically converted.

1.1.1.1.1 Base malts

These malts are used to provide the bulk of the wort's extract (fermentable carbohydrates, soluble proteins, conversion enzymes, etc.). Some of the more widely used base malts, in order of ascending order, are: pilsner, lager, pale, mild, Vienna, and Munich. The last two are closer to the specialty threshold and are usually used at 10-25% of the total grain bill, mostly for flavour contribution.

1.1.1.1.2 Specialty malts

These malts are used to provide the wort with significant colour, flavour, mouthfeel, and aroma and will contribute little to no enzymes for conversion potential. Some of the more widely used specialty malts are: caramel, crystal, amber, black, roasted, and chocolate. Higher kilning temperatures form increasing numbers of flavour-active compounds product of the Maillard reaction.

1.1.2 Yeast

The main yeast species used for brewing is *Saccharomyces cerevisiae* which was first isolated and named by E. C. Hansen in the 1880s. *S. cerevisiae* is a unicellular fungus that reproduces asexually and can live under aerobic or anaerobic conditions (Palmer, 2006). Yeast is responsible for the fermentation of the wort, during fermentation ethanol and carbon dioxide is produced from the consumption of carbohydrates in the wort. Alcohol is generated so that the yeast can replenish NAD⁺ and be able to produce energy through glycolysis. Carbon dioxide is released as a by-product of the transformation of pyruvate into acetaldehyde, the latter is subsequently reduced into ethanol (Bokulich and Bamforth, 2013).

The essential properties that brewers look for in yeasts are (Priest and Campbell, 2003):

- rapid fermentation
- consistent production of flavour and aroma compounds
- efficient fermentation, i.e. maximum production of ethanol with minimum production of biomass
- resilience to the osmotic stress of fresh wort and finished beer
- suitable flocculation and sedimentation properties at the end of fermentation
- high final viability for recovering and use in next fermentation
- high genetic stability over many generations.

1.1.3 Water

Water is the most abundant ingredient in beer (up to 90% of beer is water); brewers are interested to brew with water that is suitable for brewing a particular type of beer. Some of the aspects that are taken into consideration for good brewing water are its hardness and alkalinity. The amount of dissolved ions affects the efficiency of the extraction of fermentable sugars as well as desirable and undesirable flavour compounds from the raw materials.

1.1.4 Mashing

Mashing consists in mixing the grist with water at a controlled amount and at a desired temperature. The grist consists on the combination of milled malt grains, adjuncts, and supplementary materials.

The amount of water used can vary depending on the mashing method and the equipment configuration itself. There is controversy amongst brewers whether which methods are more efficient at extracting the most fermentable extract as a very large number of enzymes act simultaneously on the grist and the optimal conditions of activity for each enzyme are not the same. Brewers can vary the mashing regime to achieve certain desired characteristics on the final beer. Ultimately, it is agreed that much of the characteristics of the wort obtained is much more dependent on the quality of the malt and on the barley strains from which it is made (Briggs, 2004).

Based on the level of modification in the malt used, brewers can selectively mash through at different temperatures to get optimal activity of certain enzymes. Some of the most important enzymes during mashing are proteases (for protein breakdown for free amino nitrogen and haze reduction), glucanases (for gum conversion), phytases (for mash acidification), β -amylase (for the conversion of starch into simple carbohydrates), and α -amylase (for the conversion of starch into complex carbohydrates) (Palmer, 2006).

Table 1.1 Enzymatic activity along mashing temperatures

<i>Mashing Enzymes Activity</i>			
<i>Temperature</i>	<i>Working pH range</i>	<i>Enzyme</i>	<i>Activity</i>
35°C	4.5-5.5	β-glucanase	Start
38°C	5.0-5.5	Phytase	Start
40°C	4.6-5.3	Protease	Start
40°C	5.0-5.5	β-amylase	Start
45°C		β-glucanase	Peak
45-55°C		Phytase	Peak
50°C		Protease	Peak
55°C		β-glucanase	Denatured
56-63°C		Phytase	Denatured
60°C		Protease	Weaken
60°C	5.3-5.7	α-amylase	Start
65°C		β-amylase	Peak
70°C		β-amylase	Denatured
72°C		α-amylase	Peak
80°C		Protease	Denatured
80°C		α-amylase	Denatured

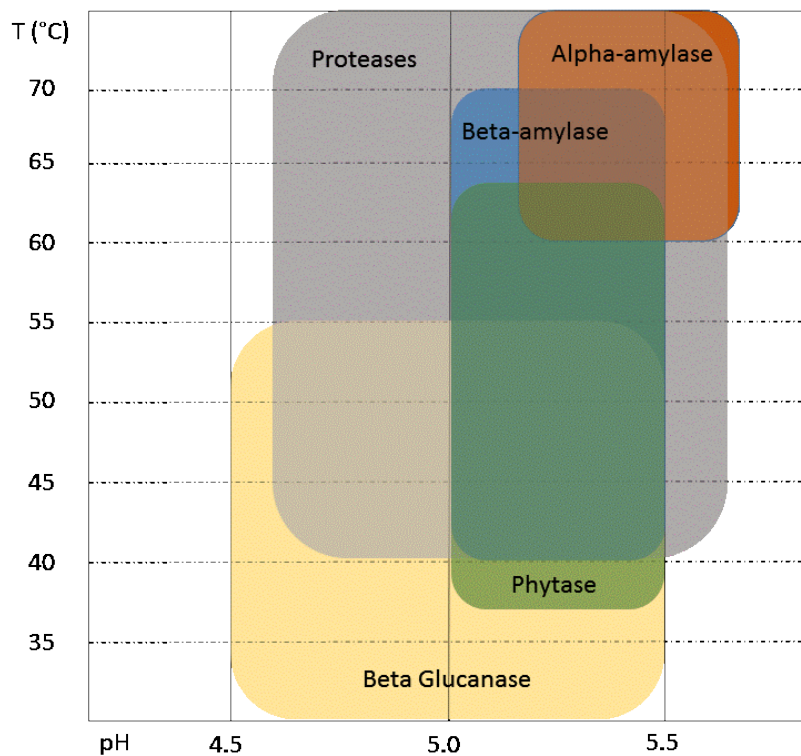


Figure 1.3 Typical pH and temperature enzyme ranges during mash (Adapted from (Palmer, 2006))

Some of the most commonly used methods of mashing are:

- Infusion mashing: Consists on mashing at set temperature (62-65°C) in a non-stirred tank for a period of time (20-60 min) to convert the most extract in a thick wort. The run-off is then washed off with sparge arms at a higher temperature (70-80°C).
- Decoction mashing: Consists on heating up (usually to boiling point) a portion of the mash and then adding it to the main mash. This method has the advantage of gelatinizing the starch and making it completely available, however it also affects the DP as the high temperatures denature the total amount of converting enzymes.
- Double mashing: consists on adding a mash separately prepared at a higher temperature to an already on-going main mash to create a ramp up in temperature in order to increase the extract content.

Although temperature has the biggest impact during the mashing, the following factors also determine the fermentability of the wort:

- pH
- mashing time
- water/grist ratio
- mash schedule.

It is evident that brewer's need to choose the mash conditions to accommodate the enzyme content of the malt. Malt modification will determine the amount and ratio of starch and enzymes. Then mashing can be customised to manage the malt in creative ways (through temperature controlled mashing) so that the optimal fermentable potential can be achieved.

1.1.5 Boiling

The boiling phase has several purposes. It is key that the boiling is vigorous and constant so that any undesirable remaining proteins, polyphenols, and other minor components evaporate or precipitate into insoluble trub (also known as hot break). Boiling achieves chemical, physical, and microbiological stability of the wort. Near the end of the boiling many brewers implement a technique known as whirlpooling, which consists in stirring (either by recirculating wort tangentially into the tank or by stirring manually) the wort to create a vortex that forces the suspended particles to come together and sink to the bottom of the tank. This action improves the clarity of the final beer.

1.1.6 Hops

Without hops, fermented unhopped malt extract is a very heavy and syrupy beverage that is very satiating. Hops give beer a unique and characteristic flavour that increases its palatability to consume in quantity. Hops come from the perennial plant *Humulus lupulus* native to North America, Europe, and Asia. There are several brewing practices used to infuse the wort with the bitter and aroma compounds from the hops. Late hopping is performed by boiling hops with the wort, whole hops can be used but hop products such as extracts and dried pellets are also popular due to their practicality

and resistance to deterioration during storage. Dry hopping is another technique that consists in adding hops to the wort after it has been cooled, this has the advantage of adding aroma without further adding bitterness to the final beer.

The resins and essential oils that impart the bitter taste and unique aromas respectively in beer are contained in the hop cones which are in the female plant; the female plant is the only one cultivated commercially. The 0.3-1.5% of dry weight in hops are essential oils, with a composition of over 300 organic compounds.

Table 1.2 Gross chemical composition of whole hops (Lewis and Young, 1995)

<i>Constituent</i>	<i>Percentage by weight</i>
Cellulose and lignin	40.4
Total resins	15
Proteins	15
Water	10
Ash	8
Tannins	4
Fats	3
Pectin	2
Sugars	2
Essential oils	0.5
Amino acids	0.1
Total	100

Hops determine, mostly, the bitterness, hoppy flavour, and foam stability of beer. The bitter taste comes from the conversion of α -acids (contained in the resin fraction) into iso- α -acids during the boiling of the wort. Iso- α -acids additionally support foam formation and in enough concentration (enough to give a low pH value) they provide anti-microbial properties that enhance the biological stability of beer, at least to a certain extent, as only gram-positive bacteria are susceptible (Priest & Campbell 2003).

1.1.7 Beer design considerations

1.1.7.1 Colour

Beer colour is measured by the ASBC in Standard Reference Method (SRM) units or in degrees Lovibond °L (which are equivalent), in the European system beer colour is expressed according to the European Brewing Convention (expressed as EBC units). SRM or EBC values are reported by maltsters and brewers can calculate the estimated beer colour using the following formula:

$$\text{Beer colour} = \frac{SRM_1 * m_1 + SRM_2 * m_2 + \dots + SRM_n * m_n}{V} \quad (\text{Dornbusch, 2010})$$

Where:

- *SRM* are the values of the malts that make up the grain bill
- *M* are the amounts of each malt in US pounds
- *V* is the amount of green beer in US gallons made from this grain bill

A formula to convert SRM values to EBC units is:

$$^{\circ}EBC = 1.98(SRM) \quad (\text{ASBC Beer-10, 2011})$$

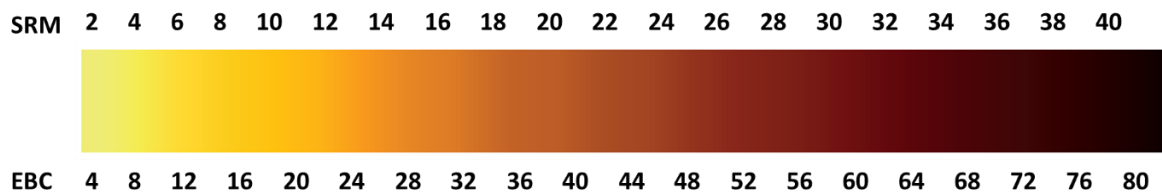


Figure 1.4 Beer's colour scale

1.1.7.2 Moisture Content

Moisture content (MC) is a measure of the malt quality, it shows it underwent a good malting and kilning process. Low moisture helps to avoid mould growth and the loss of flavour and aroma over time. Good quality malt ranges from 1.5% to 4%, anything over these range is considered poor quality. Brewers should take into account the MC to calculate the real extract potential of each batch or they may risk varying wort colour, density, and flavour.

1.1.7.3 Diastatic power

The diastatic power states the strength of the conversion enzymes in the malt, it is expressed in °Lintner (sometimes referred to as IOB) and as WK (Windisch-Kolbach units) in the EBC. A higher DP means higher protein content and thus more enzymes to reduce the starch. British pale ale malts generally have 35-45°Lintner, European lager malts around 100°Lintner, and American malts with high protein can go as high as 160°Lintner. The formula to convert WK to °Lintner is:

$$^{\circ}Lintner = \frac{(^{\circ}WK + 16)}{3.5}$$

These values are used to adjust conversion times of the mashing steps.

1.1.7.4 Protein content

Nitrogen content and protein content are usually interchangeable in the context of malting and brewing, each 1% of nitrogen is equal to 6.25% of protein. Protein values that exceed 12% indicate that the beer may haze too much or cause lautering problems, but are useful when a lot of adjuncts are used. Maltsters usually report both the total nitrogen and the soluble nitrogen, expressed as a

percentage of malt weight, these values can then be used to calculate the soluble nitrogen ratio (SNR %, also known as the Kolbach index) and this is a good measure of malt modification. It needs to be high enough to give the beer enough body, mouthfeel, to form stable beer foam, and to ensure that the lack of nitrogenous yeast nutrients does not limit fermentation. Malts used in infusion mashing have SNR values of 36-44. Undermodified malts tend not to perform well in a single infusion mash and are likely to produce thin beers, in these cases, by adding additional rests at lower temperatures, a better yield can be achieved.

1.1.7.5 Extract yield measurements

In order to measure the sugar content of wort (measure of fermentability) brewers can track it by measuring the specific gravity (SG). SG is an intensive property of a substance and it is the ratio of the density of that substance at the temperature under consideration to the density of water at a certain temperature (most commonly at 4°C but in a brewing context it is usually 20°C). SG, numerically is equal to the density (kg/L) but is denoted as a dimensionless number.

In the brewing industry the more typical scale to measure extract is °Plato, which is the percent solids (w/w) in unfermented wort. One degree Plato is approximately 0.004 SG and equals 1 g extract per 100 g wort. The formula to convert from °Plato to specific gravity is:

$$SG = \frac{^{\circ}Plato}{258.6 - \left[\left(\frac{^{\circ}Plato}{258.2} \right) * 227.1 \right]} + 1 \quad (\text{ASBC Approved Methods})$$

Extract yield can be reported in several ways, depending on whether the malt was tested on a coarse or fine grind (0.2-1.3 mm are the usual mill gap settings used), and whether it was done on a dry basis or as is. When the extract is reported as DBFG (dry basis fine grind) it indicates the maximum soluble yield possible for the malt adjusted for a uniform 0% moisture content, this can give the brewer a good idea of the quality of the grain itself. Alternatively, DBCG (dry basis coarse grind) can give a better indication of the degree of starch conversion that the grain can undergo during a typical brewhouse mashing. Extract yield can also be reported in liter degrees per kilogram units (L°/kg). L°/kg are in specific gravity and one unit means that 1 kg of the material will yield 1 L of wort with a SG of 1.001.

The ASBC provides a formula used to calculate the amount of extract required based on the desired SG of the wort and the weight of one barrel of water at 4°C.

$$\frac{(259 \frac{lbs}{bbl} + ^{\circ}Plato)(^{\circ}Plato)}{100} = lbs \text{ of extract/bbl} \quad (\text{ASBC Approved Methods})$$

Once the amount of extract needed is known, the brewer can calculate how much raw materials are needed. From the specifications sheet provided the brewer can know realistically how much can be extracted from the grain and adjust according to its MC if needed. To calculate the amount of extract required, the total volume of beer, the extract yield of the malt, and the MC of the malt are required and can be done using the following formula (Lewis and Young 1995):

$$\frac{\text{lbs of extract per bbl} \left(\frac{1 \text{ bbl}}{117 \text{ L}} \right) \left(\frac{0.454 \text{ kg}}{1 \text{ lb}} \right) (\text{volume of green wort per brew})}{(1 - MC)(DBCG)} = \text{theoretical mass of malt in kg/beer}$$

1.1.7.6 Efficiency

There are many different ways to measure efficiency in a Brewhouse, depending on where and when the amount of extract in the wort is measured. The efficiency is the comparative ratio of the extract recovered in the kettle (post-boil) against the maximum extract potential of the grain (obtained in laboratory mashes). No brewhouse is 100% efficient as there is always some amount of soluble mass that the mash is unable to extract (Palmer, 2006). The efficiency is a good measure of the effectiveness of the equipment and to see whether or not grain is being wasted.

$$\text{Brewhouse efficiency} = \frac{\text{After boil wort gravity}}{(\text{Mass of grain used})(\text{Boiler volume})(\text{Extract potential of grain})}$$

The efficiency figure will vary for each batch and depends on the type of wort and how well the equipment works. An average has to be taken along several batches and then it can be used to adjust the theoretical mass of malt needed.

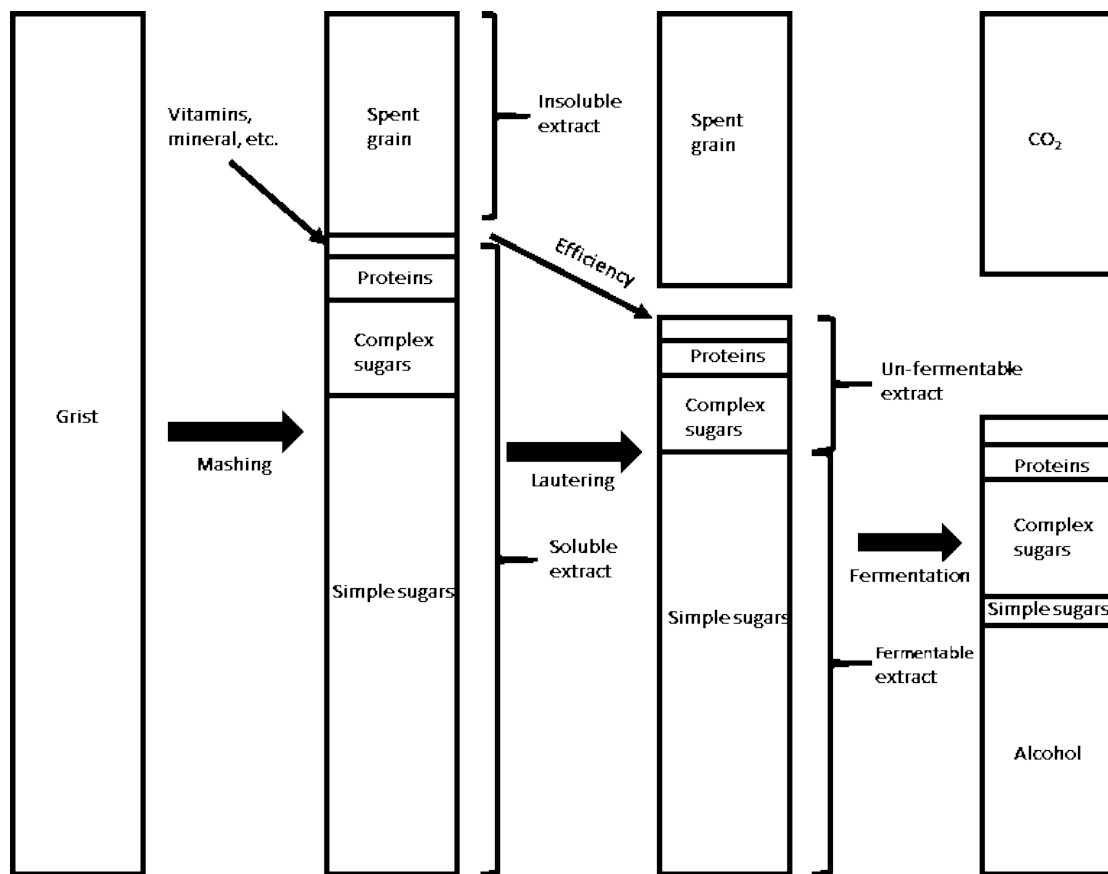


Figure 1.5 Visual diagram of the composition of wort along the brewing process (Adapted from (Palmer, 2006))

1.1.7.7 Hop Utilization

Bitterness is adjusted by international bitterness units (IBU), 1 IBU is equal to 1 mg of iso- α -acid/ 1 L of beer. The typical range found in beers is 10-50 IBU but exceptional beers with up to 100 IBUs are not unheard of. Brewers use a simple and practical formula to determine the amount of hops to use on each brew based on the α -acid content of hops and the percent of utilization of said hops. Hop utilization is defined as the ratio between the amount of iso- α -acids in beer and the amount of α -acids (non-isomerised) in hops used. When using hop cones, hop utilization rarely exceeds 40% but other hop products like pellets and isomerised extracts that enable higher rates of utilisation. Utilisation is a function of several factors such as: amount of extract in the wort, humulone solubility, and most importantly, wort boiling time.

$$\text{Weight of hops to be added} = \frac{(\text{Wort volume})(\text{Desired IBUs})}{(\% \text{ alpha acids in the hops})(\% \text{ utilization})} \quad (\text{Lewis and Young 1995})$$

Table 1.3 Hop Utilization percentage based on boiling time (Dornbusch, 2010)

<i>Minutes</i>	<i>%Utilization</i>
60+	30
55	29
50	28
45	27
40	25
35	23
30	21
25	19
20	17
15	14
10	10
5	6
0	0

1.1.7.8 Selection of yeast strain

In an active yeast data sheets, the specifications of interest to the brewer are:

- Apparent attenuation: It can be reported as high/medium/low or as a percentage (%), it indicates the degree to which a strain can consume the fermentable carbohydrates in the wort. Typical values are 65-85%. Attenuation can also be used to design beers based on desired relative dryness or sweetness of a beer; less attenuated beers are sweeter due to a less alcohol to unfermented extract ratio
- Fermentation temperature: It is the optimum fermentation temperature range, for ale yeasts it is normally 18-22°C and for lager yeasts 12-15°C
- Flocculation: It describes the tendency of yeast to aggregate into flocs and sediment out of the beer, clarifying it. It can be reported as low/medium/high.
- Alcohol tolerance: It is the concentration of alcohol at which the strain can survive. Most strains have a tolerance in the range of 9-12% ABV.

1.3 The complex nature of beer chemistry

Beer is a chemically complex beverage, comprised by many different chemical classes each of which can provide beer with various physical-chemical properties that can affect its quality. The quality of beer is most importantly dictated by its flavour (taste, aroma, and mouthfeel), by its colour, and by its ability to keep its properties through time, in other words its flavour stability. Beer is a complex mixture of volatile and non-volatile components whose formation and degradation mechanisms, their measurement, and control are a yet a challenge to fully understand.

Briefly, the most important types of reaction mechanisms involved in the formation and degradation of flavour compounds are:

- Maillard reaction and non-enzymatic browning
- Oxidation of polyphenols and reductones

- Strecker degradation
- Lipid oxidation
- Hydrolysis of precursors
- Enzymatic reactions
- Yeast metabolism

1.3.1 Vicinal diketones

Vicinal diketones (VDKs) are compounds that above a certain threshold produce stark off-flavours. Some of the more infamously well-known VDKs are 2,3-butanedione and 2,3-pentanedione that have a butterscotch and rubbery-sweet flavour (Hughes and Baxter 2001).

The precursors and mechanisms of formation and degradation of these compounds are well understood. Diacetyl (2,3-butanedione) is a product of the chemical oxidative decarboxylation of α -acetolactate and α -acetohydroxybutyrate, which are secreted by yeast into the extracellular environment when there is an excess during the biosynthetic metabolism of valine. Production of VDKs is unavoidable, however at the end of the main fermentation and maturation phase, VDK levels decrease due to the re-assimilation and reduction by yeast into acetoin and 2,3-butanediol, compounds that have higher flavour thresholds and thus negligible impact on flavour (Meilgaard, 1975a; Brányik *et al.*, 2008). Factors that can promote an excess and secretion of precursors are the yeast pitching and growth rate, amino acid content in wort, oxygen content in wort, and amino acid utilization rate (Verbelen *et al.*, 2009). By manipulating these factors, brewers can indirectly control the levels of these off-flavours.

1.3.2 Carbohydrates

1.3.2.1 Saccharides

Carbohydrates with less than four glycosil units are the main source of essential carbon to yeast and responsible for the sweetness in beer; medium sized carbohydrates are known as dextrans and are not generally consumed by yeast, they provide a richer mouthfeel and body to the finished beer. During the initial stages of the fermentation, yeast preferentially uses glucose and sucrose by downregulating the genes involved in the uptake of alternative carbon sources; as the fermentation progresses, and glucose and sucrose deplete, catabolic metabolism begins to occur and maltose and maltotriose begin to be assimilated (Cortacero-Ramírez *et al.*, 2003; Briggs *et al.*, 2004).

Carbohydrates have a varied relative sweetness so the composition and ratio of them will dictate the flavour profile directly and indirectly. Worts with a high ratio of glucose and sucrose tend to result in fermentations with a high concentration of acetate esters, which impart fruity and chemical flavour characteristics. This is undesirable for brewers and has to be considered when designing mashing

profiles. How carbohydrates are consumed is an important link between the composition of carbon source and the resulting flavour profile (Priest and Campbell, 2003; Hirst and Richter, 2016).

1.3.2.2 Cell Wall Polysaccharides

β -glucans are the main non-starch polysaccharides composed of glucose units that form a linear backbone linked by (1,3)(1,4)- β -glycosidic bonds, they constitute up to 70% of the barley endosperm cell wall and are bound to it by protein-polysaccharide and phenol-ester linkages. β -glucans modify the viscosity when dissolved in water in a process known as “gel formation” which in turn can have an effect on wort filtration and lautering, and ultimately affects extract yield and haze formation (Jin *et al.*, 2004). β -glucan levels in beer are influenced by malt quality, mash agitation, and the fineness of grists.

Arabinoxylan (AX) is another non-starch polysaccharide present in barley, it comprises 20% of the endosperm cell wall. AX is composed of two pentoses: xylose and arabinose. These two are arranged in a β -(1-4)-xylan backbone in which arabinose may be intercalated at the C2 and/or C3 position. Additionally, feruloyl and *p*-coumaroyl groups can be esterified to the arabinofuranosyl residues at the O5 position. AX is known source of phenolic compounds into beer (Vanbeneden, Van Roey, *et al.*, 2008).

It has been shown that AX is not readily degraded during the brewing process as β -glucan and can remain in beer. There have been claims that there are enough levels of AX in beer to provide the benefits of prebiotic material, but more research is necessary (Kanauchi, Ishikura and Bamforth, 2011).

Polysaccharides degradation during malting and brewing is divided in two stages: solubilisation and digestion. There are endogenous enzymes known as solubilases that attack the barley cell wall and enable hydrolysis of the polysaccharides into the medium, then glucanases and xylanases can digest the polysaccharides into oligosaccharides and monomeric units (Bamforth, 2010).

1.3.3 Fusel alcohols

Fusel alcohols are aliphatic and aromatic alcohols that impart subtle aromas which, when balanced appropriately, can provide an organoleptic fingerprint of specific fermented beverages. Fusel alcohols are products of amino acid catabolism via a pathway proposed in 1907 by Felix Ehrlich. Only the branched-chain amino acids valine, leucine, isoleucine, the sulphur-containing amino acid methionine, and the aromatic amino acids phenylalanine, tyrosine, and tryptophan are metabolised via de Ehrlich pathway. An irreversible transamination of the amino group results in an α -ketoacid that cannot be rerouted into central carbon metabolism, and before it can be excreted to the medium, yeast converts it into fusel alcohol or fusel acid. The amino group is then translocated into other structures, products of yeast metabolism (Hazelwood *et al.*, 2008; Hill and Stewart, 2019).

There are two paths of formation of the α -ketoacids: the Ehrlich pathway and an anabolic pathway that involves the *novo synthesis* of branched-chain amino acids from glucose (Eden *et al.*, 2001; Olaniran *et al.*, 2017).

Fusel alcohols are a source of flavour-active compounds. They can have desirable or undesirable organoleptic properties. In wine and cider, fusel alcohols have been described to have pungent, solvent-like aromas in high concentration, whereas in low concentration they can impart fruity characteristics. Propanol, butanol, and isobutanol have an alcoholic aroma, amyl alcohol and isoamyl alcohol have a marzipan-like or banana aroma (Hirst and Richter, 2016). Fusel alcohols are also an important intermediate in the synthesis pathway of acetate esters.

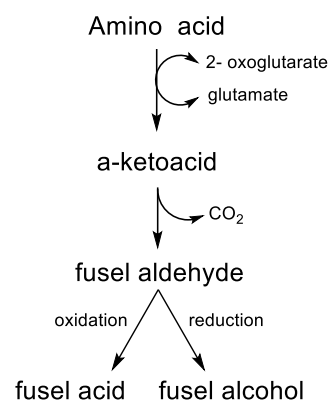


Figure 1.6 Simplified diagram of the Ehrlich pathway (adapted from (Hazelwood *et al.*, 2008))

1.3.4 Esters

Esters are one of the more volatile group of compounds that give flavour to beer (Saison *et al.*, 2009). Esters are formed by reactions between alcohols and acids during yeast fermentation; a fusel alcohol and a fatty acid react via catalysis of ester synthase. The final concentration of esters in beer is difficult to predict due to the many factors that affect their synthesis. Substrate availability is dictated by nitrogen and lipid metabolism within the yeast intracellular environment. The best characterised ester synthases are alcohol acetyl transferases I and II (EC 2.3.1.84), their activity is ruled by the corresponding genes, which are dependent on the fermentation conditions (FAN, oxygen, sugar, and lipid content in wort; temperature and fermenter design). Thus, brewers have a variety of options to control ester production (Verstrepen *et al.*, 2003).

The most abundant ester is ethyl acetate (due to acetyl CoA and ethanol as precursors) but the most contributor to flavour is iso-amyl acetate (Priest and Campbell, 2003). Esters commonly give beer fruity attributes such as banana, apple, cider, roses, tropical fruit, and others (Meilgaard, 1975a).

1.3.5 Aldehydes

These are volatile compounds formed during the processing of malt and by yeast metabolism. Aldehydes play an important role to the odour and aroma of beer, especially during ageing. Aldehydes have been identified to be responsible for green, grassy, pea-like flavours in malt kilned at low temperatures. Additionally, aldehydes can be formed during storage resulting in stale off-flavours. Aldehydes in beer can be classified into three types: Strecker aldehydes, Maillard aldehydes, and unsaturated fatty acid oxidation aldehydes (Rossi *et al.*, 2014).

1.3.5.1 Oxidation of Fatty Acids

Barley lipids are oxidised during germination to intermediate hydroperoxides by action of several mechanisms, the hydroperoxides are then broken down to flavour-active aldehydes during subsequent processing stages (malt kilting, mashing, boiling, fermentation, beer storage).

Specifically, linolenic (C18:3), linoleic (C18:2), and oleic (C18:1) acid are the precursors with higher susceptibility to oxidation (in that order) to hydroperoxy fatty acids. These three fatty acids make up 70% of the fatty acid content in malt (Kobayashi *et al.*, 1994).

During wort production, unsaturated fatty acids can go through autoxidation due to the high temperature and the presence of oxygen. If reductases are active, the aldehydes will be reduced into their corresponding alcohols as well (Moir, 1992). The particular flavour profile of a food that has the same type of enzymatic oxidation reactions is determined by the set of lipoxygenases and the resultant variety of aldehydes.

One of the more prominent aldehydes is (E)-2-nonal, a major off-flavour with a cardboard and papery flavour description and is a product of beer staling. Aged flavours are caused by a myriad of compounds and their formation pathways and control measures are still a major research area (Vanderhaegen *et al.*, 2006).

The amount of aldehydes in malts gets progressively smaller as malt is kilned at higher temperatures. Green malt and pale malt contain the highest amount and variety of aldehydes, then they are found in smaller quantities in caramelised and roasted malts. This can be explained by the inactivation of lipoxygenases at high temperatures. The exception is hexanal and 2,4-decadienal oxidation of lipid precursors by lipoxygenases during the malting (germination stage).

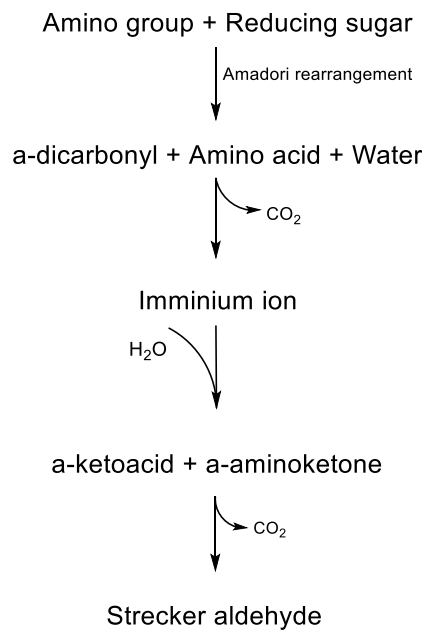


Figure 1.8 Simplified diagram of the Strecker degradation

1.3.6 Nitrogenous compounds

Nitrogenous compounds in wort include amino acids, ammonium ions, di- and tripeptides, and proteins. Assimilable nitrogen is known as free amino nitrogen (FAN). For a typical fermentation 100-140 mg of FAN/L is the minimum content required to achieve complete attenuation, however levels up to the 200-250 mg FAN/L are recommended as optimal to achieve a healthy growth phase. Nitrogenous compounds have a crucial indirect relationship to the flavour profile of the final beer. The majority of the FAN content is generated during the malting of barley, however some endoproteases in malt remain active after kilning and can be activated during the mashing. Mashing regimes of 40-50°C favour the activity of these endoproteases and can further increase the FAN content in wort (Hill and Stewart, 2019).

FAN composition and total content in wort have a direct correlation with the formation of VDKs, esters, fusel alcohols, sulphur compounds, and Maillard reaction products. Excess FAN levels can also have a detrimental effect during fermentation such as undesirable levels of diacetyl and fusel alcohols (Lodolo *et al.*, 2008).

Amino acids are classified according to the sequential manner by which they are assimilated and utilised by yeast.

Table 1.4 Amino acid classification according to their yeast uptake pattern in brewery conditions (Jones and Pierce, 1964)

<i>Group A</i> <i>Fast uptake</i>	<i>Group B</i> <i>Intermediate uptake</i>	<i>Group C</i> <i>Slow uptake</i>	<i>Group D</i> <i>Little or no uptake</i>
Glutamic acid	Valine	Alanine	Proline
Aspartic acid	Histidine	Glycine	
Asparagine	Methionine	Ammonia	
Glutamine	Isoleucine	Tryptophan	
Serine	Leucine	Phenylalanine	
Threonine		Tyrosine	
Lysine			
Arginine			

1.3.7 Sulphur compounds

The main sulphur compounds that impact beer flavour: sulphur dioxide, hydrogen sulphide, dimethyl sulphide, and mercaptan; but there are a range of different categories of sulphur compounds in beer. Most have low flavour thresholds and thus can have a high impact on the flavour profile of beer.

Hydrogen sulphide and sulphur dioxide influence the metabolism of sulphur-containing amino acids (cysteine and methionine), coenzymes (CoA, biotin, thiamine), and other cellular metabolites.

Dimethyl sulphide (DMS) is the main volatile sulphur compound derived from malt, its source is the thermal degradation of *S*-methylmethionine (SMM) which itself forms during malting (germination). DMS can be desirable or undesirable flavour characteristics depending on the style and brand; it provides a cooked vegetable and sulphur flavour; it has a high volatility and so its presence in beer can be controlled by ensuring a vigorous boiling, a healthy fermentation (due to purging by CO₂), and good quality raw materials.

1.3.8 Phenolic compounds

Phenolic compounds are chemical substances with at least one phenol unit. Phenols can be present in monomeric or polymeric forms. The phenol compounds identified in beer's ingredients can be divided in three sub-classes: phenolic acids, flavonoids, and stilbenes, the majority of them still uncharacterised (Briggs, 1998). Up to 80% of the polyphenols in beer can be derived from malt and the other 20% from hops (Aron and Shellhammer, 2010).

Benzoic, cinnamic acids and derivatives can be found as glycosides or other bound forms in malt and hops, and partially remain the brewing process all the way into beer. Along the malting, mashing, and fermentation these compounds are broken down from their combined forms or from the cell wall constituents. They can become soluble by water extraction during the mashing or by enzymatic action

during the mashing by cinnamoyl esterase and arabinoxylan (AX) hydrolases (e.g. xylanase, arabinofuranosidase, and xylosidase) (Debyser, Derdelinckx and Delcour, 1997; Briggs *et al.*, 2004; Vanbeneden, Gils, *et al.*, 2008; Callemien and Collin, 2009).

Most of them have high threshold values and do not significantly affect beer's aroma or taste, but as they are broken down into smaller more volatile compounds, these can have a greater impact in the flavour, being described as giving beer a "phenolic-like" or "solvent" taste (Vanbeneden, Gils, *et al.*, 2008). They also have an effect on the colloidal stability of beer, haze formation, and provide antioxidant properties to beer by preventing the oxidation of precursors to known off-flavour (aldehydes, VDKs, etc.). Specifically, *p*-coumaric acid and ferulic acid can be transformed into the highly volatile flavour-active phenols 4-vinylphenol and 4-vinylguaicol (Iyuke *et al.*, 2008). 4VG is produced by yeast by the decarboxylation of ferulic acid by a decarboxylase encoded in the FDC1 gene and requires the cofactor produced by the Pad1 gene, encoded in the subtelomeric region of the right arm of chromosome 4 (Gallone *et al.*, 2018); it can also be decarboxylated by thermal impact during wort boiling. Even though it is known what yeast strains are capable of enzymatic decarboxylation of phenolic compounds, brewers still experience considerable variations in final phenolic content in identical production batches, indicating a knowledge gap of how the volatile phenolic compounds are being released into the wort and beer (Vanbeneden, Van Roey, *et al.*, 2008).

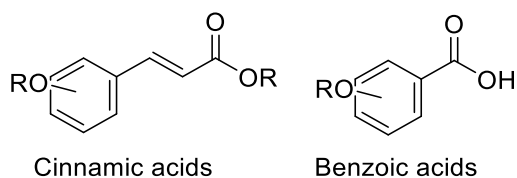


Figure 1.9 General structure of phenolic acids

1.3.9 Compounds derived from the Maillard reaction

The Maillard reaction are all the possible reactions that occur after an amine group reacts with a reducing sugar, specifically an aldose, either a hexose or pentose. These reactions are also known as "non-enzymatic browning reactions" and are the most important reactions in the cooking process of foodstuff that give rise to myriad flavour-active compounds with various chemical properties. These reactions start to occur at 50°C and pH 4-7 (Baert *et al.*, 2012).

The reaction starts with the nucleophilic condensation of an amino group and the carbonyl group in the reducing carbohydrate which yields a Schiff base (an unstable imine) which then undergoes a spontaneous conformational change known as the Amadori rearrangement (favoured by temperature) and converts into the Amadori product. The intermediate stage of the Maillard reaction comprises the fragmentation of the carbohydrate into a diverse range of products and the release of

the amino group. The final stages of the reaction involve the reintegration of amino compounds either by dehydration, fission, cyclization or polymerization and the formation of a variety of heterocyclic products with flavour-active properties. It is important to mention that due the complex factors that dictate the rate and direction of the reaction (initial reactants, temperature, pH, moisture content) the mechanisms involved in the Maillard reaction are still disputed.

Furfural and 5-hydroxymethylfurfural (5-HMF) are quantitatively the most important heterocyclic aldehydes in beer; furfural is derived from a pentose and 5-HMF from a hexose. They are synthesised during the boiling stage of the mashing process; and their concentration is indicative of the heat load the wort was subjected. The reductones produced during the Maillard reaction are involved in the Strecker degradation (explained in more detail in section 1.3.5.2 Strecker degradation) which yields aldehydes and can also lead to the formation of heterocyclic products and brown nitrogenous polymers known as melanoidins.

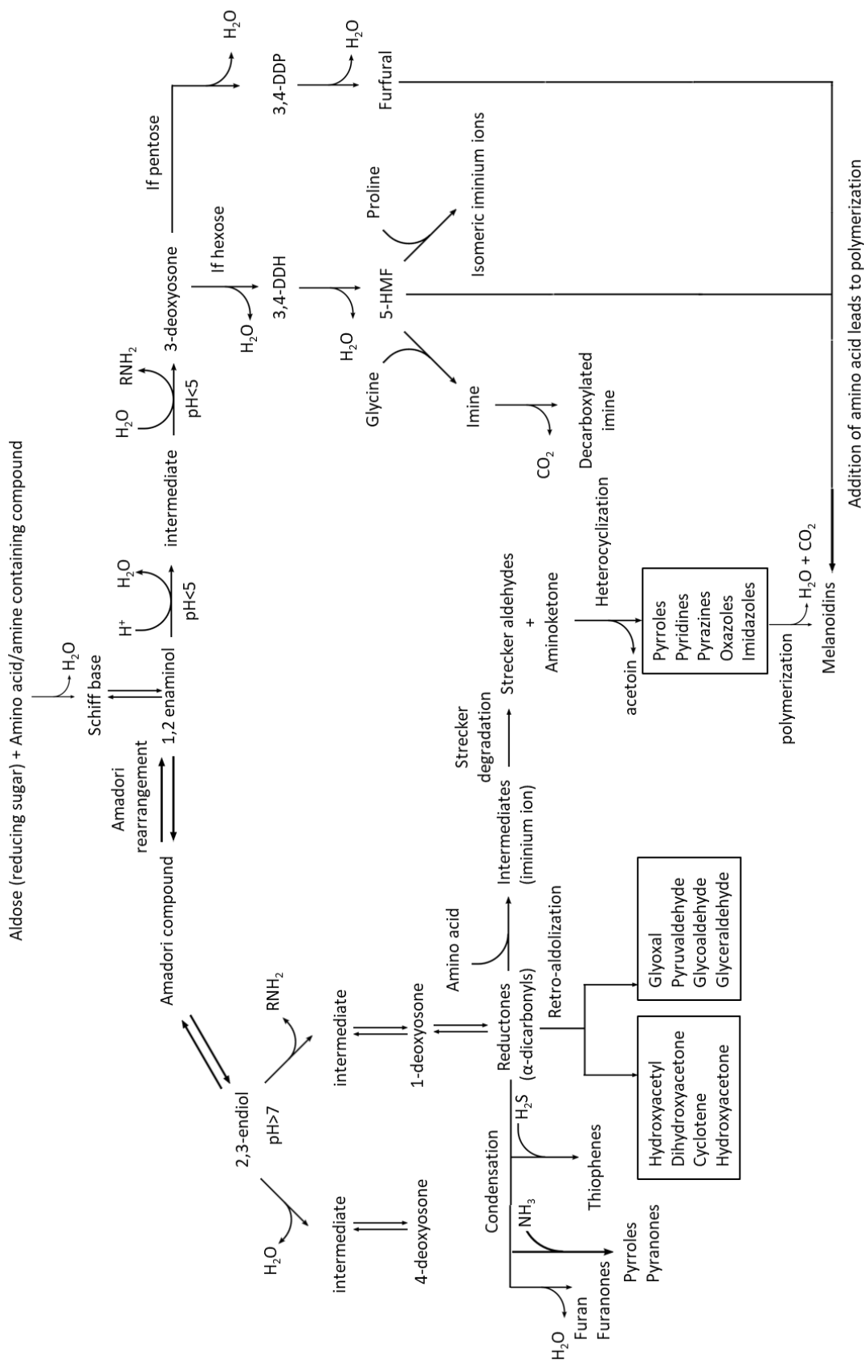


Figure 1.10 Overview scheme of the Maillard reaction and its products, adapted from (van Boekel, 2006; Baert et al., 2012)

1.4 Mass Spectrometry for beer analysis

The ASBC has a compendium of standard methods of analysis for various quality markers for raw ingredients, wort, finished beer, sensory analysis, and even adjunct materials. A vast range of techniques are used in the ASBC standard methods: gravimetric and volumetric methods, spectrophotometry, acidic hydrolysis, enzymatic methods, liquid, and gas chromatography, etc. The intention of these methods is to provide a reliable reference for the brewing industry and enable brewers to track quality markers with a common language.

The ASBC standard methods are extremely useful in the case of measuring specific parameters and very well-known compounds that affect quality in a certain way. But the greater challenge of flavour analysis resides in the vast number, complexity, and interrelated nature of compounds found in beer. To analyse a wide range of flavour compounds simultaneously, new trends of flavour compound analysis have emerged with the rise of the “-omics” fields that can be used to deal with the large quantities of data generated. Coupling high resolution analytical techniques with powerful separation methods and the automatization of sampling methods have enabled the deep analysis of organic samples in fields of biology and food science.

1.3.4 Principles of mass spectrometry

The basic goal of mass spectrometry (MS) is to generate charged particles (ions) from a sample, separate them, and detect them based on their mass-to-charge ratio (m/z); differences in the m/z detected and its relative abundance can yield valuable quantitative and qualitative information of the sample's composition. A mass spectrometer is composed of three main parts: ion source, mass analyser, and detector; the parts' function are ion production, ion separation, and ion detection respectively and can operate under vacuum conditions.

There are many ionisation methods and sources that take advantage of different operating principles; in general, ionisation methods are classified as hard or soft. Hard ionisation methods are characterised by fragmenting the sample's analytes into a spectra of charge particles. In contrast, soft ionisation methods are characterised by leaving the sample's analytes relatively intact. Soft ionisation methods have enabled widespread use of MS in the biological sciences. In this project two ionisation methods were used: electrospray ionisation (ESI) and matrix-assisted laser desorption ionisation (MALDI).

Electrospray ionisation is commonly used to detect large, non-volatile, chargeable organic molecules; however, it is still very effective at detecting small polar molecules. It is considered a very soft ionisation method that allows the transfer of ions from solution to a gas phase; it can be used to analyse extremely small sample volumes diluted in a solvent. In this method, the goal is to form a mist

with electrically charged droplets small enough to overcome surface tension interactions with electrostatic repulsion which then tears the droplets apart, this occurs repeatedly forming smaller and smaller particles which eventually form isolated gas phase ions. In ESI, mist formation occurs at atmospheric pressure, and can be implemented with virtually any standard solvent, and can be easily coupled to liquid chromatography, these are key features that have made it a highly popular method (Gross, 2017). ESI-MS tends to produce multiple-charged ions which helps extending the mass range of the analysis. One major limitation of ESI-MS is that molecular structural information cannot be obtained from the resulting mass spectrum.

In ESI the sample is pumped at a low flow rate through a capillary at atmospheric pressure until it reaches the end of the capillary tube; then the sample forms a meniscus, and the mist is formed by action of the electrostatic field. The charged aerosol is then passed to the mass analyser by means of a differential pumped interface. There are many design layouts and configurations for these basic principles; sprays can be introduced at various angles and/or redirected by pumps in a way to deliver a “cleaner” sample into the analyser; also, while the ESI occurs at atmospheric pressure, the mass analyser is at a vacuum and to prevent freezing of the sample during the transition, heat must be applied either at the capillary or by a heated counter current inert gas stream, usually nitrogen or helium.

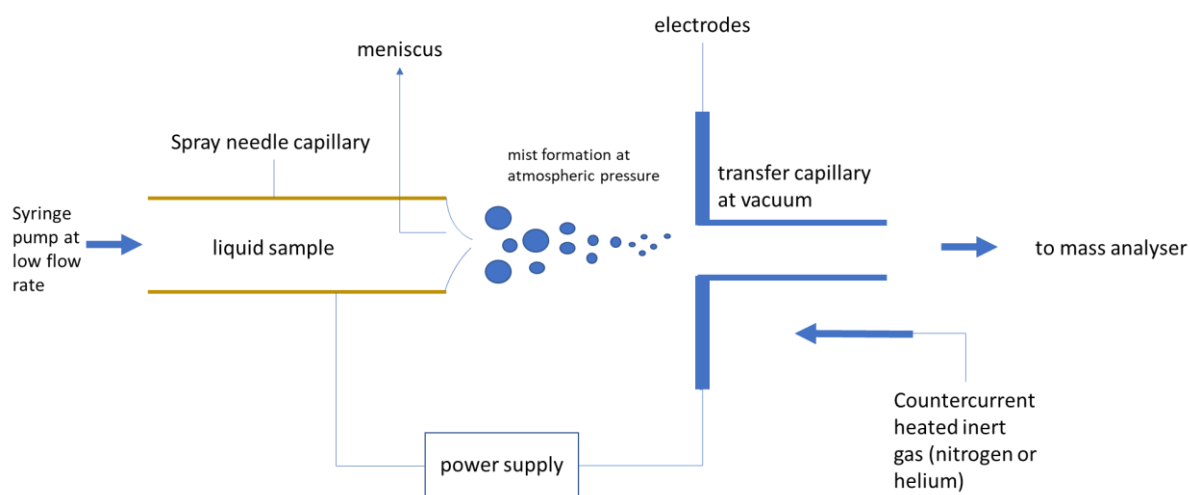


Figure 11.11 Simplified diagram of the operating principles during ESI

There are two main ionisation mechanisms proposed for ESI: the ion evaporation model (IEM) and the charge residue model (CRM). Low molecular weight compounds are thought to follow the IEM. Low molecular weight analytes are typically protonated due to the sample’s own low pH or assisted by the addition of an organic acid, IEM is based on the theory that the electric field imposed

on a small enough droplet can be strong enough to cause the ejection of the charged analyte from inside the droplet by overcoming interactions with the droplet's surface and releasing the analyte into the gas phase, ready to be analysed by the detector. Whereas high molecular weight compounds such as proteins follow the CRM model. The CRM model says the charged analyte is released into the gas phase by the result of the evaporation of the solvent from the droplet's surface towards inside the droplet, shrinking until only the charged analyte is left (Konermann *et al.*, 2013).

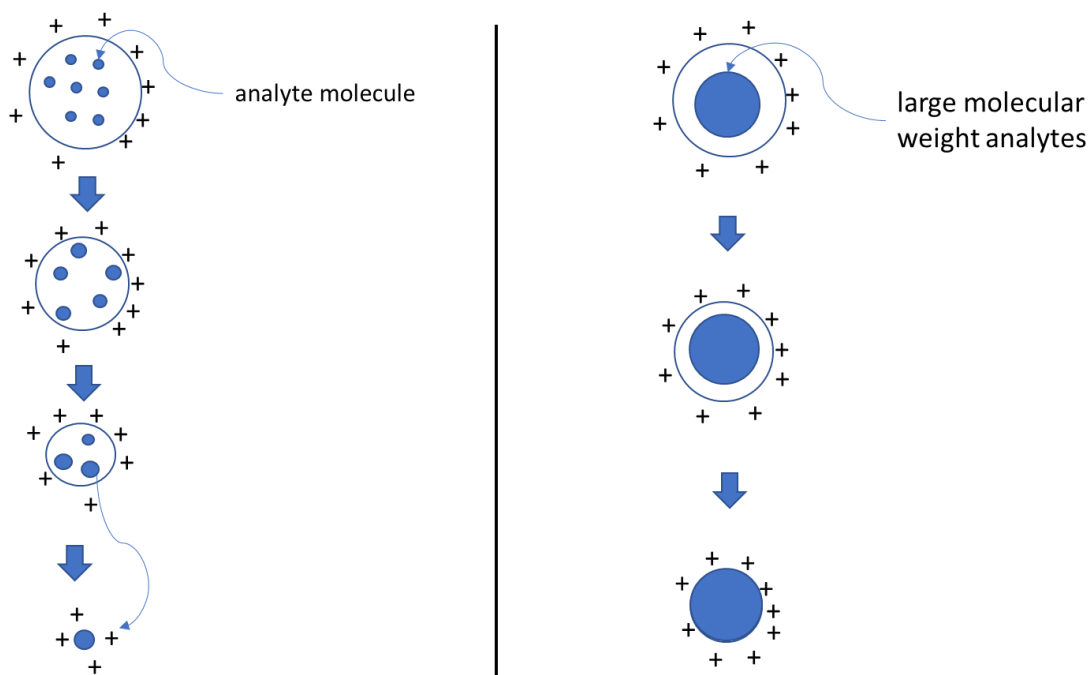


Figure 12 The two main ionisation mechanisms during ESI: IEM model showing how analyte molecule is ripped from within the charged nanodroplet by the electrostatic forces (left); CRM model showing the nanodroplet's surface evaporates until only the charged analyte is left.

It is important to say that ESI is not really an ionising method, the ions are already present in the sample and ESI delivers them into the gas phase and makes them available for detection. In reality ESI is an ionising interface method (Kandiah and Urban, 2013).

Matrix-assisted laser desorption ionization (MALDI) basic principles of operation and mechanisms are explained in Chapter 3.

1.4.1 Extraction methods

Sample preparation methods can be crucial in determining the success of any quantitative or qualitative analysis.

Gas chromatography (GC) methods require special methods of sampling and extraction to isolate the volatile compounds. Headspace sampling (HS) has been widely used to target volatile aroma compounds. HS is commonly coupled with solid-phase extraction (SPE), solid-phase microextraction

(SPME), stir bar sorptive extraction (SBSE), and derivatization (Andrés-Iglesias *et al.*, 2015). Out of these, SPME has become the most popular due to the fact that it has the advantages of simplicity, rapidity, solvent elimination, high sensitivity (capable of detecting ppb levels), high reproducibility, requires a small sample volume, lower cost, and can be automated (Cortacero-Ramírez *et al.*, 2003; Silva, Augusto and Poppi, 2008; Tian, 2010). Some of the disadvantages of using SPME are that the fibre is fragile, and volatility of analytes may vary so some derivatization may still be needed.

To target a wide range of non-volatile compounds, liquid-liquid extraction is the method of choice. By using solvents, polar and non-polar analytes will separate into phases based on their solubility. This method of extraction has the disadvantages of being time-consuming and environmentally unfriendly.

1.4.2 Chromatographic methods

Gas chromatography coupled to a flame ionization detector (GC-FID) or a mass spectrometer (GC-MS) are currently the most widely used methods to analyse volatile flavour compounds in beer. Another popular method to detect aroma compounds is GC-Olfactometry (GC-O), although some authors claim it is not enough to identify key compounds that explain the hoppy aroma character in beer. GC based methods are capable of separating and measuring ethers, esters, organic acids, aldehydes, ketones, alcohols, sulphur compounds, hydrocarbons, and aromatic compounds simultaneously (Bernotienė *et al.*, 2004; Sterckx, Saison and Delvaux, 2010).

There are many studies applying SPME-GC-MS to characterize the volatile profile and differentiate between: bottom and top fermenting yeasts (Rossi *et al.*, 2014); alcoholic and non-alcoholic beers (Andrés-Iglesias *et al.*, 2014); beer and its raw materials (Gonçalves *et al.*, 2014).

Electrospray ionization mass spectrometry (ESI-MS) has been used to analyse different types of beers and has proven to be a promising method for beer quality control (Araújo *et al.*, 2005; Almeida *et al.*, 2006). Several studies on the profiling and tracking of select metabolites that are representative of beer aging have been done by the research group of the Colorado State University (Heuberger *et al.*, 2012); their findings have shown that the purine 5-methylthioadenosine (5-MTA) plays an important role in the stability of beer flavour (Heuberger *et al.*, 2016).

1.4.3 Metabolomics approach

“The metabolome is formally defined as the collection of all small molecule metabolites or chemicals that can be found in a cell, organ or organism” (Fiehn, 2002). It includes exogenous and endogenous species ingested or synthesized. It is the study of every compound present in the biological sample. The small molecule aspect refers to anything <1500 Da. The complexity of the

metabolome can quickly rise when cell type, tissue, and environmental conditions can greatly alter its composition. It is important to report experimental conditions as exactly as possible. The main goal of metabolomics is to formulate knowledge from the features or patterns obtained from the data.

There are two approaches for generating metabolic data (Wishart, 2008):

- Chemometric approach/untargeted profiling – samples are analysed and their spectral patterns and intensities are recorded, then they are statistically compared and used to reveal the spectral features that distinguish sample classes. These statistical comparisons and feature identification techniques usually involve unsupervised clustering and/or supervised classification, allows an unbiased analysis.
- Quantitative metabolomics/targeted profiling approach – the focus is to identify or quantify as many compounds in the sample as possible. This is done by comparing the sample's NMR or MS spectrum to a spectral reference library obtained from pure compounds. Once the constituent compounds are identified and quantified, the data can then be processed to identify important biomarkers or informative metabolomics pathways. Depending on objectives and instrumental capacity, quantitative metabolomics may be either targeted (selective to certain classes of compounds) or comprehensive (covering all or almost all detectable metabolites).

Both approaches have their advantages and disadvantages, but depending on the analytical method used, metabolomics-based studies can allow the simultaneous characterization of large numbers of chemicals in biological sample matrices. Targeted profiling can take a considerable amount of time because the identification of compounds is, in most cases, a manual process.

1.4.3.1 Multivariate statistical analysis

Multivariate analysis (MVA) is an important tool used in metabolomics. For unsupervised clustering principal component analysis (PCA) is used. PCA is a statistical technique used to transfer a data space of high dimension into a featured space of lower dimension while retaining the most significant features, this allows to visually assess the data and find patterns within the data set. Other advantages of dimensionally reducing the data are that the data can be manipulated more easily, and the data is compressed so it can be stored in less space. This technique is useful when many variables are associated with a sample. PCA will find axis (components) that will explain most of the variability in the data set where these axes are completely orthogonal from each other.

Afterwards, a supervised classification must be done to find out in a more objective manner how much difference there is between the patterns or sample clusters identified by the PCA. Partial least squares discriminant analysis (PLS-DA) is an algorithm commonly used in the pre-processing stages for

the classification of sample classes (Barker and Rayens, 2003; Brereton and Lloyd, 2014). The discriminant analysis will help revealing the variables that are driving the separation between the clusters. While the unsupervised approach allows for an unbiased projection of the data set, the supervised approach requires the input of class information provided by the user to guide the algorithm into maximum separation. That is why the PCA needs to be done and interpreted beforehand. Score plots can be extracted from the model that will tell us which variables have the largest discriminatory power. Once the variables with the most significant discriminatory power are identified, inferences and hypothesis can be formulated.

There are countless approaches that can be done using metabolomics techniques, and each study has its own aim. Traditionally, GC-MS has been the gold standard to analyse beer and profile its small molecule composition. Now, numerous studies have been published using modern approaches and workflows (Heuberger *et al.*, 2012; Broeckling *et al.*, 2014; Vivian *et al.*, 2016; Bettenhausen *et al.*, 2018). There is no clear standard way of approaching the study of beer, each study uses a different combination of preparation methods, analytical method, and data processing methods. Depending on the aim of the study and the experimental design used the resulting metabolome can vary.

In this project, three different MS methods were used to analyse beer. MALDI-MS and DI-ESI-MS were compared first; their main difference being the ionisation method and the sample preparation involved. And lastly UPLC-MS was used, which is the same ionisation method as DI-ESI-MS but is now coupled to a separation method before the analysis; this technique was used in hopes of being able to use state of the art data processing algorithms which results can be easily imported into metabolic pathway databases.

1.4 Thesis aims

Firstly, a brewing process will be designed and standardised based on brewing practices used in Sheffield, UK. The brew will be analysed using the ASBC standard methods of analysis and samples will be taken at key stages of the brewing process. Additionally, a flavour and metabolome database of beer and its ingredients will be developed.

In chapter 3 MALDI-MS and DI-MS will be used to analyse the brewing samples. A metabolomics workflow will be applied to the data generated. What compounds are identified using an untargeted approach using an optimised method for small molecules found in wort and beer?

In chapter 4 UPLC-MS will be used to analyse the brewing samples. A metabolomics workflow will be applied to the data generated. Metabolites in liquid form will be targeted and identified.

The objective of this thesis is to develop and implement an analytical approach using mass spectrometric techniques and a metabolomics workflow to analyse beer's complex chemical composition, this can lead to a better understanding of how flavour arises in beer. In this thesis it has been chosen to exclude the influence of hop derived flavour to avoid the added complexity in the analysis.

2. Chapter 2: Development of a brewing process and sampling method for metabolomics analysis

2.1 Introduction

For centuries, much like many other food preparations, brewing has been considered a specialised craft almost hold to the same level as making art. Brewers have created a distinct identity separate from conventional academia, perhaps because of fears of demystifying some of the practical knowledge they have acquired of their craft for years. Long-lasting institutions have a tendency of adopting new technology at a slow pace, and sometimes only when the market pressure is so overwhelming that there is no other choice if they want to continue existing.

The newly emergent market for craft brewing calls for a deeper understanding of the mechanisms that rule the formation of flavour in beer. While brewers can in practice control the characteristics of their product in general terms, it is by using techniques that are questionable in terms of fundamental operating principles. A clear example is the method by which brewers utilise the hops. The amount of hops to be used is a function of the alpha-acid content (alpha-acid being the main precursor of bittering compounds in beer) and the boiling time. The boiling time then dictates the degree of “utilization” which must be based in infusion rate (from the hop to the wort) and conversion rate (thermal isomerisation), but in the scientific literature there is no mention of the correlation between them. Ultimately, while brewers do have in appearance extensive theoretical guidance, brewers assess the quality of their products by means of experience, pragmatism, and their own subjective tastes.

Although hops have had a big influence on the rise of the craft industry, there are countless brewers that stand by the fact that malt is the real backbone of beer’s flavour (Briggs *et al.*, 2004). And although the use of base malt is already controlled in brewing it is done based on the total amount of extraction of mass possible into the wort. This extraction comes with hundreds of compounds each of which may have different implications to the final beer quality. Only when using specialty malts are the flavour characteristics of the grain taken into consideration even though base malt also carries many relevant flavour compounds.

The complex nature of beer’s chemistry has already been described and it calls for a science-based approach that can tackle the challenge at hand. Currently the main analytical methods used to assess specific compounds in beer are focused on avoiding off-flavour or undesired descriptors. These methods make sense from a quality control perspective. However, in the future it would be greatly desired to have analytical methods that can measure desired or favourable flavour in beer. The easiest way would be for a specific flavour descriptor to come from a single compound, but the reality is much

more complicated. This why a metabolomics-based approach makes sense as a first approach, as it allows us to analyse a complicated matrix and represent chemometric profiles in visually meaningful ways. These tests can open up research areas that can be further studied to pinpoint key compounds which can then be targeted with specific analytical techniques and where infusion and reaction rate models can be developed to accurately predict flavour characteristics in beer.

Maris Otter is a two-row variety of barley popularly used by craft brewers. At the beginning of this research some breweries were visited in the area of Sheffield to talk to the brewers about their practices. It was noted that most of the brewers used the Maris Otter variety for their craft ales. Maris Otter is praised for its low nitrogen content, flavour, and suitability for brewing. By now, it has earned its status as a heritage variety and recently celebrated its 50th harvest. It has been selected in this study as a sample in order to find a possible explanation for its characteristically praised flavour (*Malting Barley Characteristics for Craft Brewers*, 2014; Herb *et al.*, 2017).

A mashing regime will be designed based on a standard method and will be used in subsequent methods to evaluate the extractable malt chemical profile.

The purpose of this chapter is to develop a consistent brewing method, starting from the milling of the malted grain, followed by a customised mashing regime, and ending with a controlled fermentation. The brew will be characterised by traditional brewing methods and its physical chemical parameters measured to assess its consistency and reproducibility. Also, samples will be taken at key points of the process, points in time where the brewing theory dictates that a change in wort and/or beer composition is supposed to happen. The samples will then be suitably stored for subsequent technical analysis.

2.2 Materials and methods

2.2.1 Brewing

Brewing practices were chosen with the objective of getting small samples (1 mL) at key stages thought to be crucial in flavour development in a practical and easy way. The equipment used allowed for easy manipulation of the brewing stages and also for multiple batches to be produced at the same time. An important consideration was to get a consistent brew and a good quality samples for analysis. The following procedure was established as the most consistent and convenient to obtain the brewing samples.

Standardization of the mill setting was done according to (ASBC Malt-4). 50 g of malt were weighed to the nearest single kernel and then milled through a previously cleaned mill. After grinding the remains on the rollers were brushed clean and added to the milled grain. The ground malt was

then put into the top sieve (largest mesh size) stacked on a column of standard sieves of several mesh sizes ranging from 4 mm to 200 μm . The sieves were then mechanically shaken for exactly 3 minutes. Afterwards the grist remaining on each pan was weighed, depending on the amount found at a certain particle size the grind is classified as fine or coarse.

Sample wort was obtained through a modified version of the ASBC hot steep malt evaluation method (ASBC sensoryanalysis-4). The mashing profile was designed to obtain wort with a variety of fermentable carbohydrates by targeting the optimum temperature range of β -amylase and α -amylase. The experimental brew was unhopped to focus on the malt's metabolite profile. 80 g of Simpson's Pale Ale Maris Otter base malt was ground in a gristmill with an aluminium unibody and stainless steel roller manufactured by Millar's Mills™. Then the malt was put inside a fine nylon bag and placed in a 1L stainless steel insulated container and 500 mL of 67°C drinking water poured in. The container was capped and shaken vigorously for 20 seconds. The mixture was left for the first mashing step of 30 min, after which the temperature was measured at 64°C. The resulting wort was poured into a beaker, heated to 75°C, poured back into the insulated container, capped, shaken, and left 15 min for the second mashing step; at the end the temperature of the wort was measured at 72°C. The procedure was repeated by heating the wort to 81°C, mash for 10 min, and measuring temperature at the end at 78°C. Finally, the wort was boiled for 60 min and cooled to 24°C, transferred to a 500 ml glass media bottle adapted with a bung hole and an airlock and pitched with 350 mg of dry yeast Safale S-04 and fermented in a controlled temperature room at 21°C for 14 days. This procedure was done three times.

1 mL samples were taken using a 1 mL micropipette, wort samples were stored as is and fermented samples were centrifuged at 4000 rpm for 5 min to remove suspended yeast. Samples were taken at the end of each mashing step and labelled M64, M72, M78, MB and then stored at -80°C. Throughout the fermentation samples were taken each day up until the fifth day and then one at the fourteenth day and labelled F1, F2, F3, F4, F5, and F14. A diagram of the mashing profile and sampling points is shown in Figure 2.2. Samples that required analysis for physical-chemical parameters was done the same day in triplicates after sampling. MS samples were stored at -80°C until needed.

Physical-chemical parameters of the brewing sample were measured according to the ASBC Standard Methods of Analysis. Specifically: alcohol, real extract, colour, pH, and specific gravity were measured by methods (ASBC beer-4a, beer-5a, beer-10a, beer-9, and beer-2a) respectively. Cell concentration and viability was analysed according to (ASBC yeast-4).

SG was measured using a 25 mL Gay-Lussac pycnometer from BLAUBRAND® calibrated to a measured volume of 25.112 cm^3 . This pycnometer was used to measure the weight of 25.112 mL

samples in order to calculate density and then obtain SG by comparing against the density of distilled water calculated by measuring its weight in the same pycnometer at 20°C. SG was calculated using the formula:

$$SG = \frac{\rho_{sample}}{\rho_{distilled\ water}}$$

Alcohol by weight measurements of the fermented samples were measured by distillation following (ASBC beer-4a). The method in detail is the following: 150 mL of fermented samples were degassed and attemperated in a temperature controlled ultrasonic water bath to 20°C, then the SG was measured using the pycnometer. 100 mL of fermented sample were poured into a distilling flask and collocated in the distilling apparatus shown in Figure 2.1. The sample was distilled into a receiving flask for 1 hr until approximately 90 mL of distillate were collected to ensure all alcohol was distilled. The distillate attemperated to 20°C and topped up to a total of 100 mL. The SG of the distillate and of the dealcoholized beer were measured using the pycnometer. Then, using the Tables Related to Determinations on Wort, Beer, and Brewing Sugars and Syrups (ASBC Technical Committee, 2011g) the alcohol by volume and alcohol by weight percentages were obtained.

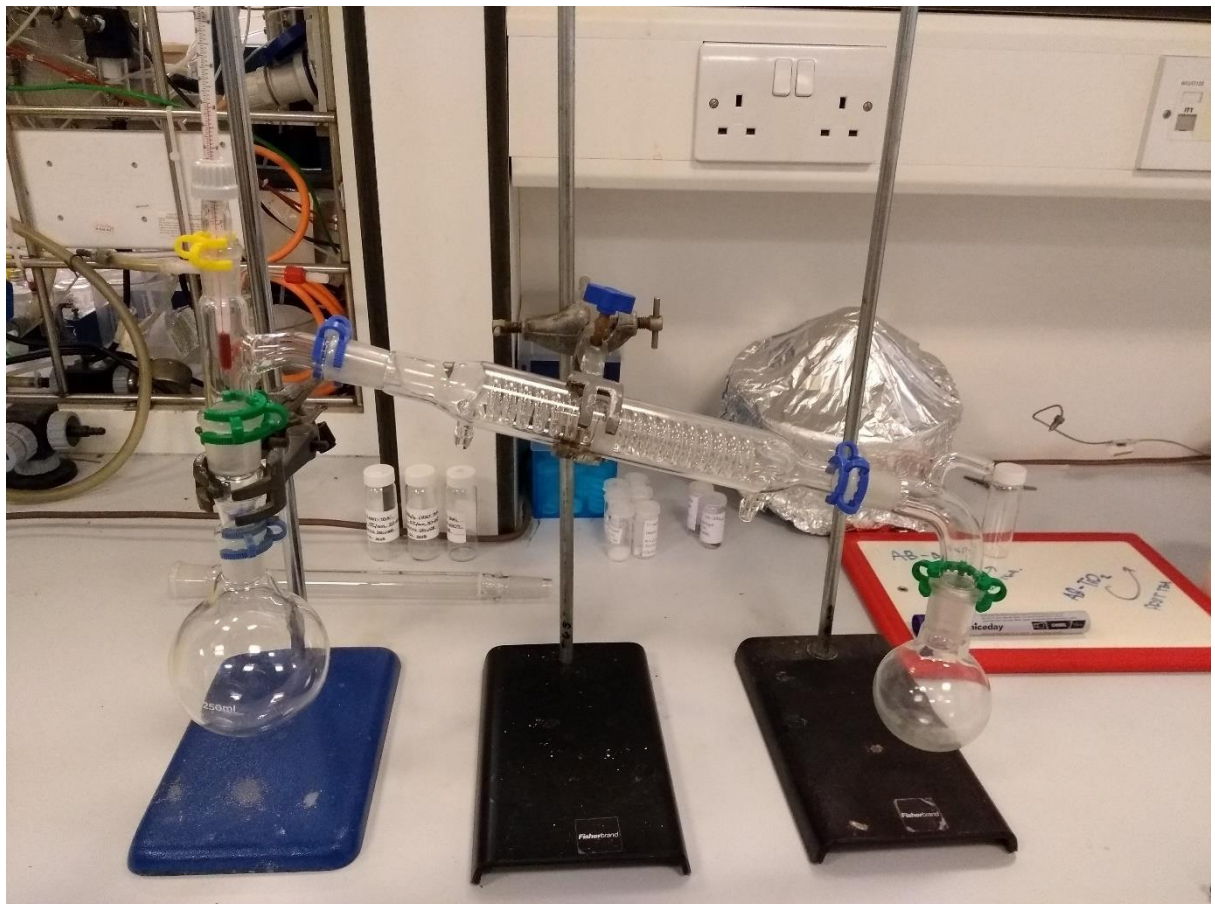


Figure 2.1 Picture of the distilling apparatus used for alcohol measurements

Real extract was then calculated using the formula where G is mass of extract in 100 g of solution of dealcoholized beer in grams (ASBC beer-5a):

$$RE = \frac{G * SG_{dealcoholised\ beer}}{SG_{beer}}$$

The apparent and real degree of fermentation were calculated using the following formulas (ASBC beer-6):

$$ADF = \frac{OG-FG}{OG} * 100$$

$$RDF = \frac{100(OG-FG)}{OG} * \frac{1}{1-(0.00516*RE)}$$

Where OG is original gravity in °Plato, FG is final gravity in °Plato, and RE is calculated real extract.

Beer colour was measured according to (ASBC beer-10a). A fully fermented sample was decarbonated and centrifuged to eliminate turbidity. Then, absorbance was measured in a calibrated spectrophotometer at a wavelength of 430 nm in 1 cm square cuvettes. Beer colour is determined by the formula:

$$Beer\ colour\ in\ SRM = 12.7 * A * F$$

Where 12.7 is the conversion factor when using 1 cm cuvettes instead of ½ in cuvettes, F is the dilution factor in case turbidity cannot be achieved easily, and A is the absorbance measured at 430 nm.

pH was measured according to (ASBC beer-9). Samples were degassed and centrifuged, then using a calibrated pH meter, pH was measured following the meter's instruction manual.

Microscopic yeast cell counting was done according to (ASBC yeast-4). A sample was taken each day during the fermentation and viable yeast cells were counted using a haemocytometer from Sigma-Aldrich following the manufacturer's instructions.

All physical-chemical parameters were measured in triplicate for all three experimental replicates.

2.4 Results and discussion

Table 2.1 Results of the sieving. Results are reported as mean and standard deviation of three replicates

Sieve Mesh Size	Crushed grain (g)
4 mm	0.53 ± 0.24
2 mm	25.03 ± 0.47
1 mm	10.2 ± 0.37
600 µm	4.63 ± 0.17
500 µm	0.7 ± 0.00
200 µm	3.1 ± 0.08
Bottom	4.27 ± 0.05

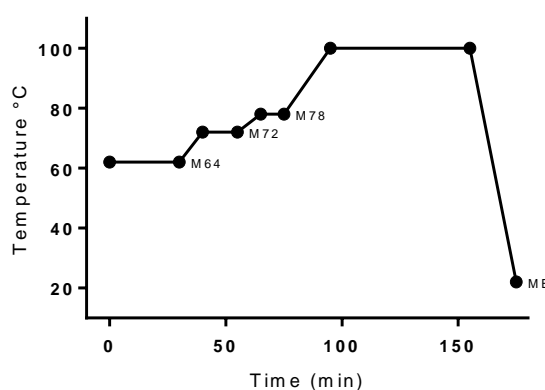


Figure 2.2 Mashing profile where the sampling points after each step are labelled.

The sieving results (Table 2.1) indicate a fine grinding setting as the grist collected at the mesh size of 600 µm is between 4.5 and 5.5 g. Brewing practices in conventional mash tuns traditionally dictate that a course grind should be used for the grain. The grinding of the grain exposes the starchy content inside the malt's husk without creating too much flour which usually is filtrated by brewers by recirculating the wort within the mashing vessel. The grist acts as a natural filter and thus improving the clarity of the wort. In this setting a fine grind was chosen because a fine nylon bag was used to filter any insoluble particles and a finer grind will yield a better extraction of malt metabolites into the wort.

The physical-chemical parameters of the experimental brews were measured at each time point sampled. The original gravity was measured at 1.052, which is a typical value of extract found in pale ale recipes (Dornbusch, 2010).

The fermentable extract appears to be consumed almost entirely by the third day, with no significant changes occurring in any parameter save for pH after that day (Table 2.2). The rate at which

the yeast reaches its maximum concentration and quickly drops by the third day of fermentation shows an unusually fast fermentation. The rapid fermentation can be explained by the fact that despite the fermentation temperature being within the recommended range by the yeast manufacturer it is in the higher limit of that range and thus increasing the metabolic rate of the yeast.

The pH keeps changing up to the fourteenth day (Figure 2.3). This suggests that the chemical makeup of the brew is still changing despite its physical-chemical parameters and viable cell count remaining constant. It can also be explained by yeast cell lysing as the population has depleted the nutrients available and has started dying. The experiment was continued to this late stage to compare the evolution of metabolites against the earlier samples.

Table 2.2 Physical-chemical parameters of brew at different sample points. Results are reported as mean and standard deviation of three replicates.

Sample	pH	SG	°Plato	ABW %	ABV %	RDF %	RE%	Colour
M64	5.69 ± 0.05							
M72	5.56 ± 0.07							
M78	5.53 ± 0.03							
MB	5.36 ± 0.07	1.052 ± 0.003	12.89	0	0	0	12.88 ± 0.68	
F1	3.77 ± 0.06	1.037 ± 0.005	9.381	1.39 ± 0.31	1.83 ± 0.40	23.29 ± 5.66	10.06 ± 1.13	
F2	3.42 ± 0.09	1.014 ± 0.001	3.585	3.86 ± 0.28	4.96 ± 0.36	59.74 ± 1.51	5.39 ± 0.27	
F3	3.34 ± 0.16	1.010 ± 0.001	2.726	4.25 ± 0.18	5.43 ± 0.23	65.13 ± 1.45	4.70 ± 0.42	
F4	3.35 ± 0.11	1.010 ± 0.000	2.76	4.11 ± 0.26	5.26 ± 0.33	64.44 ± 0.34	4.67 ± 0.22	
F5	3.44 ± 0.12	1.009 ± 0.001	2.526	4.34 ± 0.30	5.54 ± 0.39	66.26 ± 1.57	4.54 ± 0.27	
F14	3.87 ± 0.06	1.009 ± 0.001	2.404	4.51 ± 0.27	5.66 ± 0.34	66.48 ± 0.62	4.52 ± 0.26	5.80 ± 0.17

Legend: SG = specific gravity; ABW% = alcohol by weight; ABV% = alcohol by volume; RDF% = real degree of fermentation; RE% = real extract w/w; Colour = colour in SRM units

Table 2.3 Cell counting results.

Sample	Cell Concentration (cells/ml)	σ	Viability %
MB*	1.056E+07	1.232E+06	96.08
F1	3.335E+07	1.625E+06	98.49
F2	2.307E+06	3.242E+05	96.40
F3	8.025E+05	1.557E+05	92.25
F4	3.150E+05	8.042E+04	92.53
F5	1.175E+05	1.947E+04	81.75
F14	1.525E+05	8.860E+04	73.96

* MB sample count corresponds to after pitching.

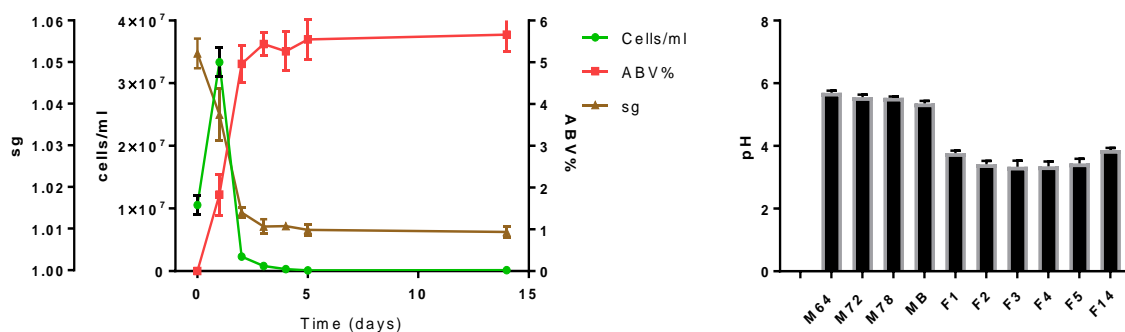


Figure 2.3 Superimposed graph of Cell concentration, specific gravity, and ABV% (left). pH measurements (right)

2.5 Conclusions

The brewing practice described in this chapter resulted in a convenient and fast method to produce a well extracted wort and beer representative of modern brewing practices and also oriented towards analysis with mass spectrometry. The physical-chemical parameters were measured and showed the consistency and reproducibility needed to confidently sample a representative sample of each stage in the brewing process. Samples of 2 mL were taken and stored in cryo-tubes at -80°C. This samples will then be analysed by various mass spectrometric techniques and submitted to a metabolomics workflow. The beer compound database developed will be used to process the data generated.

3. Chapter 3: Untargeted metabolomics analysis of brewing samples using matrix-assisted laser desorption/ionization – mass spectrometry and direct injection electron-ionisation – mass spectrometry

3.1 Introduction

The brewing samples obtained in Chapter 2 must contain a progression in terms of chemical composition according to the brewing theory described in Chapter 1. The complexity of the sample is poses a challenge in obtaining a holistic representation of the chemical composition of beer. Many different varieties of chemical compounds interact in complex reaction pathways and so the origins of many of the organoleptic properties in beer remain relatively unknown. Novel analytical approaches that can detect new chemical classes can help guide research in the right direction.

Matrix-assisted laser desorption/ionization (MALDI) is a method of soft ionization in mass spectrometry, usually time-of-flight (TOF-MS). It consists in mixing the sample with a matrix with very specific physical-chemical properties with the intent of aiding ionization, and an organic solvent that allows polar and non-polar molecules to dissolve into the solution. Afterwards, the mixture is spotted onto a metal plate and the solvent evaporates leaving the sample and matrix co-crystallized; the plate is then loaded to the machine where in a vacuum chamber a UV-laser will ablate the sample spots.

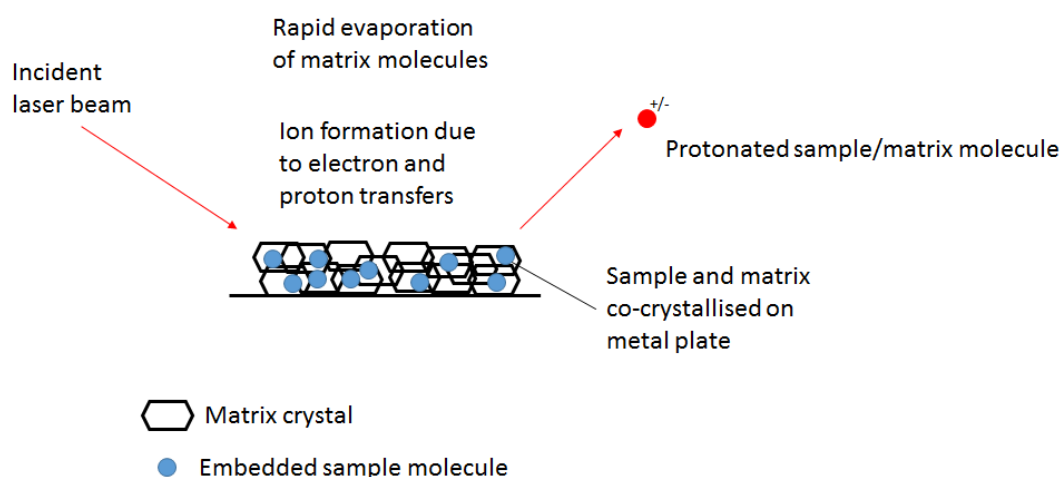


Figure 3.1 Simplified drawing of the operating principles during MALDI. The drawing shows the laser hitting the matrix:sample crystal lattice, the energy absorption, ionisation, and formation of molecular ions

Reproducibility of MALDI is a known issue where the same analysis protocol can output different mass spectra when applied in a different setting and so MALDI protocols have been mostly developed empirically through trial and error. Sample preparation is a key aspect, which involves several variability sources such as matrix choice, the analyte's physical and chemical properties, and

concentrations of the solutions. Another key aspect is the calibration of the MS, which involves the laser characteristics such as wavelength, spatial mode, and temporal pulse shape (Zenobi and Knochenmuss, 1998; Karas and Krüger, 2003). Some of its advantages are relatively low sample requirements, sensitivity, and straight-forward mixture analysis.

The laser usually shoots several times at the laser spot in a predefined pattern because the matrix-sample mixture spotted is not homogenous due to the polarity differences that lead to uneven solubilisation of the substances during co-crystallization.

MALDI-MS has been used to analyse beer and its ingredients before (Schulte, Flaschel and Niehaus, 2016). The study consisted in a proteomics study to analyse the adaptation of proteins during long storage periods where the interest was in uncovering the composition of haze proteome and ultimately better understand the colloidal stability of beer. The authors concluded that the detectable proteins correlated with haze formation contain multiple species of beer proteins rather than the hypothesised predominance of prolamins (e.g., hordeins). Maillard related reactions have been proposed as an explanation to the depletion of prolamins during storage of beer.

MALDI-MS has been used to develop a method to measure the oligosaccharides in beer (Park *et al.*, 2012). They compared 3 matrices derived from dihydroxybenzoic acid (DHB), varied the dilution factor, and compared different cationization agents to find the optimal conditions for ionization and quality of spectra. They concluded the isomer 2,6-DHB, a dilution factor of 4, and NaCl as the cationization agent provided the best results for the analysis of oligosaccharides in beer.

Characterization of the brewing process using ESI-MS (Vivian *et al.*, 2016). They were able to differentiate the stages of the brewing process and identify key compounds present at each stage. A variety of carbohydrates were identified in accordance with the brewing process and phenolic compounds related to catechin and gallic acid in the fermentation stage. The conclusion of this study was that using direct injection ESI-MS proved to be a suitable and convenient method of assessing quality of beer during its production stages allowing for quality assurance at various stages of the process.

There is extensive research on targeted analytical methods to monitor the kinetics of known flavour compounds. The untargeted approaches are sparse and not too in-depth regarding the biochemical pathways of flavour formation. The majority of the research is on pilsner/lager type malt and beer and not much on top-fermenting all grain ale beer (Andrés-Iglesias *et al.*, 2014; Spevacek *et al.*, 2016).

The aim of this chapter is to perform and optimise two MS methods to obtain a discriminant metabolic profile of an unhopped wort and beer produced from a heritage pale ale base malt (Maris Otter variety).

MALDI-MS has not been used to examine the low molecular weight metabolites in beer. In this chapter a method will be developed using MALDI-MS that will have good ion yields and reproducibility to gain access to new classes of compounds present in beer brewed from a heritage pale ale malt variety (Maris Otter). The procedure to process brewing samples by MALDI-MS went through an optimisation process described in the Appendix. The following experimental run's parameters are the result of the optimisation process. Additionally, a direct injection ESI-MS method will be developed in parallel in order to compare the resulting chemometric profiles and assess the relative merits of each approach.

3.2 Materials and methods

3.2.1 MALDI-MS

After -80°C storage, samples were prepared for MS analysis by freeze drying for 3 days, then the remaining organics were dissolved in 100 µl 70:30 v/v methanol:water solution and vortexed until there were no suspended solids. Then the samples were diluted 100 fold in the methanol:water solution. α -Cyano-4-hydroxycinnamic acid (CHCA) (Sigma Aldrich, UK) in solution (5mg/mL) with methanol and 0.1% trifluoroacetic acid as a cationization agent was used as the matrix. Then, 1 µL spot per sample of a mixture of 1:1 v/v (sample:matrix) was loaded into a 96-well target plate and allowed to crystallise on a heating block at 60°C. Three experimental replicates were divided and spotted into three technical replicates of each sample and spotted in a random sequence. Phenylalanine (monoisotopic mass 165.0789 Da) was used as a lock mass for mass drift correction and instrument calibration. Sample preparation and conditions were optimised based on previous tests described in the Appendix.

The MALDI-TOF-MS analysis was done in a Synapt G2-MS (Waters Corporation, UK) in both positive and negative ionization mode. Samples were scanned in a range of 50-1200 m/z with a scan time of 120 sec/spot. The laser energy was set at 300 (internal units) in a spiral pattern with a firing rate of 1000 Hz and N₂ was used as the carrier gas.

The Synapt G2 system has the following specifications according to the manufacturer:

Table 3.1 Synapt G2 specifications (Waters Corporation, UK)

<i>Specification</i>	<i>Value</i>
Operation mode (detector)	a) Time-of-flight (TOF) mode b) Mobility- TOF mode
TOF Mass resolution	a) Sensitivity mode – 10,000 FWHM (full width half maximum) b) Resolution mode – 20,000 FWHM c) High resolution mode – 40,000 FWHM d) MALDI resolution mode – 16,000 FWHM e) MALDI high resolution mode – 32,000 FWHM
Positive Ion MS sensitivity	a) Sensitivity mode – 1700 ions/s @ 10,000 resolution b) Resolution mode – 850 ions/s @ 20,000 resolution c) EDC – 1000 ions/s @ 20,000 resolution
Negative Ion MS sensitivity	a) Sensitivity mode – 1800 ions/s @ 10,000 resolution b) Resolution mode – 900 ions/s @ 20,000 resolution
Mass scale calibration accuracy	At high resolution mode <1 ppm over the range of 150-800 <i>m/z</i>
Mass measurement accuracy	At high resolution mode better than 1 ppm
Mass range	The TOF mass range is: a) Resolution mode 20-100,000 <i>m/z</i> b) High resolution mode – 20-32,000 <i>m/z</i>
Acquisition rate	20 scans/s
Dynamic range	At high resolution mode, defined as the range of peak intensities that will give better than 3 ppm accurate mass for 10 s of data is >4 orders of magnitude

3.2.2 DI-MS

Three experimental brewing samples were taken directly from the -80°C storage and diluted to 80% ethanol:20% sample. Then 2 mL aliquots were centrifuged at 140000 rpm for 10 min. Afterwards, the supernatant was transferred to a new centrifuge tube and centrifuged again at the same conditions as above. Finally, the supernatant was transferred to a new Eppendorf tube and mixed in a 1:1 ratio with a 50% methanol: 50% distilled water solution and 1% formic acid. All chemicals were sourced from Sigma Aldrich, UK.

Biological samples were injected into a QStar Elite MS System (Applied Biosystems), which was previously calibrated by the technical staff using sulfadimethoxine (monoisotopic mass 310.0735) as a standard, in a random order under the following operating parameters:

Table 3.2 DI-MS run parameters

<i>Specifications</i>	<i>Value/Type</i>
Component	Hybrid Quadrupole Time-of-Flight MS
Source type	Turbo spray
Source temperature	200°C
Vacuum gauge	10e-5 Torr
Injection manifold	Direct injection
Syringe diameter	2.3 mm
Flow rate	10 µL/min
Sample Acq duration	12 min
Scan polarity	Positive mode
TOF mass range	50-1200 Da
Calibration standard	Sulfadimethoxine

Of the 12 min of data acquisition, three 30 s intervals of stable signal were selected using the software Analyst QS 2.0 MarkerView™ (SCIEX) into peak lists. The QStar Elite MS system has the following specifications:

Table 3 QStar Elite MS System technical specifications (Applied Biosystems)

<i>Parameters</i>	<i>Value</i>
Operation mode (detector)	Hybrid quadrupole time-of-flight
Flow rate precision	<1 nL/min
Mass resolution in positive ion mode	8,000 FWHM @ 829 <i>m/z</i> 10,000 FWHM @ 1,163 <i>m/z</i>
Minimum accumulation time	100 ms
Mass accuracy	5 ppm
Mass range	50-40,000 <i>m/z</i>
Physical dimensions	Width 160 cm Height 107 cm Weight 592 kg Depth 79 cm

3.2.3 Data pre-processing and multivariate analysis

In both mass spectrometry runs the resulting spectra were visualised and peak corrected in MassLynx 4.0 (Waters Ltd). Noise reduction, normalization, and binning was performed as described by (Overy *et al.*, 2004) using a Visual Basic macro in Microsoft Excel (Microsoft Corp, USA). Triplicate

samples are combined to eliminate false positive peaks, only peaks that are present in all three replicates are preserved. To determine which peaks are equivalent to each other a linear function is used to define an acceptable mass variance. For positive ionisation mode the equation used is, $y < 0.00003x + 0.0033$; and for negative ionisation mode, $y < 0.00003x + 0.0044$; where y is the standard deviation of the three masses and x is the mean of the three masses. After a peak is selected as a true positive, the masses' intensities are normalised to the percentage of the total ion count (TIC) in each replicate and added together, then allocated into mass unit "bins" with a size of 0.2 amu. The resulting peak list's statistical treatment and multivariate analysis was done in SIMCA 14 (Umetrics, Sweden). The resulting peak list from the pre-processing algorithm was transposed and imported into SIMCA so that the mass bins are the independent variable and the sample label (e.g. M64, F1, etc.) are the dependent variable. Then, the data-set was Pareto scaled to reduce the relative effect of peaks with high relative intensity while partially retaining the data structure (Worley and Powers, 2015), this is done to have a higher discriminating power on changes of intensity that are otherwise too small to detect. Then, adducts related to the matrix (CHCA) were removed from the data-set. Then, the PCA was done using the default parameters provided by the software, depending on the results of the PCA, sample labels were inputted, and OPLS-DA executed. The OPLS-DA outputs loading scores which were arranged in column plots and arranged in increasing order, the top discriminating bins were selected for annotation and analysis; this step was performed for each sample label identified.

3.2.4 Development of a beer flavour compound database to use with MS data

The processing and functional interpretation of untargeted metabolomics data is a noticeable bottleneck in current research pipelines. Many methods for peak identification, spectral deconvolution, and peak annotation have been developed with the goal of streamlining the analysis; regarding the first two tasks, some excellent methods have been developed which can output practical "MS peak lists". From these lists peak annotation must be done by manually searching through relevant compound and spectral databases. Therefore, it was decided to create a database focused on grain and yeast derived flavour compounds present in beer.

The ASBC beer flavour database was used as a starting point. This database originally contained 574 unique entries of compounds found in beer. Each compound has its chemical name, synonyms, formula, average molecular weight, flavour descriptors, concentration range, flavour thresholds, flavour units, threshold in water, formation/description, compound class, and CAS number. This database was expanded, updated, and curated by scraping data from 49 academic papers to a total of 1,041 unique entries. Additional information was added: the monoisotopic mass, method of analysis/detection, extraction method, source sample, HMDB ID, KEGG ID, and its simplified molecular-input line-entry system (SMILES) was added to the database.

The new set of information added to the database can be used to identify molecular/parent ions and its adducts from MS spectral data by comparing monoisotopic mass and calculated adduct ion masses. HMDB ID represents a unique number identifier in the Human Metabolome Database (www.hmdb.ca), which is one of the most comprehensive databases today that can be used to analyse metabolomics data sets specifically (Wishart *et al.*, 2007, 2018). Additionally the HMDB acts as a “parent” database for other more context specific databases like the Yeast Metabolome Database (YMDB) (Jewison *et al.*, 2012; Ramirez-Gaona *et al.*, 2017) and the FooDB (www.foodb.ca). HMDB and KEGG ID entries were added, as much of its data can be downloaded and then used in other dependant applications for things such as pathway analysis, enrichment analysis, spectral analysis, biomarker analysis, etc. The database developed can be accessed and downloaded at:



Figure 3.2 QR code to access the beer flavour database (Permalink: https://drive.google.com/file/d/151leowuy3z3VYI5yvJTa2NvQ69-E7J_/view?usp=sharing)

3.3 Results

3.3.1 MALDI-MS

Sample spotting and loading for both positive and negative mode runs resulted in homogenous spots that crystalized in less than 1 min. The total ion counts (TIC) for both ionization modes consistently resulted in values over 1×10^6 counts (Figure 3.3), high and consistent TIC indicate a good quality mass spectrum fingerprint and good reproducibility is a key factor in the discriminatory potential of profiling methods (Qiao *et al.*, 2009). The spectra appear consistent among samples by visual inspection (data shown in the Appendix). The matrix peaks were in general the most abundant but did not completely dominate over the rest indicating a good matrix/sample ratio in the spot and ionisation efficiency.

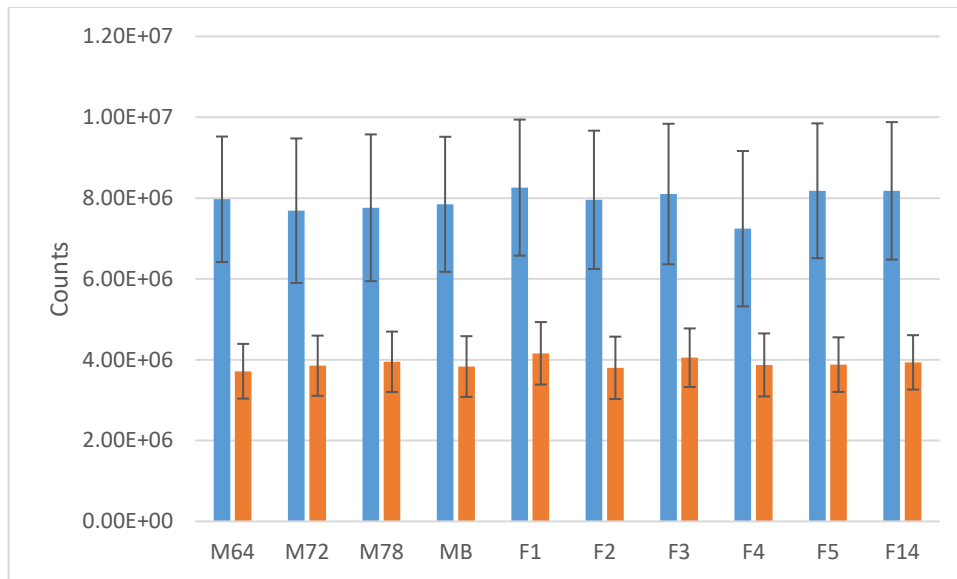


Figure 3.3 Sum total ion count (TIC) in positive (blue) and negative (orange) ionisation mode (MALDI-MS)

The positive mode samples' PCA results overall scatter plot (44.89% of the variance explained) followed the progression of the process as the wort samples clustered in the right section of the plot and the fermented samples clustered on the left side (Figure 3.4). Another PCA (42.9% of the variance explained) was applied to the pre-fermented samples and it revealed a subtle progression of the mashing process, with lower temperature samples projecting on the top side of the plot and higher temperature samples on the bottom right (Figure 3.6). Another PCA (39.6% of the variance explained) was done on the post-fermented samples and it also hints at a subtle progression between time points, as less fermented samples laid on the top side of the plot and more fermented samples on the bottom (Figure 3.5).

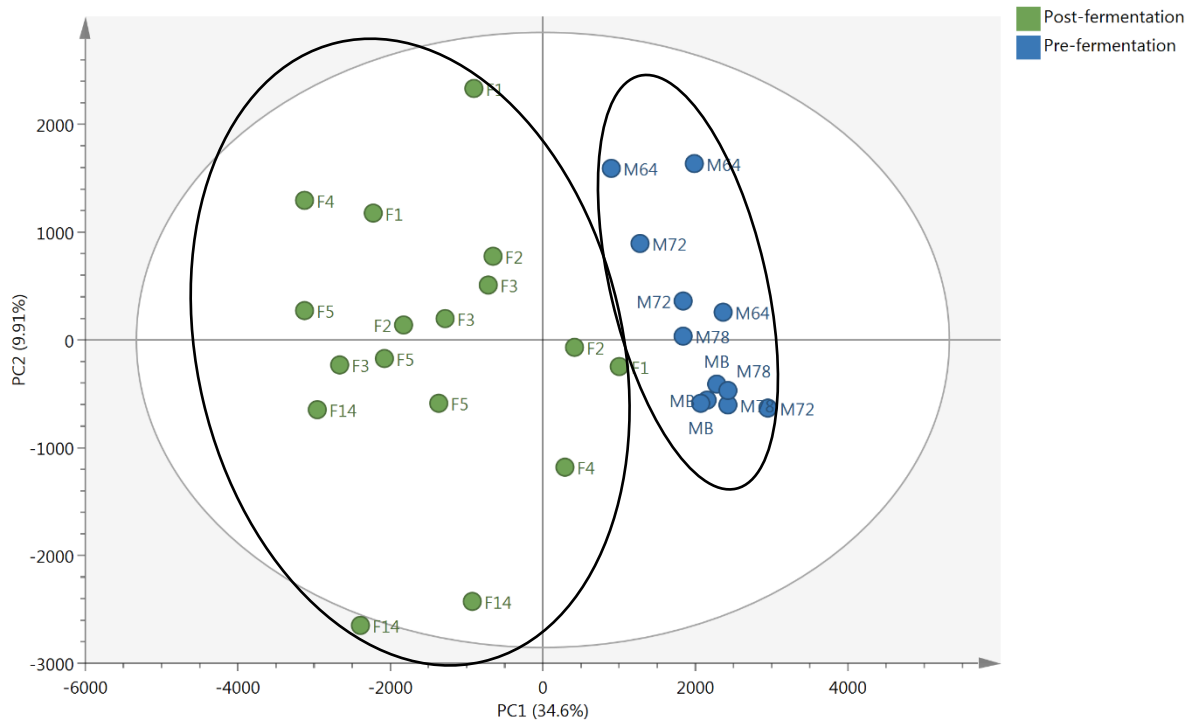


Figure 3.4 Overall PCA score scatter plot (MALDI-MS positive mode). Labels on each point correspond to the time-point named in Chapter 2

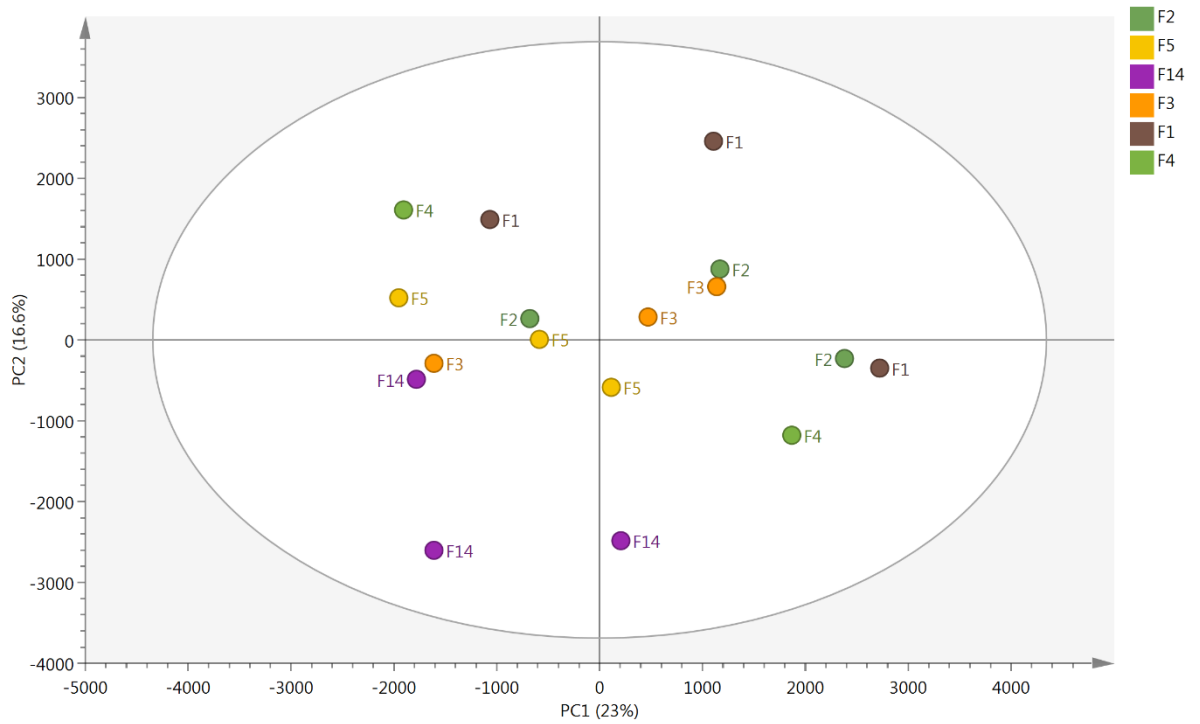


Figure 3.5 PCA score scatter plot of the post-fermentation sample class (positive mode)

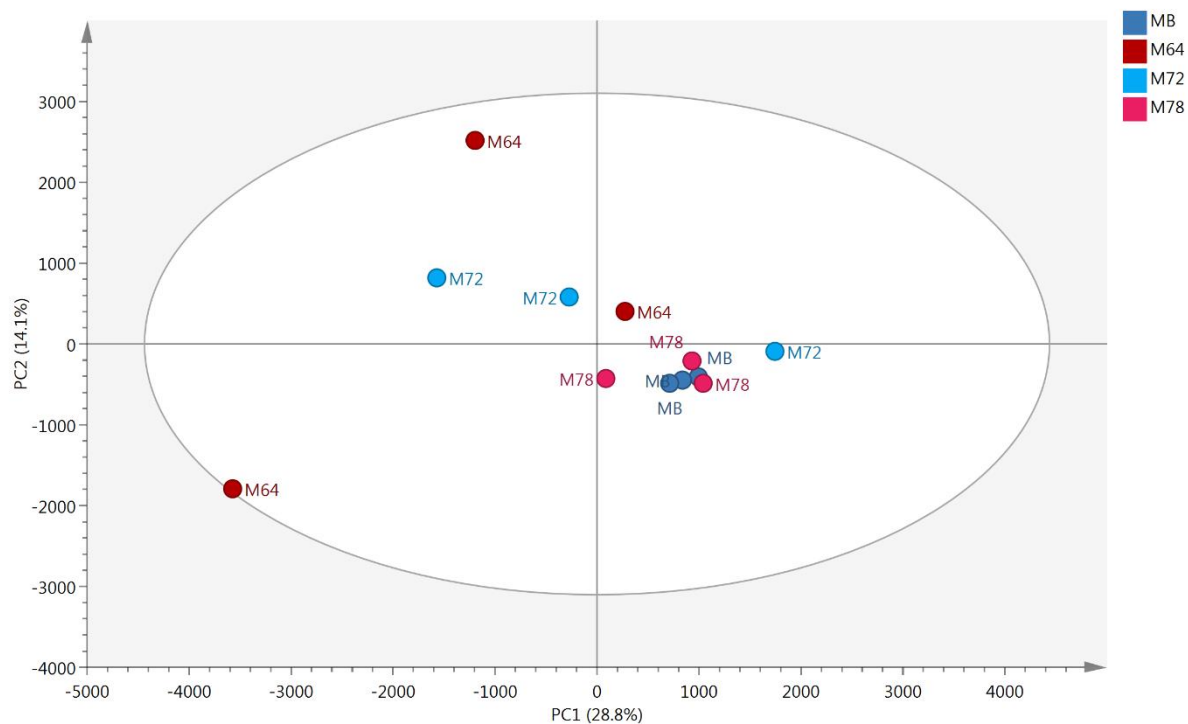


Figure 3.6 PCA score scatter plot of the pre-fermentation sample class (positive mode)

Discrete clusters for each sample-point could not be identified. Despite the subtle progression of the samples taken from the wort mashing and during each fermentation day there was considerable overlap between them in the PCAs. For the previous reasons, OPLS-DA was only applied to compare between the pre-fermentation and post-fermentation samples (Figure 3.7) classes as there was not a significant distinction within the pre-fermentation and post-fermentation samples to justify further valid interrogation of the data (Worley and Powers, 2016).

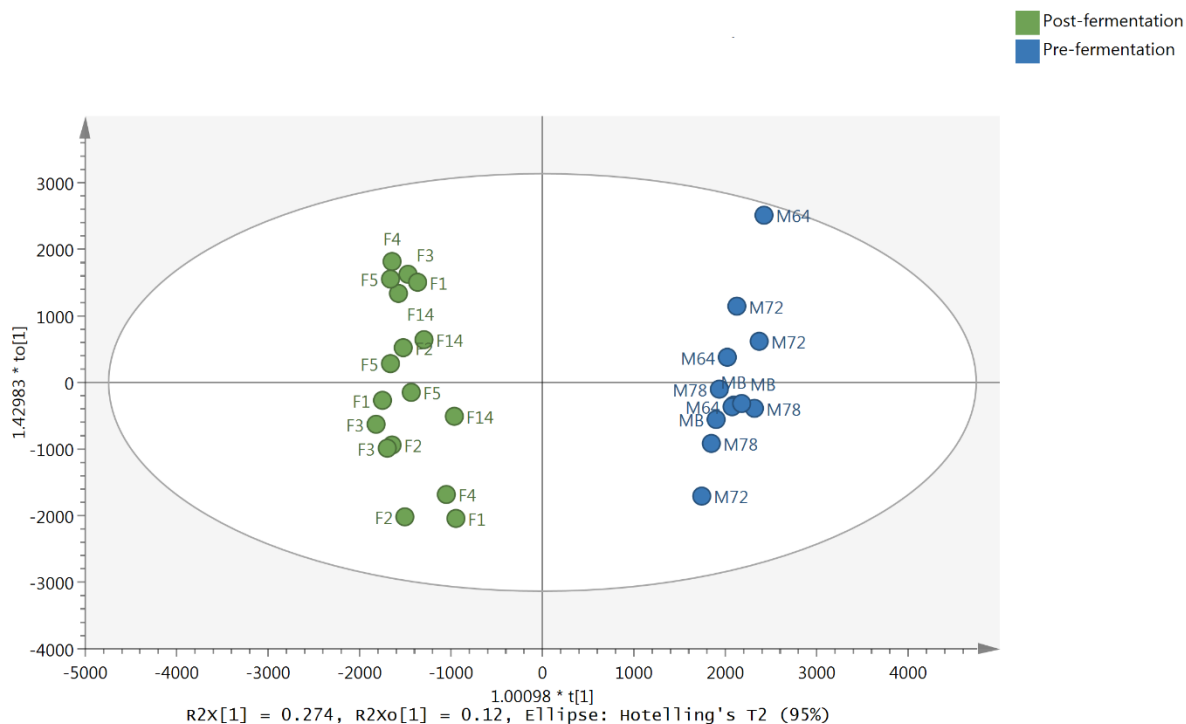


Figure 3.7 OPLS-DA score scatter plot (positive mode)

For the negative mode run, the resulting PCA overall scatter plot (47.62% of the variance explained) followed the progression of the process as the wort samples were primarily plotted on the left side, except for one M64 replicate; the fermented samples clustered, mainly, on the right side but a few overlap with the wort samples (Figure 3.8). Another PCA (43.8% of the variance explained) was applied to the post-fermentation samples and it shows no clear groups or patterns, the samples are spread all over the plot (Figure 3.9). Another PCA (47.86% of the variance explained) was done on the pre-fermentation samples and it shows a clear progression between time points, as lower temperature samples are on the right and higher temperature samples are progressively to the left of the plot (Figure 3.10).

As with the positive mode run, OPLS-DA was only applied to compare between the pre-fermentation and post-fermentation samples (Figure 3.11) classes as there was not a significant distinction amongst the pre-fermentation and post-fermentation samples to justify further valid interrogation of the data (Worley and Powers, 2016).

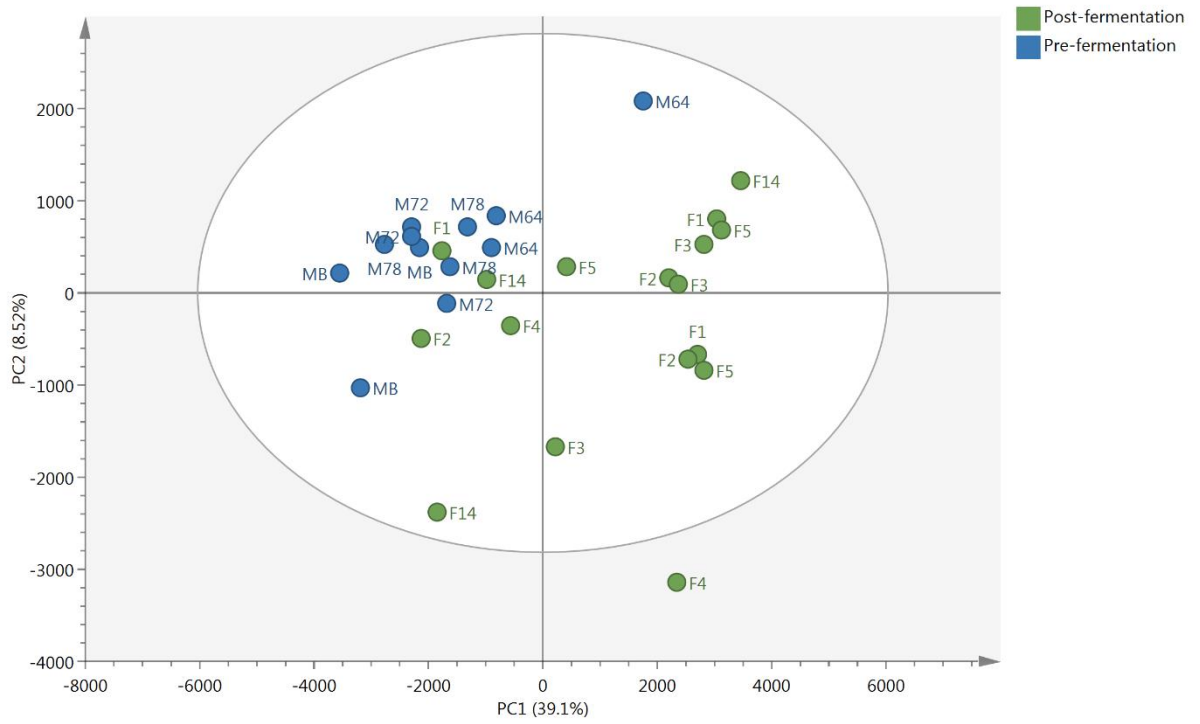


Figure 3.8 Overall PCA score scatter plot (negative mode)

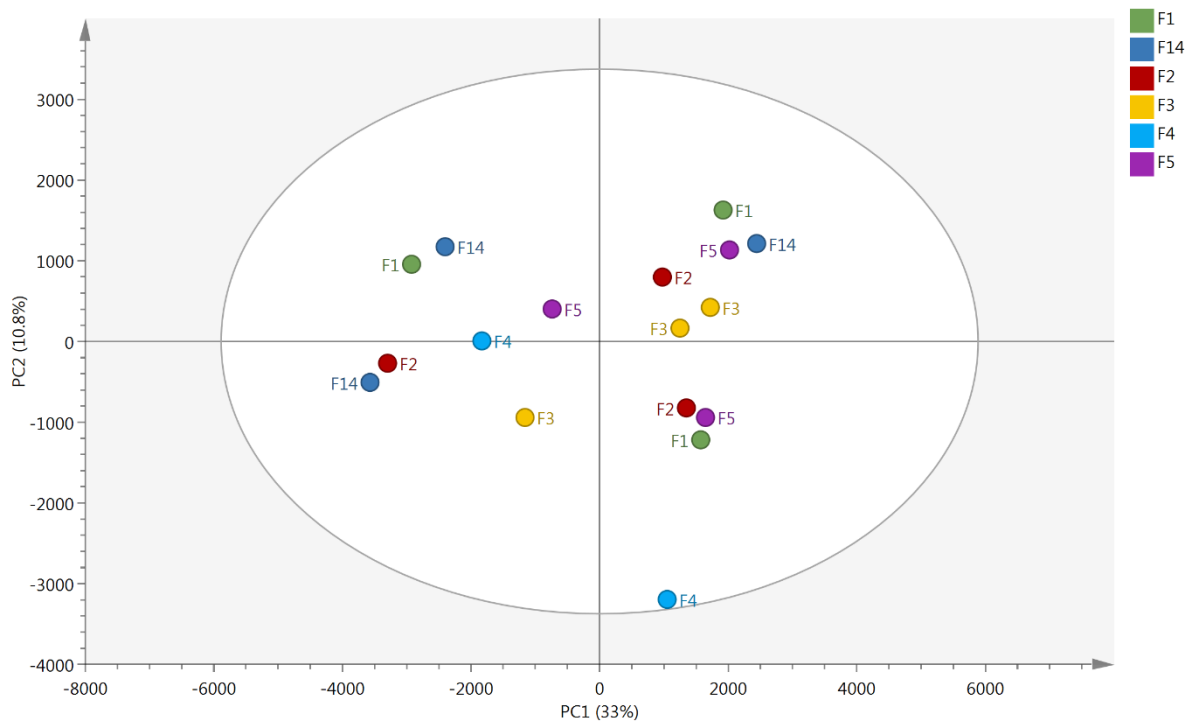


Figure 3.9 PCA score scatter plot of the post-fermentation sample class (negative mode)

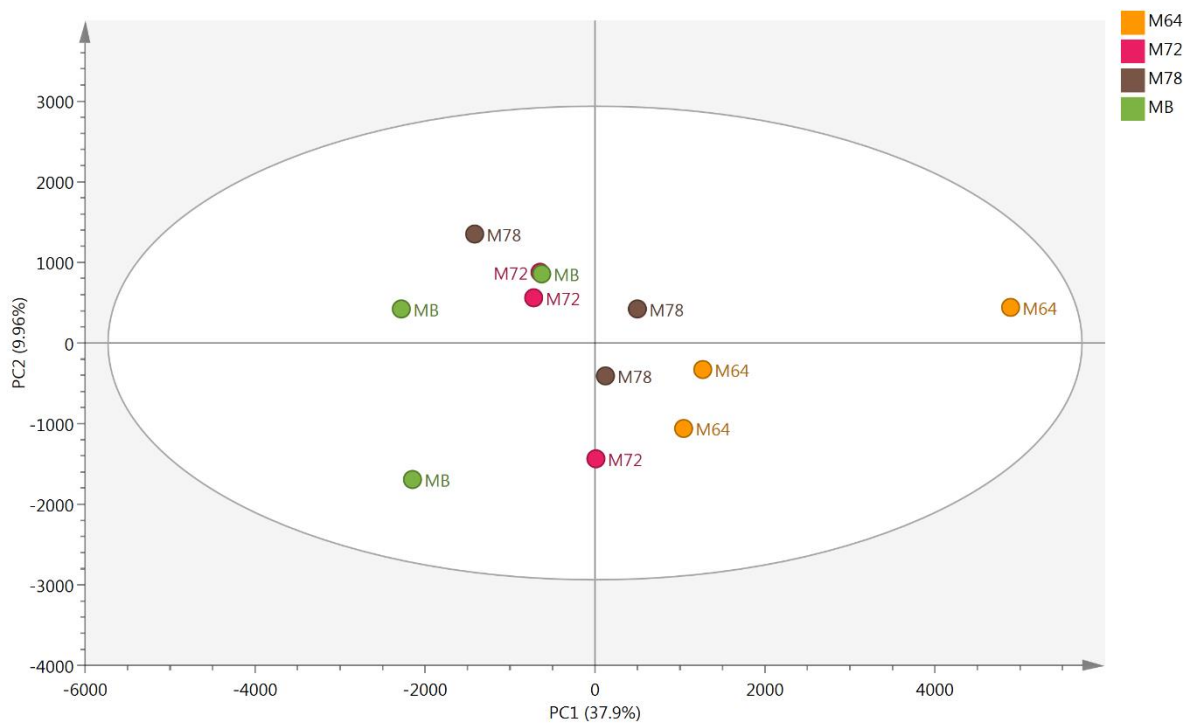


Figure 3.10 PCA score scatter plot of the pre-fermentation sample class (negative mode)

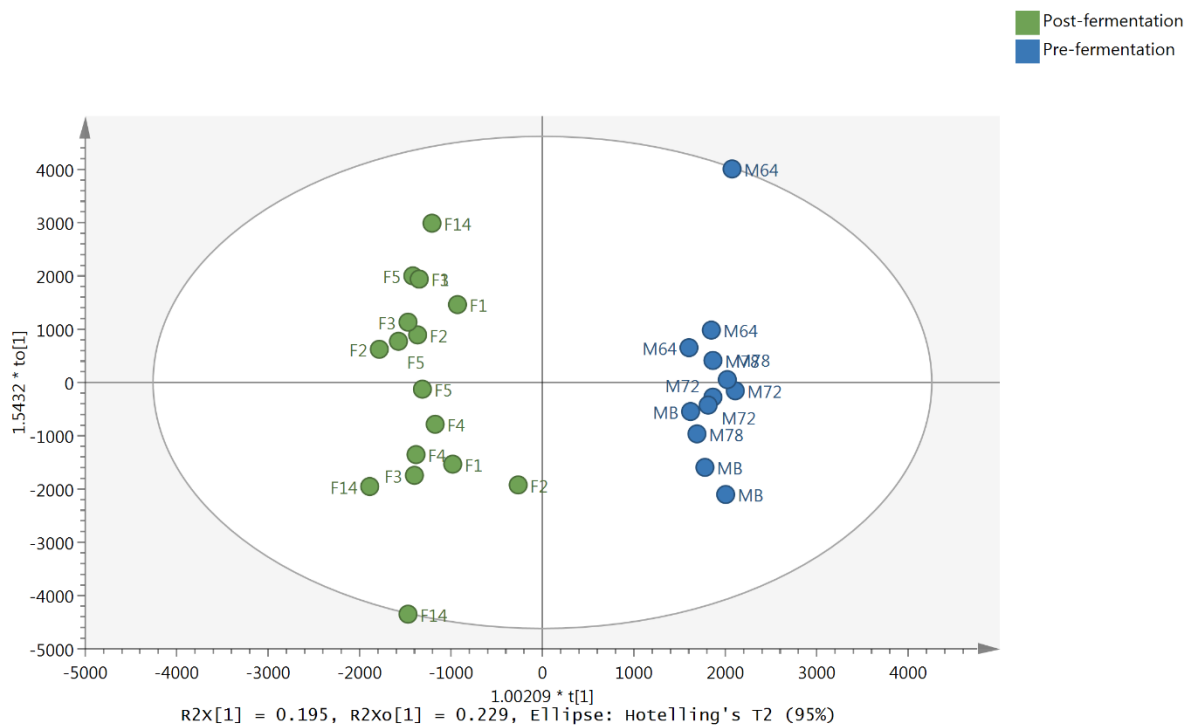


Figure 3.11 OPLS-DA score scatter plot MALDI-MS (negative mode)

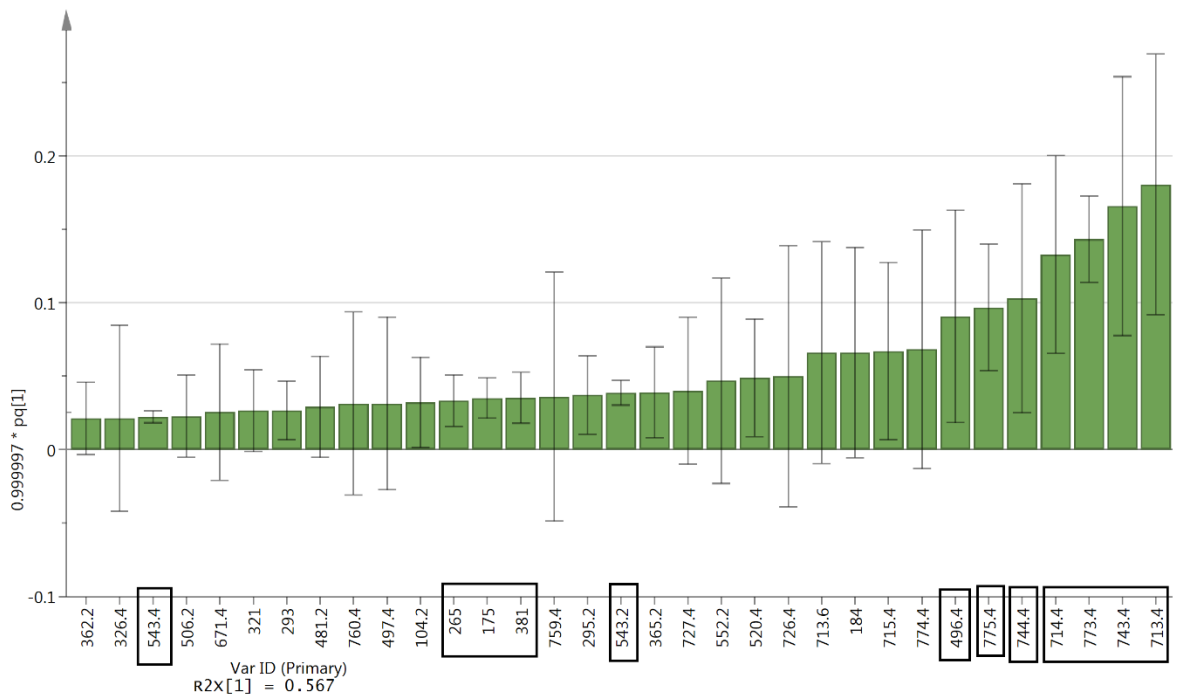


Figure 3.12 Loadings column plot showing the most discriminant bins of the pre-fermentation sample class MALDI-MS (positive mode) normalised to unit length. Top discriminant bins are enclosed in black and were chosen for annotation based on statistical significance and the standard deviation clearly not crossing into a presence into the other sample class.

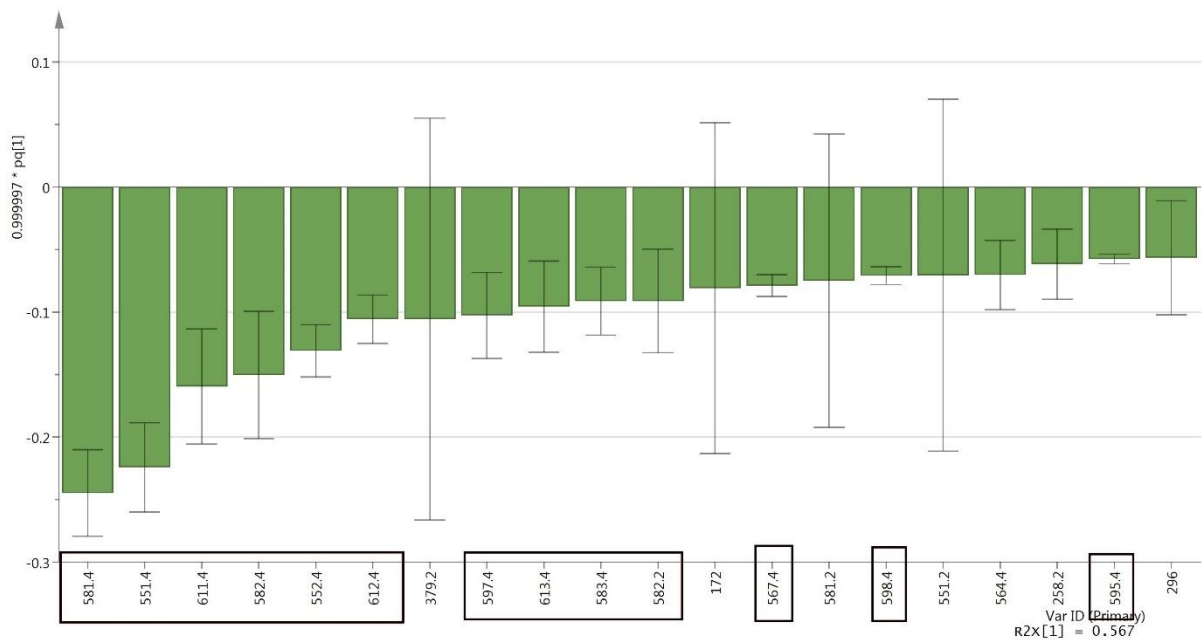


Figure 3.13 Loadings column plot showing the most discriminant bins of the post-fermentation sample class MALDI-MS (positive mode) normalised to unit length. Top discriminant bins are enclosed in black and were chosen for annotation based on statistical significance and the standard deviation clearly not crossing into a presence into the other sample class.

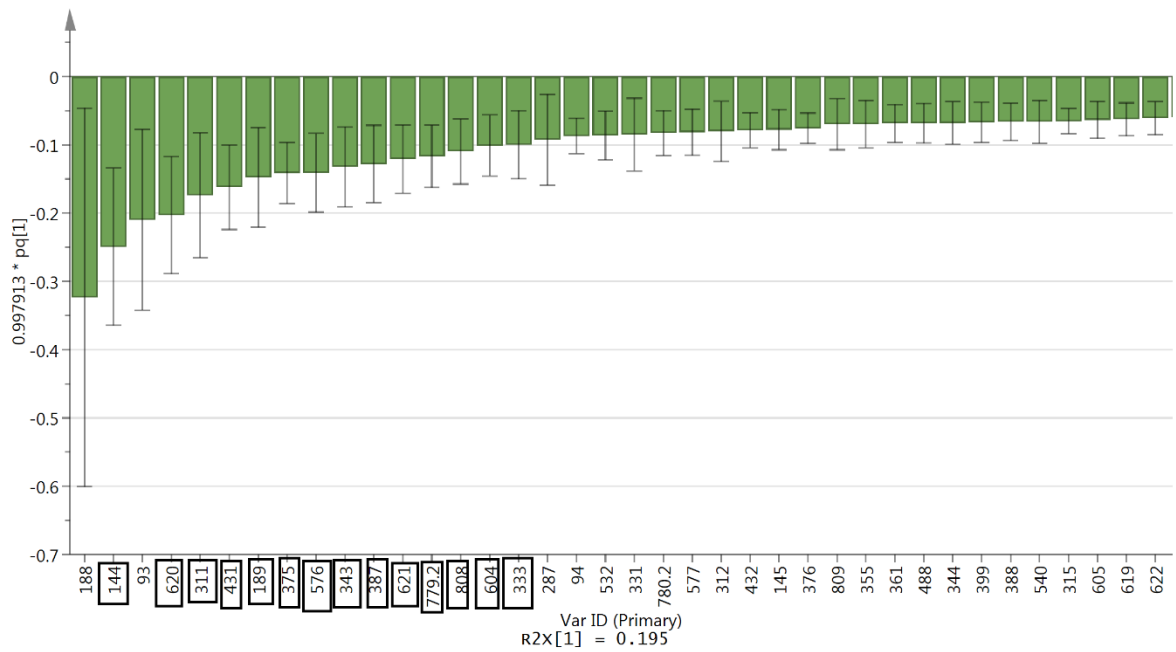


Figure 3.14 Loadings column plot showing the most discriminant bins of the post-fermentation sample class MALDI-MS (negative mode) normalised to unit length. Top discriminant bins are enclosed in black and were chosen for annotation base on apparent statistical significance and the standard deviation clearly not crossing into a presence in the other sample class.

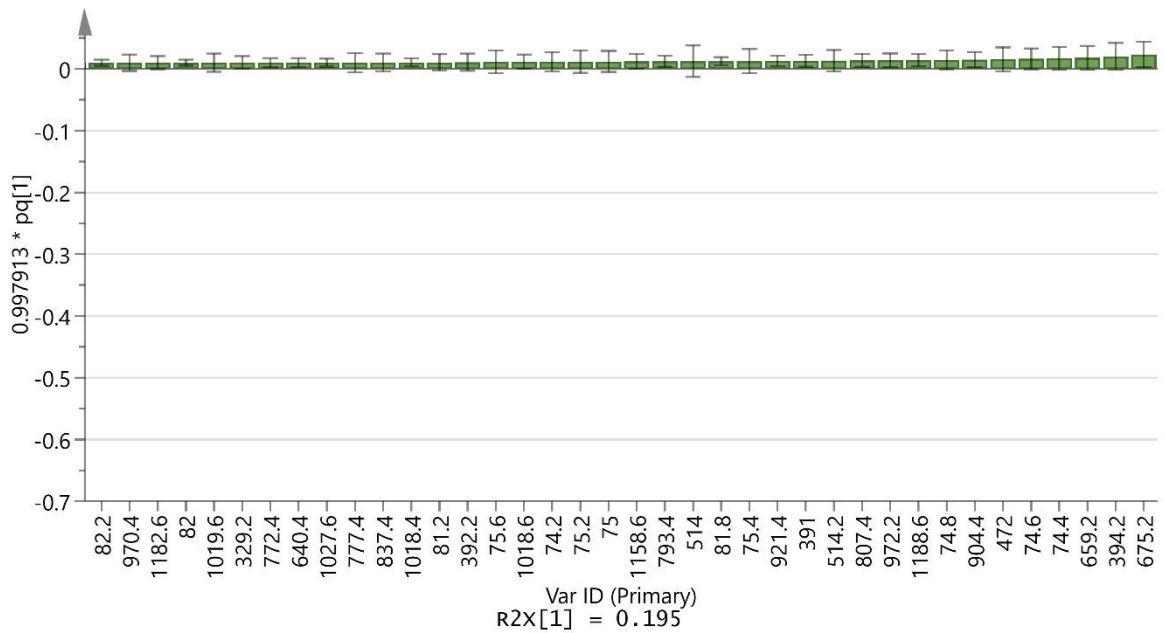


Figure 3.15 Loadings column plot showing the most discriminant bins of the pre-fermentation sample class MALDI-MS (negative mode) normalised to unit length

Table 3.4 Top discriminant bins between sample classes. Putative identification of compounds for each sample class is referenced next to it by table number.

<i>Positive mode</i>		<i>Negative mode</i>	
<i>Pre-fermentation</i> (Table 7.1)	<i>Post-fermentation</i> (Table 7.2)	<i>Pre-fermentation</i>	<i>Post-fermentation</i>
175.0	551.4	N/A*	144.0
265.0	552.4		189.0
381.0	567.4		311.0
496.4	581.4		333.0
543.2	582.2		343.0
543.4	582.4		375.0
713.4	583.4		387.0
714.4	595.4		431.0
743.4	597.4		576.0
744.4	598.4		604.0
773.4	611.4		620.0
775.4	612.4		621.0
	613.4		779.2
			808.0

* No statistically significant discriminating bins in this sample class

The OPLS-DA revealed the top discriminating bins between the pre-fermentation and post-fermentation samples in both positive and negative ionisation modes (Table 3.4) and for full loadings score visualised in Figure 3.12, Figure 3.13, Figure 3.14, and Figure 3.15. The top discriminating bins chosen to be associated to each sample class are enclosed in black boxes, the top discriminating bins were chosen based on an apparent statistical significance and the standard deviation clearly showing the bin detected is not present in the other sample class.

A visual inspection of the spectra from the MS in negative mode shows not much discrimination from the pre-fermentation and post-fermentation samples (Figure 7.20, Figure 7.21, Figure 7.22, Figure 7.23). There was also poor ionisation yield when compared to the positive mode (Figure 3.3). The most abundant peaks at m/z 93.0172 and 188.0168 correspond to the matrix [M-2H] and [M-H] adducts respectively; these two peaks have notably higher relative abundance throughout all the samples (Figure 7.20, Figure 7.21, Figure 7.22, Figure 7.23), especially the peak at m/z 188.1035. While there is a high amount of TIC in ESI- mode, it appears that the matrix is not fulfilling its purpose of providing a charge to the sample, this can be inferred by the low intensity peaks throughout the spectrum tested when compared to the matrix peaks. The chosen matrix is not suitable for negative ionisation mode mass spectrometry. For a better ionisation efficiency in negative mode samples should be alkalized instead and a nucleophile such as 9-Aminoacridine should be used to deprotonate the sample during the laser ablation and produce negative adducts (Zenobi and Knochenmuss, 1998).

No further interrogation of the data set is recommended. No further tests with other matrices were done due to lack of interest, funding, and time.

The results are corroborated by the MVA where no bins were discriminating enough to explain the small variance between the sample groups (Figure 3.15 and Table 3.4). For these reasons, the data obtained from the negative mode MS will not be processed further. Further research in negative ionisation mode was not conducted due to time constraints.

3.3.2 DI-MS

The overall PCA showed two distinct clusters of experimental samples, distinguished between the pre-fermentation and post-fermentation samples, and with a total variance explained of 82.4% (Figure 3.16). The PC2 (28.3% of the variance explained) followed the progression of the brewing process as the mashing samples clustered on the top and the beer samples clustered on the bottom of the plot.

Supervised clustering was applied to the two clusters identified and the top most statistically significant discriminating bins for each sample class were identified (Figure 3.18, Figure 3.19).

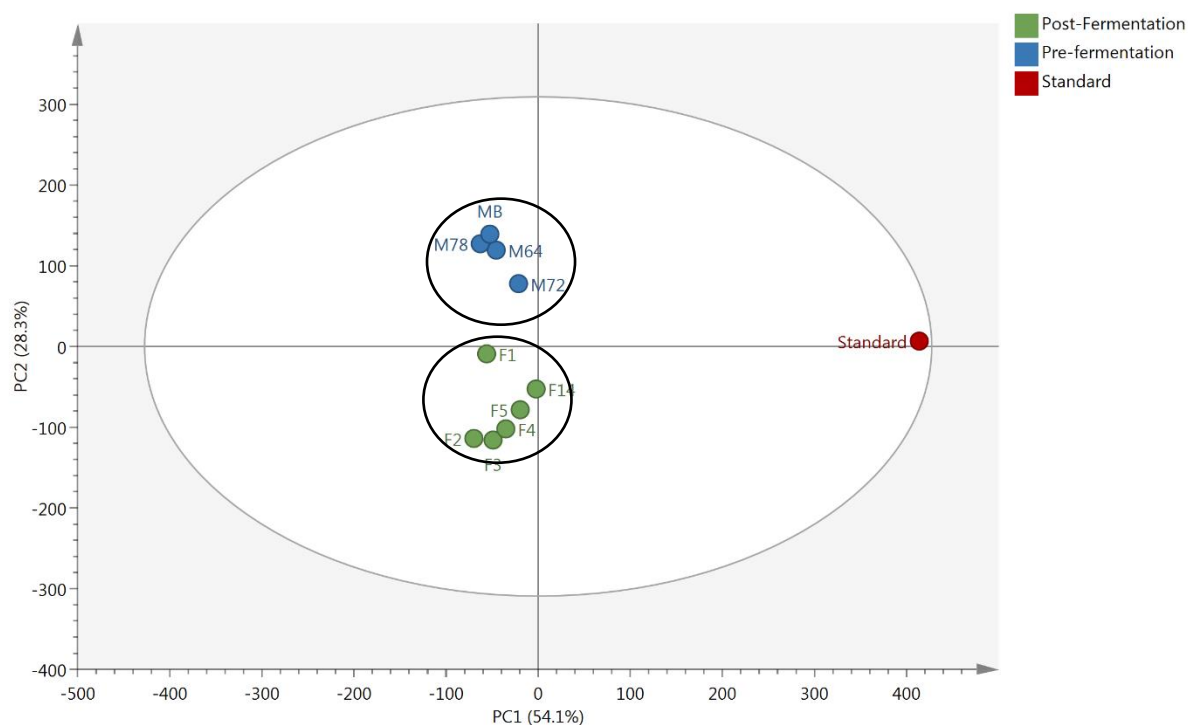


Figure 3.16 Overall PCA score scatter plot in DI-ESI-MS

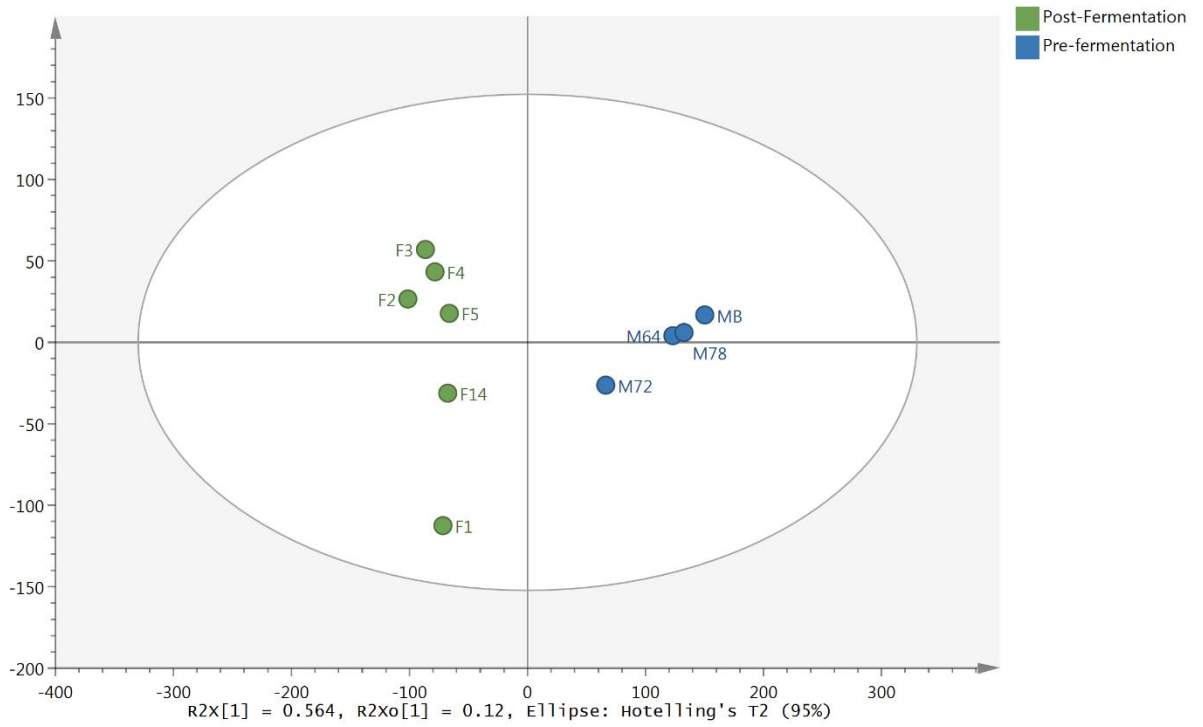


Figure 3.17 OPLS-DA score scatter plot in DI-ESI-MS

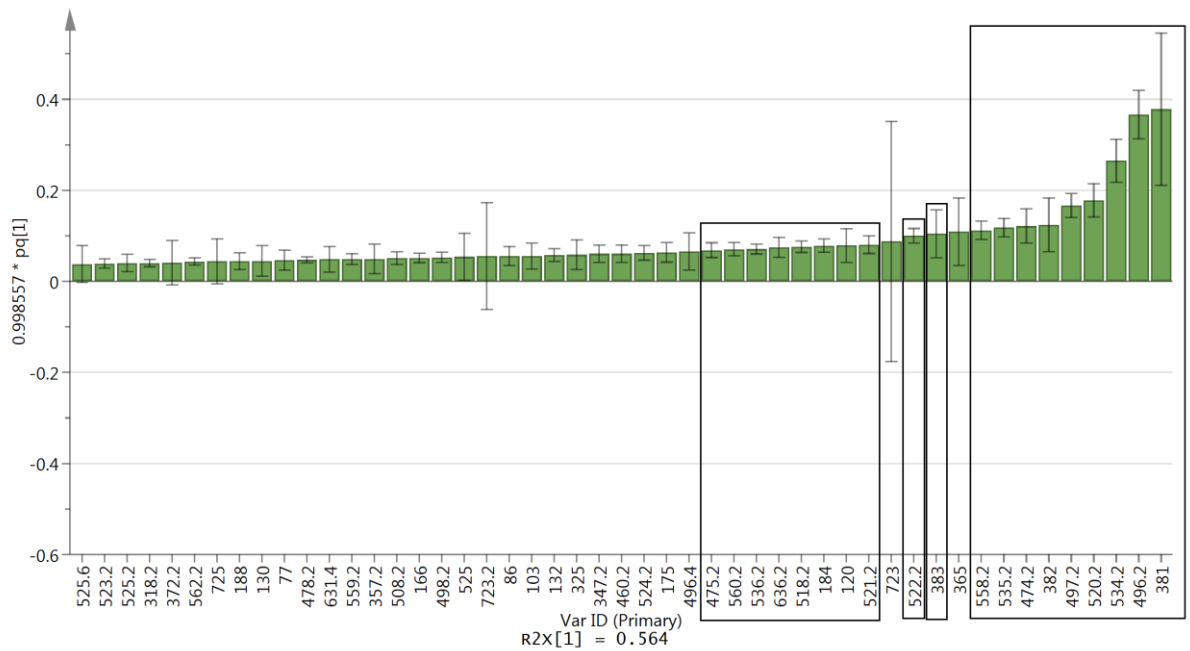


Figure 3.18 Loadings column plot showing the most discriminant bins of the pre-fermentation sample class (normalised to unit length). Top discriminant bins are enclosed in black and were chosen for annotation base on apparent statistical significance and the standard deviation clearly not crossing into a presence in the other sample class.

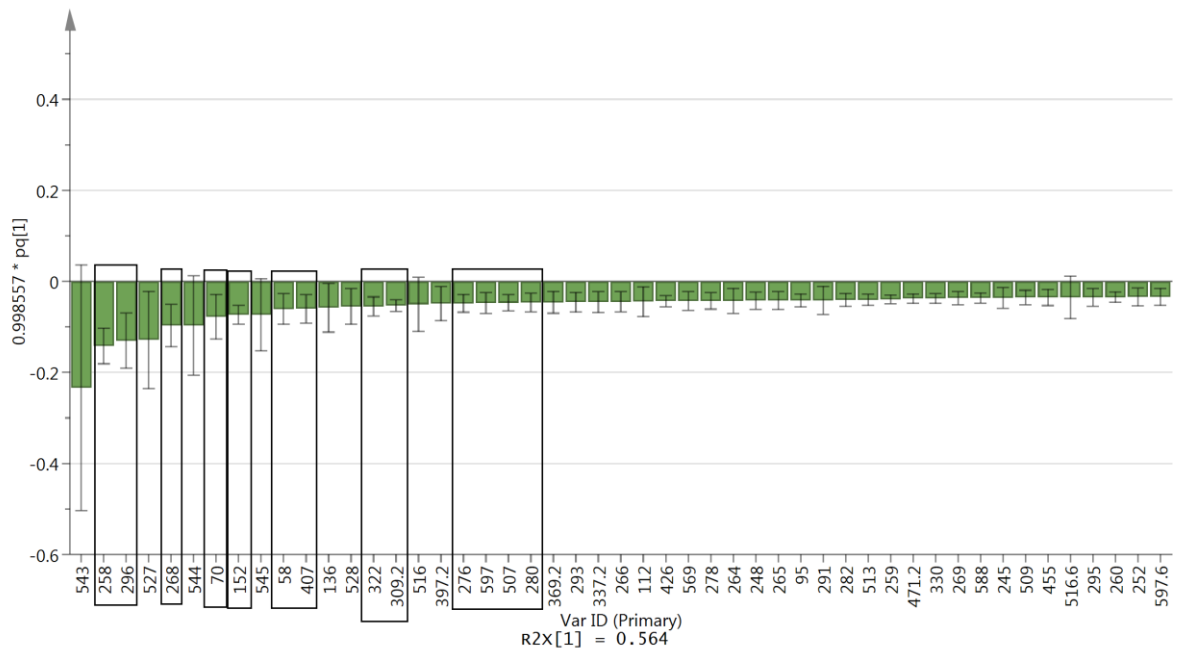


Figure 3.19 Loadings column plot showing the most discriminant bins of the post-fermentation sample class (normalised to unit length). Top discriminant bins are enclosed in black and were chosen for annotation base on apparent statistical significance and the standard deviation clearly not crossing into a presence in the other sample class.

3.3.3 Statistical significance of the relative abundance between sample classes

The relative abundance of the discriminant bins was subjected to a *t*-test in order to determine whether or not there is a significant difference between the sample classes. Despite the identification of the most discriminant bins through the supervised multivariate analysis, it is necessary to use a quantitative measure to determine the significance of each bin. A Student's *t*-test was used. The results can be seen in Table 3.5, Figure 3.20, and Figure 3.21 for MALDI-MS. In general, all except one identified bin resulted statistically different. The bin 613.4 was non-significant with a $p = 0.3$.

Table 3.5 Results of *t*-test applied to discriminant pre-fermentation bins (left table) and post-fermentation bins (right table) of MALDI-MS positive mode. P value significant if $p < 0.05$; df = degrees of freedom; t = t value

<i>Bin</i>	<i>p value</i>	<i>t</i>	<i>df</i>	<i>Bin</i>	<i>p value</i>	<i>t</i>	<i>df</i>
175	<0.0001	6.334	28	551.4	<0.0001	8.355	28
265	<0.0001	7.011	28	552.4	<0.0001	7.954	28
381	<0.0001	6.566	28	567.4	<0.0001	5.378	28
496.4	<0.0001	9.35	28	581.4	<0.0001	8.287	28
543.2	0.0001	4.505	28	582.2	0.001	3.693	28
543.4	<0.0001	7.403	28	582.4	<0.0001	7.059	28
713.4	<0.0001	7.089	28	583.4	<0.0001	5.008	28
714.4	<0.0001	6.979	28	595.4	0.04	2.154	28
743.4	0.0298	2.289	28	597.4	<0.0001	8.719	28
744.4	<0.0001	4.645	28	598.4	0.0007	3.83	28
773.4	<0.0001	8.914	28	611.4	<0.0001	15.58	28
775.4	0.0316	2.263	28	612.4	<0.0001	23.84	28
				613.4	0.3	1.056	28

The results for the DI-ESI-MS can be seen in Table 3.6, Figure 3.22, and Figure 3.23. Overall, all bins identified were statistically different between sample classes.

Table 3.6 Results of t-test applied to discriminant pre-fermentation bins (left table) and post-fermentation bins (right table) of DI-ESI-MS positive mode. P value significant if $p < 0.05$; df = degrees of freedom; t = t value

<i>Bin</i>	<i>p value</i>	<i>t</i>	<i>df</i>
120	0.0001	4.41	28
381	0.0003	4.073	28
382	0.0002	4.238	28
383	0.0003	4.183	28
474.2	<0.0001	6.171	28
496.2	<0.0001	10.4	28
497.2	<0.0001	10.76	28
520.2	<0.0001	10.83	28
522.2	<0.0001	9.091	28
534.2	<0.0001	9.388	28
535.2	<0.0001	9.097	28
558.2	<0.0001	9.719	28

<i>Bin</i>	<i>p value</i>	<i>t</i>	<i>df</i>
58	0.0003	4.175	28
70	<0.0001	4.563	28
152	<0.0001	8.45	28
258	<0.0001	6.427	28
268	<0.0001	7.286	28
280	<0.0001	8.108	28
296	0.0004	3.976	28
309.2	<0.0001	8.305	28
322	<0.0001	4.659	28
407	<0.0001	5.428	28

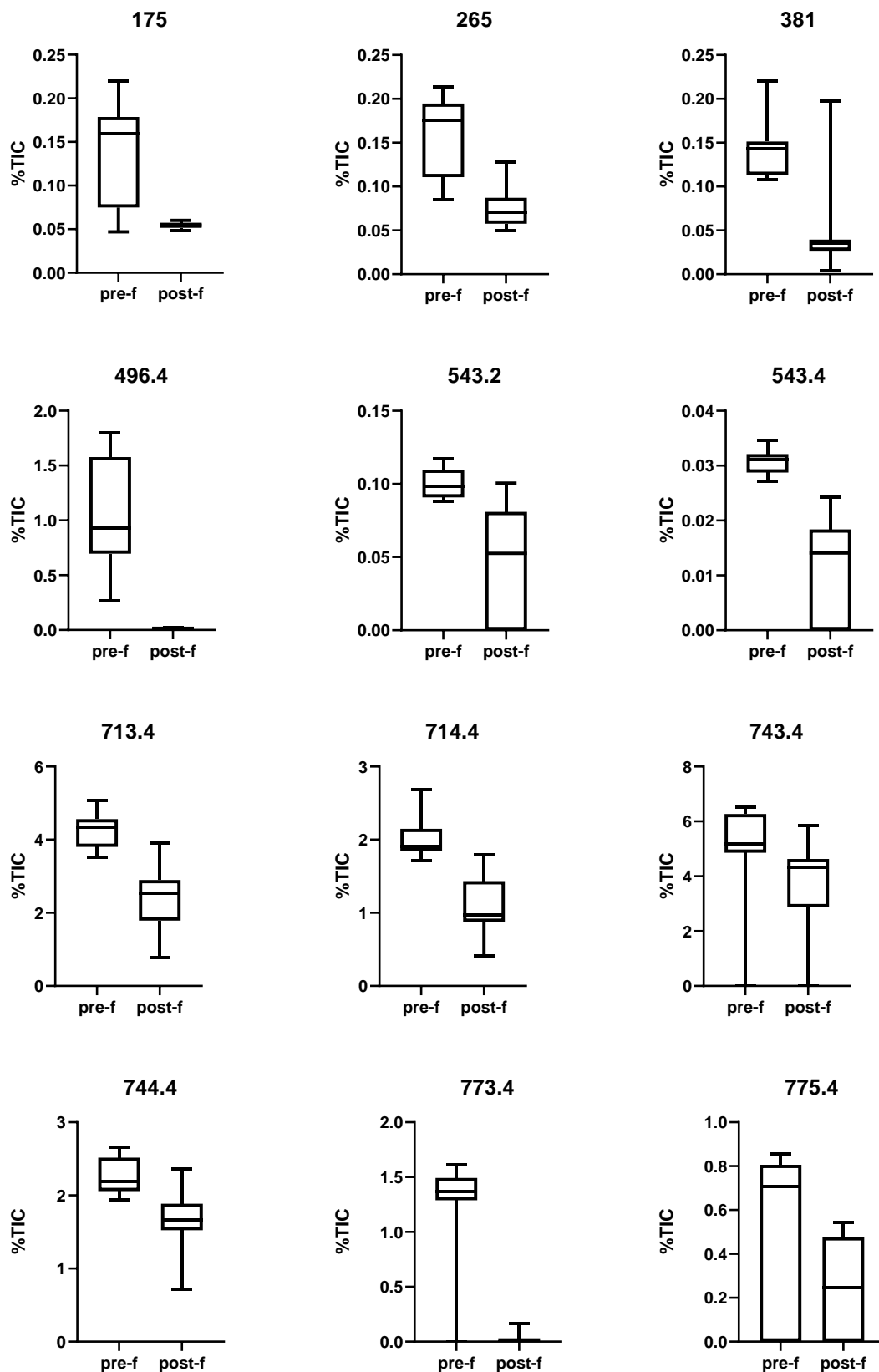


Figure 3.20 Boxplots of the average %TIC detected at each discriminant bin of the pre-fermentation sample class (MALDI-MS positive mode). Upper and lower whiskers indicate upper and lower quartiles respectively; the rectangle represents the middle quartile range divided by the median value.

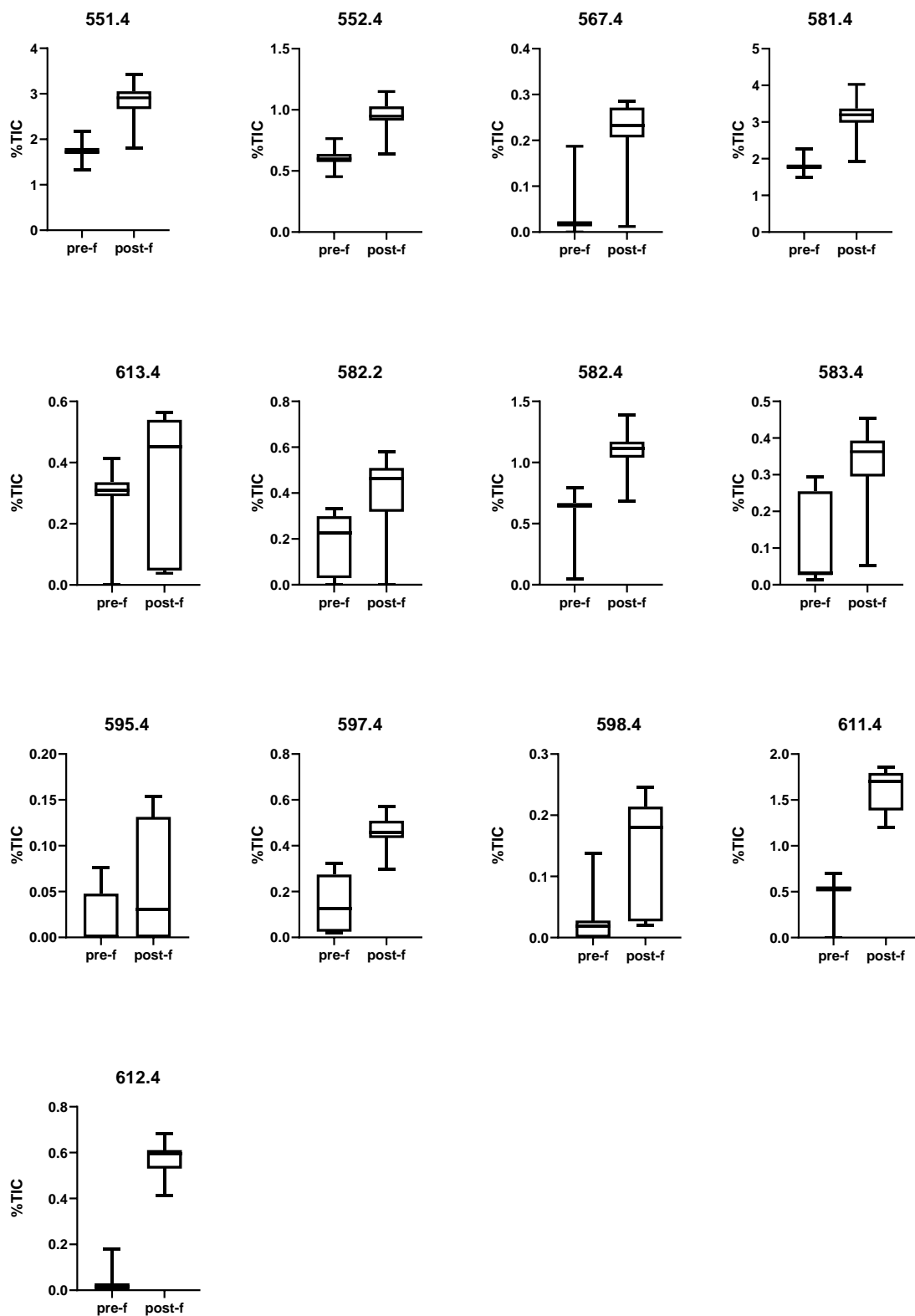


Figure 3.21 Boxplots of the average %TIC detected at each discriminant bin of the post-fermentation sample class (MALDI-MS positive mode). Upper and lower whiskers indicate upper and lower quartiles respectively; the rectangle represents the middle quartile range divided by the median value.

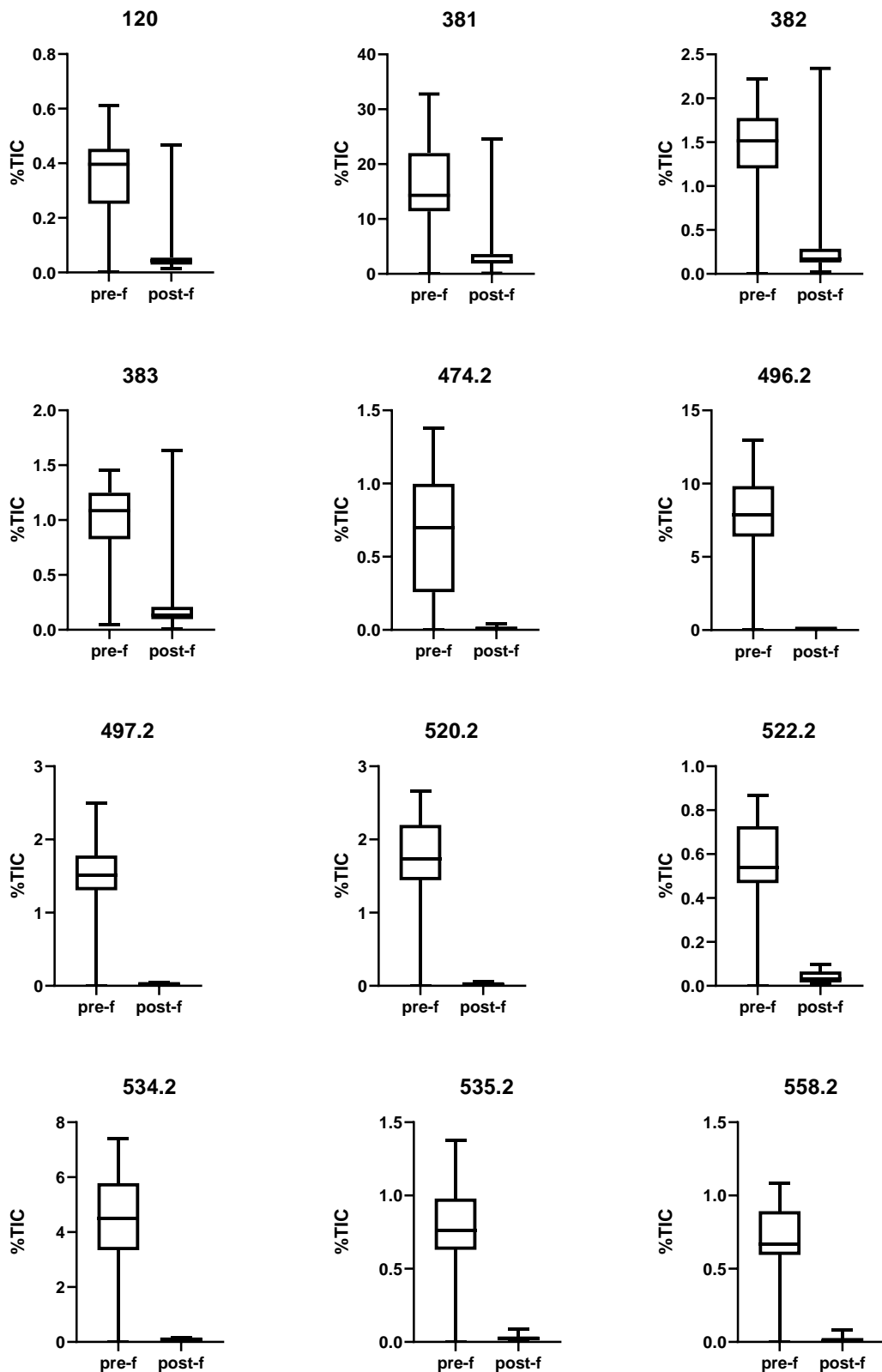


Figure 3.22 Boxplots of the average %TIC detected at each discriminant bin of the pre-fermentation sample class (DI-ESI-MS positive mode). Upper and lower whiskers indicate upper and lower quartiles respectively; the rectangle represents the middle quartile range divided by the median value.

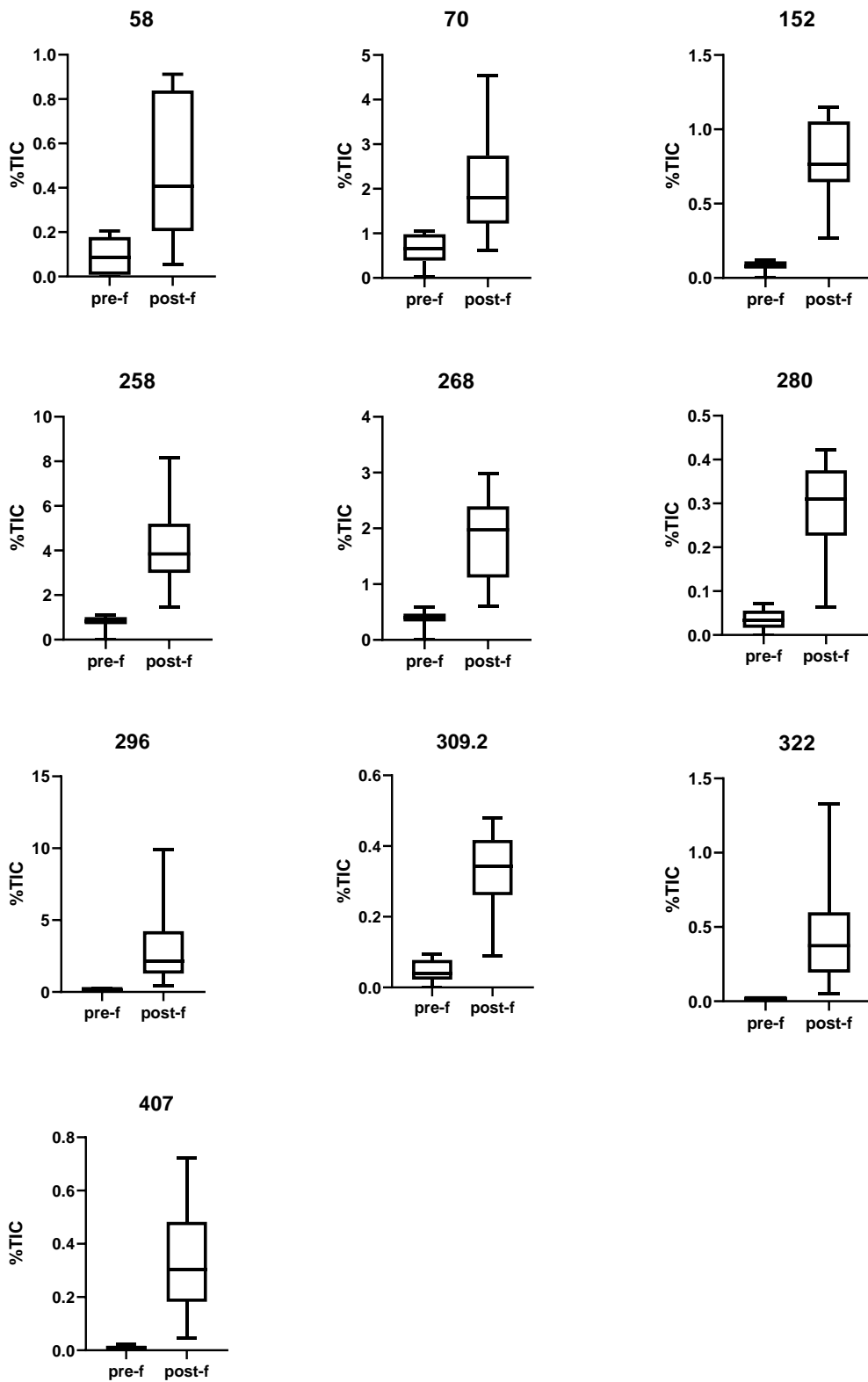


Figure 3.23 Boxplots of the average %TIC detected at each discriminant bin of the post-fermentation sample class (DI-ESI-MS positive mode). Upper and lower whiskers indicate upper and lower quartiles respectively; the rectangle represents the middle quartile range divided by the median value.

3.3.4 Data processing and putative identification of discriminant compounds

After data pre-processing, the discriminant features obtained from each MS and were annotated using the internal database developed, the HMDB, FooDB, and YMDB.

The MALDI-MS (positive mode) and DI-MS data resulted in discriminant bins for each sample class. All the masses detected in each discriminant bin were considered and searched for in three reference compound databases: the in-house flavour database previously developed, FooDB, and YMDB. An important assumption made during the annotation process was to consider the detected masses as either the molecular/parent ion of potassium $[M+K]^{1+}$, sodium $[M+Na]^{1+}$, and hydrogen $[M+H]^{1+}$ adducts only. The molecular weight tolerance was ± 30 ppm. The ppm threshold for identifying compounds used in MS is not a measure of concentration as it is traditionally used in chemistry, but a measure of the difference in the mass detected as a function of the mass expected. This process of identification corresponds to a level 2 according to the Metabolomics Standard Initiative (Sumner *et al.*, 2007). Level 2 annotation is when only one analytical measurement matches to the candidate compound, in this case the adduct's m/z . The full lists of putatively identified compounds can be seen in the Appendix (Table 7.1, Table 7.2, Table 7.3, Table 7.4).

Chemical classification of putatively identified compounds was done via the ClassyFire web-based application for automated structural classification of chemical entities (Djoumbou Feunang *et al.*, 2016) in where each compound's SMILES was inputted into the ClassyFire labelling engine and a category was chosen from the classification section; furthermore, in order to simplify and reduce the number of categories required to be plotted and analysed some compounds were lumped together into a higher parent class.

Afterwards, the matching tables of compounds were shortened through a manual process of elimination based on how contextually relevant each compound may be to the sample (wort and beer). The criteria used to shorten the list was whether the compound was found in cereal plants like wheat, barley, oats, etc.; product of roasting, baking, cooking, etc.; had relevant flavour descriptors; or is a product of fermentation or detected in alcoholic beverages. With this additional shortlisting process based on relevance to the sample the putative identification can be considered as "near positive" (Wishart, 2011).

For the MALDI-MS run pre-fermentation sample class, a total of 68 compounds were putatively identified belonging to 22 distinct chemical classes. The compounds range from carbohydrates, phenolic compounds, nitrogenous compounds, lipids, carbonyl compounds, and sulphur compounds. The overall distribution can be seen in Figure 3.24.

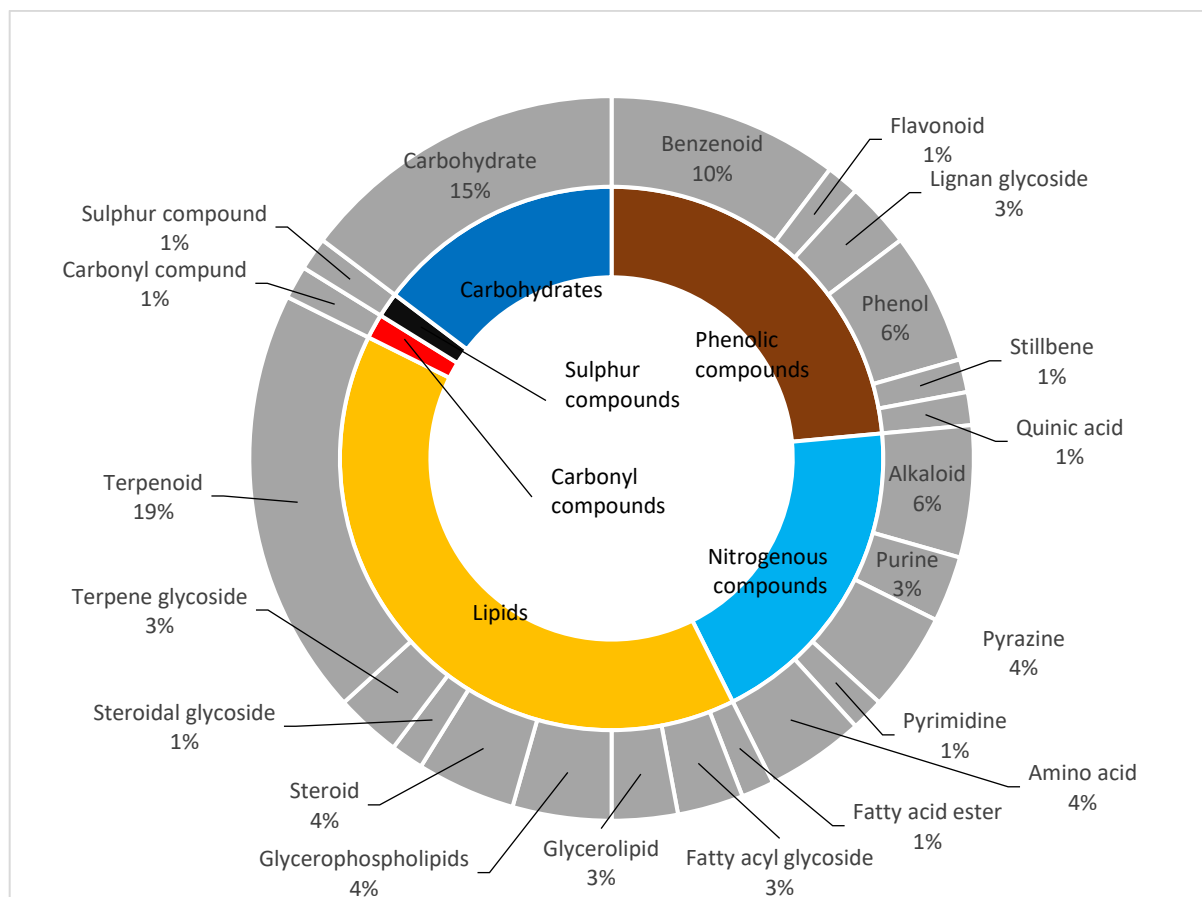


Figure 3.24 MALDI-MS pre-fermentation chemical class proportional distribution of putatively identified compounds. Outer ring show the chemical class and inner ring shows the parent class.

For the MALDI-MS run post-fermentation sample class, a total 76 compounds were putatively identified belonging to 14 distinct chemical classes. The compounds range from phenolic compounds, nitrogenous compounds, and lipids. The overall distribution can be seen in Figure 3.25.

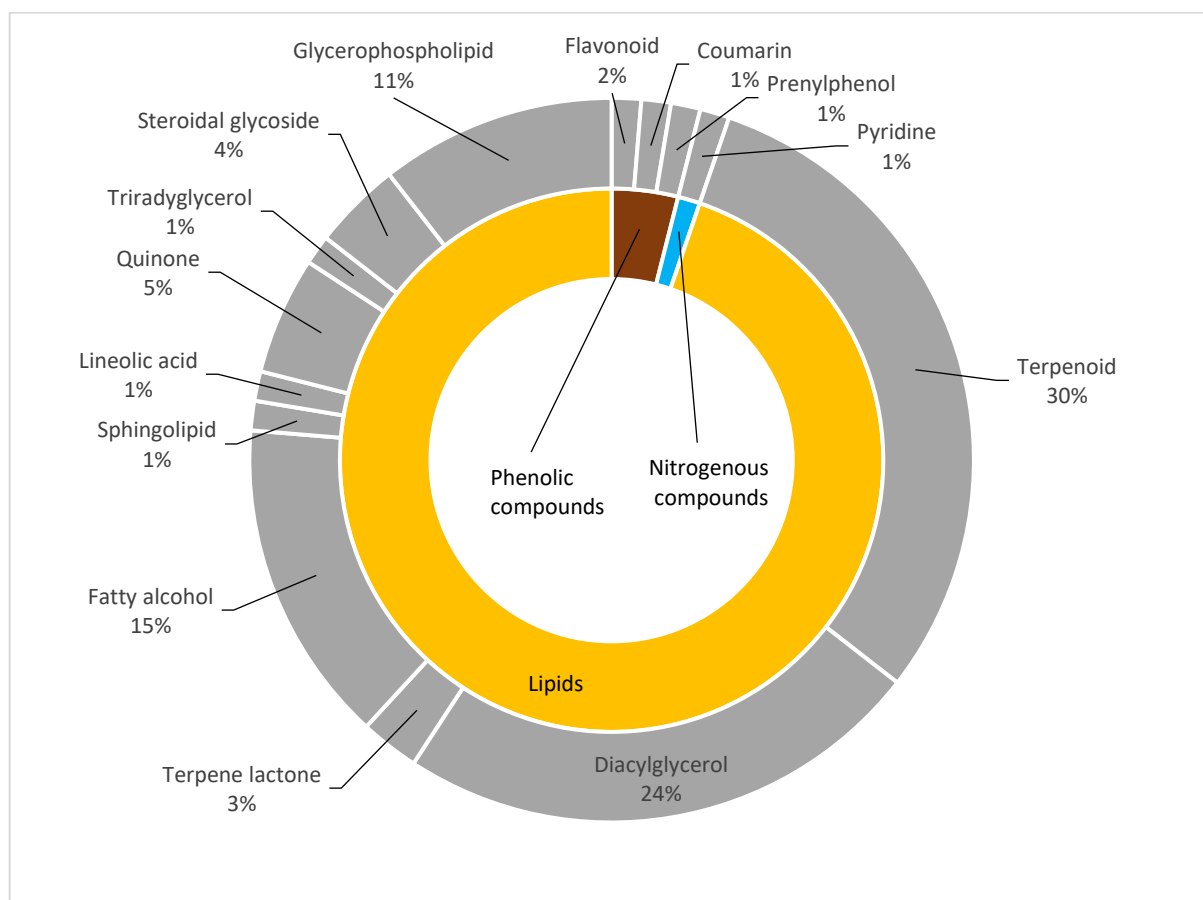


Figure 3.25 MALDI-MS post-fermentation chemical class proportional distribution of putatively identified compounds. Outer ring show the chemical class and inner ring shows the parent class.

For the DI-MS run pre-fermentation sample class, a total of 69 compounds were putatively identified belonging to 24 distinct chemical classes. The compounds range from carbohydrates, phenolic compounds, nitrogenous compounds, lipids, and carbonyl compounds. The overall distribution can be seen in Figure 3.26.

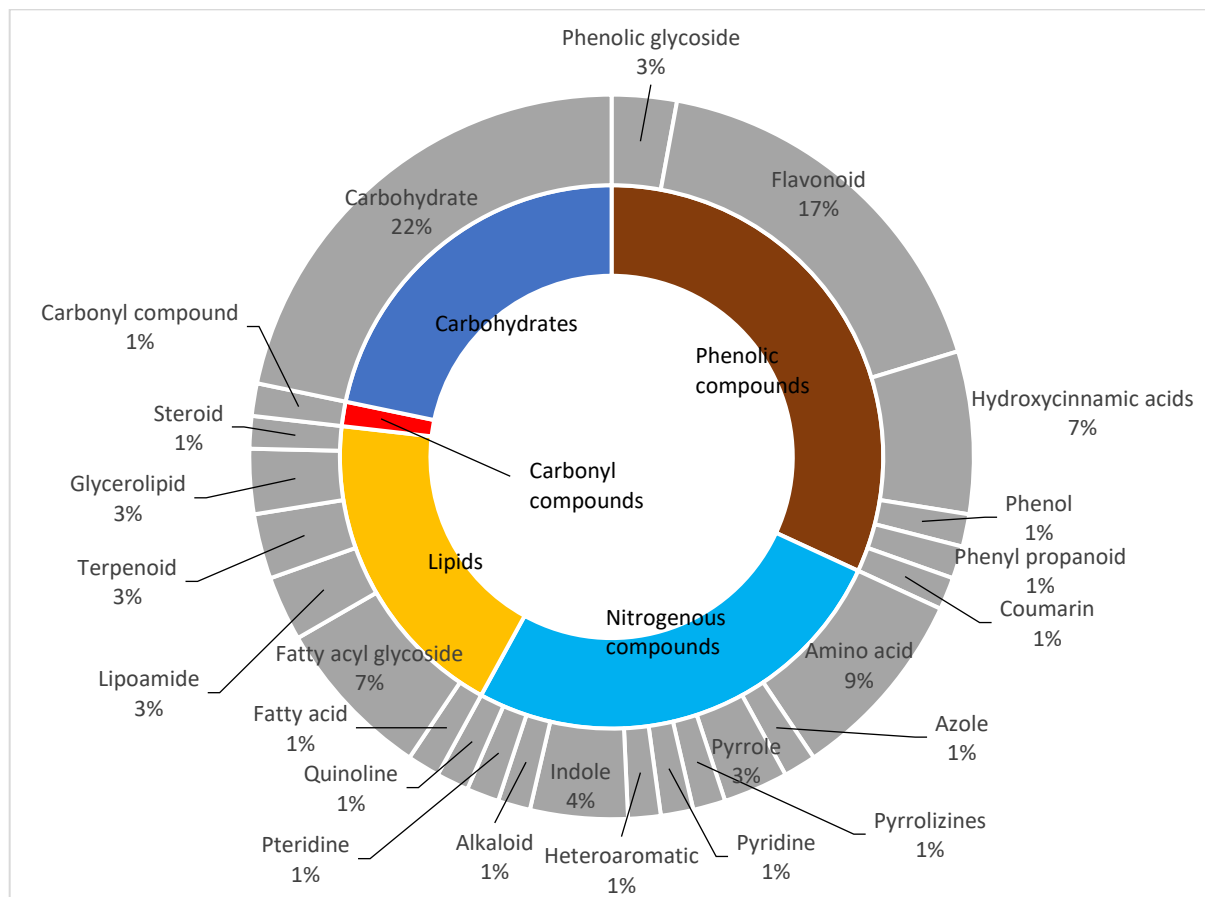


Figure 3.26 DI-ESI-MS pre-fermentation chemical class proportional distribution of putatively identified compounds. Outer ring show the chemical class and inner ring shows the parent class.

For the DI-MS run post-fermentation sample class, a total of 41 compounds were putatively identified belonging to 25 distinct chemical classes. The compounds range from carbohydrates, phenolic compounds, nitrogenous compounds, lipids, sulphur compounds, and carbonyl compounds. The overall distribution can be seen in Figure 3.27.

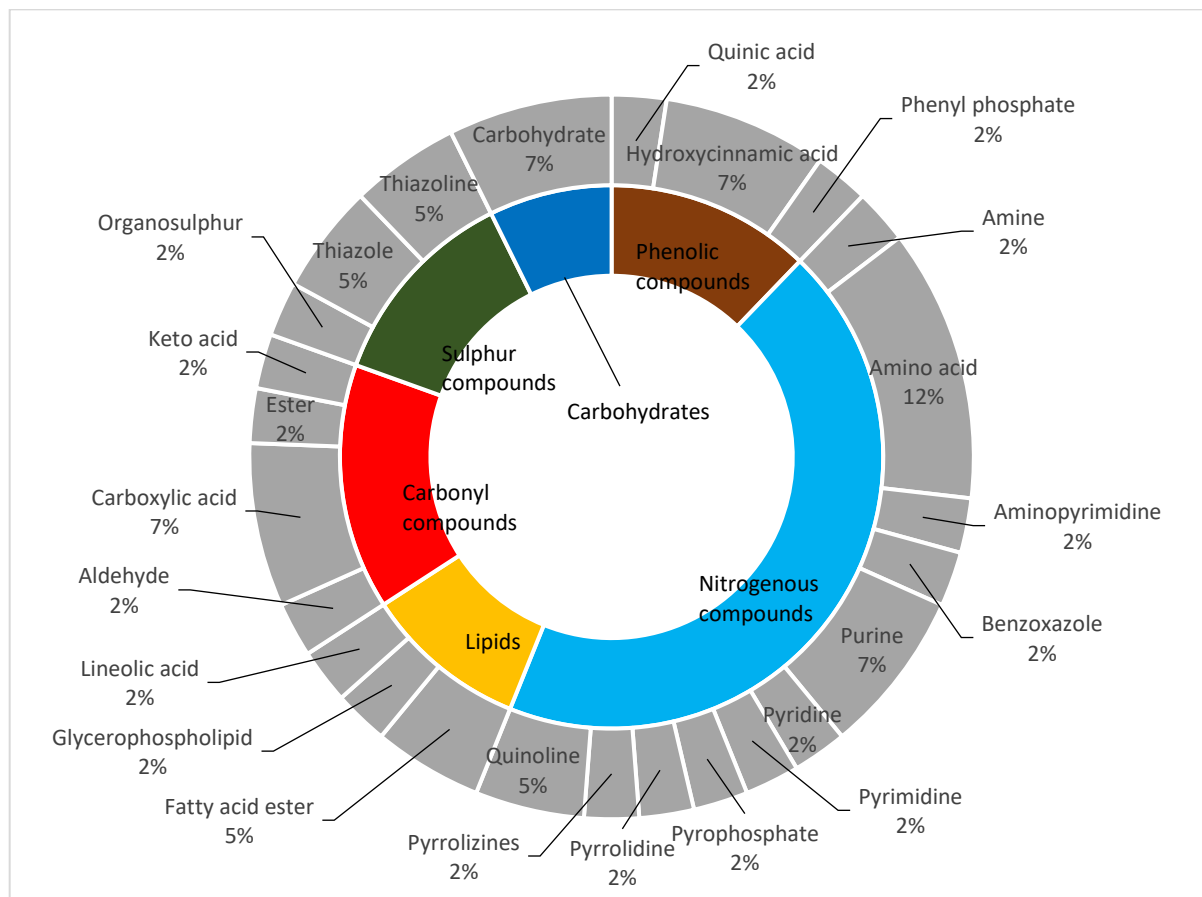


Figure 3.27 DI-ESI-MS post-fermentation chemical class proportional distribution of putatively identified compounds. Outer ring show the chemical class and inner ring shows the parent class.

It is important to state that the distribution of chemical classes previously showed includes isomeric forms of compounds identified in each discriminant bin and therefore does not represent a real proportion of the chemical diversity of each sample class in absolute terms. There is no reason to believe all isomers are present in the sample or even a single one. The selection of contextually relevant compounds in each bin went through a process of elimination that is entirely subject to individual criteria and bias. This fact is unavoidable with the nature of the data obtained as no other targeted experiments were conducted to confirm the identity of the discriminant bins.

3.4 Discussion

The brewing method developed in the brewing chapter was designed and sampled in a way that would allow the elucidation of the chemical composition of wort and beer throughout key stages in the brewing process. The PCA of both techniques resulted in only two sample clusters (labelled pre-

fermentation and post-fermentation) instead of the expected ten sample classes. These results may be explained several ways. It could be that the sampling time-window chosen is too long and the changes are happening in a shorter time interval; this can be inferred by how the physical-chemical parameters measured in Chapter 2 remain relatively constant after the F1 sample. It could also mean that the binning algorithm used to pre-process the MS raw data is masking the subtle changes amongst metabolites with similar m/z which is highly likely in compounds that are consecutive in reaction pathways.

However, the MVA and data processing workflow implemented was successful in the identification of statistically significant bins discriminant for each sample class. The significant differences between the two sample classes is also evident in the changes of relative %TIC of the discriminant mass bins. In both MS methods the separation between sample classes can be confidently tied to the action of the yeast and its metabolism. This can be inferred by the reduction of the carbohydrates in the overall distribution between the pre- and post-fermentation sample classes in both MS runs. A clear example is the reduction of D-maltose (identified in bin 381) which is the main source of carbon in yeast metabolism. However, other mechanisms should also be in play in order to explain the rise and fall of the other chemical classes identified.

The two MS techniques resulted on a markedly difference in the proportion of discriminant chemical classes identified. This shows a clear ionisation preference between both techniques. The logic behind the structuring of this discussion is to use the variation in the chemical class proportions found in each discriminant class and try to find interactions between the putatively identified compounds that are relevant in the formation or degradation of flavour compounds relevant to beer and wort. The relative intensities detected in the MS runs were not taken into consideration as an indication of importance or significance because the role each flavour compound has is related to its flavour threshold and concentration. Relative intensity can be used to indirectly get a measure of abundance in the sample but since no calibration curve was used with pure standards no concentration data can be calculated from the data. Some compounds putatively identified could not be discussed in deeper detail because no relevant explanations and interactions could be found in the literature relevant to flavour formation in beer, wort, or other related foods.

In bin 551, 567 (Table 7.2) the lipid biomolecules comprised 40% pre-fermentation class and 95% of the post-fermentation compounds in the MALDI-MS. In contrast to the reduction from 19% to 10% found in the pre- and post-fermentation samples respectively in the DI-MS. Most of the unique classes within the lipids are semi-polar amphipathic compounds with various functional groups. Considering the knowledge known of beer biochemistry, the results obtained for the MALDI-MS post-fermented

sample indicate a clear sampling error and the lipid content could be explained by yeast's cell membrane debris present in the sample; either by using an uncentrifuged sample with a significant amount of yeast cells suspended in the sample or by cell membrane debris.

Various sized tri- and diacylglycerols which are associated with the phospholipid metabolic pathway in yeast. Lipid content in beer is associated with potential off-flavour and staling compound formation through various oxidation pathways.

Carbonyl compounds were a small percentage of the compounds detected in both techniques. They comprised 1% of the pre-fermentation samples in both MS runs. Their proportion rose to 15% in the post-fermentation samples in the DI-MS. However there were no carbonyl compounds discriminant for the MALDI-MS post-fermented samples; it is surprising that carbonyl compounds were not identified in this sample class as it is well known that carbonyl compounds are product of lipid oxidation and yeast metabolism and are present in beer (Vanderhaegen *et al.*, 2006; Olaniran *et al.*, 2017). Fatty acid esters were identified in bins 152 and 309.2 (Table 7.4) ethyl-2-butenate and ethyl pentadecanoate respectively; these are volatile compounds product of yeast metabolism (reactions between ethanol and carboxylic fatty acids) with typically pleasant sweet aromas. A keto-acid (2-Keto-3-methyl-valerate) and the aldehyde 4-Acetamidobutanal were also identified in bin 152 (Table 7.4) and are involved in the Strecker degradation. Another notable carbonyl compound identified in bin 258 (Table 7.4) is pantothenic acid, a known vitamin and essential nutrient present in many foods; it is a precursor in the synthesis of coenzyme-A and is important in the characteristic bitter, astringent, and salty flavour of yeast.

Nitrogenous compounds comprised 19% and 26% of the compounds identified in the pre-fermented samples in MALDI-MS and DI-MS respectively. As with the carbonyl compounds the nitrogenous compounds were inconsistent between the two MS runs. Their proportion grew to 44% in the DI-MS and decreased to 1% in the MALDI-MS.

The majority of the nitrogenous compounds detected are products of the Maillard reaction. Some are specifically derived from reactions involving proline and 5-methylfurfural; bins 184 (Table 7.3), 258 (Table 7.4), and 309.2 (Table 7.4). While the heteroaromatics identified do not have reported flavour descriptors, 5-methylfurfural is a flavouring ingredient with almond, caramel, burnt, and spice flavours (Yahya, Linforth and Cook, 2014); its derivatives detected in bin 184 may potentially have similar flavour descriptors and have not been previously identified in wort or beer.

The phenolic compounds comprised 22% and 32% of the proportion of identified compounds of pre-fermented samples in MALDI-MS and DI-MS respectively; in both MS runs the proportion

decreased to 4% and 12%. The phenolic compounds identified are varied and participate in different metabolic pathways.

Compounds involved in the lignin biosynthesis were found in bin 381 and 543 (Table 7.1 and Table 7.3) both in pre-fermented samples. Coniferin is a glucoside of coniferyl alcohol and Matairesinose are intermediates in cell wall lignification found in many foods and vegetables. These compounds have not been previously identified in beer and are most likely released during malting and could play a role in the colloidal stability of beer by interacting with peptides and affecting the haze in beer (Briggs *et al.*, 2004).

Several compounds related to hydroxycinnamic acids have been identified. Glucocaffeic acid (identified in bin 381) (Table 7.3) is a hydroxycinnamic acid (from caffeic acid) attached to a glycosyl moiety with astringent, sour, and bitter flavour descriptors. Caffeoyl tyrosine identified in bin 382 (Table 7.3) is a cinnamic acid amide probably formed by the reaction between tyrosine and caffeic acid through an unknown mechanism during mashing. Feruloylquinic acid (identified in bin 407 DI-MS post-fermentation) (Table 7.4), is a quinic acid derivative esterified to ferulic acid; this compound has been identified but not quantified in barley and corn (Duke, 2016). Ferulic acid is a known flavour precursor known to be released from the polysaccharide arabinoxylan by action of cinnamoyl esterases (EC 3.1.1.73). The trimer 2'-(E)-Feruloyl-3-(arabinoxylxylose) was also identified in bin 497.2 (Table 7.3) which has the xylose and arabinose residues. It is unexpected to find two apparently unrelated ferulic acid copolymers, one with quinic acid and one with the already well known pentose residues from the AX main structure; this would suggest that there could be another source of ferulic acid from which it is being solubilised and released into wort or that quinic acid and ferulic acid (derived from AX) are interacting during the mash through an unknown mechanism.

In bin 175 and 265 (Table 7.1) several flavour active compounds were identified. Two isomers of hydroxyphenylacetic acid, which has no flavour properties reported, were identified along with phenylacetic acid which has civet, floral, flower, honey, sweet, and waxy properties. Phenylacetic acid is the product of the dehydration reaction of hydroxyphenylacetic acid during the metabolism of tyrosine during yeast fermentation. 4-Ethylguaiacol was also identified, it is product of the reduction of 4-vinylguaiacol which is the product of the decarboxylation of ferulic acid; it is surprising to find the end product of this flavour formation pathway in a pre-fermented sample which confirms that enzymatic activity and/or thermal degradation, and not only yeast fermentation, can produce this flavour active compounds.

Hydroxycinnamic acids are product of the metabolism of aromatic amino acids like phenylalanine and tyrosine and are part of the phenylpropanoid metabolism which is ubiquitous in plants. These

compounds are known to play an important role in the process of ripening fruits by affecting their firmness, colour, taste, aroma, and texture (Singh, Rastogi and Dwivedi, 2010). As they are, hydroxycinnamic acids do not have relevant flavour descriptors but are precursors of potent flavour compounds once they undergo decarboxylation. Decarboxylation of hydroxycinnamic acids can occur by thermal degradation during malting and boiling or by the action of yeast fermentation, specifically the POF+ phenotype of *Saccharomyces cerevisiae* and *Brettanomyces/Dekkera* (Heresztyn, 1986; Cabrita *et al.*, 2012). The mechanisms by which these compounds end up in wort and beer's chemical make-up are poorly understood. The phenolic glycosides identified in this experiment could be initial steps into what are the precursors of the hydroxycinnamic acids in wort and beer.

The sulphur compounds comprised 1% of the pre-fermented samples in the MALDI-MS run and were not identified in the DI-MS run; paradoxically they were not identified in the post-fermented samples in the MALDI-MS run and comprised 12% in the DI-MS run. In bin 152 and 268 several thiazole compounds were identified with notable flavour properties. 2,4-Dimethyl-1,3-thiazole, 2-Ethyl-1,3-thiazole, and 2-acetyl-2-thiazoline have bread, chip, corn, nutty, popcorn, potato, roast, taco, and toasted flavour descriptors and are reportedly found in yeast extract. The formation mechanism is probably the Maillard reaction, specifically the condensation of dicarbonyls derived from proline with hydrogen sulphide.

It is surprising that ethanol was not detected as a discriminant compound for the post-fermentation samples in either of the MS runs. Ethanol's positive adducts (and many other known flavour compounds in beer) would fall inside the scanned range of 50-1200 Da. It could be explained by ethanol's low vapour pressure and quick tendency to become volatile. MALDI-MS had a clear ionisation preference towards relatively larger compounds.

It is important to remember that the MALDI-MS sample preparation and analysis was optimized based on the TIC with the intention of detecting the largest number of metabolites disregarding molecular size or tendency to fragmentation. Flavour compounds tend to be relatively small polar molecules and since MALDI is considered a soft ionisation method it was assumed that no fragmentation occurred. In reality the annotation process is confounded by the fact that many ionisation products will be not only molecular ions but also salt/solvent adducts and neutral loss fragments of original metabolites. In the future, strategies that allow annotation based on all potential ionisation products can be used to process metabolomics data and obtain more accurate results (Draper *et al.*, 2009).

3.5 Conclusions

The MS techniques applied to the brewing samples were analysed through a metabolomics workflow. Two distinct sample classes' chemometric profiles were discriminated through unsupervised and supervised MVA. There was a notable difference of the discriminant features identified for each MS technique. It is not surprising due to the differences in sample preparation and operating principles of each technique that will inevitably lean toward to certain ionisation mechanisms. With some paradoxical results and a lack of holistic metabolite identification it is justifiable to analyse the samples with a more targeted and sensitive technique.

This results call for further techniques to be applied to the same samples in order to obtain a more complete analysis of beer's metabolome.

4. Chapter 4: Metabolomics of the liquid phase of brewing samples using ultra performance liquid chromatography – mass spectrometry

4.1 Introduction

Metabolites in wort and beer have the potential to be markers of flavour formation during beer production. The metabolites can be the intermediates, by-products, or end-products of complex flavour formation pathways. It is important to be aware that the true number of organoleptically meaningful compounds in beer is still unknown. The volatile phase contains the majority of the flavour active compounds but the precursors are released or synthesised during the processes of malting and brewing. Due to the complexity of the metabolites involved and the diversity in biomolecules, high resolution separation and analytical techniques are needed to profile the metabolome of biological systems.

High resolution separation techniques coupled with MS techniques with high sensitivity and then combined with MVA can be a powerful tool to identify key compounds. UPLC-MS has been used to profile molecular markers in various populations of malting barley and beer at high temperature storage (Heuberger *et al.*, 2012, 2014). It was demonstrated that some metabolites and quality traits were correlated based on genotype and growing environmental conditions; additionally, a non-volatile metabolite was identified as a candidate to predict oxidation and stale off-flavour development during beer storage.

Metabolomics strategies and MVA have been used to prove that malt's genotype, location of harvest, and degree of modification have an effect on beer's metabolome, sensory profile and flavour stability (Herb *et al.*, 2017; Bettenhausen *et al.*, 2018). However, there are still unknowns in order to establish a causal relationship between relevant genes and biochemical pathways that explain specific flavour profiles. Data indicates that flavour profiles arise by a combination of many flavour-active compounds found in beer.

The data generated in LC-MS based methods contains a signal with both mass and retention time-based specificity, these signals are commonly known as "features". In the absence of co-elution, a feature is assumed to originate from a single compound. Novel algorithms to process high-mass-accuracy data and detect features have been developed (Overy *et al.*, 2004; Smith *et al.*, 2006; Chong *et al.*, 2018); and processing methods to automate the annotation process of the detected features have also been published (Kaeffer *et al.*, 2009; Broeckling *et al.*, 2014), however all methods have assumptions that ultimately lead to bias and information can be lost in the process.

For these reasons, UPLC-MS coupled to a metabolomics workflow tailored to brewing samples has been chosen as an analytical approach to characterize the liquid phase of the samples obtained in Chapter 2. Based on the premise that flavour active compounds are derived from non-volatile and semi-volatile compounds this approach offers an in-depth analysis that can reveal metabolite pathways of flavour formation and their precursors/derivatives. Metabolites identified here can aid the identification of quality markers in beer and its ingredients in the effort of developing and improving brewing and malting processes as well as barley breeding and agronomic practices.

4.2 Materials and methods

4.2.1 UPLC-MS

Brewing samples (see 2.2.1 Brewing2.2) were taken from -80°C storage and freeze dried. Samples were then reconstituted in 1 mL of methanol 95%: distilled water 5% v/v, vortexed and centrifuged to remove the proteins. Afterwards, the supernatant was subjected to an ultra-high pressure liquid chromatography using an ACQUITY SM-FTN coupled to a Synapt G2-Si Q-TOF mass spectrometer with an electrospray (ESI) ionization source (all equipment from Waters, UK). Chromatographic separation occurred in a ACQUITY UPLC® BEH C18 column (2.1 × 50 mm, 1.7 µm). Samples were eluted using a gradient of water to acetonitrile each containing 1% formic acid. The gradient started at 0.1% and held for 1 min, then ramped up to 95% over a total of 11 min at a flow rate of 0.4 mL/min. The entire system was controlled by MassLynx v4.1 software.

Table 4.1 UPLC-MS tune settings

<i>Parameter</i>	<i>Value/Type</i>
Polarity	ESI+
Run time/sample	11 min
Target column temperature	45°C
Capillary	3.000 kV
Source temperature	100°C
Sampling cone	50 kV
Desolvation temperature	280°C
TOF Scan time	1 s
Mass range	50-1200 Da

The technical specification of the Synapt G2-Si Q-TOF mass spectrometer are the following:

Table 2 Synapt G2-Si-Q-TOF technical specifications (Waters Corporation, UK)

<i>Parameters</i>	<i>Value</i>
Operation mode	Time-of-flight Mobility-TOF
Mass resolution	a) 60,000 FWHM in positive mode @ 956 <i>m/z</i> b) 60,000 FWHM in negative mode @ 1431 <i>m/z</i>
Positive ion MS sensitivity	>31,200 ions/s
Negative ion MS sensitivity	>33,600 ions/s
Mass scale calibration accuracy	At high resolution mode <1 ppm at the range of 150-900 <i>m/z</i>
Mass measurement accuracy	>1 ppm RMS with sufficient intensity and resolution
Mass range	Operating at TOF: a) At resolution mode 20-100,000 <i>m/z</i> b) At high resolution mode 20-32,000 <i>m/z</i>
Dynamic range	At high resolution mode better than 3 ppm for 10 s of data acquisition

4.2.2 Data pre-processing and multivariate analysis

Raw data files were converted from the Waters *.raw* folders into mZML files (centroid mode) with ProteoWizard's MSConvert toolkit (Chambers *et al.*, 2012). Afterwards, the raw MS data was aligned and integrated using XCMS Online (Smith *et al.*, 2006; Gowda *et al.*, 2014). XCMS is an open source untargeted metabolite profiling method for LC-MS data; it incorporates nonlinear retention time alignment, matched filtration, peak detection, and peak matching. The raw data files were pre-processed using the pre-set parameters: UPLC – High Res POS (Waters). This pre-set's method for feature detection is centWave ($\Delta m/z = 15$ ppm, minimum peak width = 2 s, and maximum peak width = 25 s); method for retention time correction is obiwrap (profStep = 0.5); and the parameters for chromatogram alignment include bw = 2, minfrac = 0.5, and mzwid = 0.01.

Statistics, annotation, and putative identification of features were completed separately using the resulting peak list from the XCMS pre-processing. MVA was done in SIMCA 14 (Umetrics, Sweden) in the same way as explained in section (3.2.3 Data pre-processing and multivariate analysis).

4.3 Results

The total ion counts (TIC) for the MS run was consistent throughout all samples, indicating reproducibility of the method. Additionally, sufficient ion counts to ensure a good chemometric profile was achieved (Figure 4.1). Example chromatograms and mass spectra can be seen in the Appendix (A3 Chapter 4 UPLC-MS Supplementary Material).

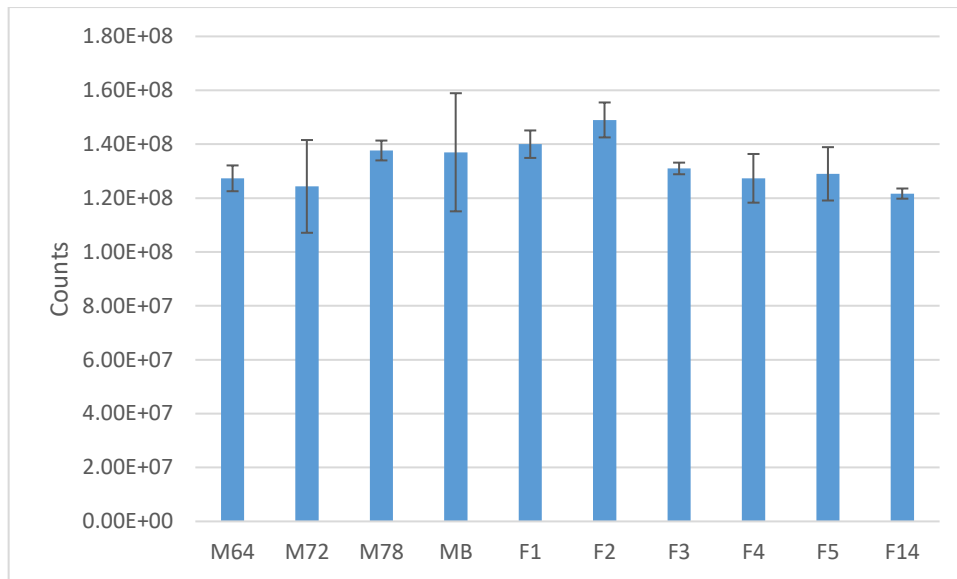


Figure 4.1 Column plot of mean total ion counts in positive mode. Error bars indicate standard deviation.

The overall PCA results can be visualised in Figure 4.2, two principal components with a total variance explained of 69%. The pre-fermented samples clustered mainly in the left side of the plot and the post-fermented samples in the right side. Three distinct sample clusters were identified. The F1 samples cluster in-between the wort and beer sample class. OPLS-DA was done to make pairwise comparisons between the three sample classes identified in order to find the most discriminant features (Figure 4.3, Figure 4.4, Figure 4.5, Figure 4.6, Figure 4.7, and Figure 4.8).

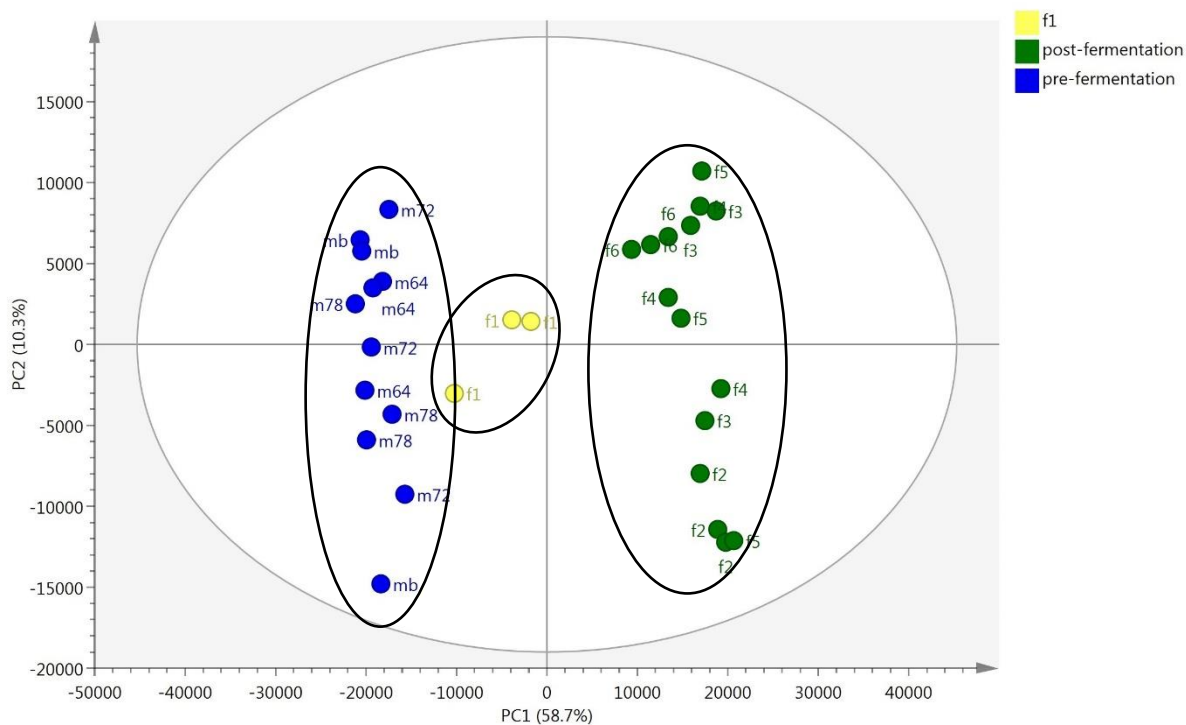


Figure 4.2 PCA score scatter plot. The enclosed samples represent the sample classes identified

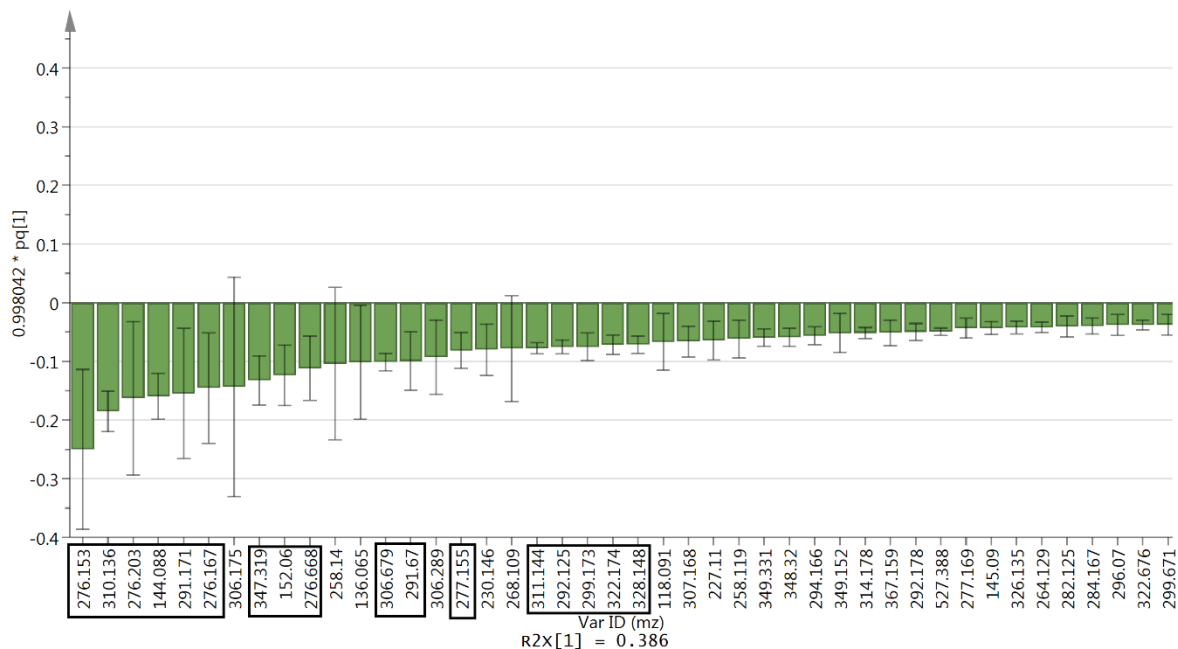


Figure 4.3 OPLS-DA Loadings column plot of the most discriminant features of the post-fermented sample class normalised to unit length (post-fermented-f1 pairwise comparison). Top discriminant bins are enclosed in black and were chosen for annotation based on apparent statistical significance and the standard deviation not crossing into a presence in the other sample class.

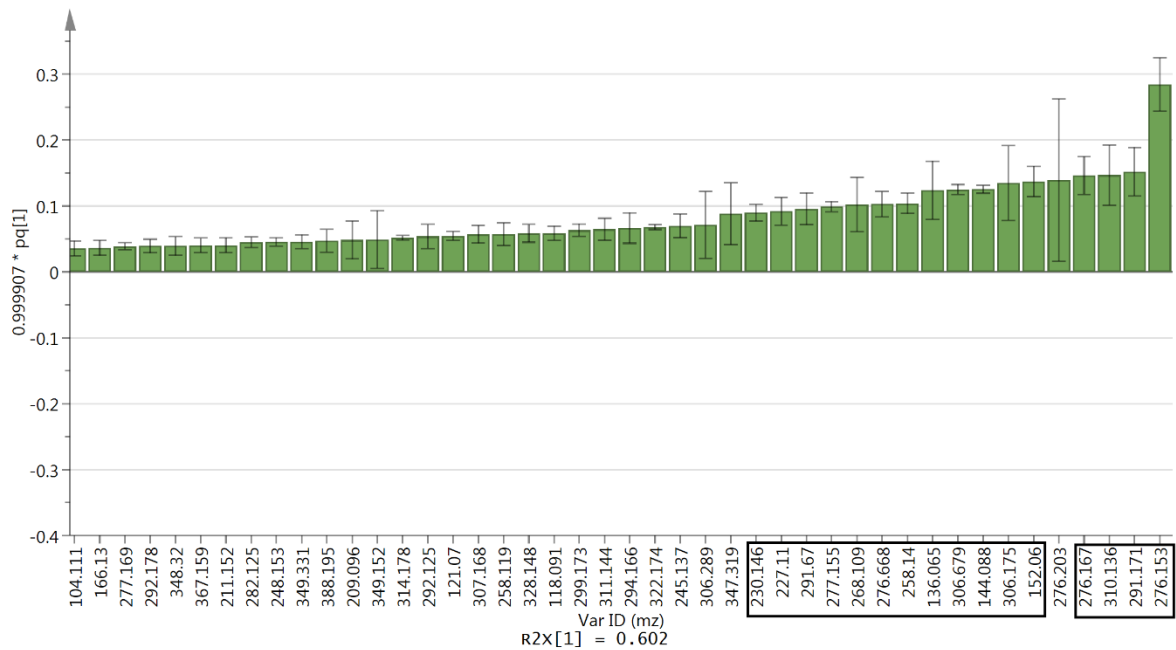


Figure 4.4 OPLS-DA Loadings column plot of the most discriminant features of the post-fermented sample class normalised to unit length (post-fermented-pre-fermented pairwise comparison). Top discriminant bins are enclosed in black and were chosen for annotation based on apparent statistical significance and the standard deviation not crossing into a presence in the other sample class.

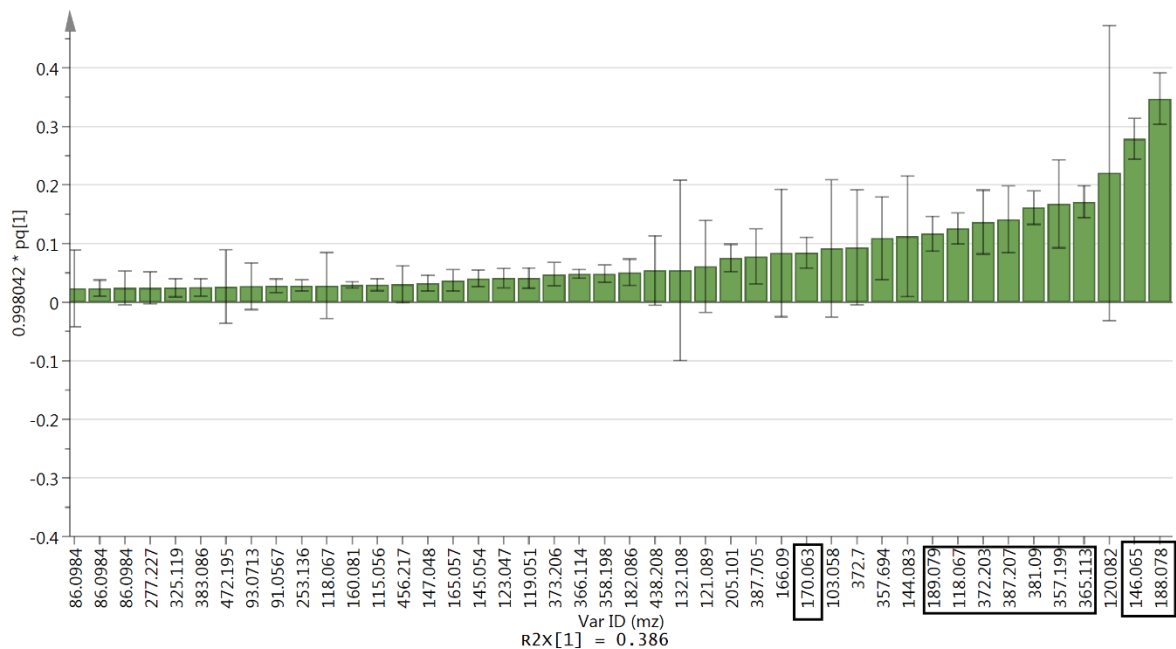


Figure 4.5 OPLS-DA Loadings column plot of the most discriminant features of the F1 sample class normalised to unit length (post-fermented-f1 pairwise comparison). Top discriminant bins are enclosed in black and were chosen for annotation based on apparent statistical significance and the standard deviation not crossing into a presence in the other sample class.

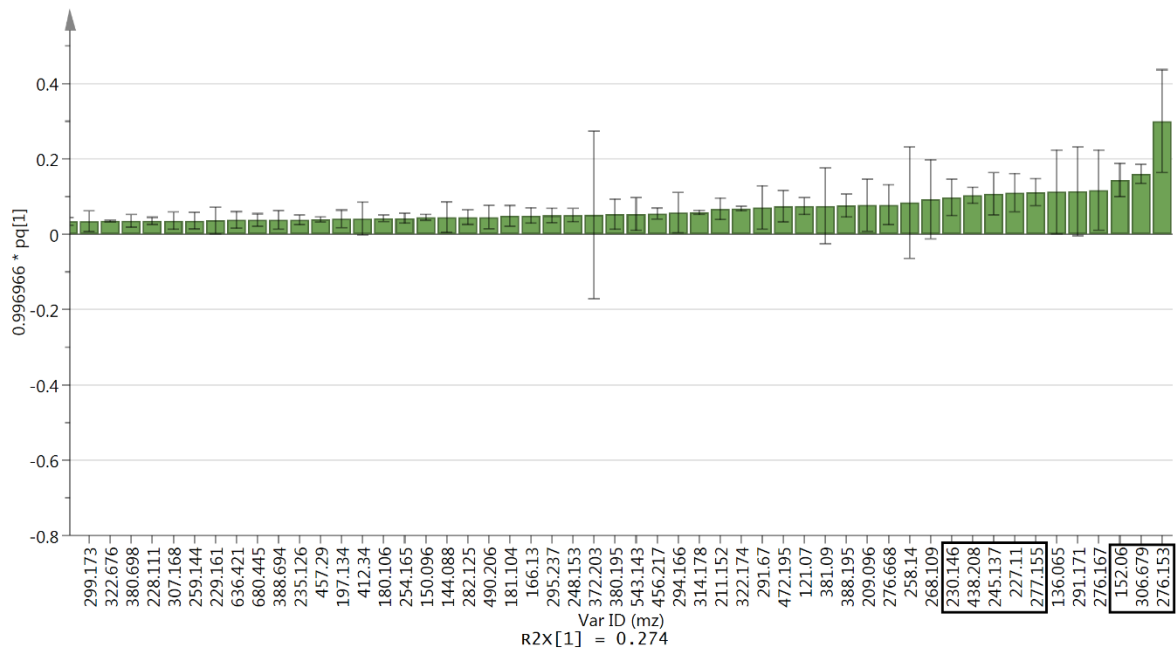


Figure 4.6 Loadings column plot of the most discriminant features of the F1 sample class normalised to unit length (pre-fermented-f1 pairwise comparison). Top discriminant bins are enclosed in black and were chosen for annotation based on apparent statistical significance and the standard deviation not crossing into a presence in the other sample class.

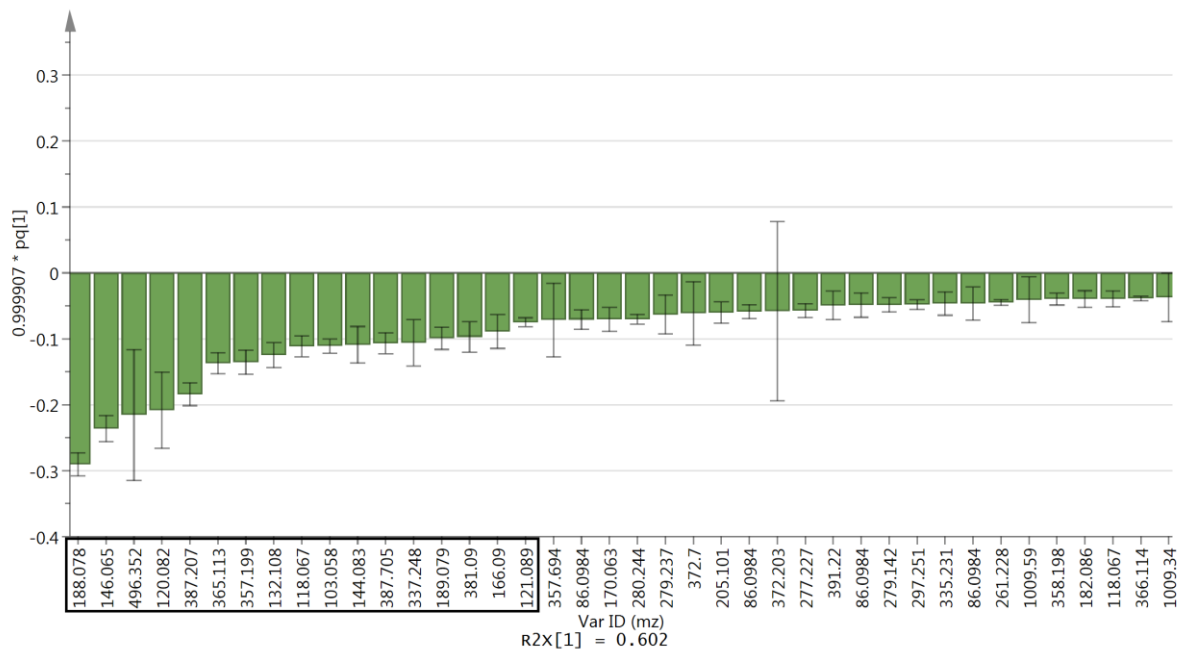


Figure 4.7 Loadings column plot of the most discriminant features of the pre-fermented sample class normalised to unit length (post-fermented-pre-fermented pairwise comparison). Top discriminant bins are enclosed in black and were chosen for annotation based on apparent statistical significance and the standard deviation not crossing into a presence in the other sample class.

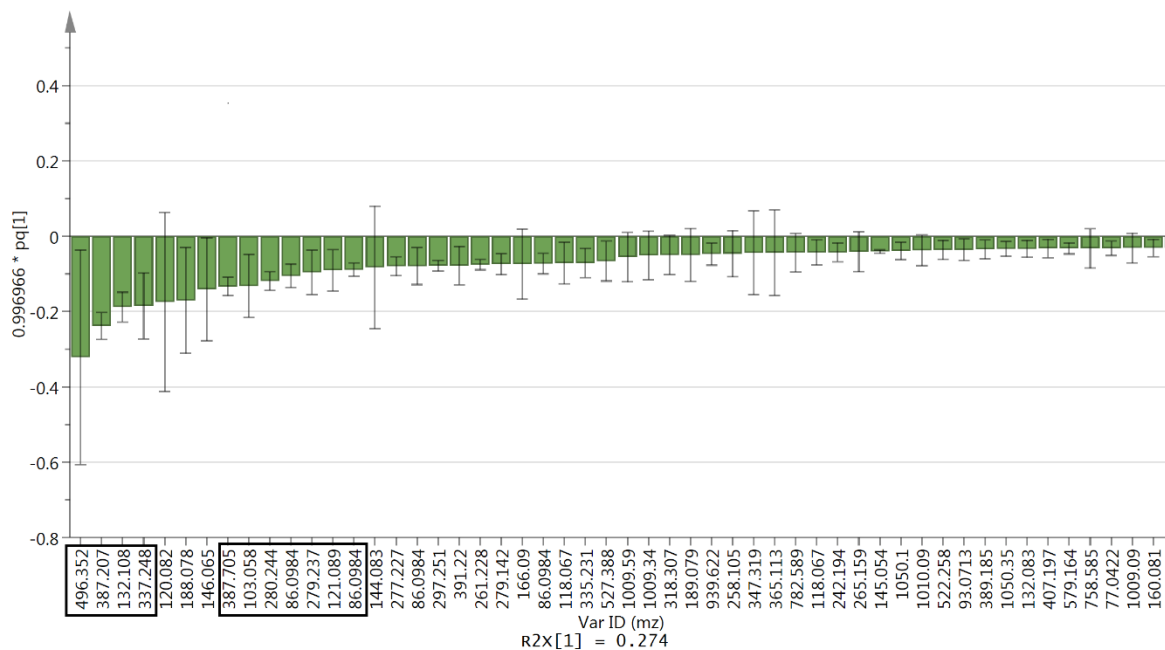


Figure 4.8 Loadings column plot of the most discriminant features of the pre-fermented sample class normalised to unit length (pre-fermented-f1 pairwise comparison). Top discriminant bins are enclosed in black and were chosen for annotation based on apparent statistical significance and the standard deviation not crossing into a presence in the other sample class.

Some discriminant features are shared between the sample classes (Figure 4.9).

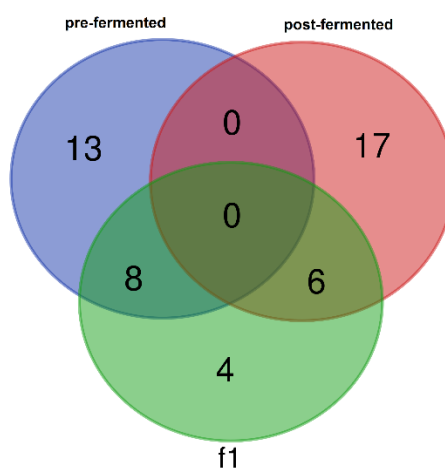


Figure 4.9 Venn diagram of the most discriminant masses of the three sample classes identified

4.3.1 Statistical significance of the relative abundance between sample classes

The relative abundance of the discriminant features was subjected to a one-way ANOVA in order to determine whether or not there is a significant difference between the sample classes. Despite the identification of the most discriminant bins through the supervised multivariate analysis, it is

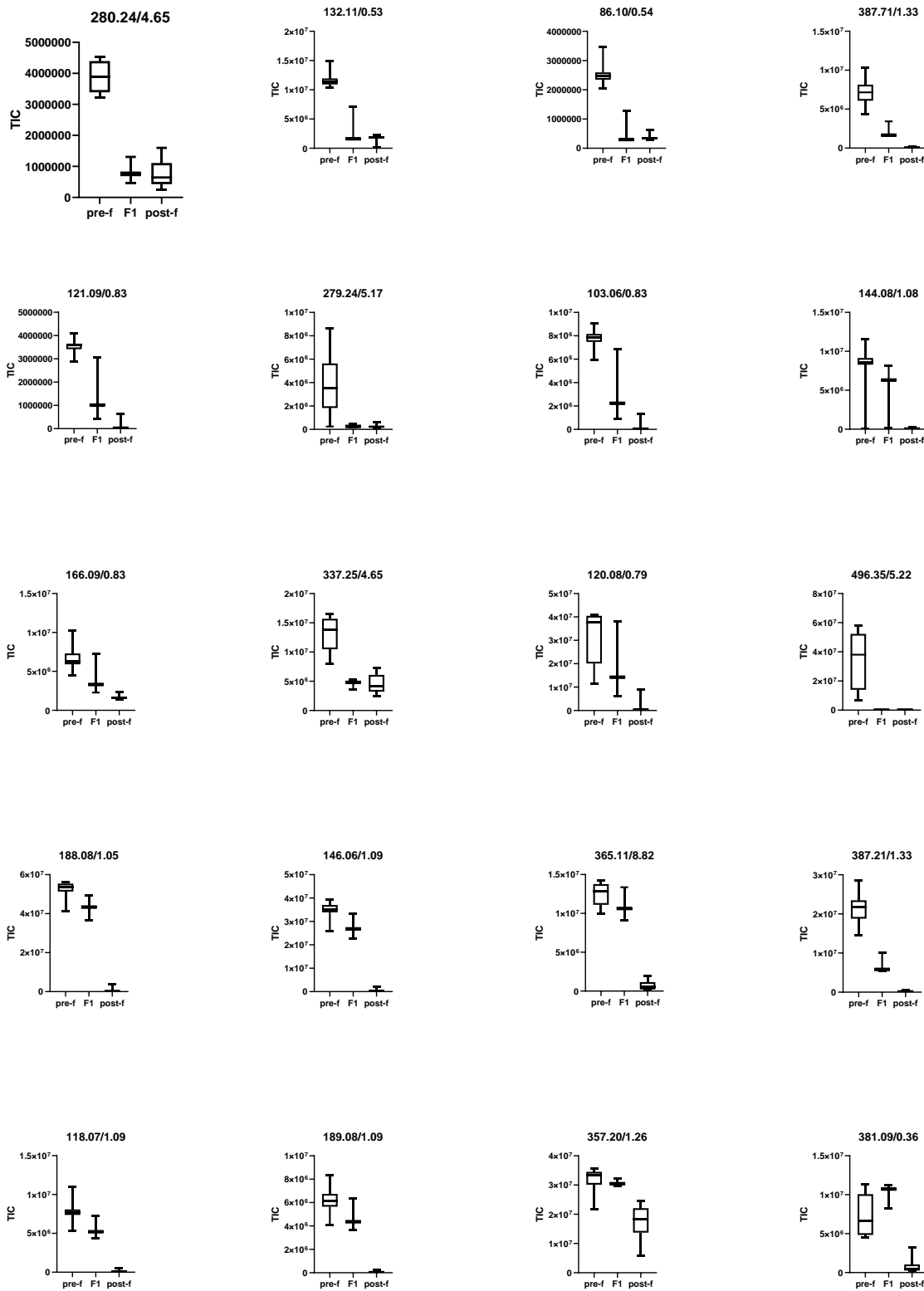


Figure 4.10 Boxplots of the TIC detected at each discriminant feature (mz/rt) of the pre-fermented sample class. Upper and lower whiskers indicate upper and lower quartiles respectively; the rectangle represents the middle quartile range divided by the median value.

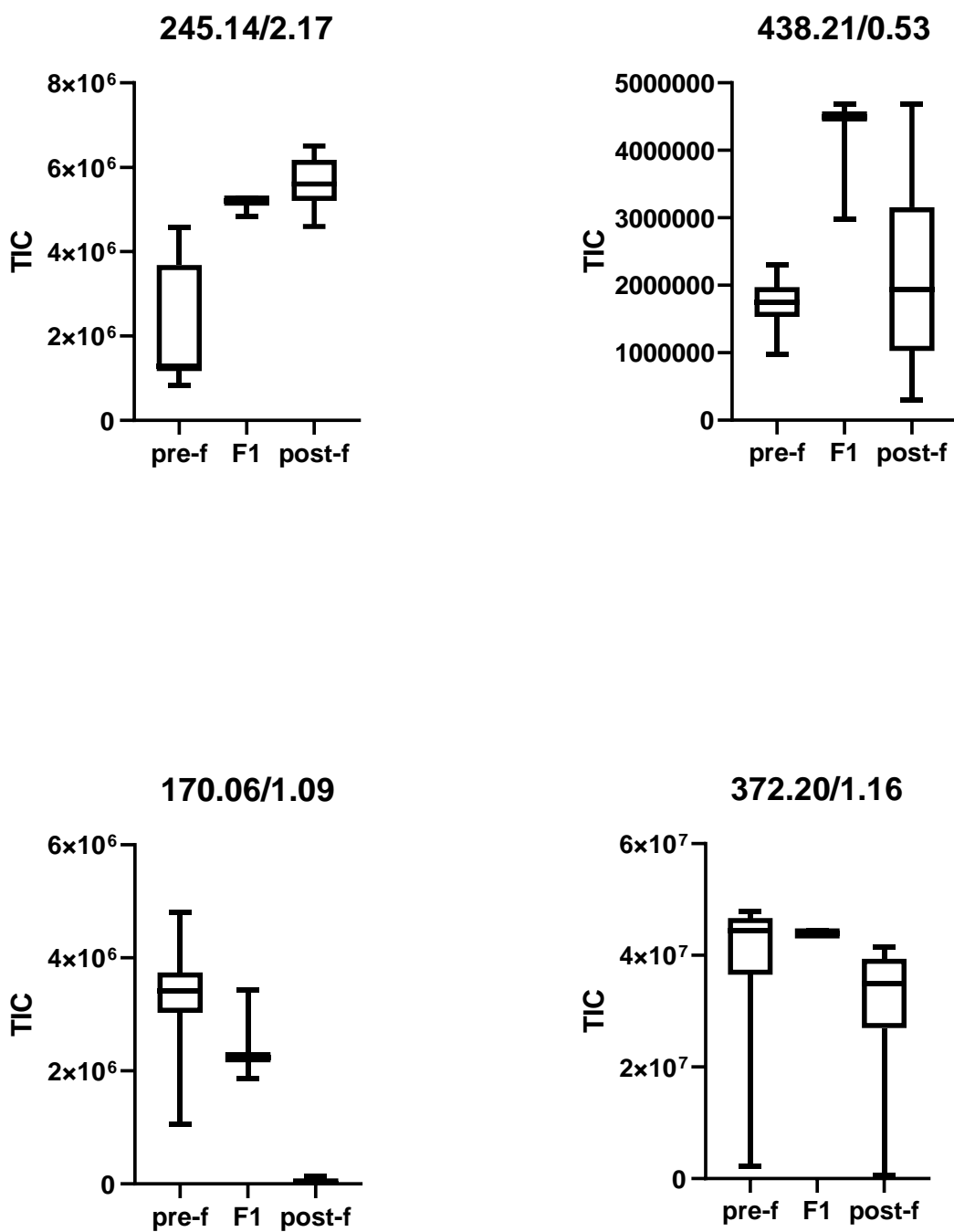


Figure 4.11 Boxplots of the TIC detected at each discriminant feature (mz/rt) of the F1 sample class. Upper and lower whiskers indicate upper and lower quartiles respectively; the rectangle represents the middle quartile range divided by the median value.

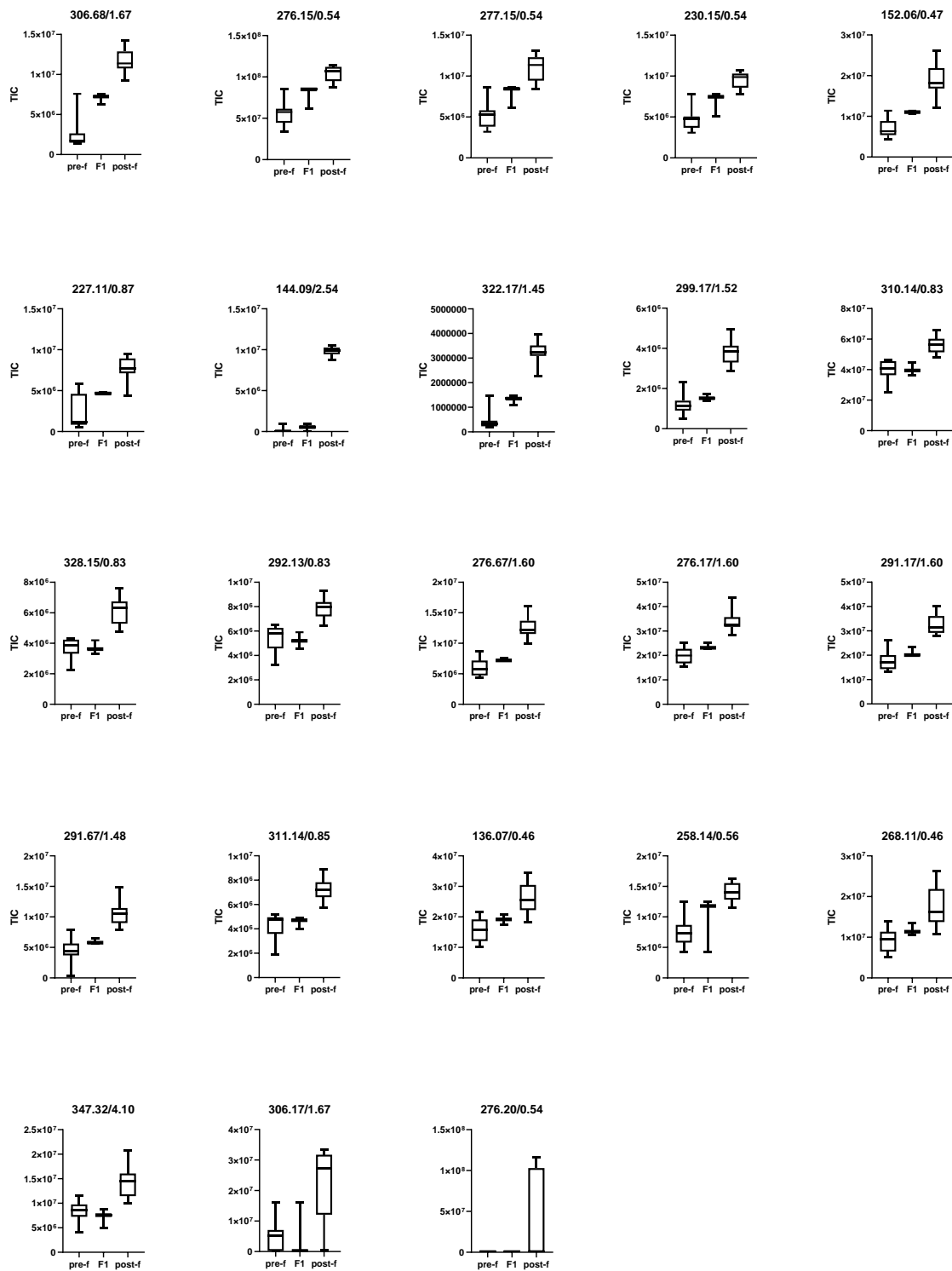


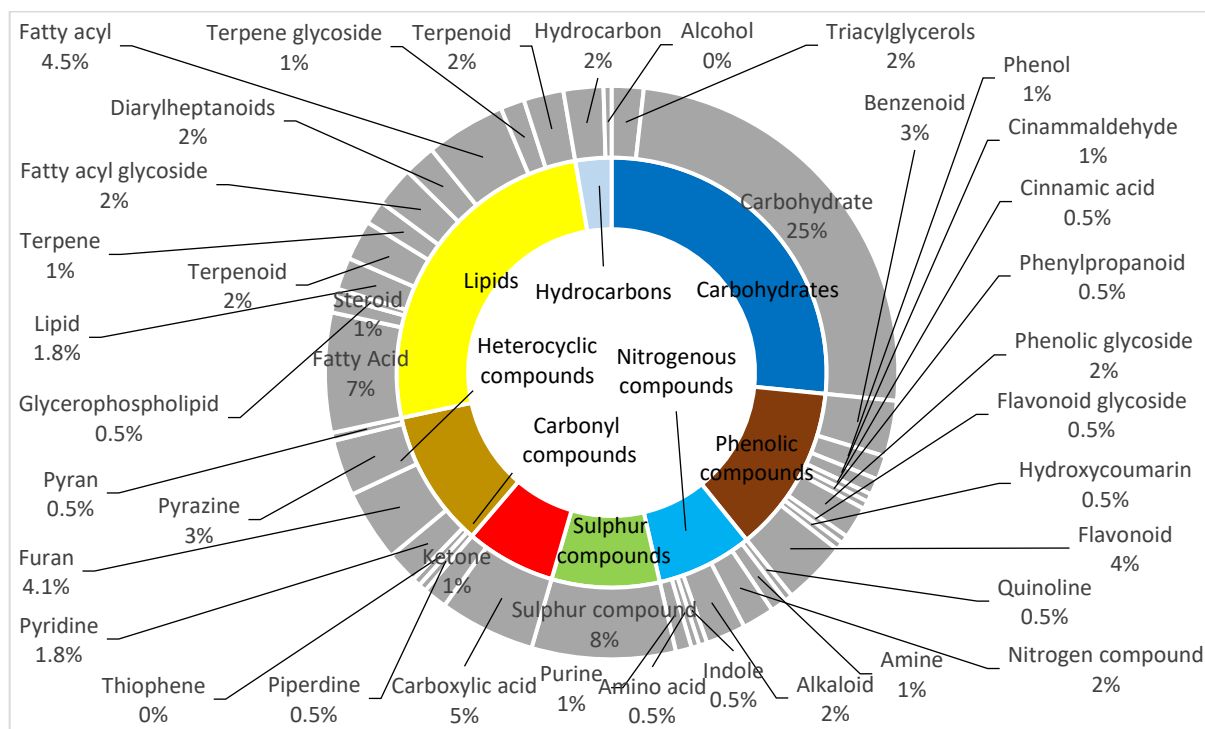
Figure 4.12 Boxplots of the TIC detected at each discriminant feature (mz/rt) of the post-fermented sample class. Upper and lower whiskers indicate upper and lower quartiles respectively; the rectangle represents the middle quartile range divided by the median value.

4.3.2 Data processing and putative identification of discriminant compounds

The discriminant features obtained from the OPLS-DA were annotated using the same criteria described in section (3.3.4 Data processing and putative identification of discriminant compounds) with the only difference being that the ammonium adduct was also considered $[M+NH_4]^{1+}$. This adduct was additionally considered because the data processing was more streamlined, and it was decided to include a wider range of adducts to increase the potential chemical diversity that could be putatively identified. The ammonium adduct was chosen due to its known presence in beer (Briggs *et al.*, 2004).

Chemical classification of putatively identified compounds was done via the ClassyFire web-based application for automated structural classification of chemical entities (Djombou Feunang *et al.*, 2016) in where each compound's SMILES was inputted into the ClassyFire labelling engine and a category was chosen from the classification section; and by subjective criteria in order to simplify and reduce the number of categories required to be plotted and analysed.

In the pre-fermented samples, a total 222 compounds were putatively identified belonging to 40 distinct chemical classes. The classes range from carbohydrates, phenolic compounds, nitrogenous compounds, sulphur compounds, carbonyl, heterocyclic compounds, lipids, and hydrocarbons. The overall distribution can be visualised in Figure 4.13.



In the F1 sample class, a total of 24 compounds were putatively identified belonging to 12 distinct chemical classes. The compounds range from phenolic, carbonyl, heterocyclic compounds, lipids, and hydrocarbons. The overall distribution can be seen in Figure 4.14.

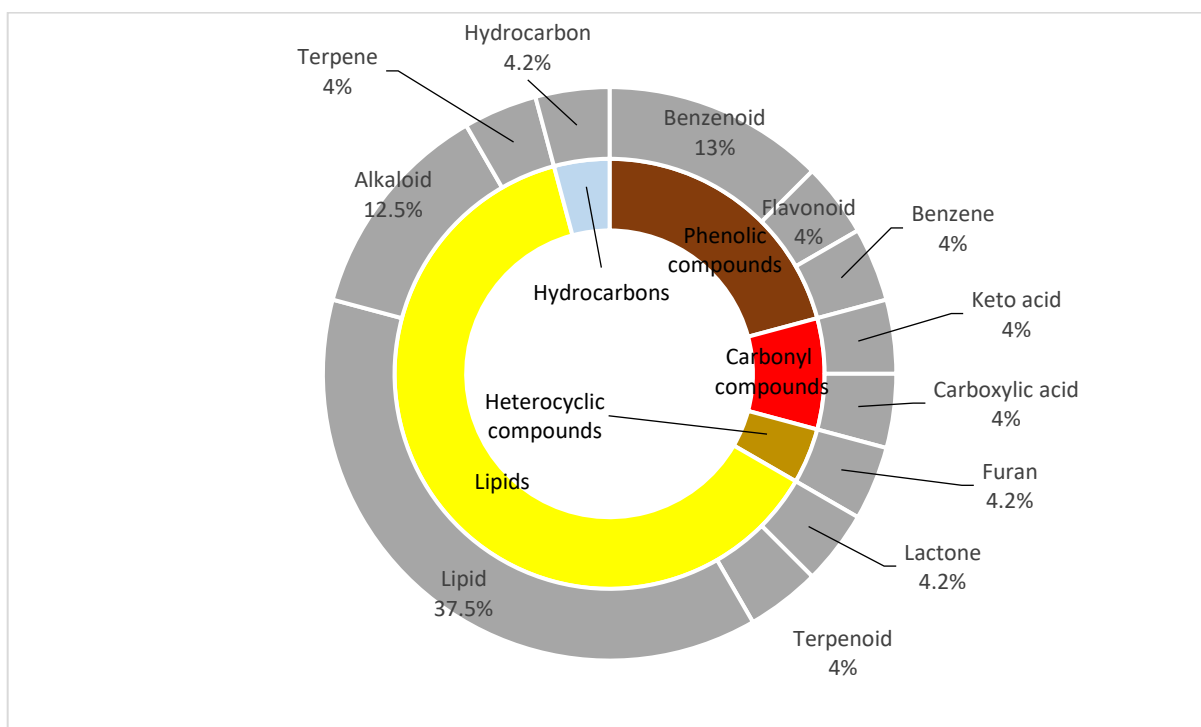


Figure 4.14 Proportional distribution of putatively identified compounds in the F1 samples. Outer ring show the chemical class and inner ring shows the parent class.

In the post-fermented samples, a total of 207 compounds were putatively identified belonging to 37 distinct chemical classes. The compounds range from carbohydrates, phenolic, nitrogenous, sulphur, carbonyl, heterocyclic compounds, and lipids. The overall distribution can be seen in Figure 4.15.

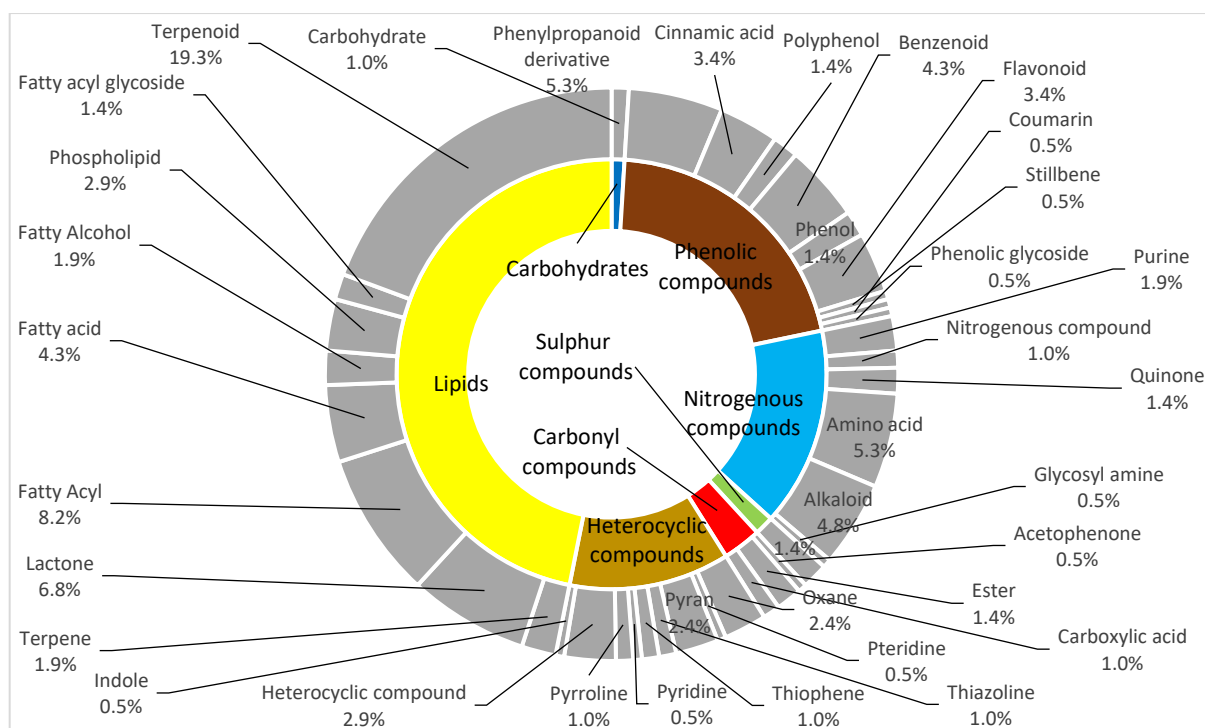


Figure 4.15 Proportional distribution of putatively identified compounds in the post-fermented samples. Outer ring show the chemical class and inner ring shows the parent class.

As it was explained in the previous chapter, the data processing presents important limitations. Peak annotation was limited to m/z matching to selected adducts and the resulting matches were shortlisted through a manual process based on subjective criteria. The resulting distribution of chemical classes of the putatively identified compounds includes isoforms and thus the true chemical class proportion of the discriminant compounds is unknown. True identification was not possible because no pure standards were used to match chromatographic conditions, in fact the retention value was not considered in the peak annotation process. In some metabolomics data processing suites, m/z and retention time can be used to match compounds to contextually relevant values, in softwares like MarVis and RAMClust (Broeckling *et al.*, 2014; Kaever *et al.*, 2015) they use metabolic pathway databases like KEGG (Kanehisa *et al.*, 2016) to perform peak annotation and pathway analysis; unfortunately, there is a lack of information regarding to food analysis and flavour formation pathways, although KEGG has yeast metabolic pathways there are no cereal grains pathways available from which a meaningful comparison could be made to barley, so they were not used in processing the present data.

4.4 Discussion

The brewing method developed in Chapter 2 was designed to obtain samples that represented the chemical evolution of the brewing process. The results from the MVA allowed for the identification of 3 sample classes instead of the expected 10. The UPLC-MS allowed for better resolution and

separation of the samples' metabolites. Also, the data pre-processing and processing workflow allowed for the identification of a large number of compounds from distinct sample classes. Several compounds were putatively identified in each discriminant feature, however only a selected number of compounds were chosen to be discussed. This was decided based on the level of information and detail found in the literature about this specific type of compound and its relevance to wort, beer, and the formation of flavour compounds in other beverages or foods that undergo similar processing as beer, i.e. fermentation, Maillard reaction, Strecker degradation, caramelisation, oxidation, etc.; also metabolic pathways involved in the common biochemical processes like germination or ripening of fruits shared between other chemically complex foods were considered for discussion. The way this discussion is structured follows the same logic as explained in 3.4 Discussion.

The carbohydrates showed a markedly difference in the proportion in compounds identified among the sample classes. They comprised 27% in the pre-fermented samples (Figure 4.13) (were among the shared features between the pre-fermented and F1 samples) and decreased to 1% in the post-fermented samples (Figure 4.15). The depletion of carbohydrates is explained by the action of yeast fermentation. Many disaccharides were identified in features 365.11/8.82 and 381.09/0.36, the most prominent being D-maltose (Table 7.6), the main source of carbon for yeast metabolism.

The phenolic compounds identified are varied and are involved in several metabolic pathways. There was a notable rise in the proportion of compounds identified from 12% in the pre-fermented samples to 20% in the post-fermented samples.

Two isomers of a benzenoid known as paradol were identified in feature 166.09/0.83 (Table 7.5). Paradol has been identified in alcoholic beverages and is a part of phenylalanine metabolism. It is a relative to a well-known flavour active compound that provides spiciness and pungency to ginger called gingerol. While paradol has no reported flavour descriptors it contains a feruloyl moiety coupled to a hydrocarbon saturated ketone chain and could be a potential precursor of other flavour compounds, especially volatile benzene substituted derivatives and carbonyl compounds. Other flavour active phenolics identified in feature 166.09/0.83 are cinnamic acid, (E)-3-(4-Hydroxyphenyl)-2-propenal, and 1-Phenyl-1,2-propanedione. These compounds have balsam, cinammon, honey, storax, sweet, buttery, honey, and pepper flavour descriptors and have been identified in many foods and spices. They are part of the phenylpropanoid pathway.

In the pre-fermented samples, flavonoid and phenolic glycosides were identified in features 188.08/1.05, 365.11/8.82, and 381.09/0.36 (Table 7.6). Acetophenone glycoside is a phenolic glycoside and was identified in two features; acetophenone has almonds, marzipan, and earthy flavour descriptors and is a known precursor of other fragrances (Siegel and Eggersdorfer, 2000). It

has been previously identified in unhopped wort and yeast exometabolome (Meilgaard, 1975b; De Schutter *et al.*, 2008; Martins *et al.*, 2017). The fact that it is bonded with a glycoside moiety suggests that it is being released from intermediates of malt polysaccharides by enzymatic action or thermal degradation during the wort mashing. Coniferin (Table 7.6) was also identified and it is also involved in cell wall lignification and has been previously described in detail in Chapter 3's discussion.

Phenolic compounds putatively identified in the post-fermented samples include p-Tolyl phenylacetate, 2-Phenylethyl benzoate, Cinnamyl isobutyrate, cis-3-Hexenyl benzoate, Cinnamyl butyrate, Butyl cinnamate, Benzyl 2,3-dimethyl-2-butenate (Table 7.8). These compound all have reported flavour descriptors relevant to beer flavour. They appear to be derived from cinnamic acids and could part of various stages of the oxidation/reduction pathway of aromatic compounds most likely the phenylpropanoid pathway and have not previously been identified in beer.

Several heterocyclic compounds known as furans were putatively identified in features 188.08/1.05 and 146.06/1.09 in the pre-fermented samples (Table 7.6). These furans have garlic, horseradish, onion, pungent, sulphurous, vegetable, beefy, cheese, coffee, minty, and spicy flavour descriptors; they are cysteine derived Maillard typically found in meat and have not been previously identified in beer or its ingredients. In pre-fermented features 189.08/1.09 (Table 7.6) a variety of pyrazines were identified with hazelnut, meaty, roasted earthy, etc. flavour descriptors. These pyrazines are Maillard reaction products as well. These pyrazines are thought to arise during malt kilning at high temperature and at the presence of oxygen from the heterocyclization of the by-products of the Strecker degradation, the α -aminoketones.

Heterocyclic sulphur compounds were putatively identified in all sample classes. Cyclopentanethiol was identified in features 120.08/0.79 and 103.06/0.83 (Table 7.5) in the pre-fermented samples and has a varied range of flavour descriptors. In feature 118.07/1.09, discriminant of the F1 samples, 2,3-Dihydro-5-methylthiophene was identified and then in feature 152.06/0.47 of the post-fermented samples, two isomers of tetrahydro-2-methyl-3-thiophenethiol and 3,3-Dimethyl-1,2-dithiolane were identified. This heterocyclic compounds have closely related structures and could potentially be part of a formation pathway of off-flavour active compounds in beer (Figure 4.16).

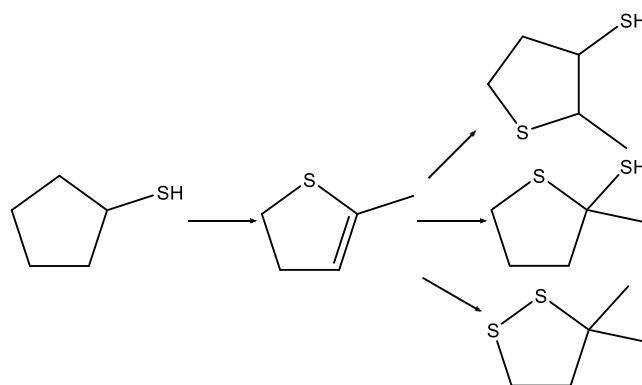


Figure 4.16 Proposed inter-relations of heterocyclic sulphur compounds.

A variety of semi-volatile fatty acid esters containing sulphur were identified in feature 166.09/0.83 (Table 7.5) of the pre-fermented samples (e.g. Ethyl 3-mercaptobutyrate, Methylthiomethyl butyrate, 3-(Methylthio)propyl acetate) with fruity, metallic, pineapple, pulpy, ripe, sulphurous, and tomato flavour properties previously found in many foods and alcoholic beverages (Duke, 2016). Unprocessed barley and green malts have a higher concentration of sulphur compounds which are believed to be volatilised during malt kilning and/or wort boiling. The presence of sulphur compounds can be indirectly controlled by brewers by a vigorous boiling. The compounds identified here suggest that they maintain their presence in beer throughout the process by interacting with carbonyl compounds and reductones and undergo heterocyclization into a variety of compounds. There are studies (Pripis-Nicolau *et al.*, 2000) that have proven the formation of Maillard heterocyclic compounds at low pH, low temperature, and in the presence of water; i.e. alcoholic beverages.

4.5 Conclusions

The data pre-processing workflow was successful, the XCMS algorithm could integrate the raw data into a comprehensive and manageable peak list that can be used as input in several metabolomics data processing platforms. However, at the moment these platforms are not well suited for food related samples and are difficult to use for flavour generation metabolic pathways.

The results of the MVA indicate that the UPLC-MS done on the brewing samples allowed for a more detailed and discriminant profiling of the chemometric profile of the samples. Three sample classes could be discriminated from the MVA, and more detailed inter-relations of flavour compounds could be proposed. In particular, the role of sulphur in the formation of heterocyclic compounds and its interaction with carbonyl compounds has the potential to be further studied. The analysis done in this dataset remains subjective and qualitative as no pure standards were used to confirm the identity of the metabolites and no quantitative data was considered during the analysis. UPLC-MS has the potential to be optimised for a more targeted application for beer analysis.

5. Chapter 5: General Discussion

The main findings of this study include: the development of a standardised brewing method and sampling method based on current brewing practices; the development of a reference flavour database of compounds found in beer; and the implementation of different mass spectrometric techniques whose results can yield variation in the metabolite profile identified. This variation can be attributed to differences in the sample preparation, separation, and ionisation mechanisms implemented for each technique. Additionally, a metabolomics workflow was applied to the data obtained in order to identify the metabolites detected and explain their contribution and effect on flavour formation pathways based on their sensory descriptors found in the literature and reference databases.

The initial intent of tracking the evolution of the chemical composition at different stages of the brewing process was achieved with various levels of success. Two main sample classes could be identified using unsupervised clustering MVA: the pre-fermentation and post-fermentation samples classes. In the UPLC-MS a higher level of discrimination between the brewing samples was achieved, and the F1 sample class was identified as a transition class between the pre-fermented and post-fermented samples.

5.1 Comparison between MS techniques

5.1.1 Comparing the putative annotation results

After data processing the metabolomics workflow used resulted in a varied number of metabolites identified. In the MALDI-MS 68 and 76 metabolites were identified for the pre-fermentation and post-fermentation sample classes respectively. In the DI-MS 69 and 41 metabolites were identified in the pre-fermentation and post-fermentation sample classes respectively. In the UPLC-MS 222, 24, and 207 metabolites were identified in the pre-fermentation, F1, and post-fermentation sample classes respectively.

A comparison of shared bins and features was made between the methods (Figure 5.5.1). Two features were shared among the three methods in the pre-fermentation sample class: bins 381 corresponding to feature 381.09/0.36 and bin 496 corresponding to feature 496.35/5.22. Bin 120 corresponding to feature 120.08/0.79 was shared between the UPLC-MS and DI-MS.

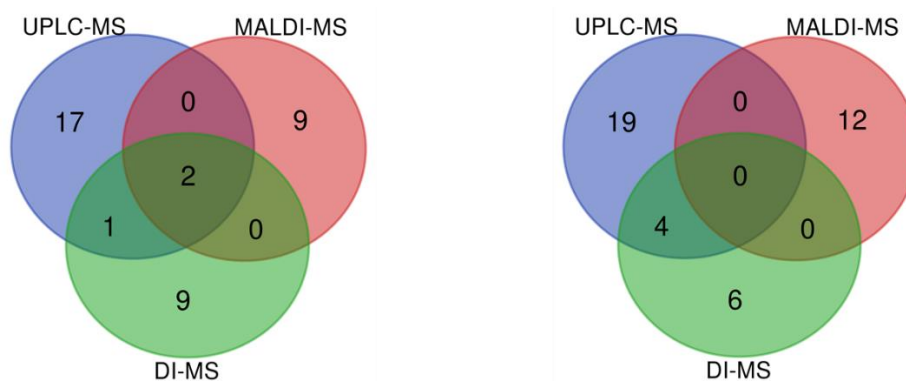


Figure 5.5.1 Venn diagrams of shared discriminant bins and features between methods. Pre-fermentation sample classes (left) and post-fermentation sample classes (right). The F1 sample class was considered as part of the post-fermented in this comparison

Bin 381 and feature 381.09/0.36 most likely identified compound is D-maltose or a similar disaccharide while bin 496 and feature 496.35/5.22 putatively identified compounds were varied. Several alkaloids, lipids, and glucosides were identified. The most likely compound could be Dhurrin 6'-glucoside, a phenol with a cyanide group attached to glycosylated moiety that has been previously identified in cereals and grains (Yannai, 2003); it is unknown how it is involved in flavour formation pathways but it is probably being released into the wort from malt polysaccharides during mashing. In bin 120 and feature 120.08/0.79 mainly products of the Maillard reaction were identified.

In the post-fermented sample classes 4 discriminant features were shared between the DI-MS and UPLC-MS: bins 322 and feature 322.17/1.45; bin 268 and feature 268.11/0.46; bin 152 and feature 152.06/0.47; and bin 258 and feature 258.14/0.56.

In Bin 322 and feature 322.17/1.45 some nitrogenous compounds related to purine metabolism as well as several phenolic dimers linked via an amide bond. These phenolic dimers are known as avenanthramides and were also identified in bin 382 in the pre-fermented samples suggesting they are not a product of yeast metabolism and were released into the wort from the mashing stage and stayed in the wort and beer. Avenanthramide has previously been identified in oats and cereals (Inglett and Chen, 2012) has no flavour descriptors reported and are derived from the common phenylpropene skeleton building block. They consist of 1-3 phenylpropanoid (*p*-coumaric, ferulic, or caffeic acid) and anthranilic acid moieties. Avenanthramides have not been identified in malt or barley but their presence indicates an interaction between phenolic acids released during mashing/boiling and nitrogenous compounds forming polyphenolic dimers that could be precursors of flavour-active aromatic compounds (Figure 5.5.2).

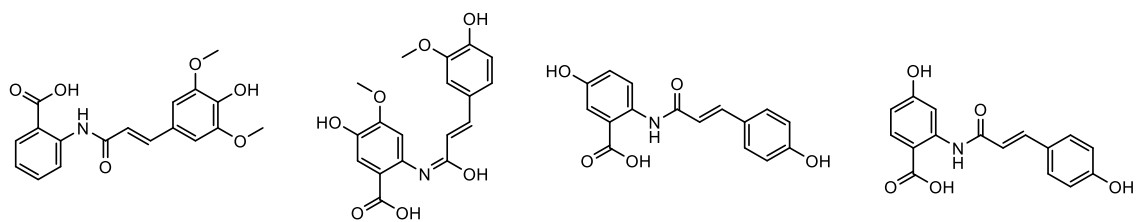


Figure 5.5.2 From left to right: Avenanthramide 1s, Avenanthramide 2, Avenanthramide A, and Avenanthramide G

In bin 268 and feature 268.11/0.46 nitrogenous compounds related to purine metabolism were identified along with some carbohydrate amides. N-(1-Deoxy-1-fructosyl)serine is the amadori product resulting from sugar-aminoacid interaction, specifically fructose and serine.

In bin 258 and feature 258.14/0.56 several nitrogenous compounds were identified. Alkaloids from the aleurone layer of cereals (Methyl 2,6-dihydroxyquinoline-4-carboxylate and N1,N10-Diferuloylspermidine) derived from quinolone and hydroxycinnamic acids. Dicarbonyl compounds were also identified and a proline derived Maillard product. Although these compounds are discriminant of the post-fermented samples it is difficult to discern whether they are products of yeast metabolism or maturation/aging related reactions occurring in the beer or a combination of both. Ketogenic amino acids are intermediates of amino acid metabolism in yeast but the presence of a proline derived Maillard product and phenolic alkaloids derived from hydroxycinnamic acids suggests they are interacting and makes possible the existence of an unknown pathway involving these compounds that results in the formation of flavour compounds. Otherwise, the fact they were putatively identified in the same discriminant bin/feature is only a coincidence and that the identification process is not very specific.

5.1.2 Relative merits of the MS methods

The metabolomics analysis applied to the brewing samples revealed a large number of metabolites involved in several flavour formation pathways. Of particular interest were the phenolic compounds derived from the phenylpropanoid pathway. Phenolic glycosides and other copolymers derived from the metabolism of phenylalanine, tyrosine, and tryptophan which are being released into the wort and undergo chemical changes into aglycones or dimers that have flavour-active properties; also, the heterocyclic compounds product of the Maillard reaction particularly derived from proline and cysteine were annotated and could have an important role in flavour formation during the brewing process.

It is surprising to see such a small number of shared features between the analytical methods, considering it was the same sample being processed. MALDI-MS and DI-MS had the same data pre-processing and processing workflow, but they had different sample preparation methods, ionisation

mechanisms, and were carried out in equipment with different specifications. DI-MS and UPLC-MS had similar ionisation mechanisms and resulted in a higher number of shared discriminant features. The retention time layer of the analysis could not be used in the processing of the data, however there were cases in which a feature had the same m/z but different retention time values; this indicates that there are compounds with the same m/z value but were eluted at a different time due to their chemical characteristics.

There are many putatively identified compounds in this study that have not been previously identified in beer and this can raise questions on the validity of the results presented, especially when they have not been confirmed with a pure standard. It is important to consider the focus chosen, looking for flavour precursors and flavour-related compounds with the aim of understanding more deeply beer's complex flavour profile. This focus has contributed heavily in a strong bias to select and discuss compounds that have not been extensively discussed in the brewing literature.

MALDI-MS has a limitation known as "matrix-related selectivity" (Kandiah and Urban, 2013). While there is no hard confirmation that matrix-related bias occurred, it can be inferred from the putative identification of phenolic acids and phenolic glycosides. The matrix used (CHCA) is a cinnamic acid which has a similar structure to many flavour related compounds derived from phenylalanine and tyrosine. On the other hand, this fact can also be an advantage towards detecting flavour related compounds. Only by doing a more targeted study with pure standards can compounds be truly identified.

The UPLC-MS appears to have the most potential for the most robust, truly untargeted analysis. The key difference in the hyphenated approach is the separation step, which improves analytical resolution and revelatory power. The literature shows the most interesting results as in beer analysis using these approach (Heuberger *et al.*, 2016; Bettenhausen *et al.*, 2018).

The sample processing approach in this research project was partially successful as at most 3 sample classes were discriminated using highly sensitive analytical methods. Perhaps the stages selected to do the sampling are not ideal considering the aim of the thesis and the data processing algorithms and MVA workflow available. The subtle changes in chemometric composition could be happening in a much shorter span of time during each stage, perhaps it would be a lot more revealing to only compare two stages at a time and narrowing down the mechanism involved, because the results as they, the results in this study need several assumptions in order for them to be analysed objectively. Too many mechanisms at play at the same time and no way of knowing exactly which one is at play.

5.2 Future recommendations

One of the purposes of this research was to identify key compounds that can impart flavour to wort or beer at certain stages of the brewing process. An important concept not considered in this research is that of the flavour threshold. The flavour threshold can determine how important a flavour is to the overall flavour profile and how much weight it has on it.

In order for brewers to determine what compounds are most important to the flavour profiles they desire, targeted and focused studies can be done on specific compounds with known flavour descriptors and thresholds as well as on the precursors of these compounds. Some better questions to ask brewers to direct further research: What makes Maris Otter malt different from other base malts? Apart from traditional quality markers in malt what type of flavours do you expect or would like to expect from base malts? With the answers of these questions in mind and using the knowledge derived from the metabolomics studies a more suitable analytical approach and experiment can be designed to elucidate in what stages are the desired flavours being developed. This further research can help the development of new malting barley varieties that can satisfy emerging craft beer markets.

Another follow-up to the experiments performed for this thesis would be to make a similar fully untargeted metabolomics analysis time-series study during the malting process and its different stages. How is the metabolite composition changing along the different stages of the malting process? What metabolic pathways are involved during the germination, steeping, and kilning stages and how much are they contributing to the development of flavour compounds and their precursors? This further research can help improve the understanding how flavour arises during malting and control it more effectively. An even more detailed approach would be to coarsely break down and separate the malt into its constituents and compare the metabolome, the hypothesis being that different compounds can be found in the aleurone layer, the husk, the endosperm, etc.

To eliminate or minimise the “matrix-related selectivity” that comes with MALDI-MS analysis: different matrices can be used to make an untargeted analysis and compare the results, it is known that other matrices, such as dihydroxybenzoic acid (DHB), can work very well with beer as the sample (Park *et al.*, 2012). If the discriminant bins are similar and comparable then we can more confidently say that the putatively identified compounds are truly discriminant of the sample class they represent. Once the results from MALDI-MS have been normalised and confirmed this way, the most interesting compounds can be confidently identified using pure standards.

The approach using UPLC-MS has the most promise and potential as a semi-targeted approach to find the precursors and pathways involved in the flavour formation in beer. A significant difference from MALDI-MS is the absence of bias in the formation of ions during ESI. The fact that the results

can be directly used as input in other metabolomics-related platforms. While there are extensively-curated databases such as KEGG (Kanehisa *et al.*, 2016), Metlin (Smith *et al.*, 2005), and HMDB (Wishart *et al.*, 2018) they are still very much focused into clinical applications and samples. The results obtained in Chapter 4 were used to implement pathway and biomarker analysis using Metaboanalyst and MarVis tools (Kaeffer *et al.*, 2015; Chong *et al.*, 2018), but the genomic platforms found are not suitable enough for food and flavour-generation related applications. While yeast's metabolic pathways can be found, they are applicable only to the post-fermented sample classes and even then it is limited to pathways that have limited involvement with flavour generation. Surprisingly, there is no suitable or comparable platform to analyse the pre-fermented samples as barley (*Hordeum vulgare*) is not included in any database (at the time this research was done), not even wheat (*Triticum aestivum*).

Future work can be structure elucidation of the putatively identified compounds with the most flavour-active related potential. Techniques such as NMR and FTIR spectroscopy could reveal the functional groups and structure that give the compound unique characteristics and allow us to infer the correct authentic standard to calibrate and properly identify the discriminant compounds. These experiments would allow us to go from a putatively identified feature (level 2) to a confidently identified compound (level 1) (Sumner *et al.*, 2007; Dias *et al.*, 2016).

Another experiment that may show valuable results is to prepare a wort enriched in phenylalanine, tyrosine, cysteine, cinnamic and benzoic acids. Different combinations could be used and compared. Based on the results of this study, these compounds could be important precursors of flavour-active compounds, and to determine whether they play a significant role in flavour-generation is a question that is worth answering in more detail. Once a more prominent precursor is identified isotopic-labelling could be a powerful tool to track the evolution of the compounds involved in flavour-generation pathways and a time series experiment like the one used in this research could be used again to find key stages where flavour arises in the brewing process.

5.3 Conclusions

The complex biochemical composition of wort and beer posed a challenge and several analytical approaches were implemented to analyse its metabolite composition. A brewing method and flavours compound database were developed to perform a metabolomics study in unhopped wort and beer with the aim of identifying key compounds involved in the formation and degradation of flavour-active compounds. Several MS based techniques were used and a large number of compounds were identified of various chemical classes and flavour descriptors. Putatively identified compounds were critically analysed in relation to the flavour formation pathways currently known and described in the literature along with the information found in public, contextually relevant reference databases.

The UPLC-MS based approach resulted in the largest number of putatively identified compounds from distinct chemical classes. The results obtained from this study have enhanced the current knowledge of precursors related to flavour formation pathways.

6. Bibliography

- Almeida, C. *et al.* (2006) 'Composition of beer by ¹H NMR spectroscopy: Effects of brewing site and date of production', *Journal of Agricultural and Food Chemistry*, 54(3), pp. 700–706. doi: 10.1021/jf0526947.
- Andrés-Iglesias, C. *et al.* (2014) 'Mass spectrometry-based metabolomics approach to determine differential metabolites between regular and non-alcohol beers', *Food Chemistry*, 157, pp. 205–212. doi: 10.1016/j.foodchem.2014.01.123.
- Andrés-Iglesias, C. *et al.* (2015) 'New trends in beer flavour compound analysis', *Journal of the Science of Food and Agriculture*, 95(8), pp. 1571–1576. doi: 10.1002/jsfa.6905.
- Araújo, A. S. *et al.* (2005) 'Electrospray ionization mass spectrometry fingerprinting of beer', *The Analyst*, 130(6), p. 884. doi: 10.1039/b415252b.
- Aron, P. M. and Shellhammer, T. H. (2010) 'A Discussion of Polyphenols in Beer Physical and Flavour Stability', *Journal of the Institute of Brewing*, 116(4), pp. 369–380. doi: 10.1002/j.2050-0416.2010.tb00788.x.
- Baert, J. J. *et al.* (2012) 'On the Origin of Free and Bound Staling Aldehydes in Beer', *Journal of Agricultural and Food Chemistry*, 60(46), pp. 11449–11472. doi: 10.1021/jf303670z.
- Bamforth, C. W. (2010) 'The Enzymology of Cell Wall Breakdown During Malting and Mashing: An Overview', *Master Brewers Association of the Americas Technical Quarterly*, (12), pp. 1–5. doi: 10.1094/TQ-47-1-0309-01.
- Barker, M. and Rayens, W. (2003) 'Partial least squares for discrimination', *Journal of Chemometrics*, 17(3), pp. 166–173. doi: 10.1002/cem.785.
- Bernotienė, G. *et al.* (2004) 'Chemical composition of essential oils of hops (*Humulus lupulus* L.) growing wild in Aukštaitija', *Chemija*, 15(2), pp. 31–36.
- Bettenhausen, H. M. *et al.* (2018) 'Influence of malt source on beer chemistry, flavor, and flavor stability', *Food Research International*. Elsevier, 113(July), pp. 487–504. doi: 10.1016/j.foodres.2018.07.024.
- van Boekel, M. A. J. S. (2006) 'Formation of flavour compounds in the Maillard reaction', *Biotechnology Advances*, 24(2), pp. 230–233. doi: 10.1016/j.biotechadv.2005.11.004.
- Brányik, T. *et al.* (2008) 'A Review of Flavour Formation in Continuous Beer Fermentations*', *Journal of the Institute of Brewing*, 114(1), pp. 3–13. doi: 10.1002/j.2050-0416.2008.tb00299.x.
- Brereton, R. G. and Lloyd, G. R. (2014) 'Partial least squares discriminant analysis: taking the magic away', *Journal of Chemometrics*, 28(4), pp. 213–225. doi: 10.1002/cem.2609.
- Briggs, D. (1998) *Malts and Malting*. First edit. Springer US. Available at: <https://books.google.co.uk/books?id=s9tf70Wk3bYC>.
- Briggs, D. *et al.* (2004) *Brewing: science and practice: brewing processes*.
- Broeckling, C. D. *et al.* (2014) 'RAMClust: A Novel Feature Clustering Method Enables Spectral-Matching-Based Annotation for Metabolomics Data', *Analytical Chemistry*, 86(14), pp. 6812–6817. doi: 10.1021/ac501530d.
- Cabrita, M. J. *et al.* (2012) 'Conversion of hydroxycinnamic acids into volatile phenols in a synthetic medium and in red wine by *Dekkera bruxellensis*', *Food Science and Technology*, 32(1), pp. 106–112. doi: 10.1590/S0101-20612012005000024.
- Callemien, D. and Collin, S. (2009) 'Structure, Organoleptic Properties, Quantification Methods, and Stability of Phenolic Compounds in Beer—A Review', *Food Reviews International*, 26(1), pp. 1–84. doi: 10.1080/87559120903157954.
- Chambers, M. C. *et al.* (2012) 'A cross-platform toolkit for mass spectrometry and proteomics', *Nature Biotechnology*, 30(10), pp. 918–920. doi: 10.1038/nbt.2377.
- Chong, J. *et al.* (2018) 'MetaboAnalyst 4.0: towards more transparent and integrative metabolomics analysis', *Nucleic Acids Research*, 46(W1), pp. W486–W494. doi: 10.1093/nar/gky310.
- Cortacero-Ramírez, S. *et al.* (2003) 'Analysis of beer components by capillary electrophoretic methods', *TrAC Trends in Analytical Chemistry*, 22(7), pp. 440–455. doi: 10.1016/S0165-9936(03)00704-0.

Debyser, W., Derdelinckx, G. and Delcour, J. A. (1997) 'Arabinoxylan and Arabinoxylan Hydrolysing Activities in Barley Malts and Worts Derived from Them', *Journal of Cereal Science*, 26(1), pp. 67–74. doi: 10.1006/jcrs.1996.0107.

Dias, D. *et al.* (2016) 'Current and Future Perspectives on the Structural Identification of Small Molecules in Biological Systems', *Metabolites*, 6(4), p. 46. doi: 10.3390/metabo6040046.

Djombou Feunang, Y. *et al.* (2016) 'ClassyFire: automated chemical classification with a comprehensive, computable taxonomy', *Journal of Cheminformatics*. Springer International Publishing, 8(1), pp. 1–20. doi: 10.1186/s13321-016-0174-y.

Dornbusch, H. (2010) *The Ultimate Almanac of World Beer Recipes*. Edited by B.-H. Group. Bamberg, Germany.

Draper, J. *et al.* (2009) 'Metabolite signal identification in accurate mass metabolomics data with MZedDB, an interactive m/z annotation tool utilising predicted ionisation behaviour "rules"', *BMC Bioinformatics*, 10(1), p. 227. doi: 10.1186/1471-2105-10-227.

Duke, J. (2016) *Dr. Duke's Phytochemical and Ethnobotanical Databases*, U.S. Department of Agriculture, Agricultural Research Service. doi: 10.15482/USDA.ADC/1239279.

Eden, A. *et al.* (2001) 'Involvement of branched-chain amino acid aminotransferases in the production of fusel alcohols during fermentation in yeast', *Applied Microbiology and Biotechnology*, 55(3), pp. 296–300. doi: 10.1007/s002530000506.

Fiehn, O. (2002) 'Metabolomics -- the link between genotypes and phenotypes', *Plant Molecular Biology*, 48(1), pp. 155–171. doi: 10.1023/A:1013713905833.

Gallone, B. *et al.* (2018) 'Origins, evolution, domestication and diversity of Saccharomyces beer yeasts', *Current Opinion in Biotechnology*. The Authors, 49, pp. 148–155. doi: 10.1016/j.copbio.2017.08.005.

Gonçalves, J. L. *et al.* (2014) 'A powerful methodological approach combining headspace solid phase microextraction, mass spectrometry and multivariate analysis for profiling the volatile metabolomic pattern of beer starting raw materials', *Food Chemistry*, 160, pp. 266–280. doi: 10.1016/j.foodchem.2014.03.065.

Gowda, H. *et al.* (2014) 'Interactive XCMS Online: Simplifying Advanced Metabolomic Data Processing and Subsequent Statistical Analyses', *Analytical Chemistry*, 86(14), pp. 6931–6939. doi: 10.1021/ac500734c.

Gross, J. H. (2017) *Mass Spectrometry*. Third, Springer. Third. Springer International Publishing. doi: 10.1007/978-3-319-54398-7.

Hazelwood, L. A. *et al.* (2008) 'The Ehrlich Pathway for Fusel Alcohol Production: a Century of Research on Saccharomyces cerevisiae Metabolism', *Applied and Environmental Microbiology*, 74(8), pp. 2259–2266. doi: 10.1128/AEM.02625-07.

Herb, D. *et al.* (2017) 'Effects of Barley (Hordeum Vulgare L.) Variety and Growing Environment on Beer Flavor', *Journal of the American Society of Brewing Chemists*, 75(4), pp. 345–353. doi: 10.1094/ASBCJ-2017-4860-01.

Heresztyn, T. (1986) 'Metabolism of volatile phenolic compounds from hydroxycinnamic acids by Brettanomyces yeast', *Archives of Microbiology*, 146(1), pp. 96–98. doi: 10.1007/BF00690165.

Heuberger, A. L. *et al.* (2012) 'Metabolomic profiling of beer reveals effect of temperature on non-volatile small molecules during short-term storage', *Food Chemistry*. Elsevier Ltd, 135(3), pp. 1284–1289. doi: 10.1016/j.foodchem.2012.05.048.

Heuberger, A. L. *et al.* (2014) 'Application of nontargeted metabolite profiling to discover novel markers of quality traits in an advanced population of malting barley', *Plant Biotechnology Journal*, 12(2), pp. 147–160. doi: 10.1111/pbi.12122.

Heuberger, A. L. *et al.* (2016) 'Evaluation of non-volatile metabolites in beer stored at high temperature and utility as an accelerated method to predict flavour stability', *Food Chemistry*. Elsevier Ltd, 200, pp. 301–307. doi: 10.1016/j.foodchem.2016.01.022.

Hill, A. and Stewart, G. (2019) 'Free Amino Nitrogen in Brewing', *Fermentation*, 5(1), p. 22. doi: 10.3390/fermentation5010022.

- Hirst, M. B. and Richter, C. L. (2016) 'Review of Aroma Formation through Metabolic Pathways of *Saccharomyces cerevisiae* in Beverage Fermentations', *American Journal of Enology and Viticulture*, 67(4), pp. 361–370. doi: 10.5344/ajev.2016.15098.
- Inglett, G. E. and Chen, D. (2012) 'Antioxidant and Pasting Properties of Oat β -Glucan Hydrocolloids', *Food and Nutrition Sciences*, 03(06), pp. 827–835. doi: 10.4236/fns.2012.36111.
- Iyuke, S. E. *et al.* (2008) 'The Effect of Hydroxycinnamic Acids and Volatile Phenols on Beer Quality', *Journal of the Institute of Brewing*, 114(4), pp. 300–305.
- Jewison, T. *et al.* (2012) 'YMDB: the Yeast Metabolome Database', *Nucleic Acids Research*, 40(D1), pp. D815–D820. doi: 10.1093/nar/gkr916.
- Jin, Y.-L. *et al.* (2004) 'Barley β -glucans and their degradation during malting and brewing', *Master Brewers Association of the Americas Technical Quarterly*, 41(3), pp. 231–240. Available at: <https://www.researchgate.net/publication/296811873>.
- Jones, M. and Pierce, J. S. (1964) 'ABSORPTION OF AMINO ACIDS FROM WORT BY YEASTS', *Journal of the Institute of Brewing*, 70(4), pp. 307–315. doi: 10.1002/j.2050-0416.1964.tb01996.x.
- Kaefer, A. *et al.* (2009) 'MarVis: a tool for clustering and visualization of metabolic biomarkers', *BMC Bioinformatics*, 10(1), p. 92. doi: 10.1186/1471-2105-10-92.
- Kaefer, A. *et al.* (2015) 'MarVis-Pathway: integrative and exploratory pathway analysis of non-targeted metabolomics data', *Metabolomics*. Springer US, 11(3), pp. 764–777. doi: 10.1007/s11306-014-0734-y.
- Kanauchi, M., Ishikura, W. and Bamforth, C. W. (2011) ' β -Glucans and Pentosans and their Degradation Products in Commercial Beers', *Journal of the Institute of Brewing*, 117(1), pp. 120–124. doi: 10.1002/j.2050-0416.2011.tb00452.x.
- Kandiah, M. and Urban, P. L. (2013) 'Advances in ultrasensitive mass spectrometry of organic molecules.', *Chemical Society reviews*, 42(12), pp. 5299–322. doi: 10.1039/c3cs35389c.
- Kanehisa, M. *et al.* (2016) 'KEGG as a reference resource for gene and protein annotation', *Nucleic Acids Research*, 44(D1), pp. D457–D462. doi: 10.1093/nar/gkv1070.
- Karas, M. and Krüger, R. (2003) 'Ion Formation in MALDI: The Cluster Ionization Mechanism', *Chemical Reviews*, 103(2), pp. 427–440. doi: 10.1021/cr010376a.
- De Keukeleire, D. (2000) 'FUNDAMENTALS OF BEER AND HOP CHEMISTRY', *Química nova*, 23(1), pp. 108–112.
- Kobayashi, N. *et al.* (1994) 'Behavior of Lipid Hydroperoxides During Mashing', *Journal of the American Society of Brewing Chemists*, 52(4), pp. 141–145. doi: 10.1094/ASBCJ-52-0141.
- Konermann, L. *et al.* (2013) 'Unraveling the Mechanism of Electrospray Ionization', *Analytical Chemistry*, 85(1), pp. 2–9. doi: 10.1021/ac302789c.
- Lodolo, E. J. *et al.* (2008) 'The yeast *Saccharomyces cerevisiae* - the main character in beer brewing', *FEMS Yeast Research*, 8(7), pp. 1018–1036. doi: 10.1111/j.1567-1364.2008.00433.x.
- Malting Barley Characteristics for Craft Brewers* (2014) *Brewers Association*.
- Martins, C. *et al.* (2017) 'Metabolomics strategy for the mapping of volatile exometabolome from *Saccharomyces* spp. widely used in the food industry based on comprehensive two-dimensional gas chromatography', *Journal of Separation Science*, 40(10), pp. 2228–2237. doi: 10.1002/jssc.201601296.
- Meilgaard, M. C. (1975a) 'Flavor chemistry in beer: Part I: Flavor interaction between principal volatiles', *Master Brewers Association of the Americas Technical Quarterly*, 12(2), pp. 107–117.
- Meilgaard, M. C. (1975b) 'Flavor Chemistry of Beer: Part II: Flavor and Threshold of 239 Aroma Volatiles', *Master Brewers Association of the Americas Technical Quarterly*, 12(3), pp. 151–168.
- Moir, M. (1992) 'The Desideratum for Flavour Control', *Journal Of The Institute Of Brewing*, 98, pp. 215–220.
- Olaniran, A. O. *et al.* (2017) 'Flavour-active volatile compounds in beer: production, regulation and control', *Journal of the Institute of Brewing*, 123(1), pp. 13–23. doi: 10.1002/jib.389.
- Overy, S. A. *et al.* (2004) 'Application of metabolite profiling to the identification of traits in a population of tomato introgression lines', *Journal of Experimental Botany*, 56(410), pp. 287–296. doi: 10.1093/jxb/eri070.

Palmer, J. J. (2006) *How to Brew: Everything you need to know to brew beer right the first time*. 3rd edn. Brewers Publications.

Park, E. *et al.* (2012) 'Analysis of oligosaccharides in beer using MALDI-TOF-MS', *Food Chemistry*, Elsevier Ltd, 134(3), pp. 1658–1664. doi: 10.1016/j.foodchem.2012.03.069.

Priest, F. G. and Campbell, I. (2003) *Brewing Microbiology*. 3rd ed. Edited by Intergovernmental Panel on Climate Change. Cambridge: Cambridge University Press. doi: 10.1017/CBO9781107415324.004.

Pripis-Nicolau, L. *et al.* (2000) 'Formation of Flavor Components by the Reaction of Amino Acid and Carbonyl Compounds in Mild Conditions', *Journal of Agricultural and Food Chemistry*, 48(9), pp. 3761–3766. doi: 10.1021/jf991024w.

Qiao, H. *et al.* (2009) 'Analyte distributions in MALDI samples using MALDI imaging mass spectrometry', *International Journal of Mass Spectrometry*, 281(1–2), pp. 41–51. doi: 10.1016/j.ijms.2008.11.015.

Ramirez-Gaona, M. *et al.* (2017) 'YMDB 2.0: a significantly expanded version of the yeast metabolome database', *Nucleic Acids Research*, 45(D1), pp. D440–D445. doi: 10.1093/nar/gkw1058.

Rossi, S. *et al.* (2014) 'Characterization of the volatile profiles of beer using headspace solid-phase microextraction and gas chromatography-mass spectrometry', *Journal of the Science of Food and Agriculture*, 94(5), pp. 919–928. doi: 10.1002/jsfa.6336.

Saison, D. *et al.* (2009) 'Determination of carbonyl compounds in beer by derivatisation and headspace solid-phase microextraction in combination with gas chromatography and mass spectrometry', *Journal of Chromatography A*. doi: 10.1016/j.chroma.2009.04.077.

Schulte, F., Flaschel, E. and Niehaus, K. (2016) 'Proteome-Based Analysis of Colloidal Instability Enables the Detection of Haze-Active Proteins in Beer', *Journal of Agricultural and Food Chemistry*, 64(35), pp. 6752–6761. doi: 10.1021/acs.jafc.6b02467.

De Schutter, D. P. *et al.* (2008) 'Characterization of Volatiles in Unhopped Wort', *Journal of Agricultural and Food Chemistry*, 56(1), pp. 246–254. doi: 10.1021/jf072619r.

Šedo, O., Márová, I. and Zdráhal, Z. (2012) 'Beer fingerprinting by Matrix-Assisted Laser Desorption-Ionisation-Time of Flight Mass Spectrometry', *Food Chemistry*, 135(2), pp. 473–478. doi: 10.1016/j.foodchem.2012.05.021.

Siegel, H. and Eggersdorfer, M. (2000) 'Ketones', in *Ullmann's Encyclopedia of Industrial Chemistry*. Weinheim, Germany: Wiley-VCH Verlag GmbH & Co. KGaA, pp. 2015–2016. doi: 10.1002/14356007.a15_077.

Silva, G. A. da, Augusto, F. and Poppi, R. J. (2008) 'Exploratory analysis of the volatile profile of beers by HS-SPME-GC', *Food Chemistry*, 111(4), pp. 1057–1063. doi: 10.1016/j.foodchem.2008.05.022.

Singh, R., Rastogi, S. and Dwivedi, U. N. (2010) 'Phenylpropanoid Metabolism in Ripening Fruits', *Comprehensive Reviews in Food Science and Food Safety*, 9(4), pp. 398–416. doi: 10.1111/j.1541-4337.2010.00116.x.

Smith, C. A. *et al.* (2005) 'METLIN: A metabolite mass spectral database', in *Therapeutic Drug Monitoring*. doi: 10.1097/01.ftd.0000179845.53213.39.

Smith, C. A. *et al.* (2006) 'XCMS: Processing Mass Spectrometry Data for Metabolite Profiling Using Nonlinear Peak Alignment, Matching, and Identification', *Analytical Chemistry*, 78(3), pp. 779–787. doi: 10.1021/ac051437y.

Spevacek, A. R. *et al.* (2016) 'Beer metabolomics: molecular details of the brewing process and the differential effects of late and dry hopping on yeast purine metabolism', *Journal of the Institute of Brewing*, 122(1), pp. 21–28. doi: 10.1002/jib.291.

Sterckx, F. L., Saison, D. and Delvaux, F. R. (2010) 'Determination of volatile monophenols in beer using acetylation and headspace solid-phase microextraction in combination with gas chromatography and mass spectrometry', *Analytica Chimica Acta*. Elsevier B.V., 676(1–2), pp. 53–59. doi: 10.1016/j.aca.2010.07.043.

Sumner, L. W. *et al.* (2007) 'Proposed minimum reporting standards for chemical analysis:

Chemical Analysis Working Group (CAWG) Metabolomics Standards Initiative (MSI)', *Metabolomics*, 3(3), pp. 211–221. doi: 10.1007/s11306-007-0082-2.

Technical Committee, A. (2011a) 'Calculated Values', in *ASBC Methods of Analysis*. American Society of Brewing Chemists, pp. 1–2. doi: 10.1094/ASBCMOA-Beer-6.

Technical Committee, A. (2011b) 'Color', in *ASBC Methods of Analysis*. American Society of Brewing Chemists, pp. 1–5. doi: 10.1094/ASBCMOA-Beer-10.

Technical Committee, A. (2011c) 'Extract', in *ASBC Methods of Analysis*. American Society of Brewing Chemists, pp. 3–5. doi: 10.1094/ASBCMOA-Malt-4.

Technical Committee, A. (2011d) 'Microscopic Yeast Cell Counting', in *ASBC Methods of Analysis*. American Society of Brewing Chemists, pp. 4–5. doi: 10.1094/ASBCMOA-Yeast-4.

Technical Committee, A. (2011e) 'pH', in *ASBC Methods of Analysis*. American Society of Brewing Chemists, p. 2018. doi: 10.1094/ASBCMOA-Beer-9.

Technical Committee, A. (2011f) 'Specific Gravity', in *ASBC Methods of Analysis*. American Society of Brewing Chemists, p. 2014. doi: 10.1094/ASBCMOA-Beer-2.

Technical Committee, A. (2011g) 'Tables Related to Determinations on Wort, Beer, and Brewing Sugars and Syrups', in *ASBC Methods of Analysis*. American Society of Brewing Chemists. doi: 10.1094/ASBCMOA-TableWortBeerBrewingSugars.

Technical Committee, A. (2017) 'Hot Steep Malt Sensory Evaluation Method', in *ASBC Methods of Analysis*. American Society of Brewing Chemists, p. 1. doi: 10.1094/ASBCMOA-Sensory Analysis-14.

Technical Committee, A. (2018a) 'Alcohol', in *ASBC Methods of Analysis*. American Society of Brewing Chemists, pp. 1–8. doi: 10.1094/ASBCMOA-Beer-4.

Technical Committee, A. (2018b) 'Real Extract', in *ASBC Methods of Analysis*. American Society of Brewing Chemists, pp. 1–2. doi: 10.1094/ASBCMOA-Beer-5.

Tian, J. (2010) 'Determination of several flavours in beer with headspace sampling–gas chromatography', *Food Chemistry*. Elsevier Ltd, 123(4), pp. 1318–1321. doi: 10.1016/j.foodchem.2010.06.013.

Vanbeneden, N., Gils, F., *et al.* (2008) 'Formation of 4-vinyl and 4-ethyl derivatives from hydroxycinnamic acids: Occurrence of volatile phenolic flavour compounds in beer and distribution of Pad1-activity among brewing yeasts', *Food Chemistry*, 107(1), pp. 221–230. doi: 10.1016/j.foodchem.2007.08.008.

Vanbeneden, N., Van Roey, T., *et al.* (2008) 'Release of phenolic flavour precursors during wort production: Influence of process parameters and grist composition on ferulic acid release during brewing', *Food Chemistry*, 111(1), pp. 83–91. doi: 10.1016/j.foodchem.2008.03.029.

Vanderhaegen, B. *et al.* (2006) 'The chemistry of beer aging – a critical review', *Food Chemistry*, 95(3), pp. 357–381. doi: 10.1016/j.foodchem.2005.01.006.

Verbelen, P. J. *et al.* (2009) 'Impact of pitching rate on yeast fermentation performance and beer flavour', *Applied Microbiology and Biotechnology*, 82(1), pp. 155–167. doi: 10.1007/s00253-008-1779-5.

Verstrepen, K. J. *et al.* (2003) 'Flavor-active esters: adding fruitiness to beer.', *Journal of bioscience and bioengineering*, 96(2), pp. 110–8. doi: 10.1016/S1389-1723(03)90112-5.

Vivian, A. F. *et al.* (2016) 'Mass spectrometry for the characterization of brewing process', *Food Research International*. Elsevier Ltd, 89, pp. 281–288. doi: 10.1016/j.foodres.2016.08.008.

Wishart, D. S. *et al.* (2007) 'HMDB: the Human Metabolome Database', *Nucleic Acids Research*, 35(Database), pp. D521–D526. doi: 10.1093/nar/gkl923.

Wishart, D. S. (2008) 'Metabolomics: applications to food science and nutrition research', *Trends in Food Science & Technology*, 19(9), pp. 482–493. doi: 10.1016/j.tifs.2008.03.003.

Wishart, D. S. (2011) 'Advances in metabolite identification', *Bioanalysis*, 3(15), pp. 1769–1782. doi: 10.4155/bio.11.155.

Wishart, D. S. *et al.* (2018) 'HMDB 4.0: the human metabolome database for 2018', *Nucleic Acids Research*, 46(D1), pp. D608–D617. doi: 10.1093/nar/gkx1089.

Worley, B. and Powers, R. (2015) 'Multivariate Analysis in Metabolomics', 1(1), pp. 92–107. doi:

10.2174/2213235X11301010092.Multivariate.

Worley, B. and Powers, R. (2016) 'PCA as a predictor of OPLS-DA model reliability', *Current Metabolomics*, 4(2), pp. 97–103. doi: 10.2174/2213235X04666160613122429.PCA.

Yahya, H., Linforth, R. S. T. and Cook, D. J. (2014) 'Flavour generation during commercial barley and malt roasting operations: A time course study', *Food Chemistry*. Elsevier Ltd, 145, pp. 378–387. doi: 10.1016/j.foodchem.2013.08.046.

Yannai, S. (2003) *Dictionary of Food Compounds with CD-ROM, New York*. Edited by S. Yannai. Chapman and Hall/CRC. doi: 10.1201/9781420068450.

Zenobi, R. and Knochenmuss, R. (1998) 'Ion formation in MALDI mass spectrometry', *Mass Spectrometry Reviews*, 17(5), pp. 337–366. doi: 10.1002/(SICI)1098-2787(1998)17:5<337::AID-MAS2>3.0.CO;2-S.

Almeida, C. *et al.* (2006) 'Composition of beer by 1H NMR spectroscopy: Effects of brewing site and date of production', *Journal of Agricultural and Food Chemistry*, 54(3), pp. 700–706. doi: 10.1021/jf0526947.

Andrés-Iglesias, C. *et al.* (2014) 'Mass spectrometry-based metabolomics approach to determine differential metabolites between regular and non-alcohol beers', *Food Chemistry*, 157, pp. 205–212. doi: 10.1016/j.foodchem.2014.01.123.

Andrés-Iglesias, C. *et al.* (2015) 'New trends in beer flavour compound analysis', *Journal of the Science of Food and Agriculture*, 95(8), pp. 1571–1576. doi: 10.1002/jsfa.6905.

Araújo, A. S. *et al.* (2005) 'Electrospray ionization mass spectrometry fingerprinting of beer', *The Analyst*, 130(6), p. 884. doi: 10.1039/b415252b.

Aron, P. M. and Shellhammer, T. H. (2010) 'A Discussion of Polyphenols in Beer Physical and Flavour Stability', *Journal of the Institute of Brewing*, 116(4), pp. 369–380. doi: 10.1002/j.2050-0416.2010.tb00788.x.

Baert, J. J. *et al.* (2012) 'On the Origin of Free and Bound Staling Aldehydes in Beer', *Journal of Agricultural and Food Chemistry*, 60(46), pp. 11449–11472. doi: 10.1021/jf303670z.

Bamforth, C. W. (2010) 'The Enzymology of Cell Wall Breakdown During Malting and Mashing: An Overview', *Master Brewers Association of the Americas Technical Quarterly*, (12), pp. 1–5. doi: 10.1094/TQ-47-1-0309-01.

Barker, M. and Rayens, W. (2003) 'Partial least squares for discrimination', *Journal of Chemometrics*, 17(3), pp. 166–173. doi: 10.1002/cem.785.

Bernotienė, G. *et al.* (2004) 'Chemical composition of essential oils of hops (*Humulus lupulus* L.) growing wild in Aukštaitija', *Chemija*, 15(2), pp. 31–36.

Bettenhausen, H. M. *et al.* (2018) 'Influence of malt source on beer chemistry, flavor, and flavor stability', *Food Research International*. Elsevier, 113(July), pp. 487–504. doi: 10.1016/j.foodres.2018.07.024.

van Boekel, M. A. J. S. (2006) 'Formation of flavour compounds in the Maillard reaction', *Biotechnology Advances*, 24(2), pp. 230–233. doi: 10.1016/j.biotechadv.2005.11.004.

Brányik, T. *et al.* (2008) 'A Review of Flavour Formation in Continuous Beer Fermentations*', *Journal of the Institute of Brewing*, 114(1), pp. 3–13. doi: 10.1002/j.2050-0416.2008.tb00299.x.

Brereton, R. G. and Lloyd, G. R. (2014) 'Partial least squares discriminant analysis: taking the magic away', *Journal of Chemometrics*, 28(4), pp. 213–225. doi: 10.1002/cem.2609.

Briggs, D. (1998) *Malts and Malting*. First edit. Springer US. Available at: <https://books.google.co.uk/books?id=s9tf70Wk3bYC>.

Briggs, D. *et al.* (2004) *Brewing: science and practice: brewing processes*.

Broeckling, C. D. *et al.* (2014) 'RAMClust: A Novel Feature Clustering Method Enables Spectral-Matching-Based Annotation for Metabolomics Data', *Analytical Chemistry*, 86(14), pp. 6812–6817. doi: 10.1021/ac501530d.

Cabrita, M. J. *et al.* (2012) 'Conversion of hydroxycinnamic acids into volatile phenols in a synthetic medium and in red wine by *Dekkera bruxellensis*', *Food Science and Technology*, 32(1), pp. 106–112. doi: 10.1590/S0101-20612012005000024.

Callemien, D. and Collin, S. (2009) 'Structure, Organoleptic Properties, Quantification Methods, and Stability of Phenolic Compounds in Beer—A Review', *Food Reviews International*, 26(1), pp. 1–84. doi: 10.1080/87559120903157954.

Chambers, M. C. *et al.* (2012) 'A cross-platform toolkit for mass spectrometry and proteomics', *Nature Biotechnology*, 30(10), pp. 918–920. doi: 10.1038/nbt.2377.

Chong, J. *et al.* (2018) 'MetaboAnalyst 4.0: towards more transparent and integrative metabolomics analysis', *Nucleic Acids Research*, 46(W1), pp. W486–W494. doi: 10.1093/nar/gky310.

Cortacero-Ramírez, S. *et al.* (2003) 'Analysis of beer components by capillary electrophoretic methods', *TrAC Trends in Analytical Chemistry*, 22(7), pp. 440–455. doi: 10.1016/S0165-9936(03)00704-0.

Debyser, W., Derdelinckx, G. and Delcour, J. A. (1997) 'Arabinoxylan and Arabinoxylan Hydrolysing Activities in Barley Malts and Worts Derived from Them', *Journal of Cereal Science*, 26(1), pp. 67–74. doi: 10.1006/jcrs.1996.0107.

Dias, D. *et al.* (2016) 'Current and Future Perspectives on the Structural Identification of Small Molecules in Biological Systems', *Metabolites*, 6(4), p. 46. doi: 10.3390/metabo6040046.

Djombou Feunang, Y. *et al.* (2016) 'ClassyFire: automated chemical classification with a comprehensive, computable taxonomy', *Journal of Cheminformatics*. Springer International Publishing, 8(1), pp. 1–20. doi: 10.1186/s13321-016-0174-y.

Dornbusch, H. (2010) *The Ultimate Almanac of World Beer Recipes*. Edited by B.-H. Group. Bamberg, Germany.

Draper, J. *et al.* (2009) 'Metabolite signal identification in accurate mass metabolomics data with MZedDB, an interactive m/z annotation tool utilising predicted ionisation behaviour "rules"', *BMC Bioinformatics*, 10(1), p. 227. doi: 10.1186/1471-2105-10-227.

Duke, J. (2016) *Dr. Duke's Phytochemical and Ethnobotanical Databases*, U.S. Department of Agriculture, Agricultural Research Service. doi: 10.15482/USDA.ADC/1239279.

Eden, A. *et al.* (2001) 'Involvement of branched-chain amino acid aminotransferases in the production of fusel alcohols during fermentation in yeast', *Applied Microbiology and Biotechnology*, 55(3), pp. 296–300. doi: 10.1007/s002530000506.

Fiehn, O. (2002) 'Metabolomics -- the link between genotypes and phenotypes', *Plant Molecular Biology*, 48(1), pp. 155–171. doi: 10.1023/A:1013713905833.

Gallone, B. *et al.* (2018) 'Origins, evolution, domestication and diversity of *Saccharomyces* beer yeasts', *Current Opinion in Biotechnology*. The Authors, 49, pp. 148–155. doi: 10.1016/j.copbio.2017.08.005.

Gonçalves, J. L. *et al.* (2014) 'A powerful methodological approach combining headspace solid phase microextraction, mass spectrometry and multivariate analysis for profiling the volatile metabolomic pattern of beer starting raw materials', *Food Chemistry*, 160, pp. 266–280. doi: 10.1016/j.foodchem.2014.03.065.

Gowda, H. *et al.* (2014) 'Interactive XCMS Online: Simplifying Advanced Metabolomic Data Processing and Subsequent Statistical Analyses', *Analytical Chemistry*, 86(14), pp. 6931–6939. doi: 10.1021/ac500734c.

Gross, J. H. (2017) *Mass Spectrometry*. Third, Springer. Third. Springer International Publishing. doi: 10.1007/978-3-319-54398-7.

Hazelwood, L. A. *et al.* (2008) 'The Ehrlich Pathway for Fusel Alcohol Production: a Century of Research on *Saccharomyces cerevisiae* Metabolism', *Applied and Environmental Microbiology*, 74(8), pp. 2259–2266. doi: 10.1128/AEM.02625-07.

Herb, D. *et al.* (2017) 'Effects of Barley (*Hordeum Vulgare* L.) Variety and Growing Environment on Beer Flavor', *Journal of the American Society of Brewing Chemists*, 75(4), pp. 345–353. doi: 10.1094/ASBCJ-2017-4860-01.

Heresztyn, T. (1986) 'Metabolism of volatile phenolic compounds from hydroxycinnamic acids by *Brettanomyces* yeast', *Archives of Microbiology*, 146(1), pp. 96–98. doi: 10.1007/BF00690165.

Heuberger, A. L. *et al.* (2012) 'Metabolomic profiling of beer reveals effect of temperature on

non-volatile small molecules during short-term storage', *Food Chemistry*. Elsevier Ltd, 135(3), pp. 1284–1289. doi: 10.1016/j.foodchem.2012.05.048.

Heuberger, A. L. *et al.* (2014) 'Application of nontargeted metabolite profiling to discover novel markers of quality traits in an advanced population of malting barley', *Plant Biotechnology Journal*, 12(2), pp. 147–160. doi: 10.1111/pbi.12122.

Heuberger, A. L. *et al.* (2016) 'Evaluation of non-volatile metabolites in beer stored at high temperature and utility as an accelerated method to predict flavour stability', *Food Chemistry*. Elsevier Ltd, 200, pp. 301–307. doi: 10.1016/j.foodchem.2016.01.022.

Hill, A. and Stewart, G. (2019) 'Free Amino Nitrogen in Brewing', *Fermentation*, 5(1), p. 22. doi: 10.3390/fermentation5010022.

Hirst, M. B. and Richter, C. L. (2016) 'Review of Aroma Formation through Metabolic Pathways of *Saccharomyces cerevisiae* in Beverage Fermentations', *American Journal of Enology and Viticulture*, 67(4), pp. 361–370. doi: 10.5344/ajev.2016.15098.

Inglett, G. E. and Chen, D. (2012) 'Antioxidant and Pasting Properties of Oat β -Glucan Hydrocolloids', *Food and Nutrition Sciences*, 03(06), pp. 827–835. doi: 10.4236/fns.2012.36111.

Iyuke, S. E. *et al.* (2008) 'The Effect of Hydroxycinnamic Acids and Volatile Phenols on Beer Quality', *Journal of the Institute of Brewing*, 114(4), pp. 300–305.

Jewison, T. *et al.* (2012) 'YMDB: the Yeast Metabolome Database', *Nucleic Acids Research*, 40(D1), pp. D815–D820. doi: 10.1093/nar/gkr916.

Jin, Y.-L. *et al.* (2004) 'Barley β -glucans and their degradation during malting and brewing', *Master Brewers Association of the Americas Technical Quarterly*, 41(3), pp. 231–240. Available at: <https://www.researchgate.net/publication/296811873>.

Jones, M. and Pierce, J. S. (1964) 'ABSORPTION OF AMINO ACIDS FROM WORT BY YEASTS', *Journal of the Institute of Brewing*, 70(4), pp. 307–315. doi: 10.1002/j.2050-0416.1964.tb01996.x.

Kaefer, A. *et al.* (2009) 'MarVis: a tool for clustering and visualization of metabolic biomarkers', *BMC Bioinformatics*, 10(1), p. 92. doi: 10.1186/1471-2105-10-92.

Kaefer, A. *et al.* (2015) 'MarVis-Pathway: integrative and exploratory pathway analysis of non-targeted metabolomics data', *Metabolomics*. Springer US, 11(3), pp. 764–777. doi: 10.1007/s11306-014-0734-y.

Kanauchi, M., Ishikura, W. and Bamforth, C. W. (2011) ' β -Glucans and Pentosans and their Degradation Products in Commercial Beers', *Journal of the Institute of Brewing*, 117(1), pp. 120–124. doi: 10.1002/j.2050-0416.2011.tb00452.x.

Kandiah, M. and Urban, P. L. (2013) 'Advances in ultrasensitive mass spectrometry of organic molecules.', *Chemical Society reviews*, 42(12), pp. 5299–322. doi: 10.1039/c3cs35389c.

Kanehisa, M. *et al.* (2016) 'KEGG as a reference resource for gene and protein annotation', *Nucleic Acids Research*, 44(D1), pp. D457–D462. doi: 10.1093/nar/gkv1070.

Karas, M. and Krüger, R. (2003) 'Ion Formation in MALDI: The Cluster Ionization Mechanism', *Chemical Reviews*, 103(2), pp. 427–440. doi: 10.1021/cr010376a.

De Keukeleire, D. (2000) 'FUNDAMENTALS OF BEER AND HOP CHEMISTRY', *Química nova*, 23(1), pp. 108–112.

Kobayashi, N. *et al.* (1994) 'Behavior of Lipid Hydroperoxides During Mashing', *Journal of the American Society of Brewing Chemists*, 52(4), pp. 141–145. doi: 10.1094/ASBCJ-52-0141.

Konermann, L. *et al.* (2013) 'Unraveling the Mechanism of Electrospray Ionization', *Analytical Chemistry*, 85(1), pp. 2–9. doi: 10.1021/ac302789c.

Lodolo, E. J. *et al.* (2008) 'The yeast *Saccharomyces cerevisiae* - the main character in beer brewing', *FEMS Yeast Research*, 8(7), pp. 1018–1036. doi: 10.1111/j.1567-1364.2008.00433.x.

Malting Barley Characteristics for Craft Brewers (2014) *Brewers Association*.

Martins, C. *et al.* (2017) 'Metabolomics strategy for the mapping of volatile exometabolome from *Saccharomyces* spp. widely used in the food industry based on comprehensive two-dimensional gas chromatography', *Journal of Separation Science*, 40(10), pp. 2228–2237. doi: 10.1002/jssc.201601296.

Meilgaard, M. C. (1975a) 'Flavor chemistry in beer: Part I: Flavor interaction between principal

- volatiles', *Master Brewers Association of the Americas Technical Quarterly*, 12(2), pp. 107–117.
- Meilgaard, M. C. (1975b) 'Flavor Chemistry of Beer: Part II: Flavor and Threshold of 239 Aroma Volatiles', *Master Brewers Association of the Americas Technical Quarterly*, 12(3), pp. 151–168.
- Moir, M. (1992) 'The Desideratum for Flavour Control', *Journal Of The Institute Of Brewing*, 98, pp. 215–220.
- Olaniran, A. O. *et al.* (2017) 'Flavour-active volatile compounds in beer: production, regulation and control', *Journal of the Institute of Brewing*, 123(1), pp. 13–23. doi: 10.1002/jib.389.
- Overy, S. A. *et al.* (2004) 'Application of metabolite profiling to the identification of traits in a population of tomato introgression lines', *Journal of Experimental Botany*, 56(410), pp. 287–296. doi: 10.1093/jxb/eri070.
- Palmer, J. J. (2006) *How to Brew: Everything you need to know to brew beer right the first time*. 3rd edn. Brewers Publications.
- Park, E. *et al.* (2012) 'Analysis of oligosaccharides in beer using MALDI-TOF-MS', *Food Chemistry*. Elsevier Ltd, 134(3), pp. 1658–1664. doi: 10.1016/j.foodchem.2012.03.069.
- Priest, F. G. and Campbell, I. (2003) *Brewing Microbiology*. 3rd ed. Edited by Intergovernmental Panel on Climate Change. Cambridge: Cambridge University Press. doi: 10.1017/CBO9781107415324.004.
- Pripis-Nicolau, L. *et al.* (2000) 'Formation of Flavor Components by the Reaction of Amino Acid and Carbonyl Compounds in Mild Conditions', *Journal of Agricultural and Food Chemistry*, 48(9), pp. 3761–3766. doi: 10.1021/jf991024w.
- Qiao, H. *et al.* (2009) 'Analyte distributions in MALDI samples using MALDI imaging mass spectrometry', *International Journal of Mass Spectrometry*, 281(1–2), pp. 41–51. doi: 10.1016/j.ijms.2008.11.015.
- Ramirez-Gaona, M. *et al.* (2017) 'YMDB 2.0: a significantly expanded version of the yeast metabolome database', *Nucleic Acids Research*, 45(D1), pp. D440–D445. doi: 10.1093/nar/gkw1058.
- Rossi, S. *et al.* (2014) 'Characterization of the volatile profiles of beer using headspace solid-phase microextraction and gas chromatography-mass spectrometry', *Journal of the Science of Food and Agriculture*, 94(5), pp. 919–928. doi: 10.1002/jsfa.6336.
- Saison, D. *et al.* (2009) 'Determination of carbonyl compounds in beer by derivatisation and headspace solid-phase microextraction in combination with gas chromatography and mass spectrometry', *Journal of Chromatography A*. doi: 10.1016/j.chroma.2009.04.077.
- Schulte, F., Flaschel, E. and Niehaus, K. (2016) 'Proteome-Based Analysis of Colloidal Instability Enables the Detection of Haze-Active Proteins in Beer', *Journal of Agricultural and Food Chemistry*, 64(35), pp. 6752–6761. doi: 10.1021/acs.jafc.6b02467.
- De Schutter, D. P. *et al.* (2008) 'Characterization of Volatiles in Unhopped Wort', *Journal of Agricultural and Food Chemistry*, 56(1), pp. 246–254. doi: 10.1021/jf072619r.
- Šedo, O., Márová, I. and Zdráhal, Z. (2012) 'Beer fingerprinting by Matrix-Assisted Laser Desorption-Ionisation-Time of Flight Mass Spectrometry', *Food Chemistry*, 135(2), pp. 473–478. doi: 10.1016/j.foodchem.2012.05.021.
- Siegel, H. and Eggersdorfer, M. (2000) 'Ketones', in *Ullmann's Encyclopedia of Industrial Chemistry*. Weinheim, Germany: Wiley-VCH Verlag GmbH & Co. KGaA, pp. 2015–2016. doi: 10.1002/14356007.a15_077.
- Silva, G. A. da, Augusto, F. and Poppi, R. J. (2008) 'Exploratory analysis of the volatile profile of beers by HS-SPME-GC', *Food Chemistry*, 111(4), pp. 1057–1063. doi: 10.1016/j.foodchem.2008.05.022.
- Singh, R., Rastogi, S. and Dwivedi, U. N. (2010) 'Phenylpropanoid Metabolism in Ripening Fruits', *Comprehensive Reviews in Food Science and Food Safety*, 9(4), pp. 398–416. doi: 10.1111/j.1541-4337.2010.00116.x.
- Smith, C. A. *et al.* (2005) 'METLIN: A metabolite mass spectral database', in *Therapeutic Drug Monitoring*. doi: 10.1097/01.ftd.0000179845.53213.39.
- Smith, C. A. *et al.* (2006) 'XCMS: Processing Mass Spectrometry Data for Metabolite Profiling

Using Nonlinear Peak Alignment, Matching, and Identification', *Analytical Chemistry*, 78(3), pp. 779–787. doi: 10.1021/ac051437y.

Spevacek, A. R. *et al.* (2016) 'Beer metabolomics: molecular details of the brewing process and the differential effects of late and dry hopping on yeast purine metabolism', *Journal of the Institute of Brewing*, 122(1), pp. 21–28. doi: 10.1002/jib.291.

Sterckx, F. L., Saison, D. and Delvaux, F. R. (2010) 'Determination of volatile monophenols in beer using acetylation and headspace solid-phase microextraction in combination with gas chromatography and mass spectrometry', *Analytica Chimica Acta*. Elsevier B.V., 676(1–2), pp. 53–59. doi: 10.1016/j.aca.2010.07.043.

Sumner, L. W. *et al.* (2007) 'Proposed minimum reporting standards for chemical analysis: Chemical Analysis Working Group (CAWG) Metabolomics Standards Initiative (MSI)', *Metabolomics*, 3(3), pp. 211–221. doi: 10.1007/s11306-007-0082-2.

Technical Committee, A. (2011a) 'Calculated Values', in *ASBC Methods of Analysis*. American Society of Brewing Chemists, pp. 1–2. doi: 10.1094/ASBCMOA-Beer-6.

Technical Committee, A. (2011b) 'Color', in *ASBC Methods of Analysis*. American Society of Brewing Chemists, pp. 1–5. doi: 10.1094/ASBCMOA-Beer-10.

Technical Committee, A. (2011c) 'Extract', in *ASBC Methods of Analysis*. American Society of Brewing Chemists, pp. 3–5. doi: 10.1094/ASBCMOA-Malt-4.

Technical Committee, A. (2011d) 'Microscopic Yeast Cell Counting', in *ASBC Methods of Analysis*. American Society of Brewing Chemists, pp. 4–5. doi: 10.1094/ASBCMOA-Yeast-4.

Technical Committee, A. (2011e) 'pH', in *ASBC Methods of Analysis*. American Society of Brewing Chemists, p. 2018. doi: 10.1094/ASBCMOA-Beer-9.

Technical Committee, A. (2011f) 'Specific Gravity', in *ASBC Methods of Analysis*. American Society of Brewing Chemists, p. 2014. doi: 10.1094/ASBCMOA-Beer-2.

Technical Committee, A. (2011g) 'Tables Related to Determinations on Wort, Beer, and Brewing Sugars and Syrups', in *ASBC Methods of Analysis*. American Society of Brewing Chemists. doi: 10.1094/ASBCMOA-TableWortBeerBrewingSugars.

Technical Committee, A. (2017) 'Hot Steep Malt Sensory Evaluation Method', in *ASBC Methods of Analysis*. American Society of Brewing Chemists, p. 1. doi: 10.1094/ASBCMOA-Sensory Analysis-14.

Technical Committee, A. (2018a) 'Alcohol', in *ASBC Methods of Analysis*. American Society of Brewing Chemists, pp. 1–8. doi: 10.1094/ASBCMOA-Beer-4.

Technical Committee, A. (2018b) 'Real Extract', in *ASBC Methods of Analysis*. American Society of Brewing Chemists, pp. 1–2. doi: 10.1094/ASBCMOA-Beer-5.

Tian, J. (2010) 'Determination of several flavours in beer with headspace sampling–gas chromatography', *Food Chemistry*. Elsevier Ltd, 123(4), pp. 1318–1321. doi: 10.1016/j.foodchem.2010.06.013.

Vanbeneden, N., Gils, F., *et al.* (2008) 'Formation of 4-vinyl and 4-ethyl derivatives from hydroxycinnamic acids: Occurrence of volatile phenolic flavour compounds in beer and distribution of Pad1-activity among brewing yeasts', *Food Chemistry*, 107(1), pp. 221–230. doi: 10.1016/j.foodchem.2007.08.008.

Vanbeneden, N., Van Roey, T., *et al.* (2008) 'Release of phenolic flavour precursors during wort production: Influence of process parameters and grist composition on ferulic acid release during brewing', *Food Chemistry*, 111(1), pp. 83–91. doi: 10.1016/j.foodchem.2008.03.029.

Vanderhaegen, B. *et al.* (2006) 'The chemistry of beer aging – a critical review', *Food Chemistry*, 95(3), pp. 357–381. doi: 10.1016/j.foodchem.2005.01.006.

Verbelen, P. J. *et al.* (2009) 'Impact of pitching rate on yeast fermentation performance and beer flavour', *Applied Microbiology and Biotechnology*, 82(1), pp. 155–167. doi: 10.1007/s00253-008-1779-5.

Verstrepen, K. J. *et al.* (2003) 'Flavor-active esters: adding fruitiness to beer.', *Journal of bioscience and bioengineering*, 96(2), pp. 110–8. doi: 10.1016/S1389-1723(03)90112-5.

Vivian, A. F. *et al.* (2016) 'Mass spectrometry for the characterization of brewing process', *Food*

- Research International*. Elsevier Ltd, 89, pp. 281–288. doi: 10.1016/j.foodres.2016.08.008.
- Wishart, D. S. *et al.* (2007) 'HMDB: the Human Metabolome Database', *Nucleic Acids Research*, 35(Database), pp. D521–D526. doi: 10.1093/nar/gkl923.
- Wishart, D. S. (2008) 'Metabolomics: applications to food science and nutrition research', *Trends in Food Science & Technology*, 19(9), pp. 482–493. doi: 10.1016/j.tifs.2008.03.003.
- Wishart, D. S. (2011) 'Advances in metabolite identification', *Bioanalysis*, 3(15), pp. 1769–1782. doi: 10.4155/bio.11.155.
- Wishart, D. S. *et al.* (2018) 'HMDB 4.0: the human metabolome database for 2018', *Nucleic Acids Research*, 46(D1), pp. D608–D617. doi: 10.1093/nar/gkx1089.
- Worley, B. and Powers, R. (2015) 'Multivariate Analysis in Metabolomics', 1(1), pp. 92–107. doi: 10.2174/2213235X11301010092.Multivariate.
- Worley, B. and Powers, R. (2016) 'PCA as a predictor of OPLS-DA model reliability', *Current Metabolomics*, 4(2), pp. 97–103. doi: 10.2174/2213235X04666160613122429.PCA.
- Yahya, H., Linforth, R. S. T. and Cook, D. J. (2014) 'Flavour generation during commercial barley and malt roasting operations: A time course study', *Food Chemistry*. Elsevier Ltd, 145, pp. 378–387. doi: 10.1016/j.foodchem.2013.08.046.
- Yannai, S. (2003) *Dictionary of Food Compounds with CD-ROM*, New York. Edited by S. Yannai. Chapman and Hall/CRC. doi: 10.1201/9781420068450.
- Zenobi, R. and Knochenmuss, R. (1998) 'Ion formation in MALDI mass spectrometry', *Mass Spectrometry Reviews*, 17(5), pp. 337–366. doi: 10.1002/(SICI)1098-2787(1998)17:5<337::AID-MAS2>3.0.CO;2-S.

7. Appendix

A1 Method optimisation supplementary material

MALDI-MS method development

The brewing samples were subjected to preliminary optimisation tests for sampling, extraction, and loading procedure in order to determine the method that would yield reproducibility and high quality data.

MALDI-MS Test 1

Materials and methods

Samples were taken directly from the brewing process in 20 mL scintillation vials and frozen in a -80°C freezer, then freeze dried until completely dry. After dry-freezing, the sample was solubilised in 2 mL of 50% methanol/50% water solution. The sample was then diluted 100 fold with 50% methanol/50% water. Then, 5 µL of the diluted samples were mixed with 5 µL of the matrix solution (5mg/mL CHCA in methanol + 0.5 % trifluoroacetic acid). Then, the sample-matrix solution was spotted onto the MALDI plate in 2 µL spots. Each sample was analysed in triplicate. Each sample was irradiated for 2 min and ions counted every 2 s, the laser moved in a spiral pattern in positive ion mode, and the mass range analysed was 50-1200 Da.

The resulting spectra were visualised and peak corrected in MassLynx 4.0 (Waters Ltd). Noise reduction, normalization, and binning was performed as described by (Overy *et al.*, 2004) using a

Visual Basic macro in Microsoft Excel (Microsoft Corp, USA). Triplicate samples are combined in order to eliminate false positive peaks, only peaks that are present in all three replicates are preserved. To determine which peaks are equivalent to each other a linear function is used to define an acceptable mass variance. For positive ionisation mode the equation used is, $y < 0.00003x + 0.0033$; and for negative ionisation mode, $y < 0.00003x + 0.0044$; where y is the standard deviation of the three masses and x is the mean of the three masses. After a peak is selected as a true positive, the masses' intensities are normalised to the percentage of the total ion count (TIC) in each replicate and added together, then allocated into mass unit "bins" with a size of 0.2 Da. The resulting peak list's statistical treatment and multivariate analysis was done in SIMCA 14 (Umetrics, Sweden). The data-set was Pareto scaled to reduce the relative effect of peaks with high relative intensity while partially retaining the data structure (Worley and Powers, 2015).

Results and discussion

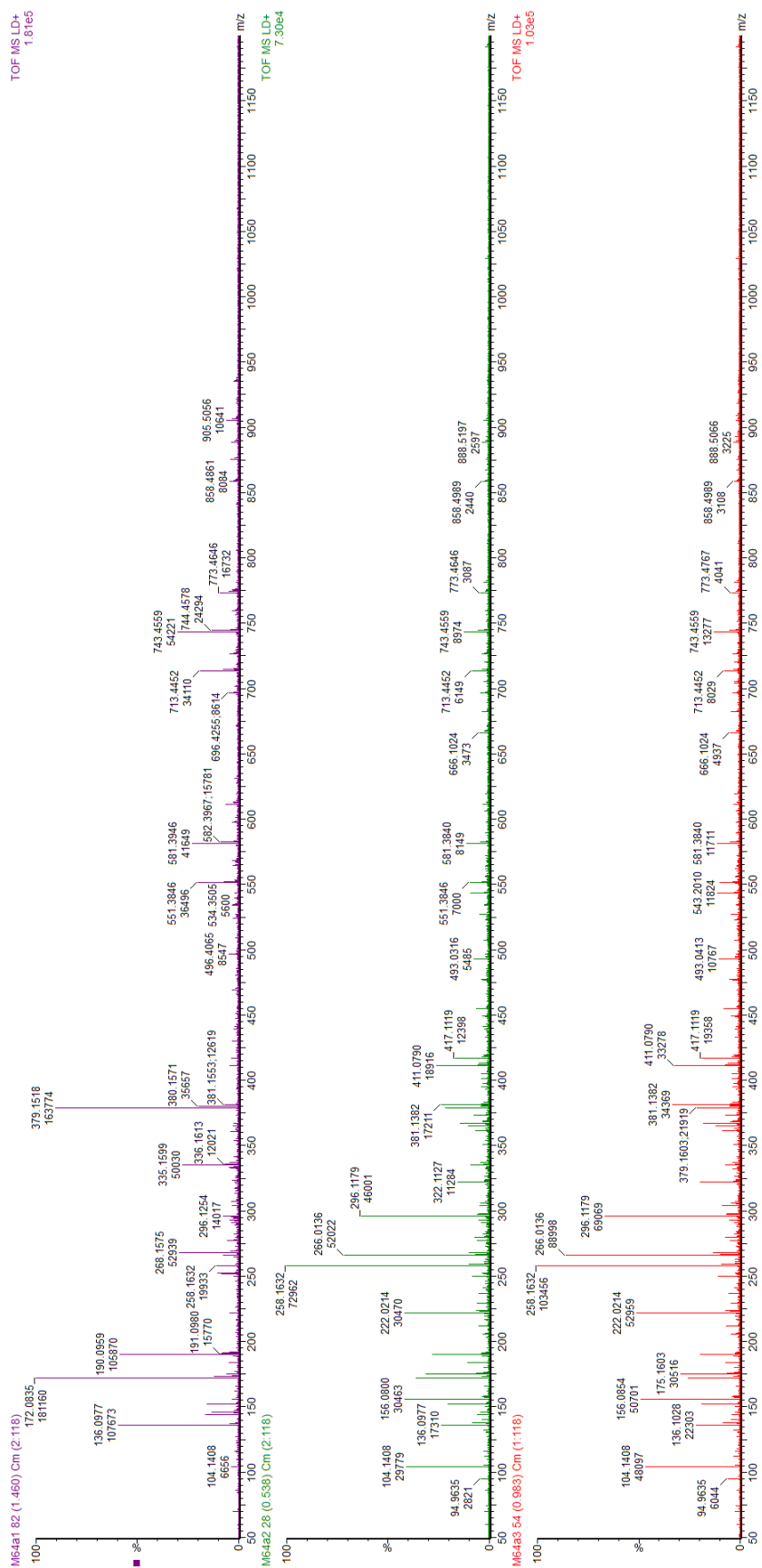


Figure 7.1 Mass spectra of three M64 replicates (MALDI-MS Positive mode Test 1)

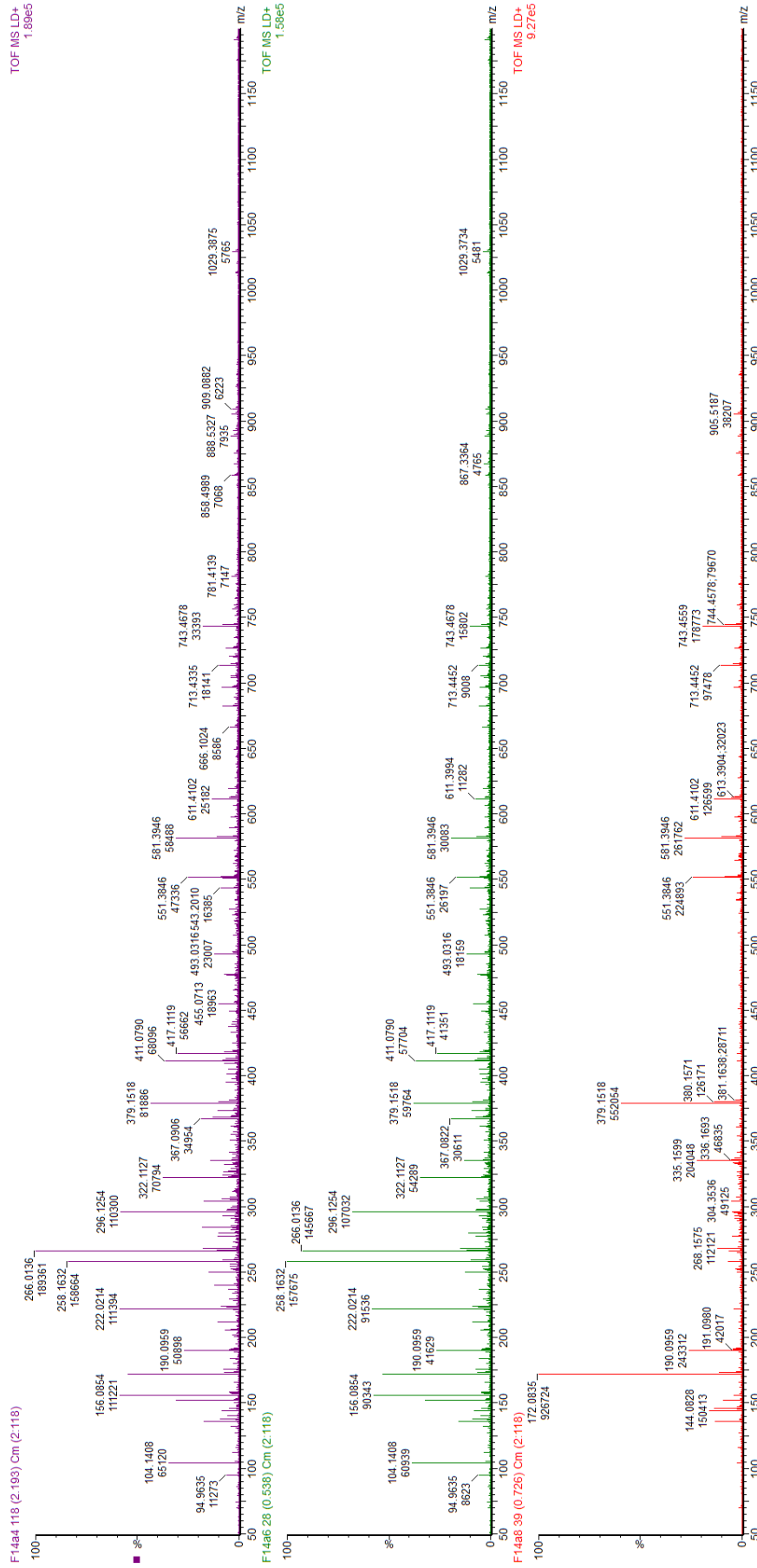


Figure 7.4 Mass spectra of three F14 replicates (MALDI-MS positive mode Test 1)

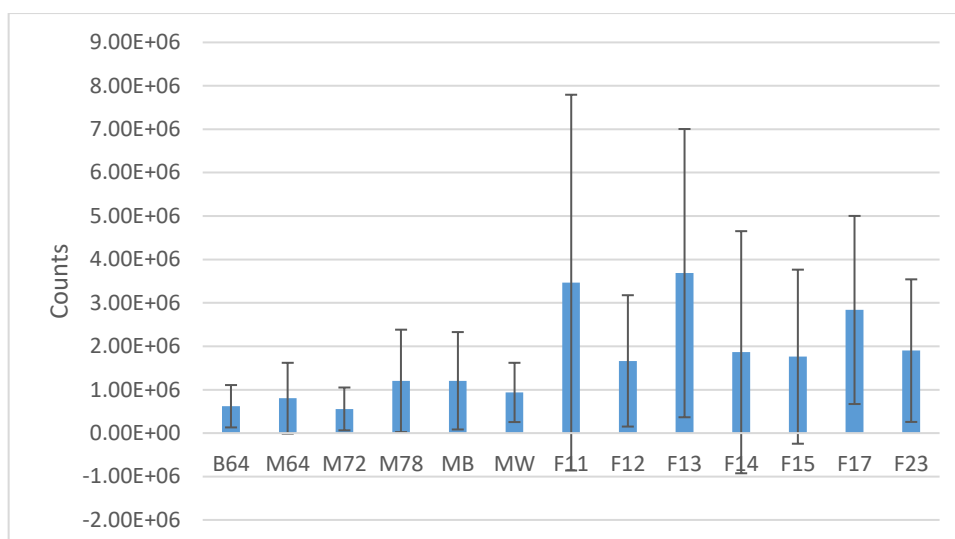


Figure 7.5 Mean total ion counts for each sample in MALDI positive mode Test 1. Error bars show standard deviation.

The target analytes in this experimental run are small organic molecules. The resulting spectra show considerable variability, indicating a lack of reproducibility and inconsistent ionisation yields amongst the samples (Figure 7.5). At the time of sample spotting it was observed that drying and crystallisation took several minutes resulting in heterogeneous spots. The ratio between matrix and sample affects the ionisation process and the ionisation of the compounds as well as temperature.

Unsupervised principal component analysis (PCA) was used to visualise the differences in the metabolic composition among the samples taken from the brewing. The resulting overall scatter plot (61.9% of the variance explained) shows layout of the samples (Figure 7.8) where, roughly the pre-fermentation samples clustered on the left and the post-fermentation samples clustered on the right side of the plot. However, there is a considerable amount of overlay within the 95% confidence ellipse. For a closer inspection of the data-set, separate PCAs were performed on the mash and fermentation samples and despite this attempt, the samples showed no discernible patterns of progression expected by the brewing and fermentation process.

Further interrogation of the data via supervised clustering (OPLS-DA) would result in significant bias where any discriminant variables identified would have a high probability of being spurious (Worley and Powers, 2016).

Further interrogation of the data will yield no qualifying discrimination between the metabolic profile of the samples. Further optimisation is required in order to extract high quality data.

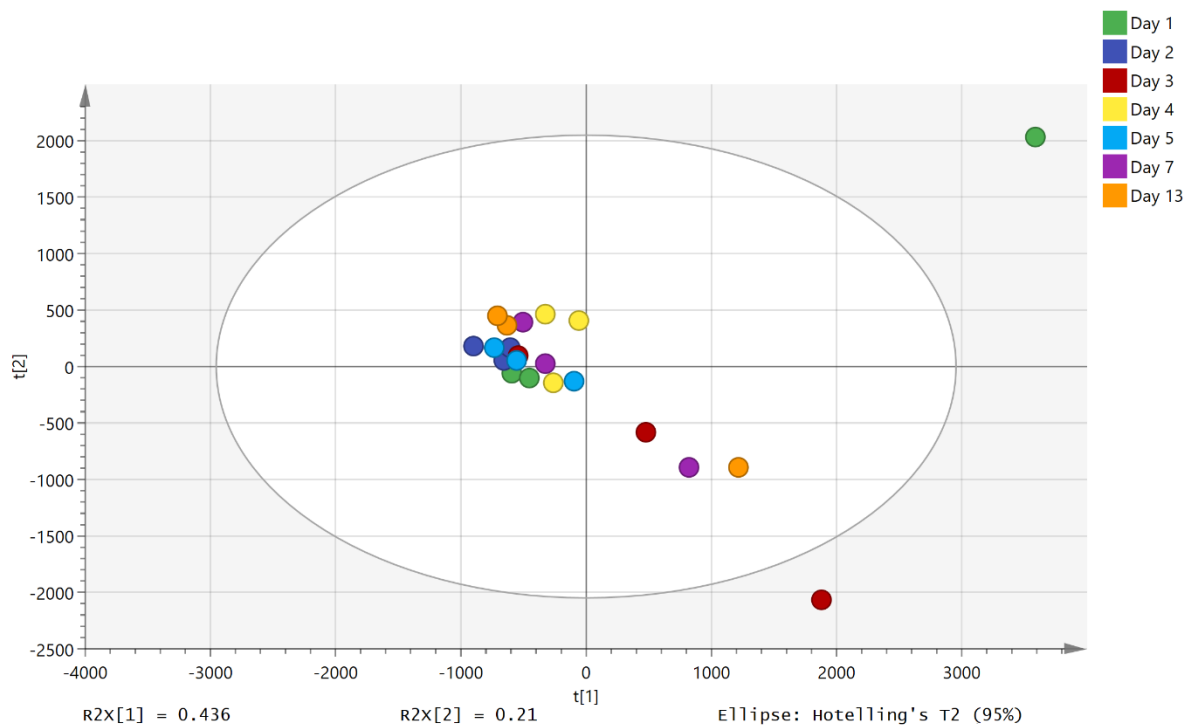


Figure 7.6 PCA scatter plot of the fermentation samples (MALDI-MS positive mode Test 1)

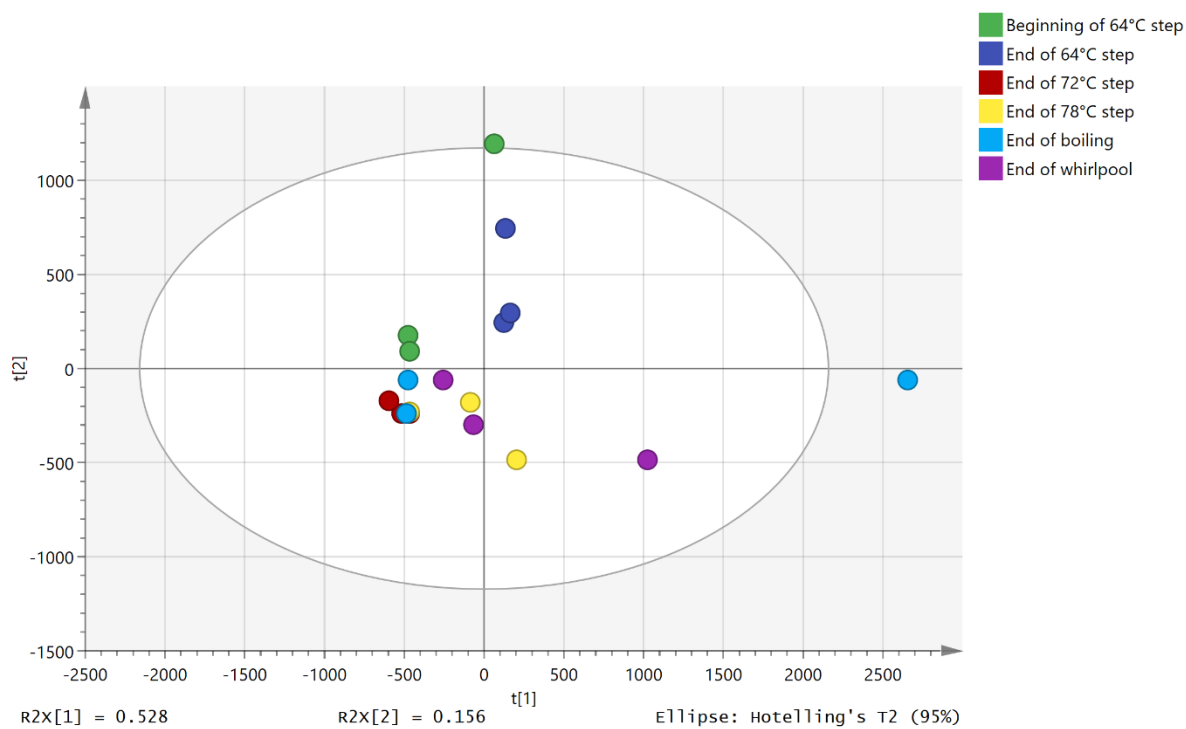


Figure 7.7 PCA scatter plot of the mash samples (MALDI-MS positive mode Test 1)

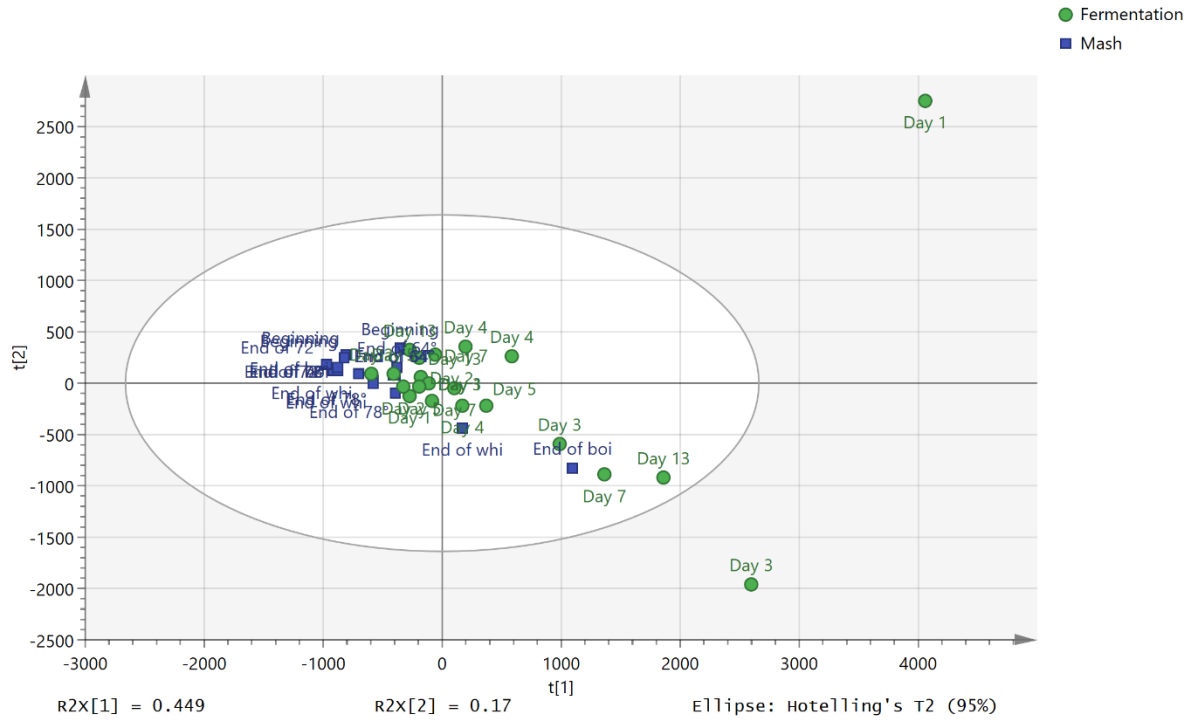


Figure 7.8 PCA scatter plot of all samples (MALDI-MS positive mode Test 1)

Test 2 Dilution test

Materials and methods

This test will make use of a single sample from the experimental brewing performed in **Error! Reference source not found.**

Mass spectrometry

The sample chosen for this test is the M78 sample. After the same sample preparation described in Test 1. After solubilisation in 50% methanol/water, the sample was further diluted three times in 70%/30% methanol:water solution: 100 fold, 1000 fold, and 10000 fold. The resulting dilution were mixed in a 1:1 ratio with matrix solution (5mg/mL CHCA in methanol + 0.5 % trifluoroacetic acid) and spotted in 2 μ L droplets onto the matrix plate heated to 60°C.

The MS parameters remained the same as described in Test 1. The resulting spectra analysis, visualisation and statistical analysis remained as described in Test 1.

Results and discussion

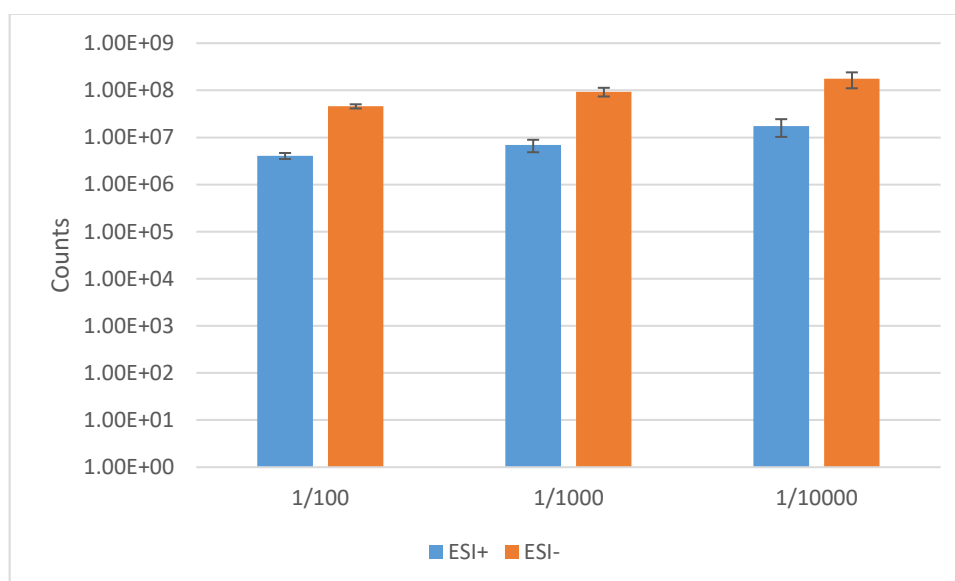


Figure 7.9 Total ion counts of the diluted samples in positive and negative ionization modes (MALDI -MS test 2)

During the sample preparation onto the MALDI plate, a focused effort was made to improve the uniformity of the sample spots ensuring that the lattice crystalized in under 1 minute and a visual inspection was made of every spot to assess its quality.

The TIC for both ionization modes consistently resulted in values over 1×10^6 counts, high and consistent TIC indicates a good quality mass spectrum fingerprint. Good reproducibility is a key factor in the discriminatory potential of profiling methods (Qiao *et al.*, 2009).

Identification of compounds requires a high degree of relative abundance (Šedo, Márová and Zdráhal, 2012).

The way of assessing the mass spectrum to identify the best dilution is to compare the matrix peaks with the other peaks. An excess of matrix is a good thing because it means that all the ionisable compounds are getting a charge but at the same time if the matrix completely dominates the spectrum it could mean that the ratio in the spot between matrix and sample is not the best. TIC

The mass spectra of each dilution was inspected to assess the resolution of the peaks and the ratio between unknown metabolites in beer to the known peaks of the matrix (α -CHCA). The most abundant matrix peaks identified in the mass spectra correspond to the peaks with m/z 172.0923 and 379.1679 which belong to the [M+H-H₂O] and [2M+H] adducts respectively.

The spectra in the 100 fold dilution samples in ESI+ (Figure 7.10) show a high relative abundance of the two matrix peaks, however it does not completely dominate over other peaks, notably at m/z 551.4059, 581.4167, and 743.4824. This indicates a good ionization efficiency of the beer's metabolites while not completely depleting the matrix. Meanwhile, the spectra of the 1000 and 10000 dilution samples (Figure 7.11 and Figure 7.12) show that the matrix peaks dominate over all the spectrum range of metabolites, indicating an overabundance of matrix to sample ratio, which could result in lost signal from low abundant metabolites as the signal to noise ratio would be much lower for metabolites of interest (Park *et al.*, 2012).

For the dilution samples in ESI- the most abundant matrix peaks are at m/z 93.0609 and 188.1035 which correspond to the [M-2H] and [M-H] adduct respectively. These two peaks have notably higher relative abundance throughout all the diluted samples (Figure 7.13, Figure 7.14, and Figure 7.15), especially the peak at m/z 188.1035. While there is a high amount of TIC in ESI- mode (Figure 7.9), it appears that the matrix is not fulfilling its purpose of providing a charge to the sample, this can be inferred by the low intensity peaks throughout the spectrum tested when compared to the matrix peaks.

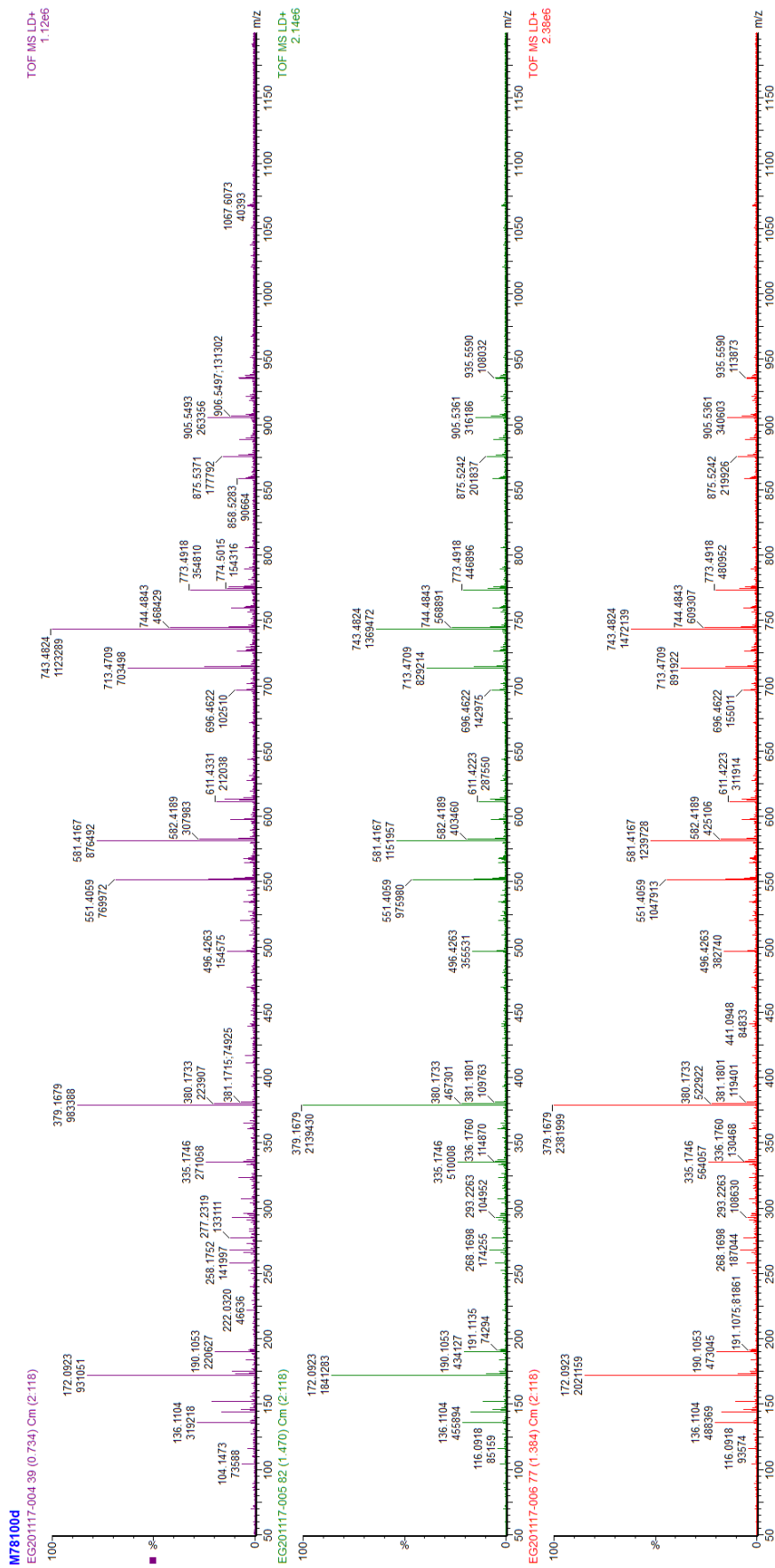


Figure 7.10 Mass spectra of three replicates of the 100 fold diluted samples in positive ionization mode (MALDI-MS positive mode Test 2)

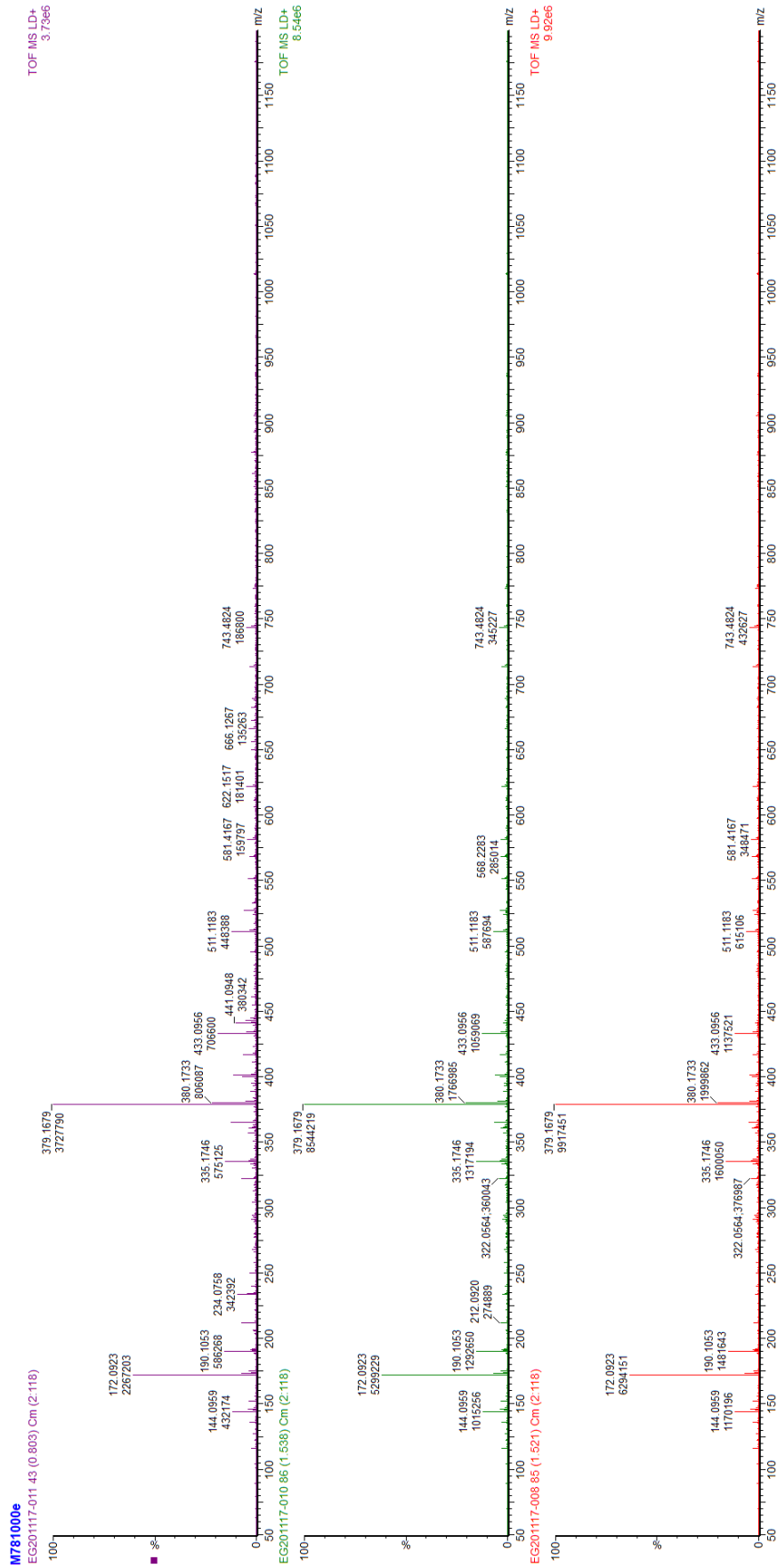


Figure 7.11 Mass spectra of three replicates of the 1000 fold diluted samples in positive ionization mode (MALDI-MS test 2)

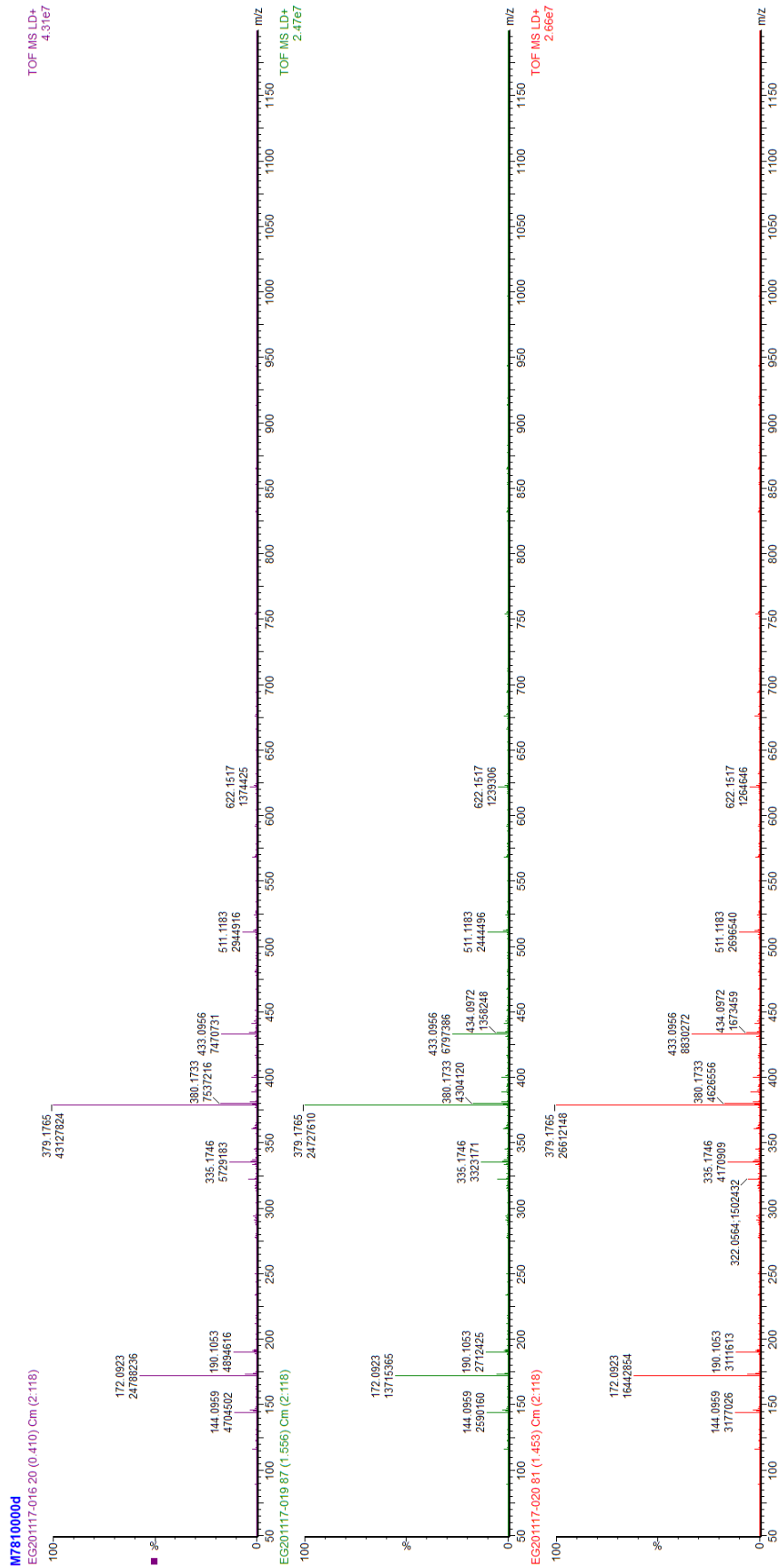


Figure 7.12 Mass spectra of three replicates of the 10000 fold diluted samples in positive ionization mode (MALDI-MS Test 2)

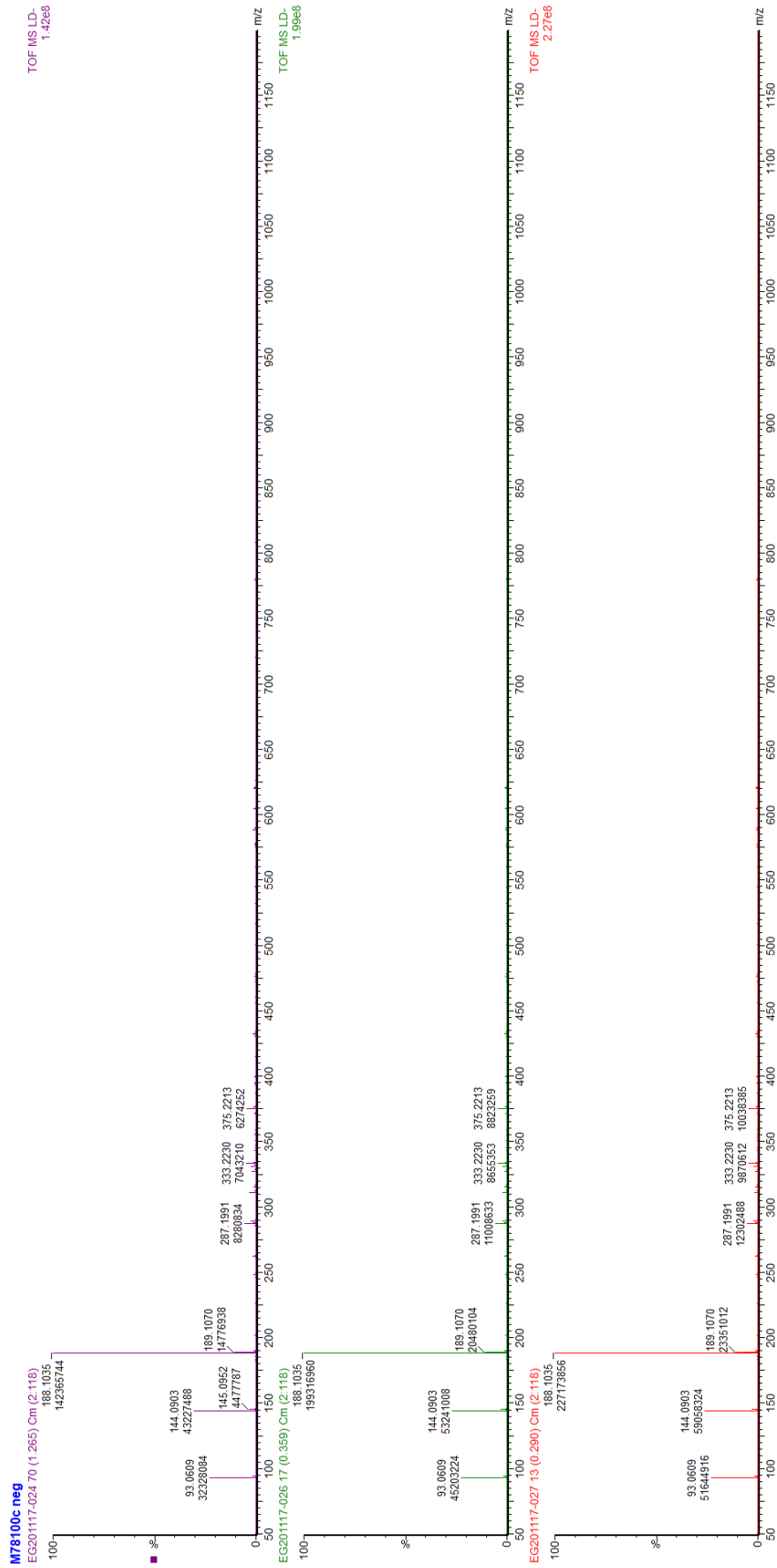
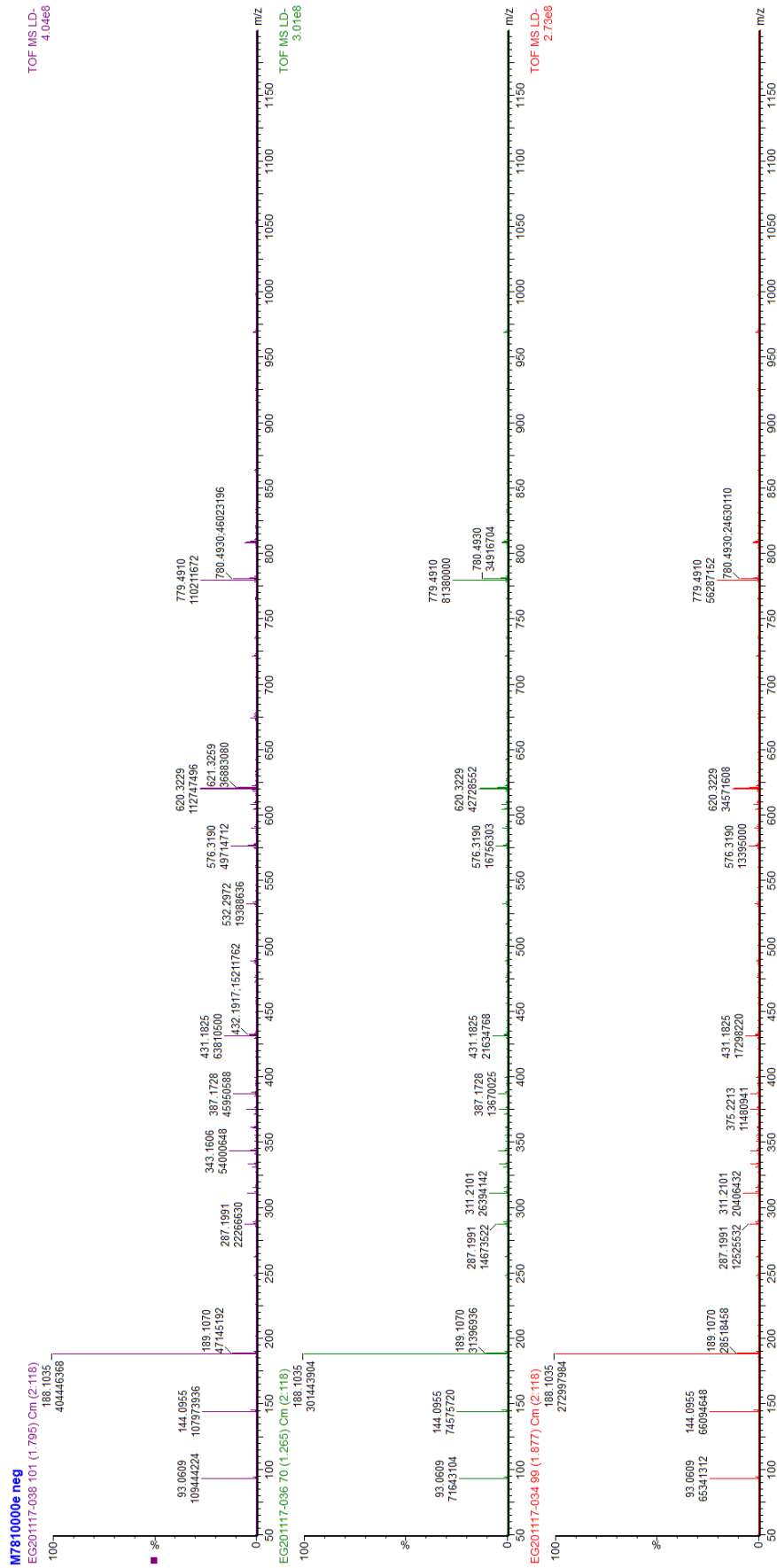


Figure 7.13 Mass spectra of three replicates of the 100 fold diluted samples in negative ionization mode (MALDI-MS Test 2)



A2 Chapter 3 Supplementary material

MALDI-MS Supplementary Material

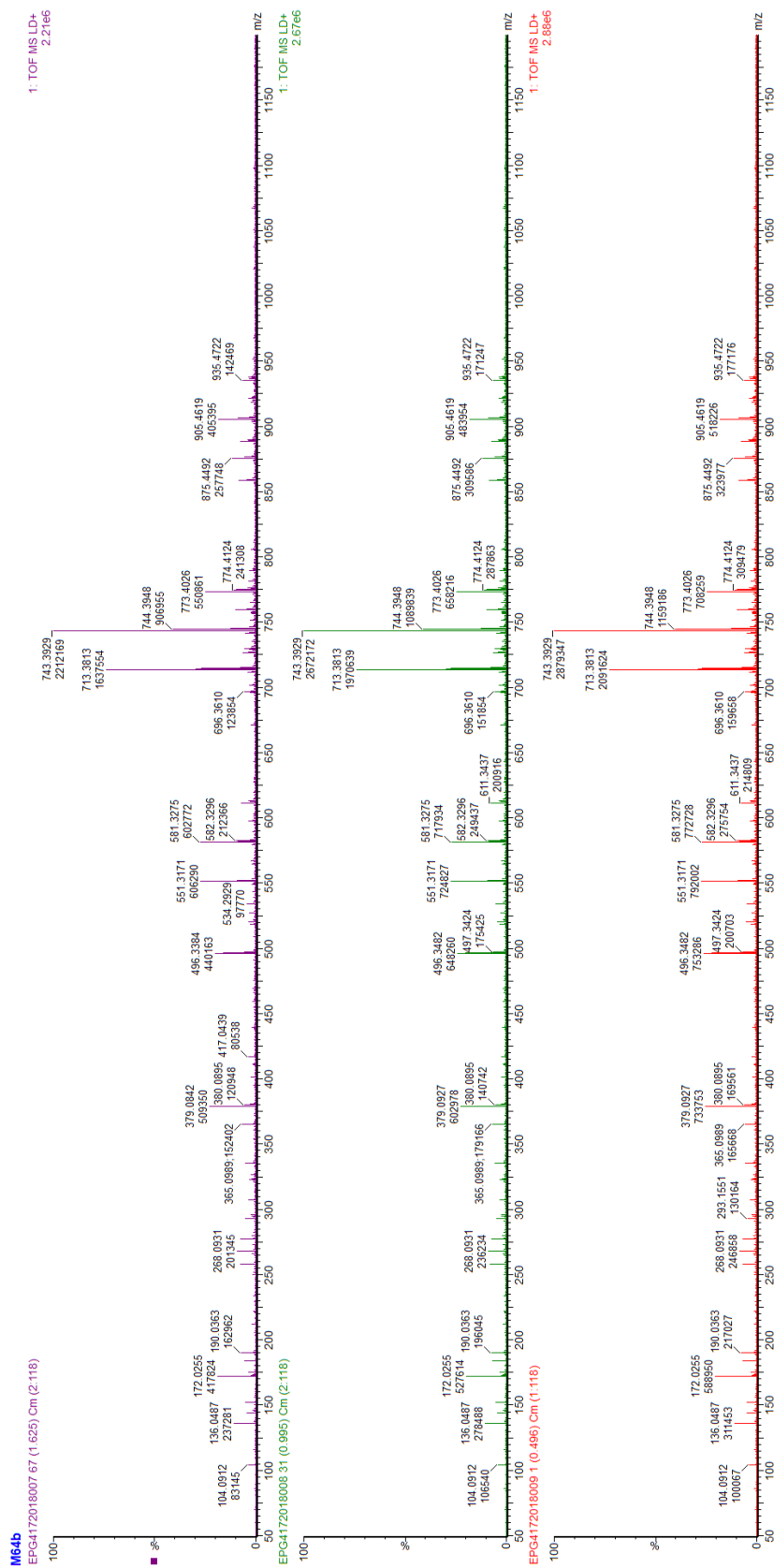


Figure 7.16 Mass spectra of three M64 replicates (MALDI-MS positive mode Chapter 3)

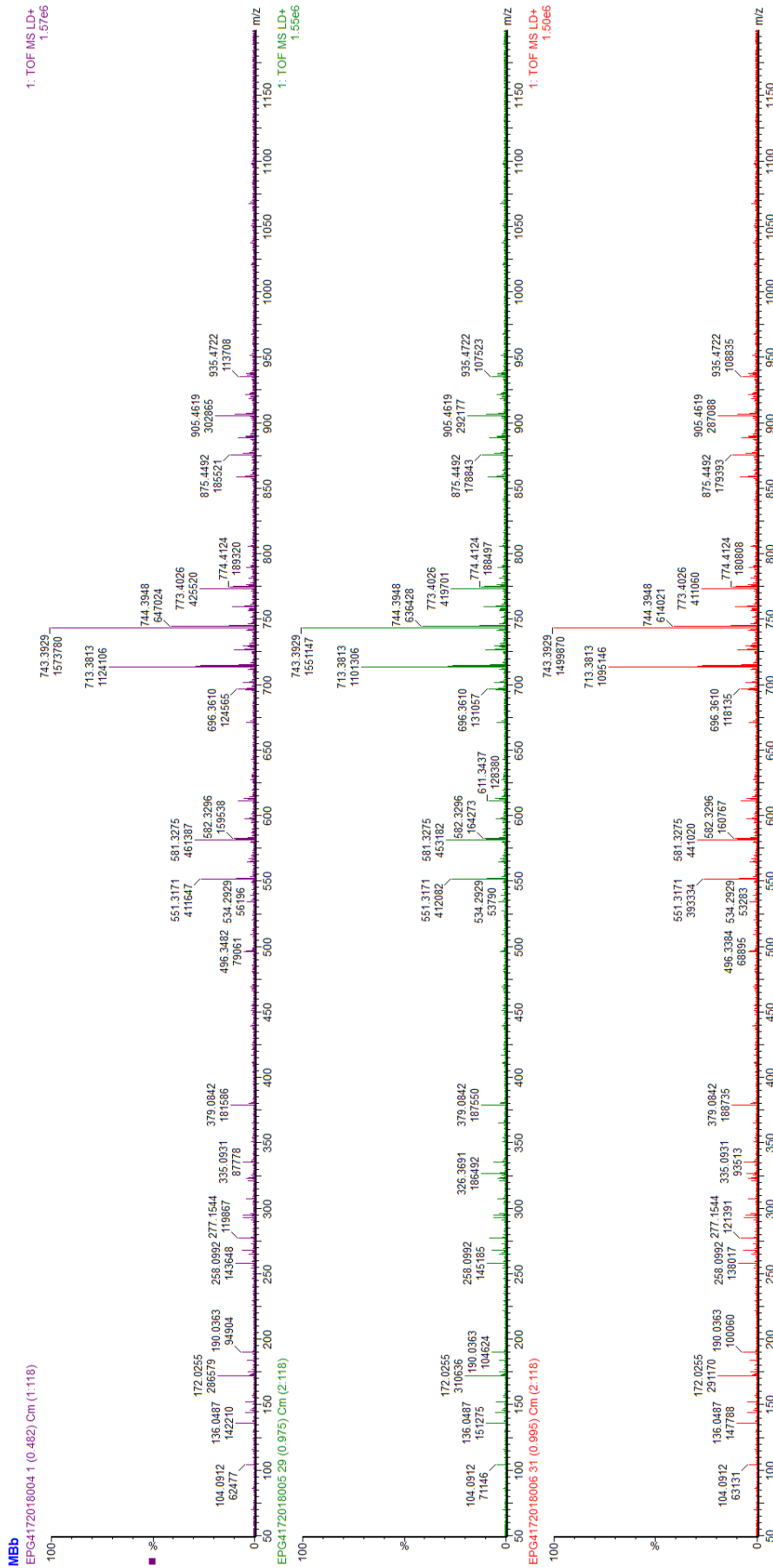


Figure 7.17 Mass spectra of three MB replicates (MALDI-MS positive mode Chapter 3)

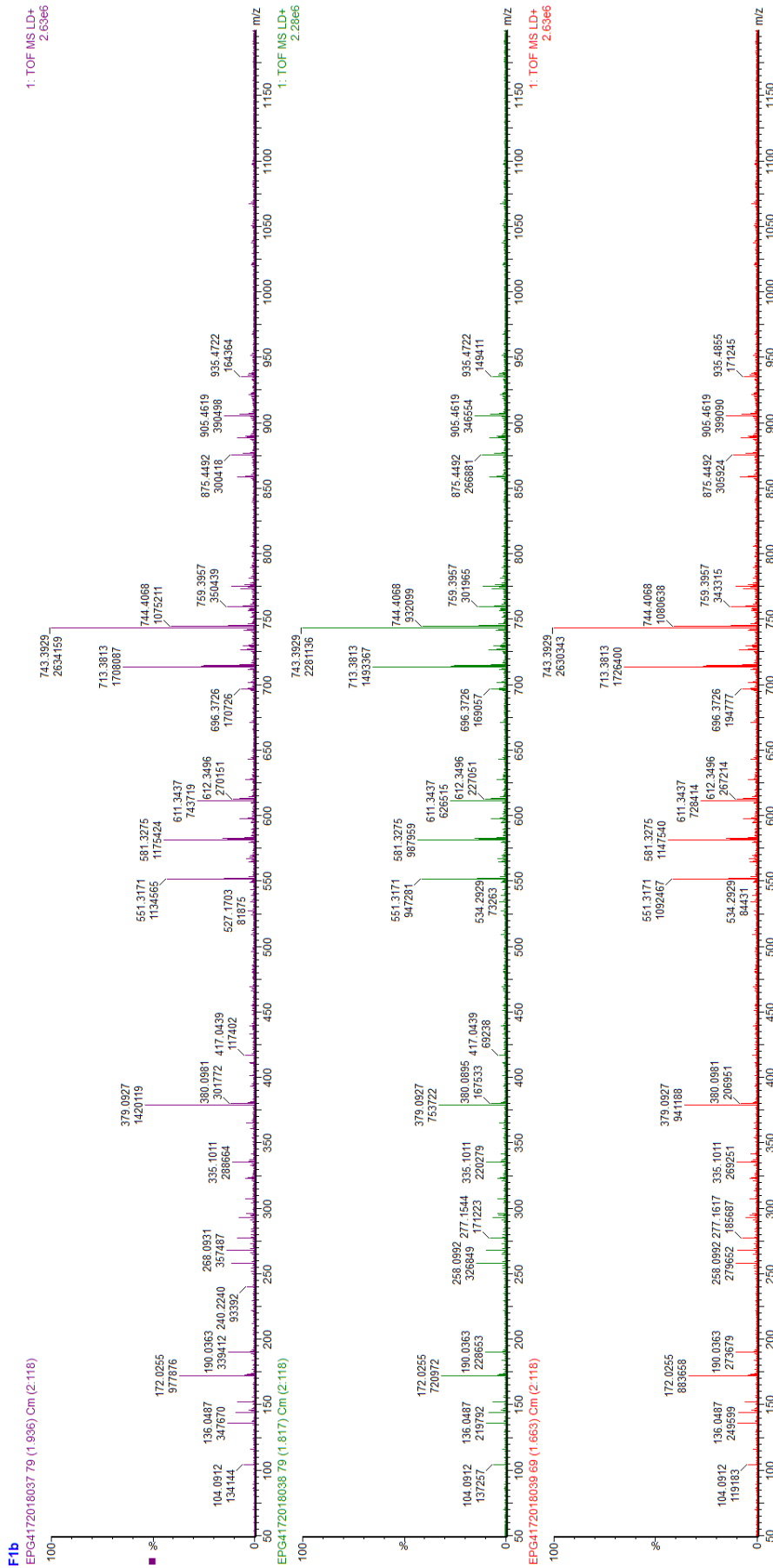


Figure 7.18 Mass spectra of three F1 replicates (MALDI-MS positive mode Chapter 3)

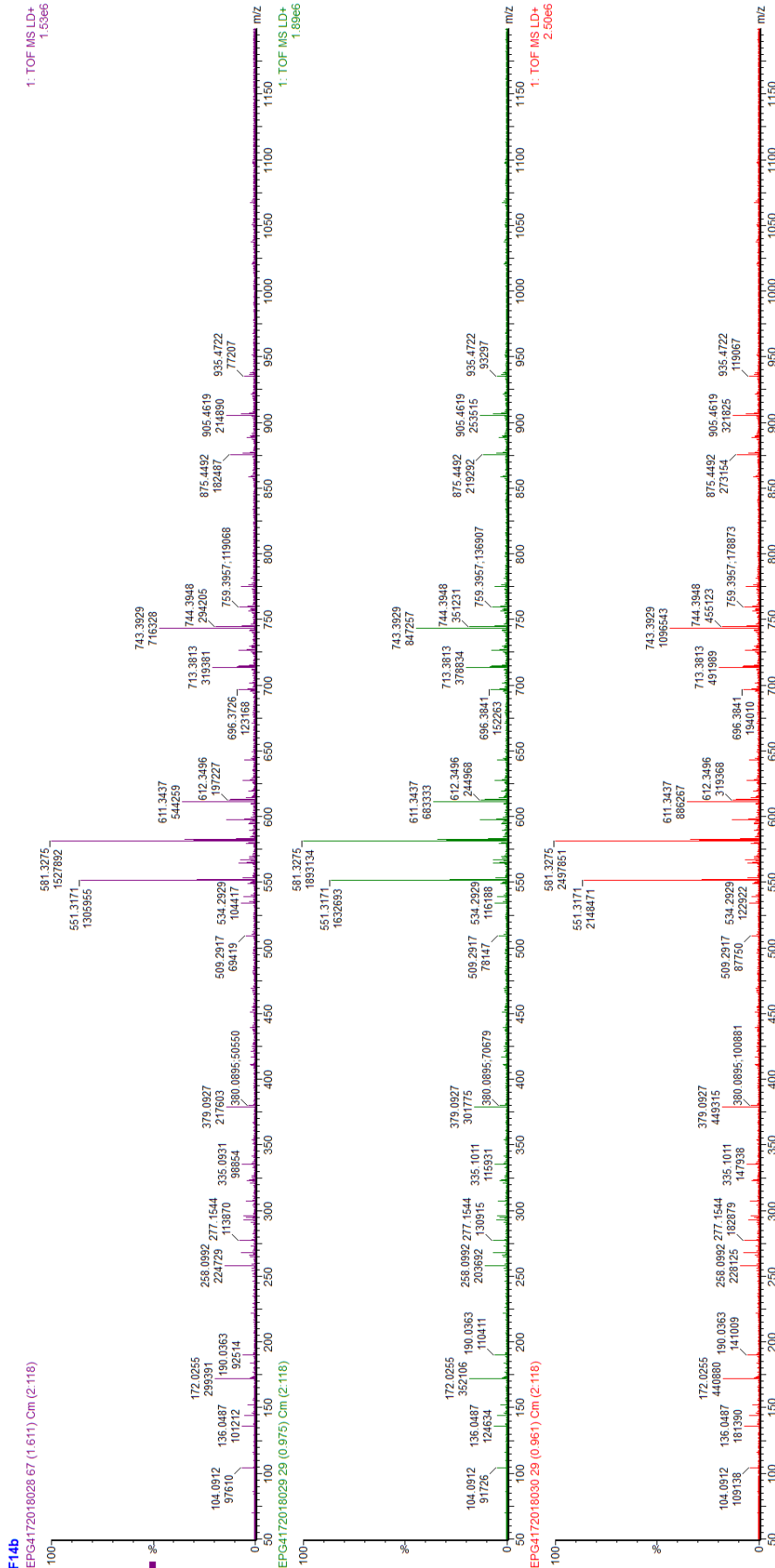


Figure 7.19 Mass spectra of three F14 replicates (MALDI-MS positive mode Chapter 3)

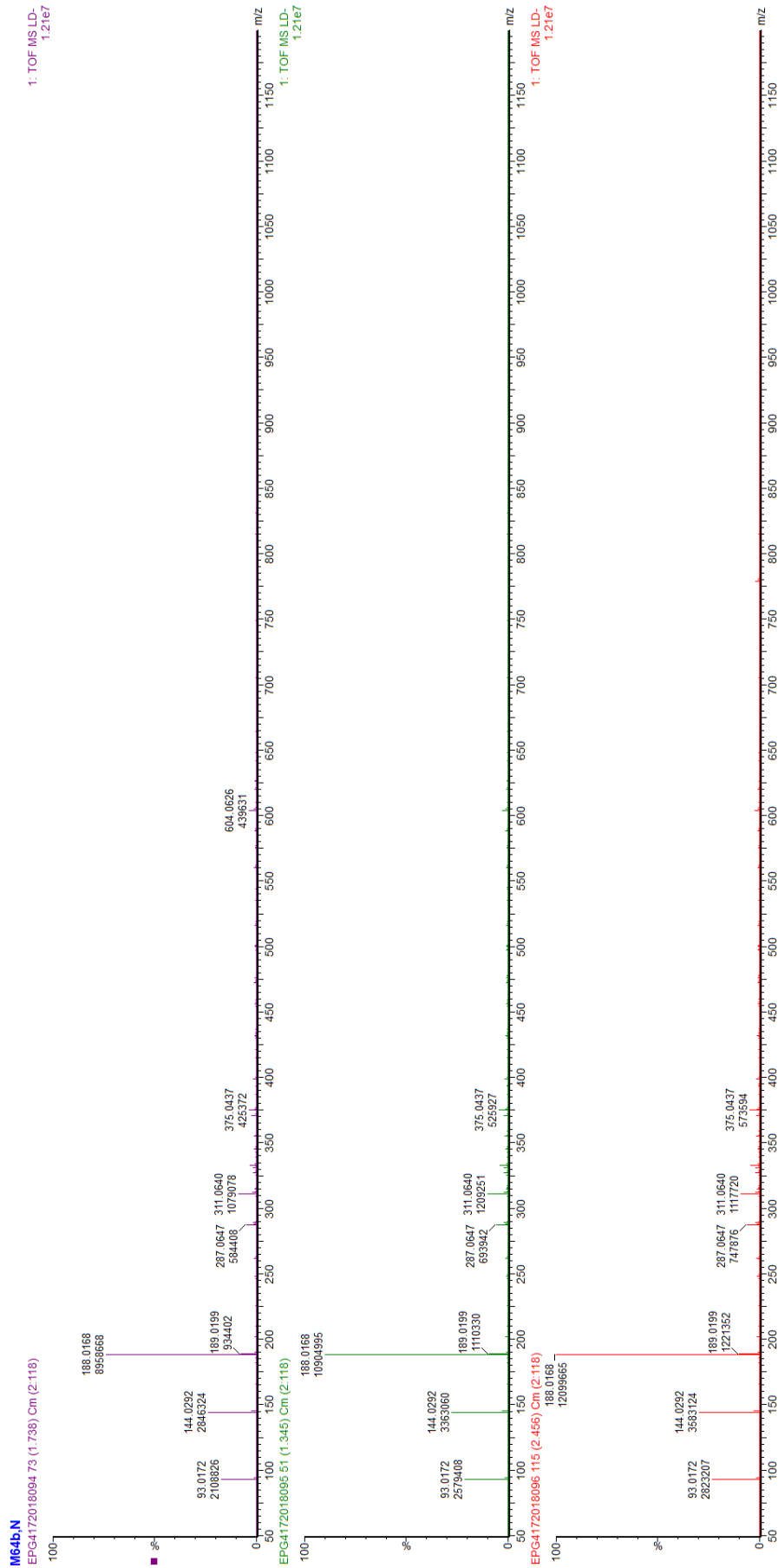


Figure 7.20 Mass spectra of three M64 replicates (MALDI-MS negative mode Chapter 3)

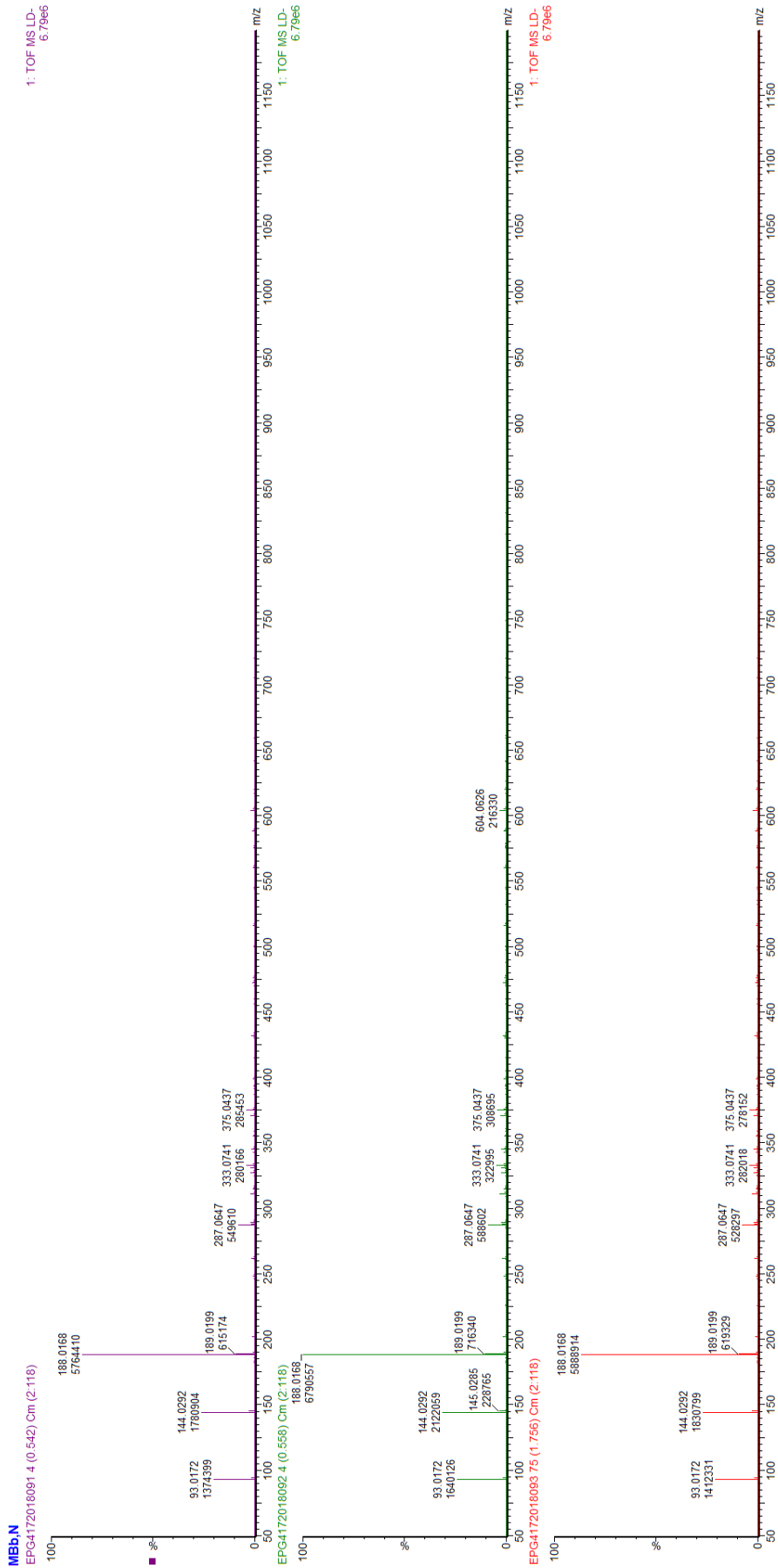


Figure 7.21 Mass spectra of three MB replicates (MALDI -MS negative mode Chapter 3)

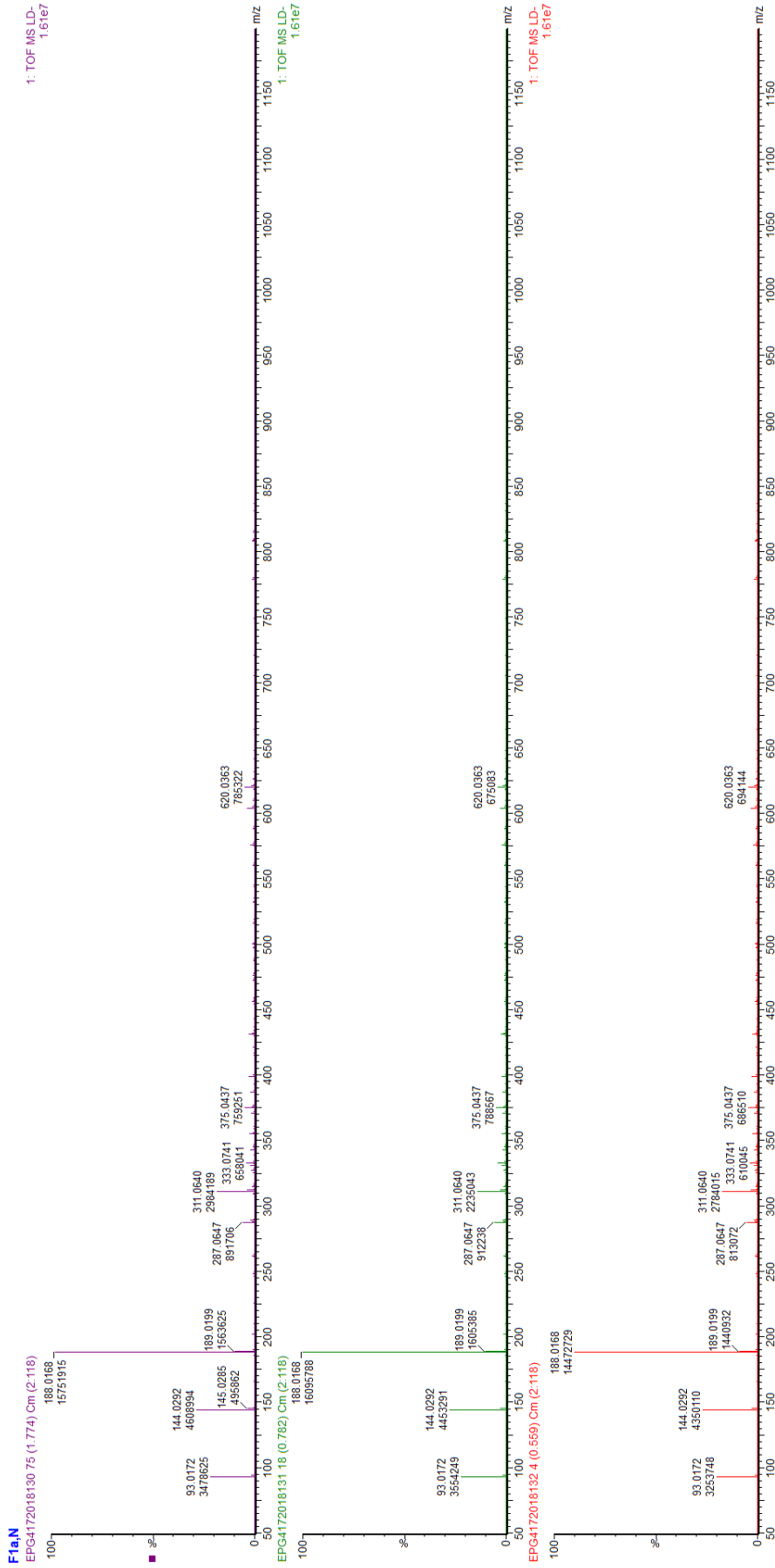


Figure 7.22 Mass spectra of three F1 replicates (MALDI-MS negative mode Chapter 3)

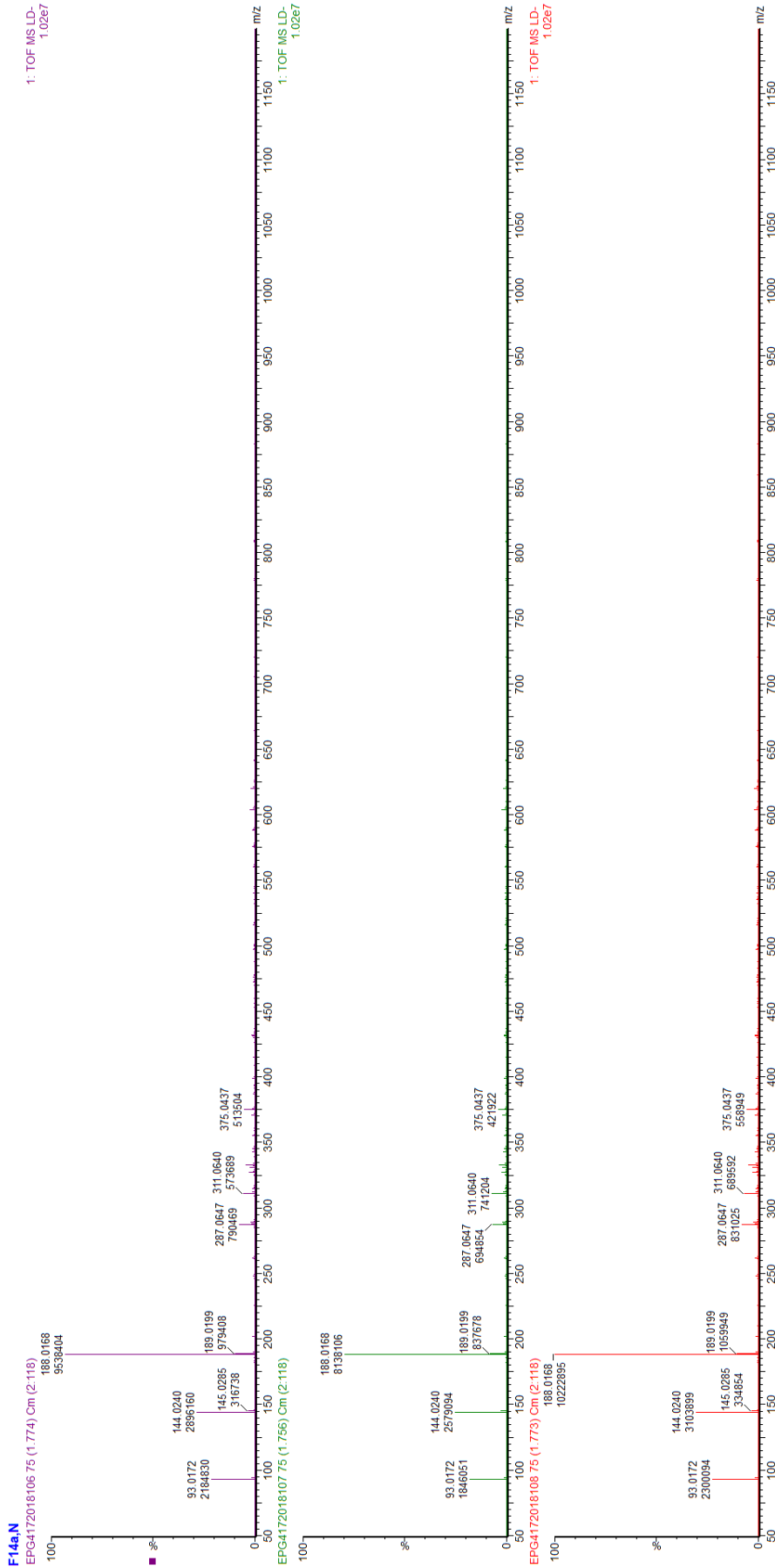


Figure 7.23 Mass spectra of three F14 replicates (MALDI-MS negative mode Chapter 3)

Table 7.1 Putative identification of compounds discriminant to the pre-fermentation sample class (MALDI-MS positive mode)

Bin	Query mass	Compound name	Formula	Monoisotopic mass	Adduct	Adduct m/z	Δppm	Flavour descriptor	Chemical class
	175.0354	Juglone	C10H6O3	174.0317	M+H	175.039	20	NIF	Napthalene
	175.0354	Methylparaben	C8H8O3	152.0473	M+Na	175.0366	7	odorless	Benzene
	175.0354	p-Hydroxyphenylacetic acid	C8H8O3	152.0473	M+Na	175.0366	7	NIF	Phenol
	175.0354	Methyl salicylate	C8H8O3	152.0473	M+Na	175.0366	7	mint, peppermit, wintergreen	Benzene
	175.0643	Tetramethylpyrazine	C8H12N2	136.1	M+K	175.0632	6	Burnt, chocolate, cocoa, coffee, lard, musty, nutty, soybean	Pyrazine
	174.9718	3-Methyl-1,2,4-trithiane	C4H8S3	151.9788	M+Na	174.968	22	NIF	Trithiane
	175.0643	2-Methyl-5-propylpyrazine	C8H12N2	136.1	M+K	175.0632	6	NIF	Pyrazine
	175.0643	2-Ethyl-3,5-dimethylpyrazine	C8H12N2	136.1	M+K	175.0632	6	Burnt almonds, coffee, potato, roast, roasted nuts	Pyrazine
	175.0354	2-Hydroxyphenylacetic acid	C8H8O3	152.0473	M+Na	175.0366	7	NIF	Benzene
	175.0354	Hypoxanthine	C5H4N4O	136.1114	M+K	175.0017	192.7353	NIF	Purine
	175.0354	Phenylacetic acid	C8H8O19	136.1479	M+K	175.0156	113.2071	civet, floral, flower, honey, sweet, waxy	Benzene
175								almond, anise, balsam, berry, bitter, cherry, chocolate, cinnamon, creamy, floral, hawthorn, mimosa, mint, minty, powdery, sweet, vanilla	
	175.0354	4-Methoxybenzaldehyde	C8H8O19	136.1479	M+K	175.0156	113.2071	floral, mint, powdery, sweet, vanilla	Benzene
	175.0354	Xanthine	C5H4N4O17	152.1108	M+Na	175.0227	72.84771	NIF	Purine
	175.0354	Mandelic acid	C8H8O18	152.1473	M+Na	175.0366	6.661465	NIF	Benzene
	175.0354	Vanillin	C8H8O18	152.1473	M+Na	175.0366	6.661465	chocolate, creamy, sweet, vanilla	phenol
	175.0354	4-Ethylguaiaicol	C9H12O17	152.1904	M+Na	175.0729	214.442	bacon, phenolic, smoky, spice, spicy	Phenol
	175.0354	Myrcene	C10H33	136.234	M+K	175.0884	302.453	NIF	Terpenoid
	175.0354	Succinic acid diethyl ester	C8H14O17	174.0892	M+H	175.0965	348.8305	apple, apricot, chocolate, cooked, cranberry, fruit, fruity, grape, mild, musty, peach, pear, wine, ylang	Fatty acid ester
	265.0906	4-Vinylsyringol	C15H14O3	242.0943	M+Na	265.0835	27	NIF	Stillbene
	265.0906	8-Phenyl-3,4-dihydro-1H-2-benzopyran-6,7-diol	C15H14O3	242.0943	M+Na	265.0835	27	NIF	Phenol
265	265.042	Benzoyl peroxide	C14H10O4	242.0579	M+Na	265.0471	19	Benzaldehyde, mild	Benzene
	265.0906	Thymidine	C10H14N2O5	242.2285	M+Na	265.0795	41.91573	NIF	Pyrimidine
	265.029	L-arogenate	C10H12NO5	226.0721	M+K	265.0353	24	NIF	Amino acid
	381.0834	Sucrose	C12H22O11	342.1162	M+K	381.0794	11	NIF	Carbohydrate
381	381.0834	Kojibiose	C12H22O11	342.1162	M+K	381.0794	11	NIF	Fatty acyl glycoside
	381.0834	Galactinol	C12H22O11	342.1162	M+K	381.0794	11	NIF	Carbohydrate

Bin	Query mass	Compound name	Formula	Monoisotopic mass	Adduct	Adduct m/z	Δppm	Flavour descriptor	Chemical class
	381.0834	D-Maltose	C12H22O11	342.1162	M+K	381.0794	11	NIF	Carbohydrate
	381.0834	beta-Mannobiose	C12H22O11	342.1162	M+K	381.0794	11	NIF	Carbohydrate
	381.0834	Melibiose	C12H22O11	342.1162	M+K	381.0794	11	NIF	Carbohydrate
	381.0834	Isomaltose	C12H22O11	342.1162	M+K	381.0794	11	NIF	Carbohydrate
	381.0834	3-Hydroxy-3-(3,4-dihydroxy-4-methylpentanoyl)-5-(3-methylbutyl)-1,2,4-cyclopentanetione	C16H22O8	342.1315	M+K	381.0946	29	NIF	Carbonyl
	381.0834	Turanose	C12H22O11	342.1162	M+K	381.0794	11	NIF	Fatty acyl glycoside
	381.0834	Fagopyritol A1	C12H22O11	342.1162	M+K	381.0794	11	NIF	Carbohydrate
	381.0834	Trehalose	C12H22O11	342.1162	M+K	381.0794	11	NIF	Carbohydrate
496.4	496.3271	23-Acetoxyisoladulcidine	C29H47NO4	473.3505	M+Na	496.3397	26	NIF	Alkaloid
	496.3531	23-Acetoxy-25-episuladulcidine	C29H47NO4	473.3505	M+Na	496.3397	27	NIF	Alkaloid
	496.3271	16-Hydroxy-5',7,9,13-tetramethyl-5-oxaspiropentacycloicosane-6,2'-piperidine]-3'-yl acetate	C29H47NO4	473.3505	M+Na	496.3397	26	NIF	Alkaloid
	543.1487	Myricatomentoside I	C26H32O10	504.1995	M+K	543.1627	26	NIF	Lignan glycoside
	543.1996	Matairesinoside	C26H32O11	520.1945	M+Na	543.1837	29	NIF	Lignan glycoside
543.2	543.1996	2-(Hydroxymethyl)-6-{4-[3-(hydroxymethyl)-5-[[12]-3-hydroxyprop-1-en-1-yl]-7-methoxy-2,3-dihydro-1-benzofuran-2-yl]-2-methoxyphenoxy}oxane-3,4,5-triol	C26H32O11	520.1945	M+Na	543.1837	29	NIF	Flavonoid
	543.2505	Cinnassiol C1 19-glucoside	C26H38O12	542.2363	M+H	543.2436	13	NIF	Terpene glycoside
	543.1487	β-Glucan	C18H32O3	504.437	M+K	543.1322	30.3885	NIF	Carbohydrate
	543.1487	Maltotriose	C18H32O3	504.437	M+K	543.1322	30.3885	NIF	Carbohydrate
543.4	543.3015	Chaetoglobosin N	C33H38N2O5	542.2781	M+H	543.2853	30	NIF	Alkaloid
	543.3015	Protobassic acid	C30H48O6	504.3451	M+K	543.3082	12	NIF	Triterpenoid
	543.3015	Tomentosic acid	C30H48O6	504.3451	M+K	543.3082	12	NIF	Triterpenoid
	543.3015	Sericic acid	C30H48O6	504.3451	M+K	543.3082	12	NIF	Triterpenoid
	543.3015	10,11,12-Trihydroxy-9-(hydroxymethyl)-hexamethyl-icosahydricene-4a-carboxylic acid	C30H48O6	504.3451	M+K	543.3082	12	NIF	Triterpenoid
	543.3015	Myrianthic acid	C30H48O6	504.3451	M+K	543.3082	12	NIF	Triterpenoid
	543.3015	3beta-Myrianthic acid	C30H48O6	504.3451	M+K	543.3082	12	NIF	Triterpenoid
	543.3015	Cyclopassifloic acid D	C30H48O6	504.3451	M+K	543.3082	12	NIF	Steroid
	543.3015	6beta-Hydroxyasiatic acid	C30H48O6	504.3451	M+K	543.3082	12	NIF	Triterpenoid

Bin	Query mass	Compound name	Formula	Monoisotopic mass	Adduct	Adduct m/z	Δppm	Flavour descriptor	Chemical class
	543.3015	Isothankunic acid	C30H48O6	504.3451	M+K	543.3082	12	NIF	Triterpenoid
	543.3015	1,10-Dihydroxy-9,9-bis(hydroxymethyl)-pentamethyl--icosahydricene-4a-carboxylic acid	C30H48O6	504.3451	M+K	543.3082	12	NIF	Triterpenoid
	543.3015	(1-{2-[2-(acetyloxy)-5-oxo-2,5-dihydrofuran-3-yl]-2-hydroxyethyl}-2-hydroxy-4b,8,8,10a-tetramethyl-tetradecahydroph enanthren-2-yl)methyl acetate	C29H44O8	520.3036	M+Na	543.2928	16	NIF	Terpenoid
	543.3525	Cyclopasiffloic acid B	C31H52O6	520.3764	M+Na	543.3656	24	NIF	Steroid
	713.3151	Nomilinic acid 17-O-beta-D-glucoside	C34H48O16	712.2942	M+H	713.3015	19	NIF	Terpene glycoside
	713.3248	Citrusin ii	C37H44N8O7	712.3333	M+H	713.3406	22	NIF	Carboxylic acid
713.4	713.4922	Dg(20:3(5z,8z,11z)/22:6(4z,7z,10z,13z,16z,19z)/0:0)	C45H70O5	690.5223	M+Na	713.5115	27	NIF	Glycerolipid
	713.4922	DG(20:3(8Z,11Z,14Z)/22:6(4Z,7Z,10Z,13Z,16Z,19Z)/0:0)[iso2]	C45H70O5	690.5223	M+Na	713.5115	27	NIF	Glycerolipid
714.4	714.4855	PC(14:0/15:0)	C37H74NO8P	691.5152	M+Na	714.5044	26	NIF	Glycerophospholipids
	714.4855	PE(14:0/18:0)	C37H74NO8P	691.5152	M+Na	714.5044	26	NIF	Glycerophospholipids
744.4	744.4008	beta1-Chaconine	C39H63NO10	705.4452	M+K	744.4084	10	NIF	Alkaloid
	744.4008	PS(14:0/16:1(9Z))	C36H68NO10P	705.4581	M+K	744.4212	27	NIF	Glycerophospholipids
773.4	773.4087	Mubenin B	C41H66O11	734.4605	M+K	773.4237	19	NIF	Triterpenoid
	775.4532	Alpha-spinasterol gentiobioside	C41H68O11	736.4762	M+K	775.4393	18	NIF	Steroid
775.4	775.3923	Cyclosquamosin f	C36H54N8O11	774.3912	M+H	775.3985	8	NIF	Carboxylic acid
	775.4532	Melilotoside B	C41H68O12	752.4711	M+Na	775.4603	9	NIF	Triterpenoid

Table 7.2 Putative identification of compounds discriminant to the post-fermentation sample class (MALDI-MS positive mode)

Bin	Query mass	Compound name	Formula	Monoisotopic mass	Adduct	Adduct m/z	Δ (ppm)	Flavour descriptor	Chemical class
551.4	551.3223	Ganoderic Acid V	C32H48O6	528.3451	M+Na	551.3343	22	NIF	Triterpenoid
	551.3223	(22S)-Acetoxy-3alpha,15alpha-dihydroxylanosta-7,9(11),24-trien-26-oic acid	C32H48O6	528.3451	M+Na	551.3343	22	NIF	Triterpenoid
	551.3223	(22S)-Acetoxy-3beta,15alpha-dihydroxylanosta-7,9(11),24-trien-26-oic acid	C32H48O6	528.3451	M+Na	551.3343	22	NIF	Triterpenoid
	551.3223	(24E)-3alpha-Acetoxy-15alpha,22S-dihydroxylanosta-7,9(11),24-trien-26-oic acid	C32H48O6	528.3451	M+Na	551.3343	22	NIF	Triterpenoid
	551.3223	Ganodermic acid TO	C32H48O5	512.3502	M+K	551.3133	16	NIF	Triterpenoid
	551.3223	Ganodermic acid TN	C32H48O5	512.3502	M+K	551.3133	16	NIF	Triterpenoid
	551.3291	Ganoderic acid S	C32H48O5	512.3502	M+K	551.3133	29	NIF	Triterpenoid
	551.3291	Ganoderic Acid Mf	C32H48O5	512.3502	M+K	551.3133	29	NIF	Triterpenoid
	551.3291	Ganoderic Acid X	C32H48O5	512.3502	M+K	551.3133	29	NIF	Triterpenoid
	551.4113	DG(14:0/14:0/0:0)	C31H60O5	512.4441	M+K	551.4072	7	NIF	Diacylglycerol
	551.4113	DG(12:0/16:0/0:0)	C31H60O5	512.4441	M+K	551.4072	7	NIF	Diacylglycerol
	551.4113	DG(10:0/18:0/0:0)	C31H60O5	512.4441	M+K	551.4072	7	NIF	Diacylglycerol
	551.4113	DG(14:0/14:0/0:0)	C31H60O5	512.4441	M+K	551.4072	7	NIF	Diacylglycerol
	551.4626	DG(15:1(11Z)/16:1(11Z)/0:0)	C34H62O5	550.4597	M+H	551.467	8	NIF	Diacylglycerol
	551.4626	DG(15:1(9Z)/16:1(11Z)/0:0)	C34H62O5	550.4597	M+H	551.467	8	NIF	Diacylglycerol
	551.4763	DG(15:1(11Z)/16:1(9Z)/0:0)	C34H62O5	550.4597	M+H	551.467	17	NIF	Diacylglycerol
551.4763	DG(15:1(9Z)/16:1(9Z)/0:0)	C34H62O5	550.4597	M+H	551.467	17	NIF	Diacylglycerol	
552.4	552.4146	LysoPC(20:0)	C28H58NO7P	551.3951	M+H	552.4024	22	NIF	Glycerophospholipid
567.4	567.3212	Ganoderic Acid V	C32H48O6	528.3451	M+K	567.3082	23	NIF	Triterpenoid
	567.3212	(22S)-Acetoxy-3alpha,15alpha-dihydroxylanosta-7,9(11),24-trien-26-oic acid	C32H48O6	528.3451	M+K	567.3082	23	NIF	Triterpenoid
	567.3212	(22S)-Acetoxy-3beta,15alpha-dihydroxylanosta-7,9(11),24-trien-26-oic acid	C32H48O6	528.3451	M+K	567.3082	23	NIF	Triterpenoid
	567.3212	(24E)-3alpha-Acetoxy-15alpha,22S-dihydroxylanosta-7,9(11),24-trien-26-oic acid	C32H48O6	528.3451	M+K	567.3082	23	NIF	Triterpenoid
	567.3212	Hovenidulcigenin A	C32H48O7	544.34	M+Na	567.3292	14	NIF	Prenol lipid
	567.3212	Cinnamoylvulgaro side	C34H46O7	566.3244	M+H	567.3316	18	NIF	Prenol lipid
	567.3281	Tsugaric acid B	C33H52O5	528.3815	M+K	567.3446	29	NIF	Triterpenoid
	567.408	Dehydroplectania xanthin	C40H54O2	566.4124	M+H	567.4197	21	NIF	Tetraterpenoid
	567.4984	Phytoene	C40H64	544.5008	M+Na	567.49	15	NIF	Tetraterpenoid
	567.4984	Phytoene	C40H64	544.5008	M+Na	567.49	15	NIF	Tetraterpenoid

Bin	Query mass	Compound name	Formula	Monoisotopic mass	Adduct	Adduct m/z	Δ (ppm)	Flavour descriptor	Chemical class
	567.4984	all-trans-Phytoene	C40H64	544.5008	M+Na	567.49	15	NIF	Tetraterpenoid
	567.4984	DG(16:0/16:1(9Z)/0:0)	C35H66O5	566.491	M+H	567.4983	0	NIF	Diacylglycerol
	567.4984	DG(10:0/22:1(11Z)/0:0)	C35H66O5	566.491	M+H	567.4983	0	NIF	Diacylglycerol
	567.4984	DG(10:0/22:1(9Z)/0:0)	C35H66O5	566.491	M+H	567.4983	0	NIF	Diacylglycerol
	567.4984	DG(12:0/20:1(11Z)/0:0)	C35H66O5	566.491	M+H	567.4983	0	NIF	Diacylglycerol
	567.4984	DG(12:0/20:1(13Z)/0:0)	C35H66O5	566.491	M+H	567.4983	0	NIF	Diacylglycerol
	567.4984	DG(14:0/18:1(11Z)/0:0)	C35H66O5	566.491	M+H	567.4983	0	NIF	Diacylglycerol
	567.4984	DG(14:0/18:1(9Z)/0:0)	C35H66O5	566.491	M+H	567.4983	0	NIF	Diacylglycerol
	567.4984	DG(14:1(11Z)/18:0/0:0)	C35H66O5	566.491	M+H	567.4983	0	NIF	Diacylglycerol
	567.4984	DG(14:1(9Z)/18:0/0:0)	C35H66O5	566.491	M+H	567.4983	0	NIF	Diacylglycerol
	567.4984	DG(16:0/16:1(11Z)/0:0)	C35H66O5	566.491	M+H	567.4983	0	NIF	Diacylglycerol
581.4	581.4909	Epomusenin A	C37H66O3	558.5012	M+Na	581.4904	1	NIF	Fatty acyl alcohol
	581.4909	Epomusenin B	C37H66O3	558.5012	M+Na	581.4904	1	NIF	Fatty acyl alcohol
	581.3363	Hordatine B	C29H40N8O5	580.3122	M+H	581.3194	29	NIF	Flavonoid
582.2	582.1766	Neoaclarimarine K	C31H29NO9	559.1842	M+Na	582.1735	5	NIF	Quinoline
	582.4791	1-(5-Decanoyl-4-nonyl-1,4-dihydropyridin-3-yl)dodecan-1-one	C36H65NO2	543.5015	M+K	582.4647	25	NIF	Dihydropyridine
	582.2873	LIPC 18:0;3	C24H50NO11P	559.3121	M+Na	582.3014	24	NIF	Sphingolipid
	582.2873	Lysopc(20:4(5Z,8Z,11Z,14Z))	C28H50NO7P	543.3325	M+K	582.2956	14	NIF	Lysophospholipid
	582.2873	Lyso-PC(20:4(5Z,8Z,11Z,14Z)/0:0)	C28H50NO7P	543.333	M+K	582.2962	15	NIF	Lysophospholipid
	582.2908	Lysopc(20:4(8Z,11Z,14Z,17Z))	C28H50NO7P	543.3325	M+K	582.2956	8	NIF	Lysophospholipid
583.4	583.4716	Phytoene	C40H64	544.5008	M+K	583.464	13	NIF	Tetraterpenoid
	583.4787	15-cis-Pytoene	C40H64	544.5008	M+K	583.464	25	NIF	Tetraterpenoid
	583.3132	Hovenidulcigenin A	C32H48O7	544.34	M+K	583.3032	17	NIF	Prenol lipid
	583.4258	DG(14:0/18:4(6Z,9Z,12Z,15Z)/0:0)	C35H60O5	560.4441	M+Na	583.4333	13	NIF	Diacylglycerol
	583.4117	2-Hexaprenyl-3-methyl-6-methoxy-1,4-benzoquinone	C38H56O3	560.4229	M+Na	583.4122	1	NIF	Quinone
	583.4769	TG(10:0/10:0/12:0)	C35H66O6	582.4859	M+H	583.4932	28	NIF	Triradylglycerol
595.4	595.469	6-Hydroxydesacetyl uvaricin	C35H62O7	594.4496	M+H	595.4568	20	NIF	Fatty acyl alcohol
597.4	597.4626	Epomusenin A	C37H66O3	558.5012	M+K	597.4644	3	NIF	Fatty acyl alcohol
	597.4626	Epomusenin B	C37H66O3	558.5012	M+K	597.4644	3	NIF	Fatty acyl alcohol
	597.4626	Muricatetrocin C	C35H64O7	596.4652	M+H	597.4725	17	NIF	Fatty acyl alcohol
	597.4626	Glacin B	C35H64O7	596.4652	M+H	597.4725	17	NIF	Fatty acyl alcohol
	597.4626	Glacin A	C35H64O7	596.4652	M+H	597.4725	17	NIF	Fatty acyl alcohol
	597.4626	Rolliacocin	C35H64O7	596.4652	M+H	597.4725	17	NIF	Fatty acyl alcohol
	597.4626	Muricatetrocin B	C35H64O7	596.4652	M+H	597.4725	17	NIF	Fatty acyl alcohol
	597.3379	Ergosteryl 3- ¹² -D-glucoside	C34H54O6	558.392	M+K	597.3552	29	NIF	Ergostane steroid
598.4	598.3359	gamma-Chaconine	C33H53NO6	559.3873	M+K	598.3504	24	NIF	Steroidal glycoside
	598.3359	gamma-Solanine	C33H53NO6	559.3873	M+K	598.3504	24	NIF	Steroidal glycoside

Bin	Query mass	Compound name	Formula	Monoisotopic mass	Adduct	Adduct m/z	Δ (ppm)	Flavour descriptor	Chemical class
	598.4143	3-Hexaprenyl-4-hydroxy-5-methoxybenzoate	C38H55O4	575.4106	M+Na	598.3998	24	NIF	Prenol lipid
611.4	611.4391	Annoglaxin	C35H62O8	610.4445	M+H	611.4517	21	NIF	Fatty acyl alcohol
	611.3527	PA(14:1(9Z)/14:1(9Z))	C31H57O8 P	588.3791	M+Na	611.3683	26	NIF	Glycerophospholipid
	611.3527	PA(14:1(9Z)/14:1(11Z))	C31H57O8 P	588.3791	M+Na	611.3683	26	NIF	Glycerophospholipid
	611.3527	PA(14:1(11Z)/14:1(9Z))	C31H57O8 P	588.3791	M+Na	611.3683	26	NIF	Glycerophospholipid
	611.3527	PA(14:1(11Z)/14:1(11Z))	C31H57O8 P	588.3791	M+Na	611.3683	26	NIF	Glycerophospholipid
613.4	613.4341	Schottenol 3-ferulate	C39H58O4	590.4335	M+Na	613.4227	19	NIF	Triterpenoid
	613.4341	Ubiquinone 6	C39H58O4	590.4335	M+Na	613.4227	19	NIF	Quinone
	613.4341	Feruloyl-beta-sitosterol	C39H58O4	590.4335	M+Na	613.4227	19	NIF	Triterpenoid
	613.4341	Ubiquinone 6	C39H58O4	590.4335	M+Na	613.4227	19	NIF	Quinone
	613.4341	Ubiquinone 6	C39H58O4	590.4335	M+Na	613.4227	19	NIF	Quinone

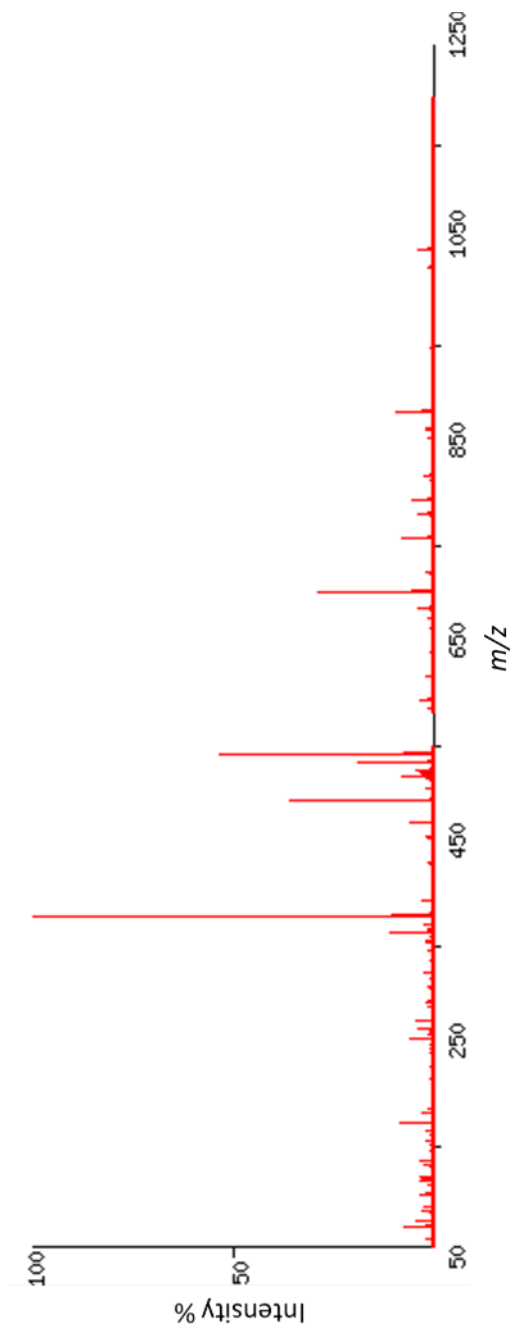


Figure 7.24 Mass spectrum of a pre-fermentation sample (DI-MS positive mode Chapter 3)

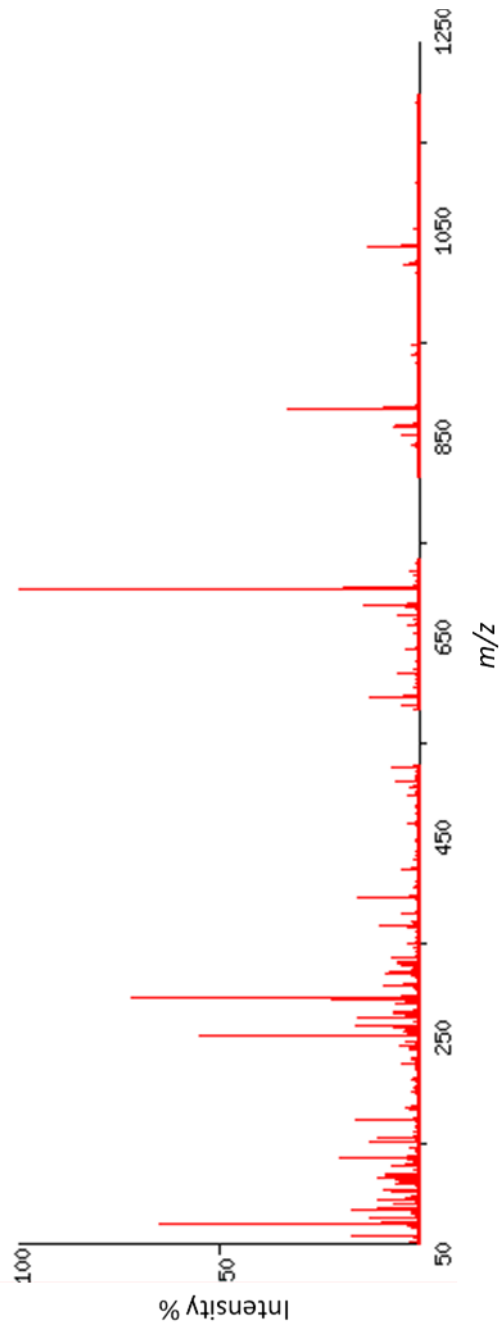


Figure 7.25 Mass spectrum of a post-fermentation sample (DI-MS positive mode Chapter 3)

Table 7.3 Putative identification of compounds discriminant to the pre-fermentation sample class (DI-MS positive mode)

Bin	Query mass	Compound name	Formula	Monoisotopic mass	Adduct m/z	Adduct type	Δ (ppm)	Flavour descriptor	Chemical class
120	120.06783	L-Homoserine	C4H9NO3	119.05824	120.06552	M+H	19	NIF	Amino acid
	120.04293	4,5-Dimethyl-1,3-oxazole	C5H7NO	97.05276	120.04198	M+Na	8	NIF	Azole
	120.02087	2-Methylpyrrole	C5H7N	81.05785	120.02101	M+K	1	bread, coumarin, licorice, musty, nut, nutty, walnut sweet, bitter, astringent	Pyrrole
	120.06783	L-Threonine	C4H9NO3	119.05824	120.06552	M+H	19	NIF	Amino acid
	120.02633	3-(methylthio)Propionate	C4H7O2S	119.01722	120.02450	M+H	15	NIF	Fatty acyl
184	184.03830	(S)-2-Amino-6-oxohexanoate	C6H11NO3	145.07389	184.03705	M+K	7	NIF	Amino acid
	184.07420	1-(2,3-Dihydro-1H-pyrrolizin-5-yl)-2-propen-1-one	C10H11NO	161.08406	184.07328	M+Na	5	NIF	Pyrrolizines
	184.04853	1-(3h-imidazo[4,5-c]pyridin-4-yl)ethan-1-one	C8H7N3O	161.05891	184.04813	M+Na	2	NIF	Imidazopyridines
	184.07420	3-(5-Methylfurfuryl)pyrrole	C10H11NO	161.08406	184.07328	M+Na	5	almond, caramel, burnt, spice	Pyrroles
	184.07420	3,4-Dihydro-4-[(5-methyl-2-furanyl)methylene]-2H-pyrrole	C10H11NO	161.08406	184.07328	M+Na	5	NIF	Heteroaromatic
	184.01773	Indole-3-carbaldehyde	C9H7NO	145.05276	184.01592	M+K	10	NIF	Indole
	184.03830	Indole-3-carboxylic acid	C9H7NO17	161.04768	184.03690	M+Na	8	NIF	Indole
	184.07420	Tryptophol/Indole-3-ethanol	C10H11NO	161.08406	184.07328	M+Na	5	almonds, solvent, unpleasant	Indole
381	381.06860	Glucocaffeic acid	C15H18O9	342.09508	381.05824	M+K	27	astringent, sour, bitter	Phenolic glycoside
	381.09070	3-b-galactopyranosyl glucose	C12H22O11	342.11621	381.07937	M+K	30	NIF	Fatty acyl
	381.09810	3-Hydroxy-3-(3,4-dihydroxy-4-methylpentanoyl)-5-(3-methylbutyl)-1,2,4-cyclopentanetrione	C16H22O8	342.13147	381.09463	M+K	9	NIF	Carbohydrate
	381.06860	5,4'-dihydroxy-3,3'-dimethoxy-6:7-methylenedioxyflavone	C18H14O8	358.06887	381.05809	M+Na	28	NIF	Flavonoid
	381.09070	Fagopyritol A1	C12H22O11	342.11621	381.07937	M+K	30	NIF	Carbohydrate
	381.09070	beta-Cellobiose	C12H22O11	342.11621	381.07937	M+K	30	NIF	Carbohydrate
	381.09810	Coniferin	C16H22O8	342.13147	381.09463	M+K	9	NIF	Phenolic glycoside
	381.09070	D-Maltose	C12H22O11	342.11621	381.07937	M+K	30	NIF	Carbohydrate
	381.09070	3-O-alpha-D-Mannopyranosyl-D-galactose	C12H22O11	342.11621	381.07937	M+K	30	NIF	Carbohydrate
	381.09070	Sucrose	C12H22O11	342.11621	381.07937	M+K	30	NIF	Carbohydrate
381.09070	Isomaltose	C12H22O28	342.11621	381.07937	M+K	30	NIF	Carbohydrate	
382	382.07823	Avenanthramide 1s	C18H17NO6	343.10559	382.06875	M+K	25	NIF	Polyphenol
	382.08563	Avenanthramide 2s	C18H17NO7	359.10050	382.08972	M+Na	11	NIF	Polyphenol
	382.07823	Caffeoyl tyrosine	C18H17NO6	343.10559	382.06875	M+K	25	NIF	Amino acid
	382.08563	Avenanthramide 2	C18H17NO7	359.10050	382.08972	M+Na	11	NIF	avenanthramides
	382.06343	DIBOA-Glc	C14H17NO9	343.09033	382.05349	M+K	26	NIF	Carbohydrate

Bin	Query mass	Compound name	Formula	Monoisotopic mass	Adduct m/z	Adduct type	Δ (ppm)	Flavour descriptor	Chemical class
	382.08563	Romucosine B	C19H18ClNO4	359.09244	382.08165	M+Na	10	NIF	aporphines
	382.06343	(R)-2,7-Dihydroxy-2H-1,4-benzoxazin-3(4H)-one 2-glucoside	C14H17NO9	343.09033	382.05349	M+K	26	NIF	Carbohydrate
	382.08563	N-(1-Deoxy-1-fructosyl)tyrosine	C15H21NO8	343.12672	382.08988	M+K	11	NIF	Amino acid
383	383.08670	1-O-alpha-D-Glucopyranosyl-D-mannitol	C12H24O11	344.13186	383.09502	M+K	22	sweet, odorless	Fatty acyl glycoside
	383.05710	Tricetin 3',4',5'-trimethyl ether	C18H16O7	344.08960	383.05276	M+K	11	NIF	flavonoid
	383.08670	Maltitol	C12H24O11	344.13186	383.09502	M+K	22	NIF	Fatty acyl glycoside
	383.08670	Melibiitol	C12H24O11	344.13186	383.09502	M+K	22	NIF	Fatty acyl glycoside
474.2	474.16760	Dhurrin 6'-glucoside	C20H27NO12	473.15333	474.16060	M+H	15	NIF	Carbohydrate
	474.18410	10-Formyltetrahydrofolate	C20H23NO7	473.16590	474.17317	M+H	23	NIF	Pteridine
496.2	496.15240	Dhurrin 6'-glucoside	C20H27NO12	473.15333	496.14254	M+Na	20	NIF	Carbohydrate
	496.16923	10-Formyltetrahydrofolate	C20H23NO7	473.16590	496.15511	M+Na	28	NIF	Pteridine
	496.16923	Pteroyl-D-glutamic acid	C20H23NO7	473.16590	496.15511	M+Na	28	NIF	Pteridine
497.10200	2'-(E)-Feruloyl-3-(arabinosylxylose) 2-(Methoxycarbonyl)-5-methyl-2,4-bis(3-methyl-2-butenyl)-6-(2-methyl-1-oxopropyl)-5-(4-methyl-3-pentenyl)cyclohexanone	C20H26O12	458.14243	497.10558	M+K	7	NIF	Coumaric acid	
497.29590	D-galactopyranosyl-(1->3)-d-galactopyranosyl-(1->3)-l-arabinose	C29H46O4	458.33961	497.30277	M+K	14	NIF	Monoterpenoid	
497.2	497.15820	alpha-D-Xylopyranosyl-(1->6)-beta-D-glucopyranosyl-(1->4)-D-glucose	C17H30O15	474.15847	497.14769	M+Na	21	NIF	Carbohydrate
497.2	497.15820	a-L-Arabinofuranosyl-(1->2)-[a-D-mannopyranosyl-(1->6)]-D-mannose	C17H30O15	474.15847	497.14769	M+Na	21	NIF	Carbohydrate
497.14693	Deoxynivalenol 3-glucoside 4'	C21H30O11	458.17881	497.14197	M+K	10	NIF	Sesquiterpenoid	
497.12730	Methylepigallocatechin 3'-glucuronide	C22H24O13	496.12169	497.12897	M+H	3	NIF	Flavonoid	
497.15820	Ethyl 6,7-dimethoxy-3-methyl-4-oxo-1-(3,4,5-trimethoxyphenyl)-1,2,3,4-tetrahydro-2-naphthalenecarboxylate	C25H30O25	372.12100	497.15722	M+K	2	NIF	Phenol	
520.2	520.19260	Gravacridonetriol glucoside	C25H29NO11	519.17406	520.18134	M+H	22	NIF	Glycerolipid
	520.25297	N1,N10-Diferuloylspermidine	C27H35NO6	497.25259	520.24180	M+Na	21	NIF	hydroxycinnamic acids
	520.28747	Vignatic acid B	C27H41NO7	519.29445	520.30173	M+H	27	NIF	cyclic peptide
522.2	522.14960	Petunidin 3-(6''-acetylglucoside)	C24H25O13	521.12952	522.13679	M+H	25	NIF	Flavonoid
534.2	534.15230	Pelargonidin 3-(6''-succinyl-glucoside) O-6-deoxy-a-l-galactopyranosyl-(1->2)-o-b-d-galactopyranosyl-(1->3)-2-(acetylamino)-1,5-anhydro-2-deoxy-d-arabino-hex-1-enitol	C25H25O13	533.12952	534.13679	M+H	29	NIF	Flavonoid
	534.18730		C20H33NO14	511.19010	534.17932	M+Na	15	NIF	Carbohydrate

Bin	Query mass	Compound name	Formula	Monoisotopic mass	Adduct m/z	Adduct type	Δ (ppm)	Flavour descriptor	Chemical class
	534.18730	O-6-deoxy-a-l-galactopyranosyl-(1->2)-o-b-d-galactopyranosyl-(1->4)-2-(acetylamino)-1,5-anhydro-2-deoxy-d-arabino-hex-1-enitol	C20H33NO14	511.19010	534.17932	M+Na	15	NIF	Carbohydrate
	535.10840	Luteolin 7-O-(6''-malonylglucoside)	C24H22O14	534.10096	535.10823	M+H	0	NIF	Flavonoid
	535.28340	7,8-Dihydrovomifoliol 9-[rhamnosyl-(1->6)-glucoside]	C25H42O12	534.26763	535.27490	M+H	16	NIF	Fatty acyl glycoside
	535.10840	Apigenin 7-(6''-malonylglucoside)	C24H22O14	534.10096	535.10823	M+H	0	NIF	Flavonoid
	535.23090	Myricatomentoside II	C27H34O11	534.21011	535.21739	M+H	25	NIF	Phenyl propanoid
535.2	535.29213	Helveticoside	C29H42O9	534.28288	535.29016	M+H	4	NIF	Steroid
	535.10840	6''-Malonylstragalol	C24H22O14	534.10096	535.10823	M+H	0	NIF	Flavonoid
	535.10840	Cyanidin 3-(6''-malonylglucoside)	C24H23O14	535.10878	535.10878	M+H	1	NIF	Flavonoid
	535.16090	Malvidin 3-(6-acetylglucoside)	C25H27O13	535.14517	535.14517	M+H	29	NIF	Flavonoid
	535.10840	(R)-Byakangelicin 3'-glucoside	C23H28O12	496.15808	535.12123	M+K	24	NIF	Coumarin
	558.14990	Malvidin 3-(6''-acetyl-galactoside)	C25H27O13	535.14517	558.13438	M+Na	28	NIF	Flavonoid
	558.14990	Gravacridonetriol glucoside	C25H29NO11	519.17406	558.13722	M+K	23	NIF	Glycerolipid
558.2	558.10230	Cyanidin 3-(3''-malonylglucoside)	C24H23O14	535.10878	558.09800	M+Na	8	NIF	Flavonoid
	558.22137	Acrimarine N	C32H31NO8	557.20497	558.21224	M+H	16	NIF	Quinoline

Table 7.4 Putative identification of compounds discriminant to the post-fermentation samples class (DI-MS positive mode)

Bin	Query mass	Compound name	Formula	Monoisotopic mass	Adduct	Adduct m/z	Δppm	Flavour descriptor	Chemical class
70	70.00430	Methylamine	CH5N	31.04220	M+K	70.00536	15	fish odor	Amine
152	151.98870	Butenyl isothiocyanate	C5H7NS	113.02992	M+K	151.99308	29	NIF	Organosulfur
	152.03223	Pyroglutamic acid	C5H7NO3	129.04259	M+Na	152.03181	3	soapy, astringent, less intense sour than other org. Acids	Amino acid
	151.98870	2,4-Dimethyl-1,3-thiazole	C5H7NS	113.02992	M+K	151.99308	29	barley, beefy, coffee, mold, roasted, rubber, tea	Azole
	152.01827	1-(4,5-Dihydro-1,3-thiazol-2-yl)ethan-1-one	C5H7NO5	129.02483	M+Na	152.01405	28	bread, chip, corn, nutty, popcorn, potato, roast, taco, toasted	Ketone
	152.05087	Quinoline	C9H7N	129.05785	M+Na	152.04707	25	Earthy, medical, musty, rubber, tobacco	Quinoline
	152.05087	2-Acetylpyrrolidine	C6H11NO	113.08406	M+K	152.04722	24	roasty	Pyrrolidine
	151.98870	2-Ethyl-1,3-thiazole	C5H7NS	113.02992	M+K	151.99308	29	Green, nutty	Azole
	152.01357	1-Pyrroline-5-carboxylic acid	C5H7NO2	113.04768	M+K	152.01084	18	NIF	Amino acid
	152.01357	2-acetyl-2-thiazoline	C5H7NO5	129.02483	M+Na	152.01405	3	bread, chip, corn, nutty, popcorn, potato, roast, taco, toasted	Ketone
	152.02757	Ethyl-2-butenate	C6H9O2	113.06025	M+K	152.02341	27	caramel, chemical, diffusive, pungent, rum, sweet	fatty acyl ester
	152.04620	2-Keto-3-methylvalerate	C6H9O3	129.05517	M+Na	152.04439	12	NIF	Fatty acyl
	152.06020	Guanine	C5H5N5O	151.04941	M+H	152.05669	23	NIF	Purine
	152.06957	4-Acetamidobutanal	C6H11NO2	129.07898	M+Na	152.06820	9	NIF	Aldehyde
	152.07887	Methyl-3-ethylbutanoate	C7H13O2	129.09155	M+Na	152.08077	13	apple-like	Fatty acyl
	152.07420	Ethyl nicotinate	C8H9NO5	151.16250	M+H	152.07060	24	medicinal, tincture, solvent, anis, stale, grainy, grape, papery	Ester
258	258.02297	Methyl 2,6-dihydroxyquinoline-4-carboxylate	C11H9NO4	219.05316	M+K	258.01632	26	NIF	Quinoline
	258.08980	1-(6-Methyl-2,3-dihydro-1H-pyrrolizin-5-yl)pentane-1,4-dione	C13H17NO2	219.12593	M+K	258.08909	3	NIF	Pyrrolizines
	257.96017	4-Nitrophenyl phosphate	C6H6NO6P	218.99327	M+K	257.95643	14	NIF	Phenyl phosphate
	258.01080	4-amino-2-methyl-5-phosphomethylpyrimidine	C6H10N3O4P	219.04089	M+K	258.00405	26	NIF	Aminopyrimidine
	258.04120	O-Succinyl-L-homoserine	C8H13NO6	219.07429	M+K	258.03745	15	NIF	Amino acid
	258.07763	Pantothenic acid	C9H17NO5	219.11067	M+K	258.07383	15	astringent, salty	Vitamin
268	268.05527	Orgothionine	C9H15NO2S	229.08850	M+K	268.05166	13	NIF	Amino acid
	268.00567	5-Phosphoribosylamine	C5H12NO7P	229.03514	M+K	267.99830	28	NIF	Pentose phosphate
	267.97477	4-Chloro-6,7-dimethoxy-1,3-benzoxazol-2-ol	C9H8ClNO4	229.01419	M+K	267.97734	10	NIF	Benzoxazole
296	296.06357	Glycerophosphocholine	C8H20NO6P	257.10282	M+K	296.06598	8	NIF	Glycerophospholipid
	296.07007	5-Aminoimidazole ribonucleotide	C8H14NO7P	295.05694	M+H	296.06421	20	NIF	Carbohydrate

Bin	Query mass	Compound name	Formula	Monoisotopic mass	Adduct	Adduct m/z	Δppm	Flavour descriptor	Chemical class
	296.07007	5-Amino-1-(5-phospho-D-riboseyl)imidazole	C8H14N3O7P	295.05694	M+H	296.06421	20	NIF	Carbohydrate
309.2	309.15260	2-Carboxy-1-[5-(2-carboxy-1-pyrrolidinyl)-2-hydroxy-2,4-pentadienylidene]pyrrolidinium	C15H20N2O5	308.13722	M+H	309.14450	26	NIF	Amino acid
	309.15260	Ethyl pentadecanoate	C17H34O2	270.45060	M+K	309.21905	215	fatty acid	fatty acids ester
	309.15260	Ethyl linoleate	C20H36O2	308.49860	M+H	309.27879	408	fatty vegetable rancid acids, oil,	Ester
322	322.07220	Avenanthramide a	C16H13NO5	299.07937	M+Na	322.06859	11	NIF	Cinnamic acid
	322.05183	(E)-Avenanthramide D	C16H13NO4	283.08446	M+K	322.04762	13	NIF	Cinnamic acid
	322.07220	Avenanthramide G	C16H13NO5	299.07937	M+Na	322.06859	11	NIF	Cinnamic acid
	322.00430	4-amino-2-Methyl-5-diphosphoxymethylpyrimidine	C6H11N3O7P2	299.00722	M+Na	321.99644	24	NIF	pyrophosphate
	322.05860	Guanosine	C10H13N5O5	283.09167	M+K	322.05483	12	NIF	Purine
	322.07220	D-4'-Phosphopantothenate	C9H18NO8P	299.07700	M+Na	322.06622	19	NIF	Amino acid
	322.08580	1-Methyl-adenosine	C11H17N5O4	283.12805	M+K	322.09121	17	NIF	Purine
407	407.08153	Feruloylquinic acid	C17H20O9	368.11073	M+K	407.07389	19	NIF	Ester
	406.97980	Orotidylic acid	C10H13N2O11P	368.02570	M+K	406.98885	22	NIF	Pyrimidine
	407.06373	2-O-Feruloylhydroxyctic acid	C16H16O11	384.06926	M+Na	407.05848	13	NIF	Carboxylic acid

A3 Chapter 4 UPLC-MS Supplementary Material

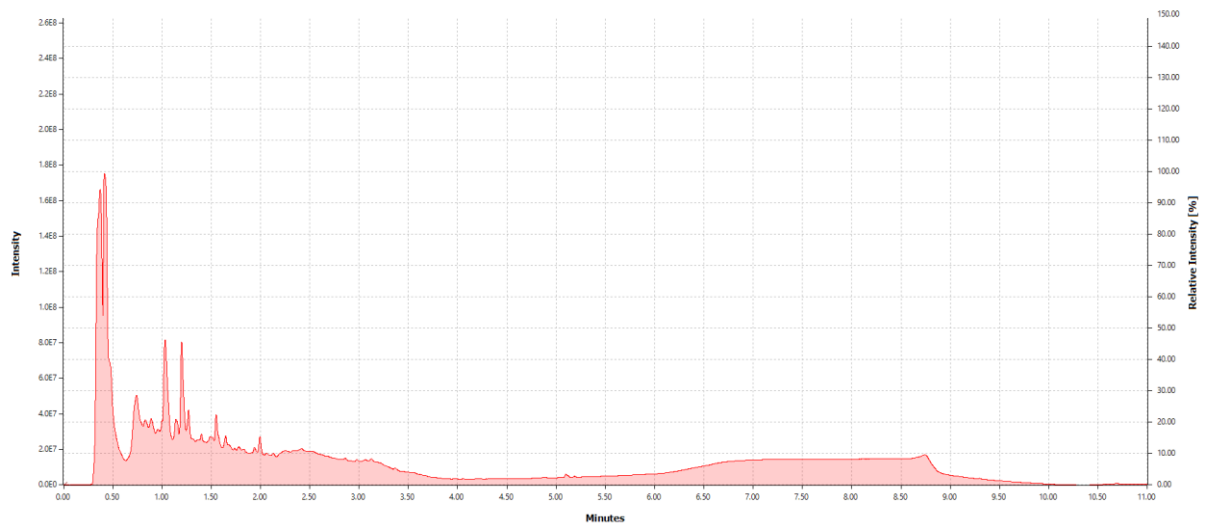


Figure 7.26 Chromatogram of a pre-fermentation sample (UPLC-MS Chapter 4)

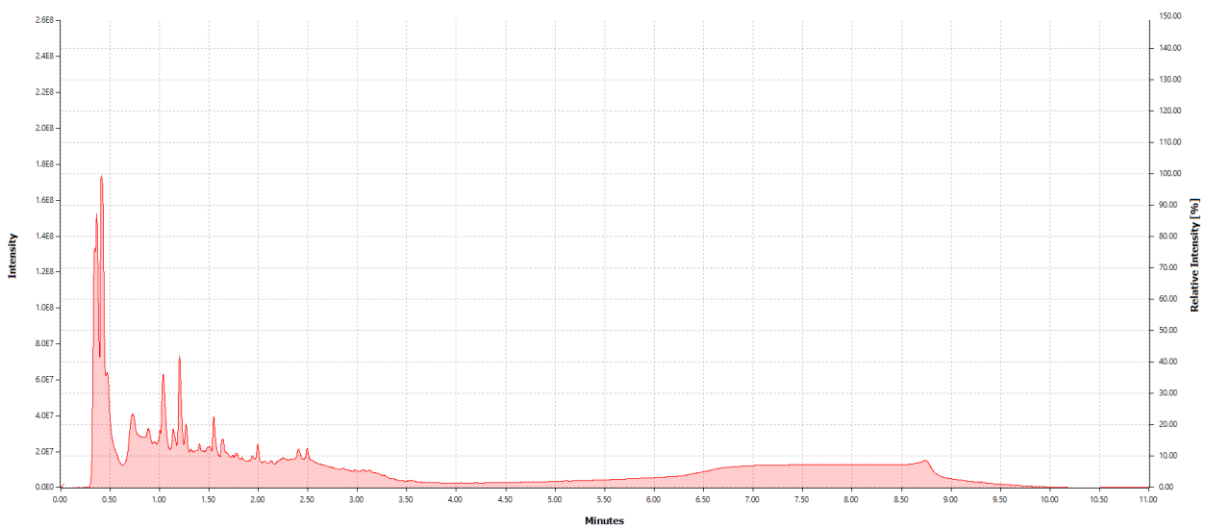


Figure 7.27 Chromatogram of a F1 sample (UPLC-MS Chapter 4)

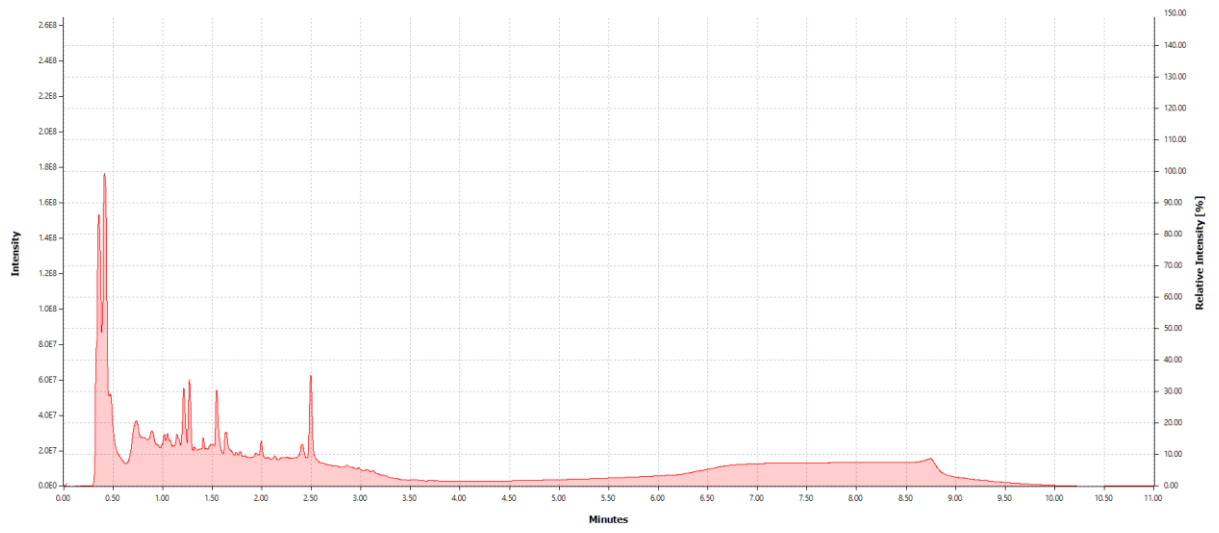


Figure 7.28 Chromatogram of a post-fermentation sample (UPLC-MS Chapter 4)

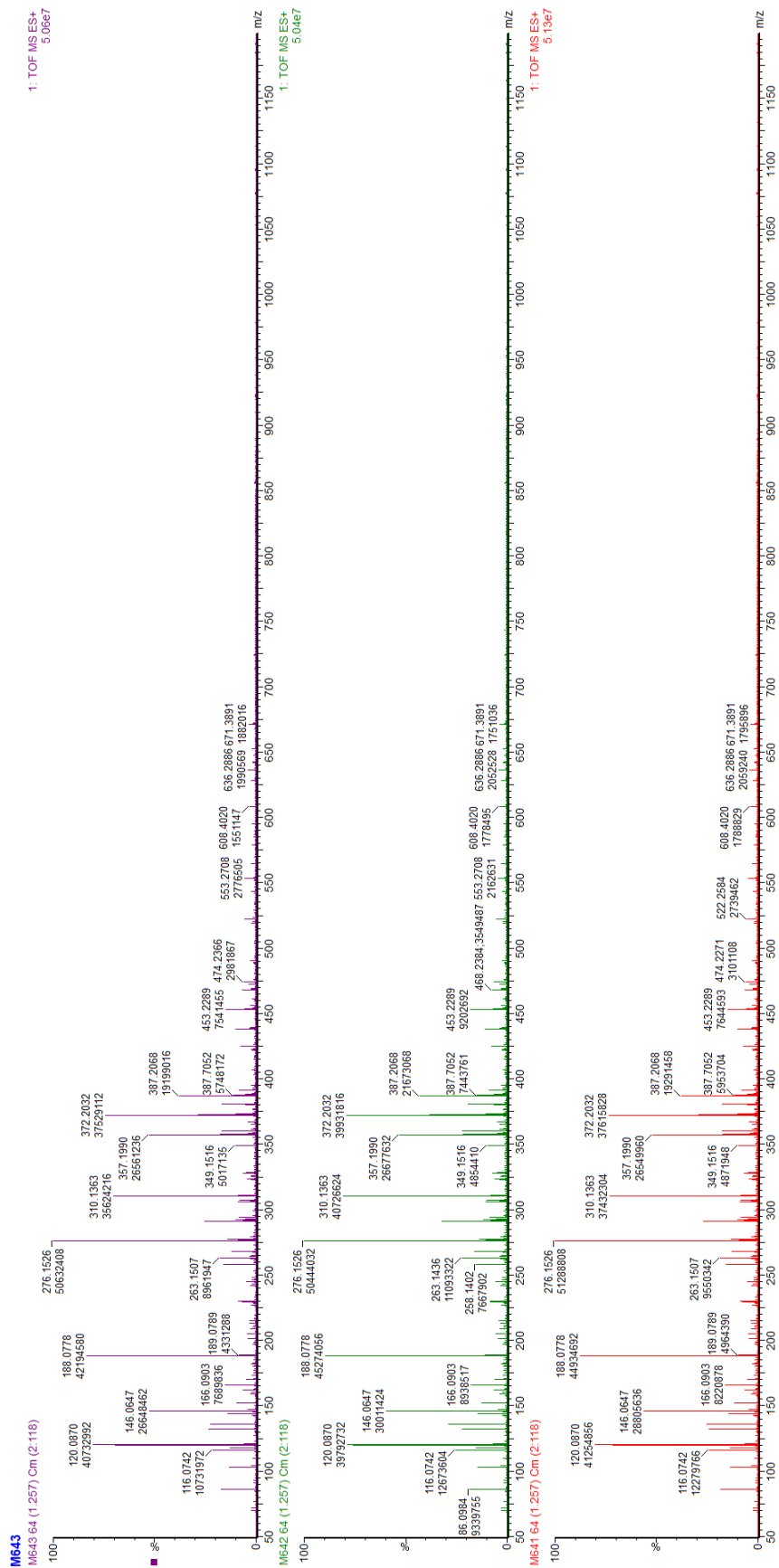


Figure 7.29 Mass spectra of three replicates of the M64 sample (UPLC-MS Chapter 4)

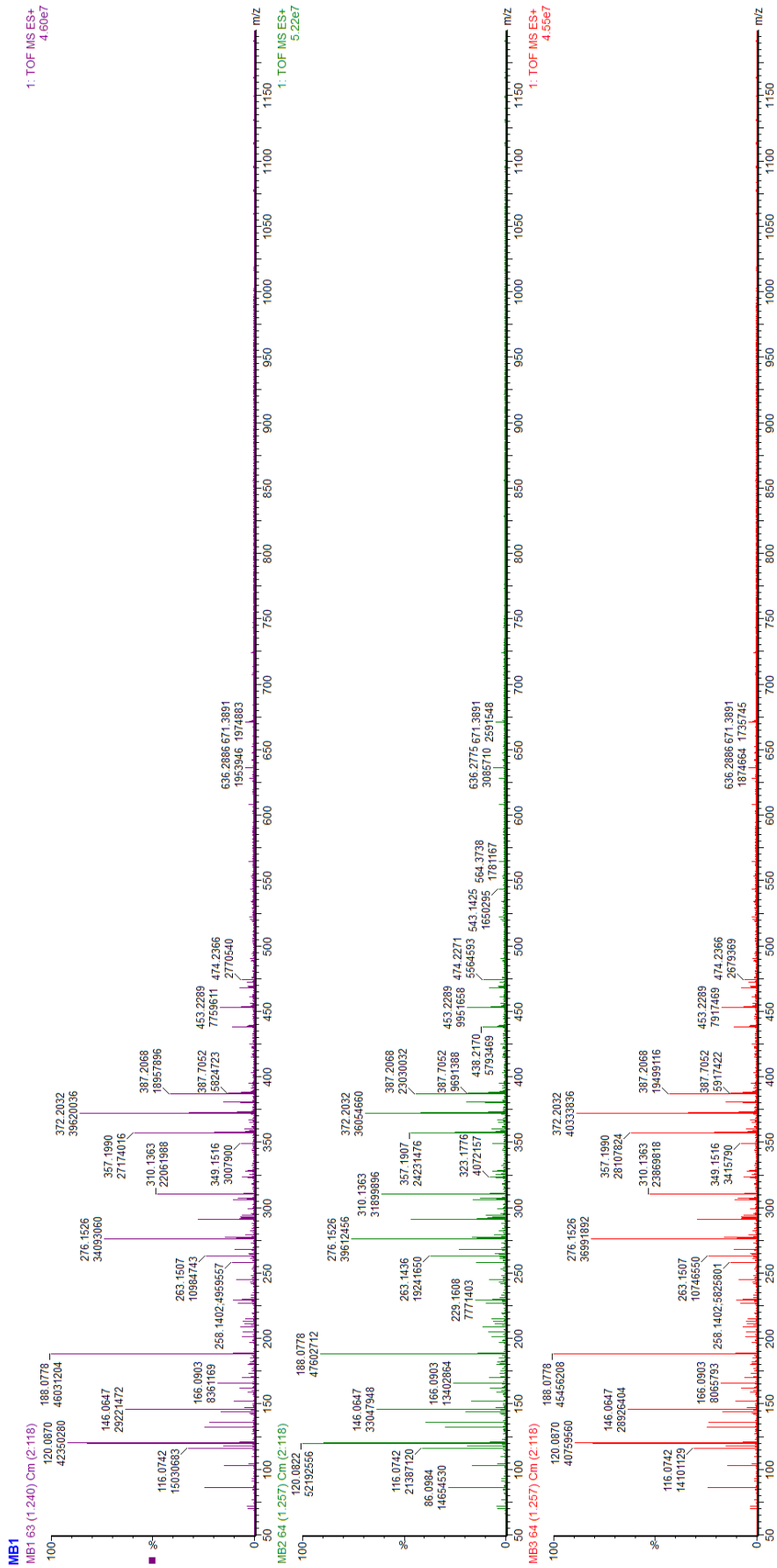


Figure 7.30 Mass spectra of three replicates of the MB sample (UPLC-MS Chapter 4)

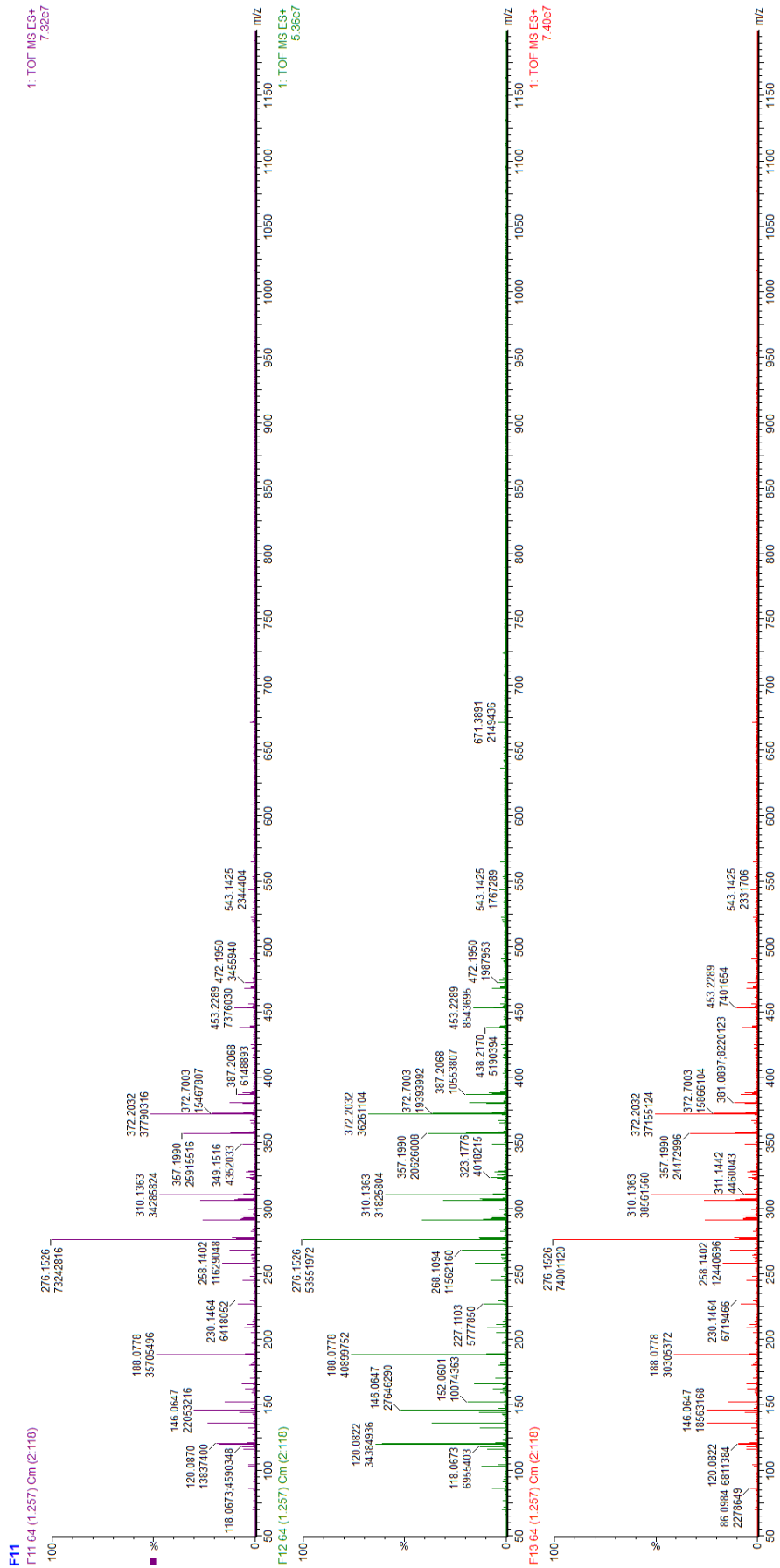


Figure 7.31 Mass spectra of three replicates of the F1 sample (UPLC-MS Chapter 4)

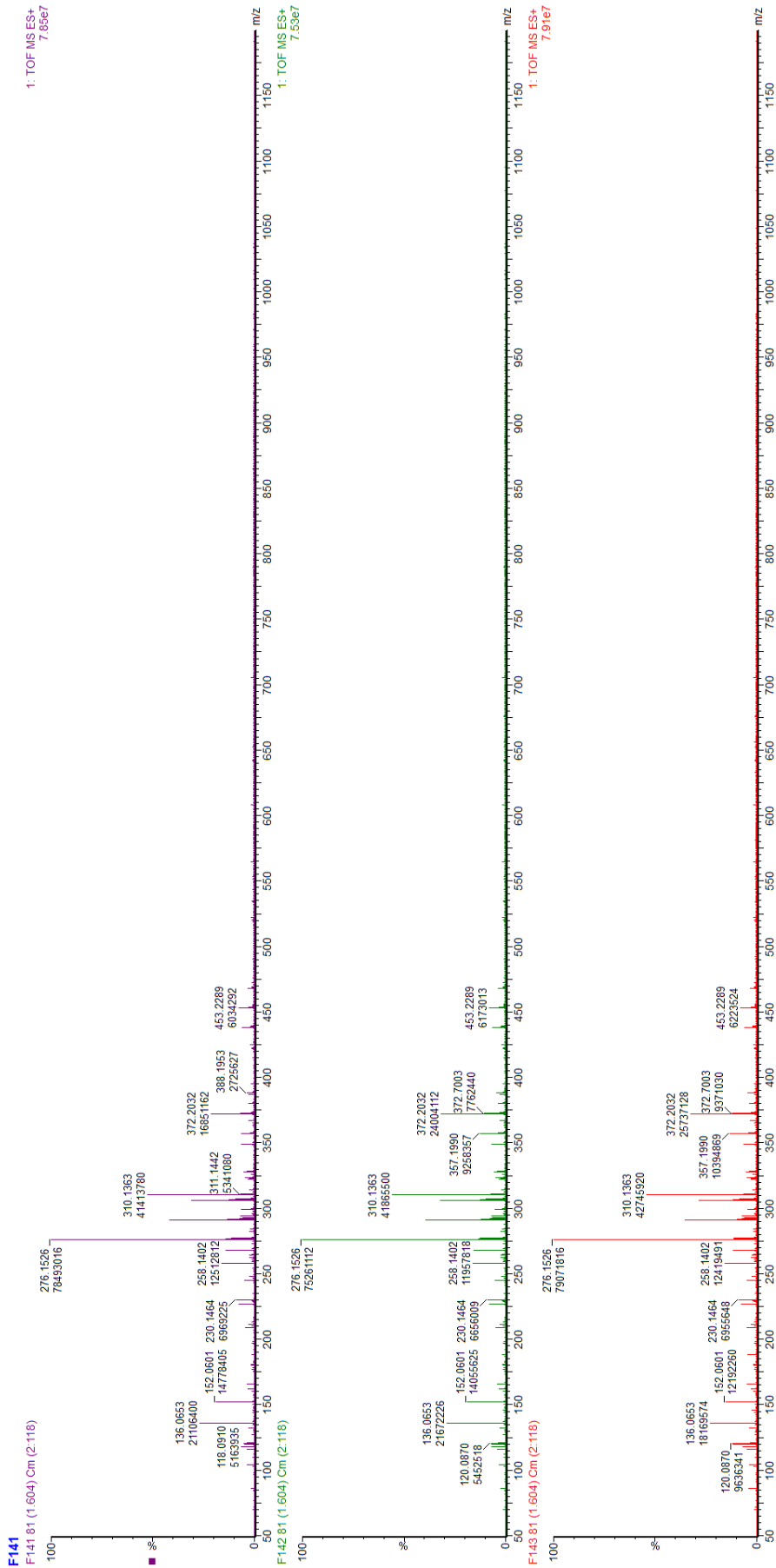


Figure 7.32 Mass spectra of three replicates of the F14 sample (UPLC-MS Chapter 4)

Table 7.5 Putative identification of features discriminant of the wort sample class (UPLC-MS)

Query mass	Compound name	Formula	Monoisotopic mass	Adduct	Adduct m/z	Δppm	Flavour descriptor	Chemical class
86.09845	Piperidine	C5H11N	85.08915	M+H	86.09643	24	animal, bitter, floral, heavy, sweet	Piperidine
86.09845	Isoprene	C5H8	68.06260	M+NH4	86.09642	24	NIF	Hydrocarbon
86.09845	Polyisoprene	C5H8	68.06260	M+NH4	86.09642	24	NIF	Hydrocarbon
103.05779	Cyclopentanethiol	C5H10S	102.05032	M+H	103.05760	2	alliacious, celery, citrus, earthy, egg, fatty, floral, fruity, garlic, green, herbaceous, horseradish, meaty, nutty, onion, spicy, vegetable, wine like, woody	Sulfur compound
103.05779	3-Methyl-2-butene-1-thiol	C5H10S	102.05032	M+H	103.05760	2	amine, leek, onion, smoke, sulfurous	Sulfur compound
103.05779	1-(Methylthio)-1-butene	C5H10S	102.05032	M+H	103.05760	2	sulfurous	Sulfur compound
120.08220	Cyclopentanethiol	C5H10S	102.05032	M+NH4	120.08414	16	alliacious, celery, citrus, earthy, egg, fatty, floral, fruity, garlic, green, herbaceous, horseradish, meaty, nutty, onion, spicy, vegetable, wine like, woody	Sulfur compound
120.08220	3-Methyl-2-butene-1-thiol	C5H10S	102.05032	M+NH4	120.08414	16	amine, leek, onion, smoke, sulfurous	Sulfur compound
120.08220	1-(Methylthio)-1-butene	C5H10S	102.05032	M+NH4	120.08414	16	sulfurous	Sulfur compound
120.08220	2-Methyl-1-propenethiol	C5H10S	102.05032	M+NH4	120.08414	16	NIF	Sulfur compound
120.08220	Hydroxydodecanoic acid	C12H24O3	216.17254	M+H+Na	120.08452	19	NIF	Acid
121.08882	8,8-Dimethoxy-2,6-dimethyl-2-octanol	C12H26O3	218.18819	M+H+Na	121.09234	29	green, lily, rose acetate, waxy	Alcohol
132.10762	1-Hexadecene	C16H32	224.25040	M+H+K	132.11042	21	NIF	Hydrocarbon
144.08260	2-Propylthiophene	C7H10S	126.05032	M+NH4	144.08414	11	roast beef	Heteroaromatic compound
144.08260	2-Ethyl-5-methylthiophene	C7H10S	126.05032	M+NH4	144.08414	11	cooked meat	Sulfur compound
144.08260	2-Ethyl-2,5-dihydro-4,5-dimethylthiazole	C7H13NS	143.07687	M+H	144.08415	11	chocolate, coffee, meat, musty, nut, raw, sulfury, vegetable	Sulfur compound
144.08260	6-Methylquinoline	C10H9N	143.07350	M+H	144.08078	13	castoreum, civet, fecal, leather, tobacco, tonka	Quinoline
144.08260	12-Oxo-2,3-dinor-10,15-phytyldienoic acid	C16H24O3	264.17254	M+H+Na	144.08452	13	NIF	Fatty Acyl
144.08260	N-Ethylaniline	C8H11N	121.08915	M+Na	144.07837	29	NIF	Amine
144.08260	N,N-Dimethylaniline	C8H11N	121.08915	M+Na	144.07837	29	NIF	Nitrogen compound
144.08260	1-Phenylethylamine	C8H11N	121.08915	M+Na	144.07837	29	NIF	Nitrogen compound
144.08260	Phenylethylamine	C8H11N	121.08915	M+Na	144.07837	29	ammoniacal, fishy	Amine
144.08260	2-Ethyl-5-methylpyridine	C8H11N	121.08915	M+Na	144.07837	29	NIF	Pyridine
144.08260	N-Methylbenzylamine	C8H11N	121.08915	M+Na	144.07837	29	NIF	Benzenoid
144.08260	5-Ethyl-2-methylpyridine	C8H11N	121.08915	M+Na	144.07837	29	Earthy, nutty, potato, raw, roasted, strong	Pyridine
144.08260	2-Methyl-6-ethylpyridine	C8H11N	121.08915	M+Na	144.07837	29	NIF	Pyridine
144.08260	2-Propylpyridine	C8H11N	121.08915	M+Na	144.07837	29	fatty, green, nutty, roasted, tobacco	Pyridine
166.09035	3-Mercapto-1-butyl acetate	C6H12O2S	148.05580	M+NH4	166.08962	4	fruity	Sulfur compound
166.09035	3-(Methylthio)propyl acetate	C6H12O2S	148.05580	M+NH4	166.08962	4	Ester, fatty	Carboxylic acid
166.09035	Methyl 4-(methylthio)butyrate	C6H12O2S	148.05580	M+NH4	166.08962	4	Cabbage, cheese, fruity, pineapple, sulfury	Fatty acid ester
166.09035	3-Mercapto-3-methylbutyl formate	C6H12O2S	148.05580	M+NH4	166.08962	4	Cat, fruity, herbal, roast, roasted, sweaty	Carboxylic acid
166.09035	2,4,6-Trimethyl-1,3,5-dioxathiane	C6H12O2S	148.05580	M+NH4	166.08962	4	onion	Sulfur compound

Query mass	Compound name	Formula	Monoisotopic mass	Adduct	Adduct m/z	Δppm	Flavour descriptor	Chemical class
166.09035	Ethyl mercaptobutyrate	C ₆ H ₁₂ O ₂ S	148.05580	M+NH ₄	166.08962	4	roasted, sour, sweet	Fatty acid ester
166.09035	Methyl (methylthio)butanoate	C ₆ H ₁₂ O ₂ S	148.05580	M+NH ₄	166.08962	4	cooked, sweet	Fatty acid ester
166.09035	Methylthiomethyl butyrate	C ₆ H ₁₂ O ₂ S	148.05580	M+NH ₄	166.08962	4	fruity, metallic, musty, onion, sulfurous, tropical, vegetable	Fatty acid ester
166.09035	beta-Methylthiopropionic acid ethyl ester	C ₆ H ₁₂ O ₂ S	148.05580	M+NH ₄	166.08962	4	fruity, metallic, pineapple, pulpy, ripe, sulfury, tomato	Carboxylic acid
166.09035	Ethyl (methylthio)propanoate	C ₆ H ₁₂ O ₂ S	148.05580	M+NH ₄	166.08962	4	NIF	Carboxylic acid
166.09035	Propyl mercaptopropionate	C ₆ H ₁₂ O ₂ S	148.05580	M+NH ₄	166.08962	4	cooked, meat, roasted	Carboxylic acid
166.09035	Methyl [6]-paradol	C ₁₈ H ₂₈ O ₃	292.20384	M+H+K	166.08714	19	NIF	NIF
166.09035	[7]-Paradol	C ₁₈ H ₂₈ O ₃	292.20384	M+H+K	166.08714	19	NIF	Phenol
166.09035	(2'E,4'Z,7'Z,8E)-Colnelenic acid	C ₁₈ H ₂₈ O ₃	292.20384	M+H+K	166.08714	19	NIF	Fatty Acid
166.09035	Gentiatibetine	C ₉ H ₁₁ N ₂ O	165.07898	M+H	166.08626	25	NIF	Pyridine
166.09035	Ethyl aminobenzoate	C ₉ H ₁₁ N ₂ O	165.07898	M+H	166.08626	25	blossom, floral, grape, orange blossom, sweet, wintergreen	Benzenoid
166.09035	Methyl methylantranilate	C ₉ H ₁₁ N ₂ O	165.07898	M+H	166.08626	25	blossom, fruity, grape, musty, neroli, orange, phenolic, powdery, wine	Benzenoid
166.09035	L-Phenylalanine	C ₉ H ₁₁ N ₂ O	165.07898	M+H	166.08626	25	bitter, odorless	Carboxylic acid
166.09035	Moupinamide	C ₁₈ H ₁₉ NO ₄	313.13141	M+H+NH ₄	166.08625	25	NIF	Phenol
166.09035	Lauroilsine	C ₁₈ H ₁₉ NO ₄	313.13141	M+H+NH ₄	166.08625	25	NIF	Aporphine
166.09035	3,4-Dihydro-2H-1-benzopyran-2-one	C ₉ H ₈ O ₂	148.05243	M+NH ₄	166.08625	25	almond, cinammon, coconut, coumarin, creamy, herbal, sweet, tobacco, tonka,	Phenol
166.09035	(E)-3-(2-Hydroxyphenyl)-2-propenal	C ₉ H ₈ O ₂	148.05243	M+NH ₄	166.08625	25	NIF	Cinammaldehyde
166.09035	(E)-3-(4-Hydroxyphenyl)-2-propenal	C ₉ H ₈ O ₂	148.05243	M+NH ₄	166.08625	25	NIF	Cinammaldehyde
166.09035	Cinnamic acid	C ₉ H ₈ O ₂	148.05243	M+NH ₄	166.08625	25	Balsam, cinammon, honey, storax, sweet	Cinnamic acid
166.09035	1-Phenyl-1,2-propanedione	C ₉ H ₈ O ₂	148.05243	M+NH ₄	166.08625	25	buttery, honey, pepper, plastic	Benzene
166.09035	Di-2-furanylmethane	C ₉ H ₈ O ₂	148.05243	M+NH ₄	166.08625	25	NIF	Heteroaromatic compound
279.23682	Sodium palmitate	C ₁₆ H ₃₁ NaO ₂	278.22217	M+H	279.22945	26	NIF	fatty acid ester
279.23682	Ethyl tetradecanoate	C ₁₆ H ₃₂ O ₂	256.24023	M+Na	279.22945	26	Ether, orris, soapy, sweet, violet, waxy	fatty acid ester
279.23682	Hexadecanoic acid	C ₁₆ H ₃₂ O ₂	256.24023	M+Na	279.22945	26	Fatty, slightly waxy	Fatty acid
279.23682	palmitate	C ₁₆ H ₃₂ O ₂	256.24023	M+Na	279.22945	26	NIF	Fatty acid
279.23682	Hexyl decanoate	C ₁₆ H ₃₂ O ₂	256.24023	M+Na	279.22945	26	fresh, green	fatty acid ester
279.23682	Octyl octanoate	C ₁₆ H ₃₂ O ₂	256.24023	M+Na	279.22945	26	coconut, fruity, oily	Fatty alcohol ester
279.23682	Butyl dodecanoate	C ₁₆ H ₃₂ O ₂	256.24023	M+Na	279.22945	26	fruity, oil, oily, peanut, soapy, waxy	fatty acid ester
279.23682	Dodecyl methylpropanoate	C ₁₆ H ₃₂ O ₂	256.24023	M+Na	279.22945	26	faint, fruity	Fatty alcohol ester
279.23682	Dodecyl butyrate	C ₁₆ H ₃₂ O ₂	256.24023	M+Na	279.22945	26	fruity	Fatty alcohol ester
279.23682	3,6,10-Trimethyltetradecane	C ₁₇ H ₃₆	240.28170	M+K	279.24486	29	NIF	Hydrocarbon
337.24847	Isopropyl hexadecanoate	C ₁₉ H ₃₈ O ₂	298.28718	M+K	337.25034	6	bland, fat, oily	Fatty acid ester
337.24847	Methyl stearate	C ₁₉ H ₃₈ O ₂	298.28718	M+K	337.25034	6	fat, oily, waxy	Fatty acid ester
496.35211	Dolicholide	C ₂₈ H ₄₆ O ₆	478.32944	M+NH ₄	496.36326	22	NIF	Steroid

Query mass	Compound name	Formula	Monoisotopic mass	Adduct	Adduct m/z	Δppm	Flavour descriptor	Chemical class
496.35211	(2R)-3-(docosa-7,10,13,16,19-pentaenoyloxy)-2-(hexadecanoyloxy)propyl docosa-4,7,10,13,16,19-hexaenoate	C63H100O6	952.75199	M+H+K	496.36121	18	NIF	Glycerol
496.35211	(2R)-3-(Icosa-5,8,11,14-tetraenoyloxy)-2-(octadec-9-enoyloxy)propyl docosa-4,7,10,13,16,19-hexaenoate	C63H100O6	952.75199	M+H+K	496.36121	18	NIF	Glycerol
496.35211	(2S)-3-(Icosa-5,8,11,14-tetraenoyloxy)-2-(octadeca-9,12-dienoyloxy)propyl docosa-7,10,13,16,19-pentaenoate	C63H100O6	952.75199	M+H+K	496.36121	18	NIF	Glycerol
496.35211	(2S)-3-(Icosa-5,8,11,14,17-pentaenoyloxy)-2-(octadec-9-enoyloxy)propyl docosa-7,10,13,16,19-pentaenoate	C63H100O6	952.75199	M+H+K	496.36121	18	NIF	Glycerol
496.35211	Polyporusterone A	C28H46O6	478.32944	M+NH4	496.36326	22	NIF	Steroid
496.35211	LysoPC(16:0)	C24H50NO7P	495.33249	M+H	496.33977	25		Glycerophospholipid
496.35211	23-Acetoxysoladulcinide	C29H47NO4	473.35051	M+Na	496.33973	25	NIF	Alkaloid
496.35211	Clupanodonyl carnitine	C29H47NO4	473.35051	M+Na	496.33973	25	NIF	Fatty acid ester

Table 7.6 Putative identification of compounds of the discriminant features in the wort-f1 sample class (UPLC-MS)

Query mass	Compound name	Formula	Monoisotopic mass	Adduct type	Adduct m/z	Δ (ppm)	Flavour descriptor	Chemical class
118.06733	2,3-Dihydro-2-methylthiophene	C5H8S	100.03467	M+NH4	118.06849	10	NIF	Sulfur Compound
118.06733	2,3-Dihydro-5-methylthiophene	C5H8S	100.03467	M+NH4	118.06849	10	NIF	Sulfur Compound
118.06733	Dihydrojasmonic acid	C12H20O3	212.14124	M+H+Na	118.06887	13	NIF	Ketone
118.06733	6-Epi-7-isocucurbitic acid	C12H20O3	212.14124	M+H+Na	118.06887	13	NIF	Acid
118.06733	Cucurbitic acid	C12H20O3	212.14124	M+H+Na	118.06887	13	NIF	Acid
118.06733	3-Ethenyl-4-hydroxy-2,5-dimethylhex-5-en-2-yl acetate	C12H20O3	212.14124	M+H+Na	118.06887	13	NIF	Acid
118.06733	Benzeneacetoneitrile	C8H7N	117.05785	M+H	118.06513	19	NIF	Nitrogen Compound
118.06733	Indole	C8H7N	117.05785	M+H	118.06513	19	animal, burnt, fecal, fishy, floral, honey, jasmine, moth ball, montball, naphthelene	Pyrrrole
118.06733	6beta,7beta,10beta-Cadina-1,4-diene	C8H4	100.03130	M+NH4	118.06512	19	fruit, fruity, mango, spice, spicy	Hydrocarbon
120.08220	Cyclopentanethiol	C5H10S	102.05032	M+NH4	120.08414	16	alliaceous, celery, citrus, earthy, egg, fatty, floral, fruity, garlic, green, herbaceous, horseradish, meaty, nutty, onion, spicy, vegetable, wine like, woody	Sulfur compound
120.08220	3-Methyl-2-butene-1-thiol	C5H10S	102.05032	M+NH4	120.08414	16	amine, leek, onion, smoke, sulfurous	Sulfur compound
120.08220	1-(Methylthio)-1-butene	C5H10S	102.05032	M+NH4	120.08414	16	sulfurous	Sulfur compound
120.08220	2-Methyl-1-propenethiol	C5H10S	102.05032	M+NH4	120.08414	16	NIF	Sulfur compound
120.08220	Dihydrozeatin	C10H15N5O	221.12766	M+H+NH4	120.08438	18	NIF	Nitrogen Compound
120.08220	xi-5-Hydroxydodecanoic acid	C12H24O3	216.17254	M+H+Na	120.08452	19	NIF	Fatty acid
146.06473	2-(Methylthiomethyl)furan	C6H8OS	128.02959	M+NH4	146.06341	9	garlic, horseradish, onion, pungent, sulfury, vegetable	Furan
146.06473	2-Methyl-3-(methylthio)furan	C6H8OS	128.02959	M+NH4	146.06341	9	beefy, cheese, coffee, minty, spicy, sulfurous	Sulfur Compound
146.06473	2,5-Dimethyl-3-furanthiol	C6H8OS	128.02959	M+NH4	146.06341	9	lamb, meat, meaty, sulfurous	Furan
146.06473	2-(1-Mercaptoethyl)furan	C6H8OS	128.02959	M+NH4	146.06341	9	NIF	Furan
146.06473	2-Methyl-5-(methylthio)furan	C6H8OS	128.02959	M+NH4	146.06341	9	coffee, garlic, horseradish, mustard, onion, sulfury	Sulfur Compound
146.06473	5-Methyl-2-furanmethanethiol	C6H8OS	128.02959	M+NH4	146.06341	9	coffee, roast, roasted, sulfur, sulfurous	Furan
188.07780	S-(2-Furanylmethyl)propanethioate	C8H10O2S	170.04015	M+NH4	188.07397	20	coffee, garlic, onion, savory, sulfurous	Furan
188.07780	2,5-Dimethyl-3-furanthiol acetate	C8H10O2S	170.04015	M+NH4	188.07397	20	floral, fruity	Furan
188.07780	Cyclodopa glucoside	C15H19NO9	357.10598	M+H+NH4	188.07354	23	NIF	phenolic glycoside
188.07780	HMBOA-Glc	C15H19NO9	357.10598	M+H+NH4	188.07354	23	NIF	Carbohydrate
188.07780	cyclo-dopa glucoside	5-O-C15H19NO9	357.10598	M+H+NH4	188.07354	23	NIF	phenolic glycoside
188.07780	Niazimicin A	C16H23NO6S	357.12461	M+H+NH4	188.08285	27	NIF	phenolic glycoside
189.07887	2,5-Diethyl-3-methylpyrazine	C9H14N2	150.11570	M+K	189.07886	0	hazelnut, meaty, toasted	Pyrazine
189.07887	2-Methyl-3-(2-methylpropyl)pyrazine	C9H14N2	150.11570	M+K	189.07886	0	green, herbal, sugar, syrup	Pyrazine

Query mass	Compound name	Formula	Monoisotopic mass	Adduct type	Adduct m/z	Δ (ppm)	Flavour descriptor	Chemical class
189.07887	2,3-Dimethyl-5-propylpyrazine	C9H14N2	150.11570	M+K	189.07886	0	NIF	Pyrazine
189.07887	3,5-Dimethyl-2-propylpyrazine	C9H14N2	150.11570	M+K	189.07886	0	burnt, hazelnut	Pyrazine
189.07887	2,3-Diethyl-5-methylpyrazine	C9H14N2	150.11570	M+K	189.07886	0	citrus, earthy, fatty, floral, fruity, green, hazelnut, herbaceous, meat, meaty, musty, nutty, potato, roast, roasted, spicy, vegetable, wine like, woody	Pyrazine
189.07887	3,5-Diethyl-2-methylpyrazine	C9H14N2	150.11570	M+K	189.07886	0	baked, meaty, nutty, vegetable	Pyrazine
189.07887	2,5-Dimethyl-3-propylpyrazine	C9H14N2	150.11570	M+K	189.07886	0	hazelnut	Pyrazine
189.07887	1-naphthoate	C11H7O2	171.04515	M+NH4	189.07898	1	NIF	Acid
189.07887	L-DOPA 3'-glucoside	C15H21NO9	359.12163	M+H+NH4	189.08137	13	NIF	Amino acid
189.07887	Isopropyl apiosylglucoside	C14H26O10	354.15260	M+H+Na	189.07455	23	NIF	Carbohydrate
189.07887	1-Deoxy-D-glucitol	C6H14O5	166.08412	M+Na	189.07334	29	NIF	Carbohydrate
189.07887	(Z)-1-(Methylthio)-5-phenyl-1-penten-3-yne	C12H12S	188.06597	M+H	189.07325	30	NIF	Sulfur compound
357.19897	Xylene	C24H30	318.23475	M+K	357.19791	3	NIF	Benzenoid
357.19897	(ent-16betaOH)-16,17-Dihydroxy-9(11)-kauren-19-oic acid	C20H30O4	334.21441	M+Na	357.20363	13	NIF	Lipid
357.19897	(ent-6alpha,7alpha)-6,7-Dihydroxy-16-kauren-19-oic acid	C20H30O4	334.21441	M+Na	357.20363	13	NIF	Terpenoid
357.19897	Phytocassane B	C20H30O4	334.21441	M+Na	357.20363	13	NIF	Terpenoid
357.19897	Crispanone	C20H30O4	334.21441	M+Na	357.20363	13	NIF	Lipid
357.19897	Jubanine A	C40H49N5O6	695.36828	M+H+NH4	357.20469	16	NIF	Alkaloid
357.19897	gamma-Crocetin	C22H28O4	356.19876	M+H	357.20604	20	NIF	Terpenoid
357.19897	Piperochromanoic acid	C22H28O4	356.19876	M+H	357.20604	20	NIF	Terpenoid
357.19897	trans-p-Menthane-7,8-diol 7-glucoside	C16H30O7	334.19915	M+Na	357.18837	30	NIF	Terpene
357.19897	3,7-Dimethyl-5-octene-1,7-diol 1-glucoside	C16H30O7	334.19915	M+Na	357.18837	30	NIF	Fatty Acyl glycoside
357.19897	2,6-Dimethyl-7-octene-1,6-diol 8-O-glucoside	C16H30O7	334.19915	M+Na	357.18837	30	NIF	Fatty Acyl glycoside
357.19897	trans-p-Menthane-7,8-diol 8-glucoside	C16H30O7	334.19915	M+Na	357.18837	30	NIF	Carbohydrate
365.11276	Starch, bleached	C27H46O20	690.25824	M+H+K	365.11434	4	NIF	Carbohydrate
365.11276	Dictyoquinazol C	C18H18N2O5	342.12157	M+Na	365.11079	5	NIF	Alkaloid
365.11276	(+)-Galeon	C20H22O4	326.15181	M+K	365.11497	6	NIF	Diarylheptanoids
365.11276	(-)-Galeon	C20H22O4	326.15181	M+K	365.11497	6	NIF	Diarylheptanoids
365.11276	Gingerenone C	C20H22O4	326.15181	M+K	365.11497	6	NIF	Diarylheptanoids
365.11276	1-(4-Hydroxy-3-methoxyphenyl)-7-phenyl-3,5-heptanedione	C20H22O4	326.15181	M+K	365.11497	6	NIF	Diarylheptanoids
365.11276	1,2-Dihydrodehydroguaiaretic acid	C20H22O4	326.15181	M+K	365.11497	6	NIF	Benzenoid
365.11276	5,5-Diisopropyl-2,2'-dimethylbiphenyl-3,3',4,4'-tetrone	C20H22O4	326.15181	M+K	365.11497	6	NIF	Lipid
365.11276	Poncitrin	C20H22O4	326.15181	M+K	365.11497	6	NIF	Pyran

Query mass	Compound name	Formula	Monoisotopic mass	Adduct type	Adduct m/z	Δ (ppm)	Flavour descriptor	Chemical class
365.11276	Peonidin 3-(6''-malonyl-glucoside) 5-glucoside	C31H35O19	711.17725	M+H+NH4	365.10918	10	NIF	Phenolic
365.11276	Epimelibiose	C12H22O11	342.11621	M+Na	365.10543	20	NIF	Carbohydrate
365.11276	Isomaltose	C12H22O11	342.11621	M+Na	365.10543	20	NIF	Carbohydrate
365.11276	Gentiobiose	C12H22O11	342.11621	M+Na	365.10543	20	NIF	Carbohydrate
365.11276	Melibiose	C12H22O11	342.11621	M+Na	365.10543	20	NIF	Carbohydrate
365.11276	Mannobiose	C12H22O11	342.11621	M+Na	365.10543	20	NIF	Carbohydrate
365.11276	Allolactose	C12H22O11	342.11621	M+Na	365.10543	20	NIF	Carbohydrate
365.11276	Trehalulose	C12H22O11	342.11621	M+Na	365.10543	20	NIF	Carbohydrate
365.11276	Kojibiose	C12H22O11	342.11621	M+Na	365.10543	20	NIF	Fatty Acyl
365.11276	Fagopyritol A1	C12H22O11	342.11621	M+Na	365.10543	20	NIF	Carbohydrate
365.11276	Fagopyritol B1	C12H22O11	342.11621	M+Na	365.10543	20	NIF	Carbohydrate
365.11276	Glucinol	C12H22O11	342.11621	M+Na	365.10543	20	NIF	Carbohydrate
365.11276	Sakebiose	C12H22O11	342.11621	M+Na	365.10543	20	NIF	Carbohydrate
365.11276	Inulobiose	C12H22O11	342.11621	M+Na	365.10543	20	NIF	Carbohydrate
365.11276	DEAE-cellulose	C12H22O11	342.11621	M+Na	365.10543	20	NIF	Carbohydrate
365.11276	Lactose	C12H22O11	342.11621	M+Na	365.10543	20	NIF	Carbohydrate
365.11276	D-Maltose	C12H22O11	342.11621	M+Na	365.10543	20	NIF	Carbohydrate
365.11276	Cellobiose	C12H22O11	342.11621	M+Na	365.10543	20	NIF	Carbohydrate
365.11276	Sucrose	C12H22O11	342.11621	M+Na	365.10543	20	NIF	Carbohydrate
365.11276	Sugars	C12H22O11	342.11621	M+Na	365.10543	20	NIF	Carbohydrate
365.11276	Olestra	C12H22O11	342.11621	M+Na	365.10543	20	NIF	Carbohydrate
365.11276	Galactinol	C12H22O11	342.11621	M+Na	365.10543	20	NIF	Carbohydrate
365.11276	alpha,alpha-Trehalose	C12H22O11	342.11621	M+Na	365.10543	20	NIF	Carbohydrate
365.11276	Trehalose	C12H22O11	342.11621	M+Na	365.10543	20	NIF	Carbohydrate
365.11276	Coniferin	C16H22O8	342.13147	M+Na	365.12069	22	NIF	Carbohydrate
365.11276	Veranisatin A	C16H22O8	342.13147	M+Na	365.12069	22	NIF	Terpene
365.11276	4-Hydroxy-3-(2-hydroxyethyl)acetophenone 4-glucoside	C16H22O8	342.13147	M+Na	365.12069	22	NIF	Carbohydrate
365.11276	Sphalleroside A	C16H22O8	342.13147	M+Na	365.12069	22	NIF	Carbohydrate
365.11276	3-Hydroxy-3-(3,4-dihydroxy-4-methylpentanoyl)-5-(3-methylbutyl)-1,2,4-cyclopentanetrione	C16H22O8	342.13147	M+Na	365.12069	22	NIF	Carbonyl compound
365.11276	Citrusin D	C16H22O8	342.13147	M+Na	365.12069	22	NIF	Fatty Acyl
365.11276	Gerberinol	C21H16O6	364.09469	M+H	365.10196	30	NIF	Hydroxycoumarin
381.08972	3-O-beta-D-Galactopyranosylproanthocyanidin A5'	C36H34O17	738.17960	M+H+Na	381.08805	4	NIF	Flavonoid
381.08972	ent-Epicatechin-(2alpha->7,4alpha->8)-epicatechin 3-galactoside	C36H34O17	738.17960	M+H+Na	381.08805	4	NIF	NIF
381.08972	Cyclic pyranopterin monophosphate	C10H14N5O8P	363.05800	M+NH4	381.09182	6	NIF	Pterine
381.08972	5'-Guanylic acid	C10H14N5O8P	363.05800	M+NH4	381.09182	6	odorless	Purine

Query mass	Compound name	Formula	Monoisotopic mass	Adduct type	Adduct m/z	Δ (ppm)	Flavour descriptor	Chemical class
381.08972	Guanosine monophosphate	C10H14N5O8P	363.05800	M+NH4	381.09182	6	NIF	Purine
381.08972	Pantetheine phosphate	C11H23N2O7PS	358.09636	M+Na	381.08558	11	NIF	Carboxylic acid
381.08972	Gardenin B	C19H18O7	358.10525	M+Na	381.09447	12	NIF	Flavonoid
381.08972	5,8-Dihydroxy-3-(4-hydroxybenzyl)-7-methoxy-4-chromanone acetate	C19H18O7	358.10525	M+Na	381.09447	12	NIF	Flavonoid
381.08972	Chrysoobtusin	C19H18O7	358.10525	M+Na	381.09447	12	NIF	Benzenoid
381.08972	3'-Hydroxy-4',5',7,8-tetramethoxyflavone	C19H18O7	358.10525	M+Na	381.09447	12	NIF	NIF
381.08972	7-Hydroxy-3',4',5,6-tetramethoxyflavone	C19H18O7	358.10525	M+Na	381.09447	12	NIF	NIF
381.08972	5-Hydroxy-3',4',7,8-tetramethoxyflavone	C19H18O7	358.10525	M+Na	381.09447	12	NIF	Flavonoid
381.08972	4'-Hydroxy-5,6,7,8-tetramethoxyflavone	C19H18O7	358.10525	M+Na	381.09447	12	NIF	Flavonoid
381.08972	3-Hydroxy-3-(3,4-dihydroxy-4-methylpentanoyl)-5-(3-methylbutyl)-1,2,4-cyclopentanetrione	C16H22O8	342.13147	M+K	381.09463	13	NIF	Carbonyl compound
381.08972	Citrusin D	C16H22O8	342.13147	M+K	381.09463	13	NIF	Fatty Acyl
381.08972	Coniferin	C16H22O8	342.13147	M+K	381.09463	13	NIF	Carbohydrate
381.08972	Veranisatin A	C16H22O8	342.13147	M+K	381.09463	13	NIF	Terpene
381.08972	4-Hydroxy-3-(2-hydroxyethyl)acetophenone 4-glucoside	C16H22O8	342.13147	M+K	381.09463	13	NIF	Carbohydrate
381.08972	Dictyoquinazol C	C18H18N2O5	342.12157	M+K	381.08473	13	NIF	Alkaloid
381.08972	Fagopyritol A1	C12H22O11	342.11621	M+K	381.07937	27	NIF	Carbohydrate
381.08972	Fagopyritol B1	C12H22O11	342.11621	M+K	381.07937	27	NIF	Carbohydrate
381.08972	Glucinol	C12H22O11	342.11621	M+K	381.07937	27	NIF	Carbohydrate
381.08972	Sakebiose	C12H22O11	342.11621	M+K	381.07937	27	NIF	Carbohydrate
381.08972	Inulobiose	C12H22O11	342.11621	M+K	381.07937	27	NIF	Carbohydrate
381.08972	beta-Lactose	C12H22O11	342.11621	M+K	381.07937	27	NIF	Carbohydrate
381.08972	Mannobiose	C12H22O11	342.11621	M+K	381.07937	27	NIF	Carbohydrate
381.08972	Allolactose	C12H22O11	342.11621	M+K	381.07937	27	NIF	Carbohydrate
381.08972	Trehalulose	C12H22O11	342.11621	M+K	381.07937	27	NIF	Carbohydrate
381.08972	Sucrose	C12H22O11	342.11621	M+K	381.07937	27	NIF	Carbohydrate
381.08972	Sugars	C12H22O11	342.11621	M+K	381.07937	27	NIF	Carbohydrate
381.08972	Olestra	C12H22O11	342.11621	M+K	381.07937	27	NIF	Carbohydrate
381.08972	DEAE-cellulose	C12H22O11	342.11621	M+K	381.07937	27	NIF	Carbohydrate
381.08972	Cellobiose	C12H22O11	342.11621	M+K	381.07937	27	NIF	Carbohydrate
381.08972	Maltose	C12H22O11	342.11621	M+K	381.07937	27	NIF	Carbohydrate
381.08972	Lactose	C12H22O11	342.11621	M+K	381.07937	27	NIF	Carbohydrate
381.08972	Alpha-Lactose	C12H22O11	342.11621	M+K	381.07937	27	NIF	Carbohydrate
381.08972	alpha,alpha-Trehalose	C12H22O11	342.11621	M+K	381.07937	27	NIF	Carbohydrate

Query mass	Compound name	Formula	Monoisotopic mass	Adduct type	Adduct m/z	Δ (ppm)	Flavour descriptor	Chemical class
381.08972	Trehalose	C ₁₂ H ₂₂ O ₁₁	342.11621	M+K	381.07937	27	NIF	Carbohydrate
381.08972	Kojibiose	C ₁₂ H ₂₂ O ₁₁	342.11621	M+K	381.07937	27	NIF	Fatty Acyl
381.08972	Galactinol	C ₁₂ H ₂₂ O ₁₁	342.11621	M+K	381.07937	27	NIF	Carbohydrate
381.08972	Epimelibiose	C ₁₂ H ₂₂ O ₁₁	342.11621	M+K	381.07937	27	NIF	Carbohydrate
381.08972	Isomaltose	C ₁₂ H ₂₂ O ₁₁	342.11621	M+K	381.07937	27	NIF	Carbohydrate
381.08972	Gentiobiose	C ₁₂ H ₂₂ O ₁₁	342.11621	M+K	381.07937	27	bitter	Carbohydrate
381.08972	Melibiose	C ₁₂ H ₂₂ O ₁₁	342.11621	M+K	381.07937	27	NIF	Carbohydrate
381.08972	Maltobionic acid	C ₁₂ H ₂₂ O ₁₂	358.11113	M+Na	381.10034	28	NIF	Fatty Acyl
381.08972	Calcium lactobionate	C ₁₂ H ₂₂ O ₁₂	358.11113	M+Na	381.10034	28	NIF	Fatty Acyl
387.20685	6e,9e-Dihydroxy-4,7E-megastigmadien-3-one 9-glucoside	C ₁₉ H ₃₀ O ₈	386.19407	M+H	387.20134	14	NIF	Fatty glycoside
387.20685	Corchoionol C 9-glucoside	C ₁₉ H ₃₀ O ₈	386.19407	M+H	387.20134	14	NIF	Fatty glycoside
387.20685	Vomifoliol 9-glucoside	C ₁₉ H ₃₀ O ₈	386.19407	M+H	387.20134	14	NIF	Fatty glycoside
387.20685	Sonchuionoside C	C ₁₉ H ₃₀ O ₈	386.19407	M+H	387.20134	14	NIF	Terpene glycoside
387.20685	Citroside A	C ₁₉ H ₃₀ O ₈	386.19407	M+H	387.20134	14	NIF	Terpene glycoside
387.20685	Citroside B	C ₁₉ H ₃₀ O ₈	386.19407	M+H	387.20134	14	NIF	Terpene glycoside
387.20685	Vanillin 3-(L-menthoxy)propane-1,2-diol acetal	C ₂₁ H ₃₂ O ₅	364.22497	M+Na	387.21419	19	minty, vanilla	Monoterpenoid
387.20685	Sativic acid	C ₁₈ H ₃₆ O ₆	348.25119	M+K	387.21435	19	NIF	Fatty Acyl
387.20685	Mubenin B	C ₄₁ H ₆₆ O ₁₁	734.46051	M+H+K	387.21547	22	NIF	Lipid

Table 7.7 Putative identification of compounds discriminant for the F1 sample class (UPLC-MS)

Query mass	Compound name	Formula	Monoisotopic mass	Adduct type	Adduct m/z	Δ (ppm)	Flavour descriptor	Chemical class
170.063	S-Methyl benzenecarbothioate	C8H8OS	152.0296	M+NH4	170.0634	2	cabbage, garlic, potato, sulfurous, vegetable	Benzenoid
170.063	5'-Hydroxy-3',4',7-trimethoxyflavan	C18H20O5	316.1311	M+H+Na	170.0638	5	NIF	Flavonoid/phenylpropanoid derivative
170.063	Verimol B	C18H20O5	316.1311	M+H+Na	170.0638	5	NIF	Benzenoid
170.063	Sorgolactone	C18H20O5	316.1311	M+H+Na	170.0638	5	NIF	Lactone
170.063	2-trans,-6-trans-farnesyl monophosphate	C15H25O4P	300.1501	M+H+K	170.0603	16	NIF	Terpenoid
245.1371	Polyethylene, oxidized	C12H20O5	244.1311	M+H	245.1384	5	NIF	Acid
245.1371	Sodium stearoyl 2-lactylate	C24H43NaO6	450.2957	M+H+K	245.1331	16	NIF	Carboxylic acid
245.1371	(±)-(E)-3-Methyl-4-(2,6,6-trimethyl-2-cyclohexen-1-yl)-3-buten-2-one	C14H22O	206.1671	M+K	245.1302	28	NIF	Lipid
245.1371	3-Methyl-4-(2,6,6-trimethyl-2-cyclohexen-1-yl)-3-buten-2-one	C14H22O	206.1671	M+K	245.1302	28	floral, powdery, violet, woody	Lipid
245.1371	Etaspirene	C14H22O	206.1671	M+K	245.1302	28	blackcurrant	Furan
245.1371	4-(1,1,3,3-Tetramethylbutyl)-phenol	C14H22O	206.1671	M+K	245.1302	28	NIF	Benzenoid
245.1371	1-(2,6,6-Trimethyl-1-cyclohexen-1-yl)-1-penten-3-one	C14H22O	206.1671	M+K	245.1302	28	floral, woody	Lipid
245.1371	delta-Methylionone	C14H22O	206.1671	M+K	245.1302	28	amberggris, floral, orris, waxy, woody	Lipid
245.1371	10-Isopropyl-2,7-dimethyl-1-oxaspiro[4.5]deca-3,6-diene	C14H22O	206.1671	M+K	245.1302	28	blackcurrant	Lipid
245.1371	1-(2,6,6-Trimethyl-2-cyclohexen-1-yl)-1-penten-3-one	C14H22O	206.1671	M+K	245.1302	28	floral, fruity, orris, powdery, sweet, violet, woody	Lipid
245.1371	alpha-Irone	C14H22O	206.1671	M+K	245.1302	28	berry, floral, orris, powdery, violet, woody	Lipid
245.1371	Methyl-delta-ionone	C14H22O	206.1671	M+K	245.1302	28	musk. oakmoss, patchouli	Lipid
245.1371	(all-E)-1,7,9-Heptadecatriene-11,13,15-tri-ene	C17H18	222.1409	M+Na	245.1301	29	NIF	Hydrocarbon
245.1371	3-Methyl-4-(2,6,6-trimethyl-2-cyclohexen-1-yl)-3-buten-2-one	C14H22O	206.1671	M+K	245.1302	28	NIF	Lipid
245.1371	2,4-di-tert-Butylphenol	C14H22O	206.1671	M+K	245.1302	28	NIF	Benzene
372.2032	Mahanimbine	C23H27NO2	349.2042	M+Na	372.1934	26	NIF	Alkaloid
372.2032	Murrayazoline	C23H27NO2	349.2042	M+Na	372.1934	26	NIF	Alkaloid
438.2079	Lucyoside M	C44H68O15	836.4558	M+H+K	438.2131	12	NIF	Terpene
438.2079	Murrastifoline F	C28H24N2O2	420.1838	M+NH4	438.2176	22	NIF	Alkaloid

Table 7.8 Putative identification of discriminant feature of the beer-f1 sample class (UPLC-MS)

Query mass	Compound name	Formula	Monoisotopic mass	Adduct type	Adduct m/z	Δppm	Flavour descriptor	Chemical class
152.06009	(E,E)-1,7-Diphenyl-4,6-heptadien-3-ol	C19H20O	264.15142	M+H+K	152.06093	5	NIF	Heptanoid/phenylpropanoid derivative
152.06009	Subaphylline	C14H20N2O3	264.14739	M+H+K	152.05891	8	NIF	cinnamic acid/phenylpropanoid derivative
152.06009	Vulgarolide	C15H20O5	280.13107	M+H+Na	152.06378	24	NIF	Oxane
152.06009	Nigelllic acid	C15H20O5	280.13107	M+H+Na	152.06378	24	NIF	Terpenoid
152.06009	13-Hydroxyabscisic acid	C15H20O5	280.13107	M+H+Na	152.06378	24	NIF	Terpenoid
152.06009	8-Deoxy-11,13-dihydroxygrosheimin	C15H20O5	280.13107	M+H+Na	152.06378	24	NIF	Terpene
152.06009	Artabsinolide B	C15H20O5	280.13107	M+H+Na	152.06378	24	NIF	Lactone
152.06009	Artabsinolide A	C15H20O5	280.13107	M+H+Na	152.06378	24	NIF	Lactone
152.06009	(1β,4α,5α,6β,8α,10β)-1,10:4,5-Diepoxy-6-hydroxy-7(11)-germacren-12,8-olide	C15H20O5	280.13107	M+H+Na	152.06378	24	NIF	Terpene
152.06009	Hexyl glucoside	C12H24O6	264.15729	M+H+K	152.06386	25	NIF	Fatty Acyl
152.06009	Tetrahydro-2-methyl-3-thiophenethiol	C5H10S2	134.02239	M+NH4	152.05622	25	NIF	Sulfur compound
152.06009	Tetrahydro-2-methyl-2-thiophenethiol	C5H10S2	134.02239	M+NH4	152.05622	25	NIF	Sulfur compound
152.06009	3,3-Dimethyl-1,2-dithiolane	C5H10S2	134.02239	M+NH4	152.05622	25	NIF	Sulfur compound
152.06010	Guanine	C5H5N5O	151.04940	M+H	152.05670	22	NIF	Purine
227.11030	O-acetylcarnitinium	C9H18NO4	204.12360	M+Na	227.11280	11	NIF	Nitrogenous compound
227.11030	Carnosine	C9H14N4O3	226.10660	M+H	227.11390	16	NIF	Peptide
227.11030	(6R)-6-(1-erythro-1,2-dihydroxypropyl)-5,6,7,8-tetrahydro-4a-hydroxypterin	C9H14N4O3	226.10660	M+H	227.11390	16	NIF	NIF
227.11030	7,8-Diaminononanoate	C9H20N2O2	188.15250	M+K	227.11560	23	NIF	Fatty acid
227.11031	3-[(2-Methyl-3-furanyl)thio]-4-heptanone	C12H18O2S	226.10275	M+H	227.11003	1	meaty, roasted	thioester
227.11031	3-Mercaptohexyl butyrate	C10H20O2S	204.11840	M+Na	227.10762	12	fruity, override fruit, passion fruit, sulfurous, tropical	fatty acyl ester
227.11031	Hexyl mercaptobutanoate	C10H20O2S	204.11840	M+Na	227.10762	12	fruity, herbal, spicy	fatty acyl ester
227.11031	(S)-3-Mercaptohexyl butyrate	C10H20O2S	204.11840	M+Na	227.10762	12		fatty acyl ester
227.11031	p-Tolyl phenylacetate	C15H14O2	226.09938	M+H	227.10666	16	animal, honey, hyacinth, lily, narcissus, rose	Polyphenol
227.11031	2-Phenylethyl benzoate	C15H14O2	226.09938	M+H	227.10666	16	balsam, floral, honey, rose, soft	Polyphenol
227.11031	2-Phenylethyl benzoate	C15H14O2	226.09938	M+H	227.10666	16		polyphenol
227.11031	7,8-Diaminononanoate	C9H20N2O2	188.15248	M+K	227.11564	23	NIF	Fatty acid
227.11031	6-(4-methyl-2-oxopentyl)-4-hydroxy-2-pyrone	C11H13O4	209.08193	M+NH4	227.11576	24	NIF	Pyran
227.11031	Ascorbyl palmitate	C22H38O7	414.26175	M+H+K	227.11609	25	citrus	Fatty acid ester
227.11031	3-Hydroxycapric acid	C10H20O3	188.14124	M+K	227.10440	26	NIF	Fatty acid
227.11031	2-Hexyl-1,3-dioxan-5-ol	C10H20O3	188.14124	M+K	227.10440	26	NIF	Heterocyclic
227.11031	xi-5-Hydroxydecanoic acid	C10H20O3	188.14124	M+K	227.10440	26	NIF	Fatty acid
227.11031	(1R,2R,4S)-p-Menthane-1,2,8-triol	C10H20O3	188.14124	M+K	227.10440	26	NIF	Terpenoid
227.11031	(1S,2S,4R,8R)-p-Menthane-1,2,9-triol	C10H20O3	188.14124	M+K	227.10440	26	NIF	Terpenoid
227.11031	2,6-Dimethyl-7-octene-2,3,6-triol	C10H20O3	188.14124	M+K	227.10440	26	NIF	Fatty Alcohol
227.11031	2,6-Dimethyloct-7-ene-2,3,6-triol	C10H20O3	188.14124	M+K	227.10440	26	NIF	Fatty Alcohol

Query mass	Compound name	Formula	Monoisotopic mass	Adduct type	Adduct m/z	Δppm	Flavour descriptor	Chemical class
227.11031	7-Methyl-3-methylene-1,6,7-octanetriol	C10H20O3	188.14124	M+K	227.10440	26	NIF	Fatty Alcohol
227.11031	2-Hexyl-1,3-dioxolane-4-methanol	C10H20O3	188.14124	M+K	227.10440	26	earthy, fundal, sweet	Oxolane
227.11031	cis-p-Menthane-1,7,8-triol	C10H20O3	188.14124	M+K	227.10440	26	NIF	Terpenoid
227.11031	trans-p-Menthane-1,7,8-triol	C10H20O3	188.14124	M+K	227.10440	26	NIF	Terpenoid
227.11031	Ethyl (±)-3-hydroxyoctanoate	C10H20O3	188.14124	M+K	227.10440	26	floral, fruity, winey	Fatty Alcohol
227.11031	Cinnamyl isobutyrate	C13H16O2	204.11503	M+Na	227.10425	27	almond, cinnamyl, fruity, spicy, sweet, tropical	Benzene
227.11031	4-Hydroxy-3-(3-methyl-2-butenyl)acetophenone	C13H16O2	204.11503	M+Na	227.10425	27	NIF	Carbonyl compounds
227.11031	cis-3-Hexenyl benzoate	C13H16O2	204.11503	M+Na	227.10425	27	balsam, fatty, floral, fresh, green, leaf, orchid	Benzenoid
227.11031	Isobutyl cinnamate	C13H16O2	204.11503	M+Na	227.10425	27	balsam, fruity, labdanum, sweet	Ester
227.11031	Plastoquinone	C13H16O2	204.11503	M+Na	227.10425	27	NIF	Quinone
227.11031	Phenethyl tiglate	C13H16O2	204.11503	M+Na	227.10425	27	green, herbal, leaf, natural, oily, rose, sweet	Fatty Acid
227.11031	Cinnamyl butyrate	C13H16O2	204.11503	M+Na	227.10425	27	balsamic, cinnamyl, cognac, fruity, soft, winey	Benzene
227.11031	2-Phenylethyl 3-methyl-2-butenolate	C13H16O2	204.11503	M+Na	227.10425	27	deep, herbal, sweet, wine	Ester
227.11031	Butyl cinnamate	C13H16O2	204.11503	M+Na	227.10425	27	balsam, cocoa, fruity, spicy, sweet	Ester
227.11031	Benzyl 2,3-dimethyl-2-butenolate	C13H16O2	204.11503	M+Na	227.10425	27	fruity, herbal, spicy, warm	Benzene
227.11031	6-(1-Hydroxyethyl)-2,2-dimethyl-2H-1-benzopyran	C13H16O2	204.11503	M+Na	227.10425	27	NIF	Pyran
227.11031	alpha, alpha-Dimethylanisalacetone	C13H16O2	204.11503	M+Na	227.10425	27	NIF	Esther
230.14642	L-prolyl-L-proline	C10H16N2O3	212.11609	M+NH4	230.14992	15	NIF	Carboxylic acid
230.14642	2-Amino-3,4-dimethylimidazo[4,5-f]quinoline	C12H12N4	212.10620	M+NH4	230.14002	28	NIF	Nitrogenous compound
276.15259	gamma-L-Glutamyl-L-pipecolic acid	C11H18N2O5	258.12157	M+NH4	276.15540	10	NIF	Carboxylic acid
276.15259	(2S,2'S)-Pyrosaccharopine	C11H18N2O5	258.12157	M+NH4	276.15540	10	NIF	Carboxylic acid
276.15259	4,5-Dihydropiperlonguminine	C16H21NO3	275.15214	M+H	276.15942	25	NIF	Alkaloid
276.15259	11a,12a-Epoxy-3b-hydroxy-28,13-oleananolate 3-acetate	C32H48O5	512.35017	M+H+K	276.16030	28	NIF	Terpenoid
276.15259	3beta-Acetoxy-12-oxo-28,13beta-oleananolate	C32H48O5	512.35017	M+H+K	276.16030	28	NIF	Terpenoid
276.15259	3alpha-Acetoxy-11-keto-beta-boswellic acid	C32H48O5	512.35017	M+H+K	276.16030	28	NIF	Terpenoid
276.15260	sn-Glycero-3-phosphocholine	C8H21NO6P	258.11060	M+NH4	276.14450	29	NIF	Lipid
276.16708	11a,12a-Epoxy-3b-hydroxy-28,13-oleananolate 3-acetate	C32H48O5	512.35017	M+H+K	276.16030	25	NIF	Terpenoid
276.16708	3beta-Acetoxy-12-oxo-28,13beta-oleananolate	C32H48O5	512.35017	M+H+K	276.16030	25	NIF	Terpenoid
276.16708	3alpha-Acetoxy-11-keto-beta-boswellic acid	C32H48O5	512.35017	M+H+K	276.16030	25	NIF	Terpenoid
276.16708	4,5-Dihydropiperlonguminine	C16H21NO3	275.15214	M+H	276.15942	28	NIF	Alkaloid
277.15454	Kukoamine A	C28H42N4O6	530.31044	M+H+Na	277.15347	4	NIF	Phenol
277.15454	(S)-Nerolidol 3-O-[a-L-rhamnopyranosyl-(1->2)-b-D-glucopyranoside]	C27H46O10	530.30910	M+H+Na	277.15280	6	NIF	Fatty acyl glycoside
277.15454	linalyl pentanoate	C15H26O2	238.19328	M+K	277.15644	7	apricot, citrus, fruity, lavender	Terpenoid
277.15454	Pentadecadienoic acid	C15H26O2	238.19328	M+K	277.15644	7	NIF	unsaturated fatty acid

Query mass	Compound name	Formula	Monoisotopic mass	Adduct type	Adduct m/z	Δppm	Flavour descriptor	Chemical class
277.15454	Bornyl isovalerate	C15H26O2	238.19328	M+K	277.15644	7	amphor, earth, green, herb, valerian,	Terpenoid
277.15454	Terpenyl isovalerate	C15H26O2	238.19328	M+K	277.15644	7	bitter, incense, olibanum, orange, pine, sweet	Terpenoid
277.15454	Bornyl valerate	C15H26O2	238.19328	M+K	277.15644	7	NIF	Terpenoid
277.15454	Tricyclohumuladiol	C15H26O2	238.19328	M+K	277.15644	7	NIF	Terpenoid
277.15454	alpha-Bisabolol oxide A	C15H26O2	238.19328	M+K	277.15644	7	NIF	Oxacyclic compounds
277.15454	5(1->10)-Abeo-1,12-patchoulanediol	C15H26O2	238.19328	M+K	277.15644	7	NIF	Alcohol
277.15454	Isocalamendiol	C15H26O2	238.19328	M+K	277.15644	7	NIF	Sesquiterpenoid
277.15454	Calamendiol	C15H26O2	238.19328	M+K	277.15644	7	NIF	Sesquiterpenoid
277.15454	(3S,4S,6R,7S)-1,10-Bisaboladiene-3,4-diol	C15H26O2	238.19328	M+K	277.15644	7	NIF	Sesquiterpenoid
277.15454	Isobornyl isovalerate	C15H26O2	238.19328	M+K	277.15644	7	NIF	Terpenoid
277.15454	2,5-Dihydroxybisabola-3,10-diene	C15H26O2	238.19328	M+K	277.15644	7	NIF	
277.15454	beta-Kessyl alcohol	C15H26O2	238.19328	M+K	277.15644	7	NIF	Sesquiterpenoid
277.15454	Germacrenone	C15H26O2	238.19328	M+K	277.15644	7	NIF	Sesquiterpenoid
277.15454	Methyl (Z,Z)-5,8-tetradecadienoate	C15H26O2	238.19328	M+K	277.15644	7	NIF	fatty acyl ester
277.15454	alpha-Terpinyll pentanoate	C15H26O2	238.19328	M+K	277.15644	7	floral, fruity	terpenoid
277.15454	Geranyl methylbutanoate	3- C15H26O2	238.19328	M+K	277.15644	7	apple, blueberry, fruity, green, pineapple, rose	fatty acyl alcohol ester
277.15454	Geranyl methylbutanoate	3- C15H26O2	238.19328	M+K	277.15644	7		fatty acyl alcohol ester
277.15454	Geranyl valerate	C15H26O2	238.19328	M+K	277.15644	7	fruit, fruity, pineapple, rose	fatty acyl alcohol ester
277.15454	2,10-Bisaboladiene-1,4-diol	C15H26O2	238.19328	M+K	277.15644	7		sesquiterpenoid
277.15454	Linalyl isovalerate	C15H26O2	238.19328	M+K	277.15644	7	apple, apricot, bergamot, citrus, lavender, peach, sage, sweet	Terpenoid
277.15454	2-Propenyl cyclohexanehexanoate	C15H26O2	238.19328	M+K	277.15644	7	fatty, fruity	fatty acyl ester
277.15454	Linatine	C10H17N3O5	259.11682	M+NH4	277.15064	14	NIF	amino acid

Table 7.9 Putative identities of features discriminant to the beer sample class (UPLC-MS)

Query mass	Compound name	Formula	Monoisotopic mass	Adduct type	Adduct m/z	Δppm	Flavour descriptor	Chemical class
136.0653	Nicotinamide riboside	C11H15N2O5	255.0981	M+H+NH4	136.0623	22	NIF	Glycosyl amine
136.0653	Adenine	C5H5N5	135.0545	M+H	136.0618	26	NIF	Purine
136.0653	Dihydroferuloylglycine	C12H15NO5	253.095	M+H+NH4	136.0681	20	NIF	Phenol
136.0653	abscisic aldehyde	C15H20O3	248.1412	M+H+Na	136.0689	26	NIF	Lipid
136.0653	8-Epiisovangustin	C15H20O3	248.1412	M+H+Na	136.0689	26	NIF	Lipid
136.0653	[4]-Shogaol	C15H20O3	248.1412	M+H+Na	136.0689	26	NIF	Phenol
136.0653	2α-Hydroxylantolactone	C15H20O3	248.1412	M+H+Na	136.0689	26	NIF	Terpene
136.0653	Artabsin	C15H20O3	248.1412	M+H+Na	136.0689	26	NIF	Lactone
136.0653	1α-1-Hydroxy-2,4(18),11(13)-eudesmatrien-12-oic acid	C15H20O3	248.1412	M+H+Na	136.0689	26	NIF	Terpenoid
136.0653	Eugenyl isovalerate	C15H20O3	248.1412	M+H+Na	136.0689	26	clove, fruity	Ester
136.0653	Parthenolide	C15H20O3	248.1412	M+H+Na	136.0689	26	bitter	Lipid
136.0653	(E)-2-Methyl-2-buten-1-ol O-beta-D-Glucopyranoside	C11H20O6	248.126	M+H+Na	136.0612	30	NIF	Fatty glycoside
136.0653	Prenyl glucoside	C11H20O6	248.126	M+H+Na	136.0612	30	NIF	Fatty glycoside
144.0878	α-Butyl-omega-hydroxypoly(oxyethylene) poly(oxypropylene)	C13H28O4	248.1988	M+H+K	144.0846	22	NIF	Ether
144.0878	12-Oxo-2,3-dinor-10,15-phytodienoic acid	C16H24O3	264.1725	M+H+Na	144.0845	23	NIF	Fatty Acyl
144.0878	2-Ethyl-2,5-dihydro-4,5-dimethylthiazole	C7H13NS	143.0769	M+H	144.0841	26	chocolate, coffee, meat, musty, nut, raw, sulfury, vegetable	Sulfur compound
144.0878	2-Propylthiophene	C7H10S	126.0503	M+NH4	144.0841	26		Heteroaromatic compound
144.0878	2-Ethyl-5-methylthiophene	C7H10S	126.0503	M+NH4	144.0841	26		Sulfur compound
144.0878	2-(3-Carboxy-3-(methylammonio)propyl)-L-histidine	C11H19N4O4	271.1406	M+H+NH4	144.0836	29	NIF	Carboxylic acid
258.1402	3-(3,4,5-Trimethoxyphenyl)propanoic acid	C12H16O5	240.0998	M+NH4	258.1336	25	NIF	phenylpropanoic acid
258.1402	Isopropyl 3-(3,4-dihydroxyphenyl)-2-hydroxypropanoate	C12H16O5	240.0998	M+NH4	258.1336	25	NIF	Phenol
258.1402	N1,N10-Diferuloylspermidine	C27H35N3O6	497.2526	M+H+NH4	258.1468	26	NIF	Cinnamic acid
268.1094	Adenosine	C10H13N5O4	267.0968	M+H	268.104	20	NIF	Purine
268.1094	Deoxyguanosine	C10H13N5O4	267.0968	M+H	268.104	20	NIF	Purine
268.1094	Neopellitorine A	C15H19NO	229.1467	M+K	268.1098	2	NIF	Fatty amide
268.1094	2,4,6,8-Decatetraenoic acid dehydropiperidide	C15H19NO	229.1467	M+K	268.1098	2	NIF	Pyridine
268.1094	2,4-Undecadiene-8,10-dienoic acid isobutylamide	C15H19NO	229.1467	M+K	268.1098	2	NIF	Fatty amide
268.1094	N-(1-Deoxy-1-fructosyl)serine	C9H17NO8	267.0954	M+H	268.1027	25	NIF	Carboxylic acid
276.1671	11α,12α-Epoxy-3β-hydroxy-28,13-oleananolate	C32H48O5	512.3502	M+H+K	276.1603	25	NIF	Terpenoid
276.1671	3β-Acetoxy-12-oxo-28,13β-oleananolate	C32H48O5	512.3502	M+H+K	276.1603	25	NIF	Terpenoid

Query mass	Compound name	Formula	Monoisotopic mass	Adduct type	Adduct m/z	Δppm	Flavour descriptor	Chemical class
276.1671	3alpha-Acetoxy-11-keto-beta-boswellic acid	C32H48O5	512.3502	M+H+K	276.1603	25	NIF	Terpenoid
276.1671	4,5-Dihydropiperlonguminine	C16H21NO3	275.1521	M+H	276.1594	28	NIF	Benzodioxole
276.2034	DG(14:0/14:0/0:0)	C31H60O5	512.4441	M+H+K	276.2073	14	NIF	Diacylglycerol
276.2034	Citronellyl anthranilate	C17H25NO2	275.1885	M+H	276.1958	27	fruity, neroli, petitgrain, rose, sweet	Terpenoid
276.2034	1,7,7-trimethylbicyclo[2.2.1]heptan-2-ol benzoate	C17H22O2	258.162	M+NH4	276.1958	27	balsam, balsamic, pine	Terpenoid
276.2034	Linalyl benzoate	C17H22O2	258.162	M+NH4	276.1958	27	bergamot, broom, gardenia, genet, heather, lily, tuberose	Terpenoid
276.2034	Geranyl benzoate	C17H22O2	258.162	M+NH4	276.1958	27	amber, rose, sweet, ylang	Terpenoid
276.2034	Falcarinolone	C17H22O2	258.162	M+NH4	276.1958	27	NIF	Fatty acyl alcohol
276.6679	Corchoroside A	C29H42O9	534.2829	M+H+NH4	276.662	21	NIF	Steroid Lactone
276.6679	Helveticoside	C29H42O9	534.2829	M+H+NH4	276.662	21	NIF	Lactone
291.1711	Platydesminium	C16H20NO3	274.1443	M+NH4	291.1709	1	NIF	Nitrogenous aromatic heterocyclic compound
291.1711	(2E)-Piperamide-C5:1	C16H19NO3	273.1365	M+NH4	291.1703	3	NIF	Nitrogenous heterocyclic compound
291.1711	(E,E)-Piperlonguminine	C16H19NO3	273.1365	M+NH4	291.1703	3	NIF	Nitrogenous heterocyclic compound
291.1711	Geranyl hexanoate	C16H28O2	252.2089	M+K	291.1721	3	fruity, geranium, rose, waxy	Fatty alcohol ester
291.1711	D6-Ambrettolide	C16H28O2	252.2089	M+K	291.1721	3	amber, berry, fruity, soapy, sweet	phenylpropanoid derivative
291.1711	Linalyl hexanoate	C16H28O2	252.2089	M+K	291.1721	3	animal, fruity, green, pear, pineapple, warm	Terpenoid
291.1711	Geranyl 2-ethylbutyrate	C16H28O2	252.2089	M+K	291.1721	3	NIF	Fatty alcohol ester
291.1711	Isoambrettolide	C16H28O2	252.2089	M+K	291.1721	3	ambrettek, fruity, musk, sweet, waxy	phenylpropanoid derivative
291.1711	Hexadecadienoic acid	C16H28O2	252.2089	M+K	291.1721	3	NIF	Fatty acid
291.1711	Diisopentyl thiomalate	C14H26O4S	290.1552	M+H	291.1625	30	bread, coffee, dark, fermented, rye, yeast	Fatty acid ester
292.1253	Lyso-PS(20:4(5Z,8Z,11Z,14Z)/0:0)	C26H43NO9P	544.2681	M+H+K	292.1193	21	NIF	lysophospholipid
292.1253	Lyso-PS(0:0/20:4(5Z,8Z,11Z,14Z))	C26H43NO9P	544.2681	M+H+K	292.1193	21	NIF	lysophospholipid
292.1253	Lyso-PI(0:0/14:0)	C23H45O12P	544.2649	M+H+K	292.1176	26	NIF	lysophospholipid
292.1253	Lyso-PI(14:0/0:0)	C23H45O12P	544.2649	M+H+K	292.1176	26	NIF	lysophospholipid
292.1253	PI(14:0/0:0)	C23H45O12P	544.2649	M+H+K	292.1176	26	NIF	phospholipid
292.1253	Charine	C9H14N4O6	274.0913	M+NH4	292.1252	1	NIF	Carbohydrate
292.1253	1,6-anhydro-N-acetyl-beta-muramate	C11H16NO7	274.0927	M+NH4	292.1265	4	NIF	Nitrogenous compound
292.1253	(1 <i>α</i> ,3 <i>S</i>)-1,2,3,4-Tetrahydro-1-methyl-beta-carboline-1,3-dicarboxylic acid	C14H14N2O4	274.0954	M+NH4	292.1292	13	NIF	Alkaloid
292.1253	Physagulin F	C30H40O9	544.2672	M+H+K	292.1188	22	NIF	Lactone
292.1253	Morellic acid	C33H36O8	560.241	M+H+Na	292.1188	23	NIF	Pyran

Query mass	Compound name	Formula	Monoisotopic mass	Adduct type	Adduct m/z	Δppm	Flavour descriptor	Chemical class
292.1253	Isomorellic acid	C33H36O8	560.241	M+H+Na	292.1188	23	NIF	Pyran
292.1253	(-)-Epiarfelechin	C15H14O5	274.0841	M+NH4	292.1179	25	NIF	flavonoid/phenylpropanoid derivative
292.1253	Phloretin	C15H14O5	274.0841	M+NH4	292.1179	25	odorless	phenylpropanoid derivative
292.1253	(E)-4-Methoxy-3,3',5,5'-tetrahydroxystilbene	C15H14O5	274.0841	M+NH4	292.1179	25	NIF	Stillbene
292.1253	2,3-Epoxy sesamone	C15H14O5	274.0841	M+NH4	292.1179	25	NIF	Lipid
292.1253	11-Methoxynoryangonin	C15H14O5	274.0841	M+NH4	292.1179	25	NIF	Lactone
292.1253	(2xi,4xi)-4,4',5,7-Tetrahydroxyflavan	C15H14O5	274.0841	M+NH4	292.1179	25	NIF	Flavonoid
292.1253	Apiforol	C15H14O5	274.0841	M+NH4	292.1179	25	NIF	Flavonoid
292.1253	(2S,3S,4R)-3,4,4',7-Tetrahydroxyflavan	C15H14O5	274.0841	M+NH4	292.1179	25	NIF	Flavonoid
292.1253	5'-Hydroxy-O-desmethylangolensin	C15H14O5	274.0841	M+NH4	292.1179	25	NIF	phenylpropanoid derivative
292.1253	Bakers yeast extract	C19H14O2	274.0994	M+NH4	292.1332	27	NIF	benzenoid
299.173	Floribundine	C18H19NO2	281.1416	M+NH4	299.1754	8	NIF	Aporphine
299.173	3-Benzoyloxy-6-oxo-12-ursen-28-oic acid	C37H50O5	574.3658	M+H+Na	299.1812	27	NIF	Terpenoid
299.173	4-(3-Hydroxy-7-phenyl-6-heptenyl)-1,2-benzenediol	C19H22O3	298.1569	M+H	299.1642	29	NIF	phenylpropanoid derivative
299.173	Auraptene	C19H22O3	298.1569	M+H	299.1642	29	NIF	Terpene
306.1747	Ethylsuberenol	C17H20O4	288.1362	M+NH4	306.17	16	NIF	Coumarin
306.1747	Angeloylsenkyunolide F	C17H20O4	288.1362	M+NH4	306.17	16	NIF	Benzofuran
306.1747	(ΔΔ)-Rollipyrrole	C16H20N2O3	288.1474	M+NH4	306.1812	21	NIF	Pyrroline
310.1363	(2S,4S)-Monatin	C14H16N2O5	292.1059	M+NH4	310.1397	11	NIF	Carboxylic acid
310.1363	Hordatine B	C29H40N8O5	580.3122	M+H+K	310.1413	16	NIF	flavonoid/phenylpropanoid derivative
310.1363	Piperanine	C17H21NO3	287.1521	M+Na	310.1414	16	NIF	Heterocyclic compound
310.1363	Feruperine	C17H21NO3	287.1521	M+Na	310.1414	16	NIF	Phenol
310.1363	Pipericyclobutanamide B	C36H40N2O6	596.2886	M+H+Na	310.1426	20	NIF	Heterocyclic compound
310.1363	N-gamma-Glutamyl-S-propylcysteine	C11H20N2O5S	292.1093	M+NH4	310.1431	22	NIF	Carboxylic acid
310.1363	indole-3-acetyl-isoleucine	C16H19N2O3	287.1401	M+Na	310.1293	23	NIF	Carboxylic acid
310.1363	indole-3-acetyl-leucine	C16H19N2O3	287.1401	M+Na	310.1293	23	NIF	Carboxylic acid
310.1363	(all-E)-1,7-bis(4-hydroxyphenyl)-1,4,6-heptatrien-3-one	C19H16O3	292.1099	M+NH4	310.1438	24	NIF	Heptanoid/phenylpropanoid derivative
310.1363	Koenigine	C19H19NO3	309.1365	M+H	310.1438	24	NIF	Carbazole
310.1363	trans-Grandmarin	C15H16O6	292.0947	M+NH4	310.1285	25	NIF	Pyranocoumarin/phenylpropanoid derivative
310.1363	cis-Grandmarin	C15H16O6	292.0947	M+NH4	310.1285	25	NIF	Pyranocoumarin/phenylpropanoid derivative
310.1363	(S)-Angelicaicain	C15H16O6	292.0947	M+NH4	310.1285	25	NIF	Pyran
311.1442	(3R)-3,4-Dihydroxy-3-(hydroxymethyl)butanenitrile 4-glucoside	C11H19NO8	293.1111	M+NH4	311.1449	2	NIF	Lipid
311.1442	4-Hydroxyproline galactoside	C11H19NO8	293.1111	M+NH4	311.1449	2	NIF	Fatty Acyl
311.1442	Galactosyl 4-hydroxyproline	C11H19NO8	293.1111	M+NH4	311.1449	2	NIF	Carboxylic acid
311.1442	Geranyl phenylacetate	C18H24O2	272.1776	M+K	311.1408	11	honey	Fatty Acyl

Query mass	Compound name	Formula	Monoisotopic mass	Adduct type	Adduct m/z	Δppm	Flavour descriptor	Chemical class
311.1442	Linalyl phenylacetate	C18H24O2	272.1776	M+K	311.1408	11	honey, neroli, rose, sick, sweet	Terpenoid
311.1442	(Δ±)-Rollipyrrole	C16H20N2O3	288.1474	M+Na	311.1366	24	NIF	Pyrroline
322.1739	(1α,3β,20S,22R,24S,25S)-Pubescenin	C34H52O10	620.356	M+H+Na	322.1763	7	NIF	steroid Lactone
322.1739	Physagulin D	C34H52O10	620.356	M+H+Na	322.1763	7	NIF	steroid Lactone
322.1739	3'-Deoxyoleacein	C17H20O5	304.1311	M+NH4	322.1649	28	NIF	Phenol
322.1739	Matricarin	C17H20O5	304.1311	M+NH4	322.1649	28	NIF	Lactone
328.1481	Dihydro-2,4,6-tris(2-methylpropyl)-4h-1,3,5-dithiazine	C15H31NS2	289.1898	M+K	328.1529	15	bacon, meaty, smoked	heterocyclic Sulfur compound
328.1481	Hydroxytanshinone	C19H18O4	310.1205	M+NH4	328.1543	19	NIF	Terpenoid
328.1481	Moracin N	C19H18O4	310.1205	M+NH4	328.1543	19	NIF	flavonoid/phe nylpropanoid derivative
328.1481	Artocarbene	C19H18O4	310.1205	M+NH4	328.1543	19	NIF	Stillbene/phe nylpropanoid derivative
328.1481	Moracin C	C19H18O4	310.1205	M+NH4	328.1543	19	NIF	flavonoid/phe nylpropanoid derivative
328.1481	(S)-scoulerine	C19H21NO4	327.1471	M+H	328.1543	19	NIF	Alkaloid
328.1481	(S)-corytuberine	C19H21NO4	327.1471	M+H	328.1543	19	NIF	Alkaloid
328.1481	(S)-Boldine	C19H21NO4	327.1471	M+H	328.1543	19	NIF	Alkaloid
328.1481	Norcorydine	C19H21NO4	327.1471	M+H	328.1543	19	NIF	Alkaloid
328.1481	(R)-Norisocorydine	C19H21NO4	327.1471	M+H	328.1543	19	NIF	Alkaloid
328.1481	Litcubine	C19H22NO4	328.1549	M+H	328.1549	21	NIF	heterocyclic Nitrogenous compound
328.1481	Pentaporphyrin I	C20H14N4	310.1218	M+NH4	328.1557	23	NIF	Alkaloid
328.1481	N-(1-Deoxy-1-fructosyl)phenylalanine	C15H21NO7	327.1318	M+H	328.1391	28	NIF	Amadori product
328.1481	1-Pentadecanecarboxylic acid	C15H18O7	310.1053	M+NH4	328.1391	28	NIF	phenolic glycoside
328.1481	trans-cinnamoyl-β ² -D-glucoside	C15H18O7	310.1053	M+NH4	328.1391	28	NIF	cinnamic acid ester/phenylpr oanoid derivative
328.1481	(E)-2-O-Cinnamoyl-beta-D-glucofuranose	C15H18O7	310.1053	M+NH4	328.1391	28	NIF	Carbohydrate
328.1481	1-O-E-Cinnamoylglucose	C15H18O7	310.1053	M+NH4	328.1391	28	NIF	Ester
328.1481	1-O-Cinnamoylglucose	C15H18O7	310.1053	M+NH4	328.1391	28	NIF	Ester
347.3188	Dihydroceramide	C19H39NO3	329.293	M+NH4	347.3268	23	NIF	Carboxylic acid